RAINFALL SIMULATOR CONSTRUCTION AND EVALUATION OF EROSION CONTROL PRACTICES

by

Christin Jennifer Weeks Manning

A thesis submitted to the Graduate Faculty of
Auburn University
in partial fulfillment of the
requirements for the Degree of
Master of Science

Auburn, Alabama
December 11, 2021

Keywords: erosion, rainfall simulation,
construction stormwater, polyacrylamide

Approved by

Michael A. Perez, Chair, Assistant Professor of Civil and Environmental Engineering
Wesley N. Donald, Research Fellow IV Civil and Environmental Engineering
Xing Fang, Professor of Civil and Environmental Engineering

Abstract

This thesis addresses the performance of erosion control products using the Auburn University Stormwater Research Facility ASTM D6459 rainfall simulators. Five products were tested for the ALDOT project *Evaluation of ALDOT Erosion Control Practices using Rainfall Simulation*. The Cover factors (C-factors) for jute, jute with polyacrylamide (PAM), jute with gypsum, ProMatrix™ hydro mulch, and EarthGuard™ EDGE™ pellets were found to be 0.35, 0.45, 0.12, 0.42, and 0.45, respectively. Data from previous testing was compared. No product types differed significantly at the 2 in./hr (5.1 cm/hr). Hydro mulches performed mostly similarly with some failing to meet their minimum C-factor criteria. PAM was highly effective at the 2 in./hr (5.1 cm/hr) but failed similarly to the hydro mulches at higher intensities. Gypsum performed similarly to erosion control blankets. Additionally, PAM testing for residual runoff concentration using a spectroscopic method with centrifuging found high concentrations (>100 mg/L in some samples). Finally, in partial fulfillment of the ALDOT project *Evaluation of ALDOT Erosion Control Practices using Rainfall Simulation on Various Soil Types and Slope Gradients,* six new rainfall simulators were constructed, including literature review, soil testing and selection, design and modeling, grading, and assembly.

Acknowledgements

The author would first like to thank Dr. Mike Perez and Dr. Wesley Donald for their invaluable support and guidance throughout the work of this thesis. The author would also like to acknowledge the support of the Auburn Stormwater research team, including Jaime Schussler, Billur Kazaz, Blake Whitman, Guy Savage, Brian Faulkner, and many undergraduate assistants, and a special thanks to Jacob Etheridge for his assistance with Phase II. The expertise and assistance of Dr. Gerald John is also gratefully acknowledged, as well as the laboratory space and material support of the National Center for Asphalt Technology and the Auburn University Department of Civil and Environmental Engineering. Finally, the author would like to gratefully recognize the Alabama Department of Transportation for their financial support of this project.

Table of Contents

List of Figures

List of Tables

CHAPTER 1: INTRODUCTION

1.1 MOTIVATION AND IMPORTANCE

Sediment pollution from construction stormwater runoff poses a significant source of contamination to water bodies. Construction activities such as clearing and grading strip land of its protective vegetative cover, leaving bare soil vulnerable to raindrop impact forces and overland flow forces which dislodge and transport the soil particles. While seemingly less innocuous than other pollutants such as heavy metals, sediment harms water bodies for the following reasons (Ryan 1991). An increase in turbidity causes a decrease in sunlight penetration which can both decrease temperature and stymie aquatic plant growth, which is problematic since aquatic plants represent the bottom of the food chain and provide habitats to many animals. Recently, over 500 manatees have starved to death in Florida because the increased turbidity of their lagoons has restricted seagrass growth (Anderson 2021). The reduced visibility can inhibit predator's ability to find food as well. Severe sediment concentrations can infiltrate fish gills, making breathing and swimming more difficult. Excess sediment deposition raises channel depths which increase the risk of flooding. It can also alter flow patterns and clog up catch basins and drains. Other pollutants like heavy metals can bond with fine soil particles which then carry them into receiving waters. For construction sites, these pollutants can include hydrocarbons used in fuel and oil, and residual material waste from concrete, paint, and others. Construction runoff contains by far the greatest concentration of sediment pollution as compared to all other sources of nonpoint source pollution, releasing 600,000 tons (544,310 metric tons) of sediment into water bodies in the U.S. each year (EPA 2008) or between 20 and 200 tons per acre, up to 1,000 times greater than undisturbed soil.

Due to the impacts of construction sediment pollution, in 1990 a Clean Water Act (CWA) revision began to require construction sites disturbing five or more acres of land to take substantial measures to reduce erosion and sedimentation pollution stemming from site (Illinois Environmental Protection Agency [EPA] 2002). In 2003, this requirement was increased to include construction sites disturbing more than one acre. The National Pollutant Discharge Elimination System (NPDES), created with the original CWA in 1972, currently requires contractors managing such sites to obtain coverage under the state's Construction General Permit (CGP) through submission of a comprehensive Stormwater Pollution Prevention Plan (SWPPP). The SWPPP is site-specific and must detail all practices used to manage and mitigate sediment pollution from site stormwater runoff. The requirements are even more stringent for construction occurring in or near waters, wetlands, streams, and those waterbodies that have certain total maximum daily loads (TMDLs) or are considered a revered or pristine waterbody. Failure to adequately adhere to the approved SWPPP may result in hefty EPA fines. In fact, in 2008 four homebuilders were fined $4.3 million dollars for CWA violations due to sediment pollution (EPA 2008). Figure 1.1 illustrates some consequences of poor construction erosion control. It depicts scenes from the 7,000-ac (2,833 ha) Chatham Park development in Chatham County, North Carolina after a two-year, 24-hour storm event in February 2020 (River Issues, 2020). Not only did the polluted water ultimately drain into the nearby Haw River, but the incident sparked public outcry and delayed construction by revocation of at least one developer's sediment control permit. Many civil engineering problems have environmental, economic, and social consequences, and construction stormwater is no exception.

(a) Stormwater runoff from Chatham Park, North Carolina

(b) Flooding of the Haw River from Chatham Park

(c) A sediment-laden stream resulting in a $10,000 fine

FIGURE 1.1: Consequences of Construction Site Erosion, Chatham Park, North Carolina (River Issues 2020)

1.2 OBJECTIVES AND OUTLINE OF PROJECT

The following presents an overview of the goals of the project coupled with an outline of how those goals are achieved and documented in this thesis.

1.2.1 Objectives

The primary objective of this research was to assess performance of various erosion control products designed for slope applications in construction using ASTM D6459

Standard Test Method for Determination of Rolled Erosion Control Product (RECP) Performance in Protecting Hillslopes from Rainfall-Induced Erosion. While numerous studies have been performed evaluating erosion control product performance, very few have done so using ASTM standard guidance. The primary motivation of this research was to aid in assessing best practices for reducing slope erosion on construction sites for the Alabama Department of Transportation (ALDOT). The products tested were selected from their Approved Product List (APL). The hope is that through uncovering new information about product performance under different conditions, the project can assist in the adoption of optimal erosion control techniques, aid in NPDES compliance, and reduce pollution in receiving water bodies. The research conducted for this thesis is part of two ongoing projects at the Auburn University - Stormwater Research Facility (formerly the Erosion and Sediment Control Testing Facility), an outdoor research laboratory created in partnership with the Highway Research Center at Auburn University and ALDOT to evaluate products and practices for better stormwater runoff management. The first project, referred to as Phase I and entitled *Evaluation of ALDOT Erosion Control Practices using Rainfall Simulation*, called for testing 14 various erosion control products and practices on an ASTM D6459 rainfall simulator constructed at the facility for that purpose. The second project, referred to as Phase II and entitled *Evaluation of ALDOT Erosion Control Practices using Rainfall Simulation on Various Soil Types and Slope Gradients*, aims to take testing a step further by evaluating two temporary and two permanent erosion control practices/products on three different soil types (clay, loam, and sand), two different slopes (3:1 and 4:1), with and without topsoil and under standard and longevity analysis. Twelve additional ASTM-D6459 rainfall simulators are to be constructed at the AU- Stormwater Research Facility for this purpose. The work conducted for this thesis encompasses the last five products tested under Phase I, includes additional residual testing for polyacrylamide (PAM) that was requested by the project advisory committee at ALDOT, and begins the construction of the twelve additional simulators needed for Phase II.

1.2.2 Research Tasks

To meet the research objectives, the following tasks were performed. Phase I testing was concluded by evaluating five additional products on the ASTM rainfall simulator: ProMatrix™ hydro mulch; jute matting; jute with PAM; jute with gypsum; and EarthGuard™ EDGE™ hydro mulch pellets. Residual PAM detection was performed through spectroscopic analysis of centrifuged runoff samples. Absorbance readings were compared to those of a calibrated solution to estimate PAM concentration. Phase II construction tasks accomplished included soil testing and selection, pump selection, catch basin design, sprinkler assembly, electrical assembly, re-grading, construction of one fully operational plot, construction of five additional plots awaiting water supply, re-stabilization, and preliminary calibration.

1.3 Organization of Thesis

The thesis is organized as follows. Chapter 1 opens with an overview of the importance of proper erosion control at construction sites, laying the groundwork for the relevance of the results of the project. It also includes a background of the *Evaluation of ALDOT Erosion Control Practices using Rainfall Simulation* projects, situating the work of this thesis within Phases I and II and reviewing the precise tasks accomplished. Chapter 2 details five products tested as part of Phase I on the existing ASTM D6459 rainfall simulator. Sections 2.1 - 2.4 discuss Phase I work performed as part of this thesis. They include a brief review of the fields of rainfall simulation and erosion control products, describe the methods and procedures of ASTM D6459, and presents the test results of jute, jute with PAM, jute with gypsum, ProMatrix™ Engineered Fiber Matrix™ hydro mulch and EarthGuard™ EDGE™ pellets. It also describes small-scale gypsum testing to aid in gypsum type selection. Sections 2.5 – 2.8 analyze all Phase I test results including those obtained before this thesis. They present bare soil results complied over all control tests and comments on any deviations. Then, results obtained during this thesis are compared to previous Phase I testing results as well as to manufacturer results. Differences in available methods to obtain C-factor are briefly discussed as well as differences between C-factor and Soil Loss Ratio (SLR). Chapter 3 concerns the residual PAM testing requested by the research advisory committee. It opens with an overview of the functions and impacts of PAM as well as methods used for aqueous detection, then discusses the detection method selected for the study, and finally dives into the results of residual testing including residual testing of an alternate PAM application technique and mulch applications. Chapter 4 summarizes construction of the new rainfall simulators. It begins with a discussion of literature relevant to the project including soil types in Alabama, the interaction of erosivity and soil properties, the interaction of erosivity and slope, and rainfall simulator calibration methods. It also details design information such as hydraulic modeling, describes soil selection data and results, denotes progress made on construction, and presents preliminary calibration data. Lastly, Chapter 5 concludes by recapping tasks and results, presenting some key implications, and suggesting avenues for future work, emphasizing recommendations for Phase II and beyond.

CHAPTER 2: ASTM D6459 RAINFALL SIMULATOR TESTING

2.1 INTRODUCTION

This chapter opens with a brief review prior research related to rainfall simulation. The opening section also summarizes the varieties of erosion control products and how they are typically tested. The chapter then presents the parameters of the ASTM D6459 rainfall simulator and details the procedures used in testing. It then reviews the products tested and the results, including results of supplementary small-scale testing. It contains a comparison of these results to results obtained from prior Phase I testing, specifically comparing C-factors, and a comparison of all bare soil results. It ends with a discussion of various alternative methods used to obtain C-factor.

2.1.1 Rainfall Simulation

Rainfall simulators are used to study hydrologic processes on land or soil including erosion, infiltration, sediment transport, and runoff. They may be used to model land use changes and hydrologic processes, to evaluate the effects of tillage, crop management, or erosion control practices, or to study means of erosion (Ries et. al 2009). Simulators may be unpressurized (drop-forming) or pressurized (nozzle) (Bubenzer 1979, Pall et. al 1983) as illustrated in Figure 2.1. Drop-forming systems rely on gravity to generate drops. In such systems, water accumulation on a surface such as a needle or capillary tube overcomes the surface tension to break free and fall to the testing surface with an initial zero velocity. These simulators produce uniform drop size distributions that tend towards the high range of drop size (0.23 in. [6 mm]) but require a former from a height of greater than 6 ft (2 m) for drops over 0.04 in. (1mm) in diameter to obtain terminal velocity (Boxel 1998). Nozzle style simulators generate a spray by passing pressurized water through the shape features of the nozzle. These simulators are more widely used and can generate a greater variety of rainfall characteristics.

(a) Drip forming rainfall simulator (Naves et. al 2020)

(b) Pressurized nozzle rainfall simulator (Yosuf et. al 2017)

FIGURE 2.1: Types of Rainfall Simulators

The goal in rainfall simulation is for the simulated rainfall to mimic natural rainfall. Thus, the macro-parameters of intensity and uniformity, and the micro-parameters of drop size distribution, mass distribution, velocity, and kinetic energy, should be targeted to imitate natural rainfall as closely as possible (Regmi and Thompson 2000, Elbasit et. al 2015). There is no uniform standard for rainfall simulation design in literature. Rather, durations and intensities are either selected to most closely reflect a geographical area of interest (for example Chouksey et al 2016, Kato et. al 2009), to most closely reflect a possible worst-case scenario (detailed in Dunkerley 2008) or are selected with no rationale given (for example, Paterson et. al 2011). Uniformity and drop size distribution should generally fall within certain targets regardless of duration and intensity. The Christiansen Uniformity Coefficient (CUC), a dimensionless number between 0 and 1 that describes the spatial uniformity of measured rainfall amount, for natural rainfall in southern Australia was measured to be over 0.95 (Kathiravelu et. al 2014) and a study in China found values above 0.99 (Liu et. al 2017) in natural rain. While typical rainfall simulators cannot achieve CUCs in these ranges, it is generally desirable to obtain a CUC above 0.70 (de Sousa Junior et. al 2017) or 0.80 (Lora et. al 2016). For drop size distribution, many natural rains have a D_{50} (size at which 50% of the raindrops have a smaller diameter) between 0.08-0.10 in. (2.0-2.5 mm) (Sousa et. al 2017) with a mean diameter less than 0.06 in. (1.5 mm) (Assouline et. al 1997) and a maximum diameter of 0.28 in. (7.0 mm) (Yakubu et. al 2014). These size parameters typically increase with increasing intensity, as does the corresponding mass and terminal velocity. Kinetic energy, the sum of the energy transferred to the soil surface as a result of raindrop impacts, may then be calculated using the raindrop size and fall velocity (Lassu et. al 2015). Many studies have attempted to determine kinetic energy as a function of storm intensity (Van Dijk et. al 2002, Kathiravelu et. al 2014) and rainfall simulator projects sometimes select one of these proxy relationships to determine kinetic energy from their storm intensity rather than run through a more complex calibration process.

2.1.2 Erosion Control Testing and Products

The National Transportation Product Evaluation Program (NTPEP) is a program of the American Association of State Highway and Transportation Officials (AASHTO) whose purpose is to provide consistent and streamlined evaluation of products and materials used by Departments of Transportation. NTPEP recognizes three classes of accepted ASTM testing related to erosion control (NTPEP 2015). Index tests examine material properties of erosion control products such as specific gravity (ASTM D792), water absorption (ASTM D1117), light penetration (ASTM D6567), tensile strength (ASTM D6818), thickness (ASTM D6525) and mass per unit area (ASTM D6475 and D6566). Bench-scale or small-scale tests are available for slope erosion/runoff (ASTM D7101) using a drip-style rainfall simulator, channel erosion/channel shear (ASTM D7207), and vegetation enhancement for RECPs (ASTM D7322). Finally, two large-scale tests are available: one for slope erosion (ASTM D6459,) utilizing a nozzle-style rainfall simulator, and one for channel erosion (ASTM D6460). NTPEP stresses that bench-scale tests should not be used for design purposes or in conjunction with calculations such as the Revised Universal Soil Loss Equation (RUSLE). Rather, they are best suited for quality control in detecting product variations and for a quick, informal benchmark of product performance. In the same vein, ASTM D7322 *Standard Test Method for Determination of Rolled Erosion Control Product (RECP) Ability to Encourage Seed Germination and Plant Growth Under Bench-Scale Conditions* (ASTM 2013) states that the test method should "not be interpreted as indicative of field performance" and that is it "not intended to replace full-scale simulation or field testing". Thus, in terms of accepted erosion testing standards, the work done at the time of this thesis conforms to the only AASHTO recognized standard for measuring and evaluating slope erosion control products at a design scale, ASTM D6459.

Most erosion control products are applied to cover the surface of disturbed soil, especially on slopes, to protect soil from the kinetic energy of falling rain and thus prevent the soil detachment which starts the erosion process. Erosion control products for slopes typically fall into four broad categories (Tyner et. al 2011): mulches, rolled erosion control products (RECPs), hydraulically applied erosion control products (HECPs), and soil conditioners. Non-product-based practices could include bulldozer tracking or diversion structures, but these are not addressed in this thesis. Figure 2.2 presents photo examples of each product type. Mulches are layers of organic material typically composed of straw or wood chips. Mulches may be installed with a tackifying agent to bond the loose material together or may be crimped to depress them into the ground. RECPs are woven blankets or netting that contain material such as coir, jute, straw, excelsior (i.e., wood shavings), plastic, or other interstitial material. They are rolled out onto the soil surface and installed with pins or staples. RECPs typically fit into one of five types according to the Erosion Control Technology Council (ECTC n.d.) and described in further detail by the South Carolina Department of Transportation (SCOT 2011): Type 1 have ultra-short-term longevity lasting three months or less, Type 2 have longevity lasting up to 12 months and contain a tackifier, Type 3 last up to two years and are considered a stabilized mulch matrix (SMM), products lasting up to three years are considered Type 4 and contain a bonded fiber matrix (BFM), and permanent products with a special engineered fiber matrix (EFM) are considered Type 5. A bonded fiber matrix (BFM) is a specific type of HECP that contains elongated fibers designed to facilitate plant growth and soil bonding. HECPs are also further divided with a letter designation indicating the maximum design slope. HECPs utilize equipment to spray a mixture of water, organic fiber, and bonding agent/tackifier onto the soil surface. The mixture quickly hardens into an absorbent covering as it dries and may be applied with seed or other additives in the wet mix.

Unlike the previous products described, soil conditioners are not intended to protect slopes via absorption of the kinetic energy of water. Rather, they are intended to chemically alter soil properties to make the soil itself more erosion resistant. They may improve infiltration or soil structure and are often used in conjunction with other erosion control practices or products. Compost is a common organic conditioner used because increasing organic matter in soil improves infiltration, strengthen soil structure, and reduces runoff and erosion (Faucette et. al 2005). Synthetic biopolymers such as those composed of lignin, cornstarch, and others (Soo Lee et. al 2013) and biochar (Soo Lee et. al 2015) have also be used. Polyacrylamide (PAM) is a common inorganic conditioner, an absorbent polymer whose acrylamide chains form a protective coating over the soil when wet. Gypsum is another inorganic conditioner, used extensively in agriculture and often combined with PAM (Akbarzadeh et. al 2009), which increases infiltration and helps flocculate fine particles (Miller 1987) and reduce sediment loss (Ben-Hur et. al 1992). Polysaccharides also help reduce runoff and sediment loss (Lu et. al 2018), as does zeolite (He and Huang 2001). Soil conditioners may be applied hydraulically, via a broadcast spreading device, by hand, or mixed with other erosion control products (ECPs).

(a) Mulch (Brian Faulkner)

(b) RECP (Oklahoma State University 2021)

(c) HECP (Mike Perez) (d) Soil conditioner (Gypsoil® 2021)

FIGURE 2.2: Erosion Control Examples

2.2 MEANS AND METHODS

The rainfall simulator used in this project is located at the Auburn University Stormwater Research Facility, formerly the Auburn University Erosion and Sediment Control Testing Facility. The Stormwater Research Facility, seen in Figure 2.3, is a 10-acre outdoor research lab dedicated to erosion and sediment control practice evaluation. The facility was originally constructed in 2009, and in 2020 during the course of this thesis, underwent a 7-acre expansion to accommodate the new rainfall simulators, new channelized testing, and space for future projects. The facility has housed testing on inlet protection practices, ditch check practices, lamella settlers, skimmers, sediment barriers, sediment basin parameters, rainfall simulators, and more. Training and outreach opportunities are held regularly, and the facility also provides independent, third-party product testing.

(a) Training event at original area (Mike Perez) (b) Expansion area during construction (Billur Kazaz)

FIGURE 2.3: Auburn University Stormwater Research Facility

The rainfall simulator used in this section, depicted in Figure 2.4, conforms to ASTM D6459-19 *Standard Test Method for Determination of Rolled Erosion Control Product (RECP) Performance in Protecting Hillslopes from Rainfall-Induced Erosion* (ASTM 2019). It consists of an 8 ft (2.4m) wide by 40 ft (12.2m) long test bed inclined on a 3H:1V slope. The test slope contains 1.5 ft (0.5m) deep loam soil that has been sifted, tilled, graded and compacted to 90% $\pm$ 10% of standard Proctor optimum. The ASTM standard specifies compaction percentage for building the slope, but only specifies to "lightly compact with a turf roller" for rebuilding between tests. Therefore, the compaction range given above was deemed a satisfactory range in absence of other information. The soil contains 48% sand, 41% silt, and 11% clay, with a Plasticity Index of 5. Ten sprinkler risers standing 15 ft (4.6 m) tall and powered by electric solenoid valves supply water at a rate of 2.0 in./hr (5.1 cm/hr), 4.0 in./hr (10.2 cm/hr), or 6.0 in./hr (15.2 cm/hr). Over the course of this thesis the simulator underwent official ASTM certification from the Geosynthetic Institute, consisting of an inspection, document review, and bare soil demonstration, becoming only the second D6459-conforming facility in the nation with third-party ASTM approval.

FIGURE 2.4: Existing ASTM D6459 Rainfall Simulator at the Auburn Stormwater Research Facility (Wes Donald)

2.2.1 Slope Preparation

Prior to conducting a simulated rainfall experiment, the slope undergoes a preparation process. First, the slope is allowed sufficient time to dry after the previous test, returning to approximately optimum moisture content. Then, the slope is hand-tilled with shovels to a depth of at least 4 in. (10 cm) and the clumps raked out and an even grade achieved with stiff rakes. Next, fresh loam soil is added to replenish soil lost through the previous test, and the plot is graded more precisely by screeding with a straight rod as seen in Figure 2.5(a). This replacement soil is sifted in a mechanical sieve with 0.25 in. (0.64 cm) openings prior to placement on the plot. Then, to compact the newly placed soil, a 4 ft (1.2 m) turf roller is rolled up and down the plot using a winch, with three passes on the right side, three passes on the left side, and two passes in the middle. Drive cylinder compaction testing is performed on three locations selected with a random number generator – one from the top third of the plot, one from the middle third, and one from the bottom third. Figure 2.5 depicts some of the process.

(a) Grading the slope

(b) Drive cylinder testing

(c) Roller compaction (Faulkner 2020)

FIGURE 2.5: Slope Preparation Examples

Per ASTM D 2937 *Standard Test Method for Density of Soil in Place by the Drive-Cylinder Method* (ASTM 2010), compaction is determined through the following equations. The wet density is first found using Equation 2.1:

$$p_{wet} = \frac{M_1 - M_2}{Vol} \qquad (2.1)$$

Where M_1 is the mass of the soil and cylinder, M_2 is the mass of the cylinder, and *Vol* is the volume of the cylinder. Dry density is determined through Equation 2.2:

$$p_{dry} = \frac{p_{wet}}{1 - \frac{w}{100}} \qquad (2.2)$$

Where p_{dry} is the dry density and w is the water content, determined through Equation 2.3:

$$w = \frac{M_{dry} - M_{wet}}{M_{dry}} \qquad (2.3)$$

Where M_{wet} is the moist weight of the soil sample and M_{dry} is the same sample after drying in a microwave to a constant weight. With the dry density, unit weight is determined through Equation 2.4:

$$\gamma_{dry} = 62.4 * p_{dry} \qquad (2.4)$$

Provided that γ_{dry} and p_{dry} are in US standard units. Percent compaction is then taken as the fraction of dry unit weight over the maximum dry unit weight as determined through Proctor compaction testing. The max dry density for the loam soil was 96 lb/ft^3 (1,538 kg/m^3).

2.2.2 Testing

The ASTM D6459-19 simulation entails three 20-min. storm events run back-to-back for a total of one hour. The first event constitutes a rainfall intensity of 2.0 in. (5.1 cm) per hour, the second at 4.0 in. (10.2 cm) per hour, and the last at 6.0 in. (15.2 cm) per hour. The water supply for this simulator is a nearby retention pond. There is a brief two- to three-minute pause between events to allow for reading of rain gages. Runoff samples are collected every 3 minutes in an 8-oz (237 mL). Runoff from the 2.0 in./hr (5.1 cm/hr) and 4.0 in./hr (10.2 cm/hr) intensities is funneled separately into holding tanks, and runoff from the 6.0 in./hr intensity is funneled directly into the catch basin at the base of the slope. Wind readings are taken prior to testing with an anemometer, and if greater than 1.0 mph (1.6 km/hr) and less than 5.0 mph (8.0 km/hr), wind curtains are drawn to break any interference. Testing is not performed in wind speeds greater than 5.0 mph. Figure 2.6 illustrates the runoff management process.

(a) Funnel for sample collection

(b) Runoff from each intensity pumped to separate holding tanks

FIGURE 2.6: Testing Procedure Examples

2.2.3 Analysis

After testing, the runoff samples are taken to the lab and analyzed for Total Suspended Solids (TSS) according to *ASTM D5907 Standard Test Method for Filterable Matter (Total Dissolved Solids) and Nonfilterable Matter (Total Suspended Solids) in Water* (ASTM 2013), and turbidity according to *ASTM D7315 Standard Test Method for Determination of Turbidity Above 1 Turbidity Unit (TU) in Static Mode* (ASTM 2017). Because of the high sediment content, 0.8-0.4 oz (25-12.5 mL) of sample may be used for TSS analysis to avoid straining the vacuum pump. A turbidity meter is used to determine turbidity and is re-calibrated before each lab session. To measure sediment loss, runoff in each holding area is kept stationary for at least 24 hours to allow sufficient settling of the sediment. Then the supernatant is carefully pumped from the top, and the sediment scooped out by hand into buckets and weighed. Several moisture samples are taken to determine the moisture content of each strata of settled sediment. Often sediment at the bottom of the tanks contains less water content than the top, so each moisture sample is paired with the appropriate layer for analysis. To isolate the total sediment weight, the moisture content is subtracted out of the total weight of each strata.

The primary objective of ASTM D6459 testing is to ascertain the cover factor, or C-factor, for each product tested. The Revised Universal Soil Loss Equation (RUSLE), described by Renard et. al 1997 and Renard et. al 1991, is employed for this purpose. RUSLE was developed from the Universal Soil Loss Equation (USLE) using improvements in isoerodent mapping technology in the 1980s. The purpose of both equations is to predict soil loss from certain predictive factors. RUSLE is given by Equation 2.5

$$A = R * K * LS * C * P \qquad (2.5)$$

Where *A* is soil loss in tons per acre per year, *R* characterizes the erosive potential of the rainfall in hundreds of foot-ton-inches per acre per hour and is called the rainfall erosivity factor, *K* characterizes the erosive properties of soil in ton-acre-hours per hundred foot-tons per inch and is called the soil erodibility factor, *LS* characterizes the erosive potential of the geography and is called the length-slope factor, *C* characterizes the erosive resistance of ground cover and is called the cover-factor, and *P* characterizes the erosive resistance of land management and is called the practice factor. *LS*, *C*, and *P* are dimensionless. For the purpose of this analysis, *P* is always set equal to 1.

Researchers often use a nomograph described in Renard et. al 1991 to obtain the K-factor. However in this method a new K-factor is determined for each product using its bare soil control. This can help capture changes in moisture or stockpile conditions in real time. To obtain K-factor from a bare soil test, C-factor is set equal to 1 representing no erosion control practice applied to the plot. LS-factor is obtained by selecting from a series of equations based on geometric properties of the study area. For slopes less than 9%, *S* is given by Equation 2.6

$$S = 10.8 sin\theta + 0.03 \qquad (2.6)$$

Where θ is the angle of the slope. And for slopes greater than 9%, *S* is given by Equation 2.7

$$S = 16.8 sin\theta + 0.05 \qquad (2.7)$$

L is calculated using Equation 2.8

$$L = (\frac{\lambda}{72.6})^m \qquad (2.8)$$

Where 72.7 is the standard plot length (feet) used to develop RUSLE, λ is the horizontal projection of the slope length, and *m* is a slope-length exponent calculated using Equation 2.9

$$m = \frac{\beta}{1+\beta} \qquad (2.9)$$

β is a function of slope angle given by Equation 2.10

$$\beta = \frac{\frac{sin\theta}{0.0896}}{3.0(sin\theta)^{0.8} + 0.56} \qquad (2.10)$$

A is calculated from sediment loss in the units given above, and *R* is calculated using Equation 2.11

$$R = EI_{30} \qquad (2.11)$$

Where *E* is the kinetic energy obtained from calibration testing and I_{30} is the maximum 30-minute intensity as prescribed by the ASTM standard. *K* may then be solved for.

The obtained K-factor is used in the RUSLE equation for the subsequent three product tests. When the average A-factor from all product tests is used along with the R-factor obtained through the actual observed rainfall rather than the calibrated rainfall, C-factor may then be solved for. This is the “average” C-factor method. A second method is to plot the C-factor against the measured R-factor for each intensity across each test and, using the resulting trendline, report the C-factor that corresponds to the theoretically optimal R-factor. This is the “regression” C-factor method. In some cases, in previously tested Phase I products, the 2 in./hr results substantially skewed the trendline. In these instances, the 2 in./hr results were simply eliminated from the analysis. All reported overall C-factors in the Results section are taken from the regression method to be consistent with industry reporting (Sprague 2018), although a discussion of the differences is presented later. Any C-factors for individual tests were obtained using the average method, since creating a regression of C-factor against R-factor of all previous results is not possible when analyzing an individual test.

2.2.4 Products and Applications

Five products were tested on the ASTM rainfall simulator as part of the work of this thesis. Jute matting was tested first as a control benchmark for the PAM, which was to be installed in conjunction with the matting. Then, PAM with jute was tested. ProMatrix™ Engineered Fiber Matrix (EFM)™ hydro mulch by Profile Products LLC was also tested. Two additional products approved by the advisory committee remained, both hydro mulches. However, there was substantial difficulty in obtaining them. One manufacturer had supply chain difficulties in getting the product to Alabama, and the other decided to refrain from having the product tested at all. Alternatives of interest were presented to the ALDOT advisory committee, and two innovative products were selected: EarthGuard™ EDGE™ pellets by LSC Environmental Products, LLC™, a hydro mulch in dry, pelletized form that can be applied without water yet intended to provide the same coverage and function of a hydraulically-applied wet mulch; and gypsum, a soil amendment that has been extensively used in agriculture to control erosion but not in construction to date.

2.2.4.1 Jute Matting Product and Installation

The jute matting used was manufactured by L&M Supply Company in Willacoochee, GA and consisted of 70-75% open area, 0.43 in. x 0.71 in. (11mm x 18mm) mesh size, 0.24 in. (6.0 mm) thickness, and 450% absorption capability by weight. Jute was the first erosion control blanket technology available, and theoretically works when the open weave serves as a system of thousands of small check dams, trapping sediment (Theisen 1992). The matting was applied to the bare soil and secured with 6 in. (15.2 cm) sod staples. “Reverse trenching” was used to begin installation at the top of the slope, whereby a 6 in. by 6 in. (15.2 cm by 15.2 cm) trench was created, the matting was placed inside the trench, and then the soil was replaced and compacted. The matting was then overlapped on top of the trench and allowed to continue down the slope. One vertical seam down the middle of the test slope was overlapped 6 in. (15.2 cm) and stapled every 12 in. (30.4 cm). The remainder of the matting was stapled every 12 in. (30.4 cm) at the edges of the plot and once per yard in the field. Details are shown in Figure 2.7.

(a) Reverse trench preparation (b) Overlap in the center of plot

FIGURE 2.7: Jute Installation

2.2.4.2 PAM Product and Installation

For the main three PAM iterations, polyacrylamide was applied directly onto the soil at a rate of 25 lb/acre (28 kg/ha), a rate determined through recommendation from a technical statement from the manufacturer (APS 2002). The PAM product used was Applied Polymer Systems Silt Stop® 715, selected from the 700 series through jar testing performed by the manufacturer with a sample of the loam soil from the plot. The charge of clay particles coupled with surface area and pH of soil all influence ideal product type and dose (Deng 2006). Silt Stop® 715 is a dry, white, granular powder. Jute matting was then applied on top of the soil and secured with 6 in. (15.2 cm) sod staples as an additional erosion control measure, typically recommended with PAM. Then, one additional test was run utilizing an alternative application method. In this method, the jute matting was installed first and then the PAM sprinkled on top rather than on the soil, at the same application rate. This "PAM-on-matting" method was intended to simulate "soft-armoring" installation technique, commonly used in industry, where the polymer intertwines on the mesh openings of the jute to aid the check dams in trapping sediment, rather than acting directly on the soil.

*2.2.4.*3 *ProMatrix™ Engineered Fiber Matrix™*

ProMatrix™ EFM™ is a bonded fiber matrix hydro mulch manufactured by Profile Products LLC. The product contains 77% thermally processed wood fibers, 18% binders (polysaccharides, biopolymers and water absorbents), 2.5% crimped interlocking fibers and 2.5% micropore granules. It was installed at a rate of 3,000 lb/ac (1,361 kg/ha) onto the test plot. The correct application rate was determined by testing different numbers of passes of the sprayer over 2 ft by 4 ft (61 cm by 122 cm) sheets of plywood placed at the same angle as the plot. The product was then scraped of the sheets and weighted. The number of passes selected corresponded to the sheet matching the appropriate application rate. A 300-gal (1,136 L) TurfMaker® 800 mechanical hydro seeder was used for the installation depicted in Figure 2.8. While manufacturer recommendations are to mix 60 lb (27.2 kg) dry mulch per 100 gallons (379 liters) water, a ratio of 150 gal (568 L) was used instead due to prior experience with workability of the TurfMaker®. One 50 lb (22.7 kg) bundle was shredded and agitated for at least 30 minutes per installation. After agitation, the product was sprayed evenly from the opposite direction onto the plot.

FIGURE 2.8: TurfMaker Hydro Seeder

2.2.4.4 Gypsum Product and Installation

The gypsum product selected was calcium sulfate dihydrate, or "agricultural" gypsum, manufactured by USA Gypsum®. The product is a white dry powder of 85% purity at 35 lb/ft^3. The gypsum was applied evenly in dry form directly to the soil at a rate of 4,461 lb/ac (5,000 kg/ha) as commonly encountered in the literature (Miller 1987, Yu et. al 2003). Jute matting was then installed on top of the gypsum, secured at the top of the slope with the reverse trenching technique, and anchored with sod staples at a minimum of one per yard.

2.2.4.5 EarthGuard™ EDGE™ Pellet Product and Installation

EarthGuard™ EDGE™ Pellets are a dry, pelletized form of EarthGuard® Fiber Matrix™ hydro mulch manufactured by LSC Environmental Products, LLC™ (previously manufactured by Terra Novo, Inc.). The product is intended to be utilized in applications where a hydraulically applied mulch product may be desired, but water is scarce or logistics are unfavorable. The pellets are composed of wood fiber with 1% PAM/sodium acrylate soil stabilizer and have 1400% moisture-holding capacity. Figure 2.9 illustrates the product. Pellets were spread by hand directly onto the slope at a rate of 3000 lb/ac (1,361 kg/ha). The product was activated by spraying with a hose until just wet and then allowed to dry before testing commenced.

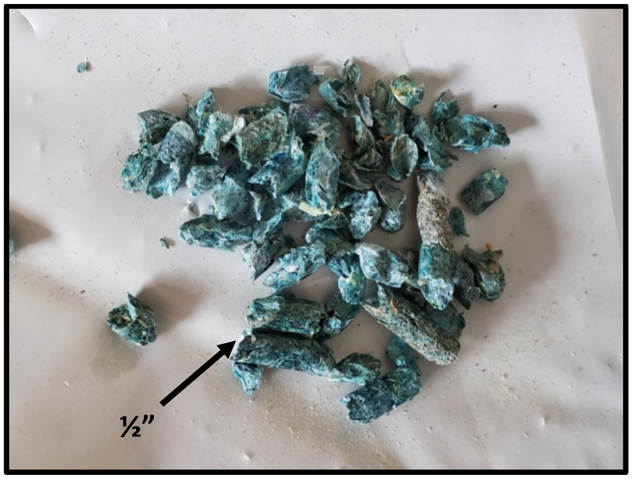

FIGURE 2.9: EarthGuard^{TM} EDGE^{TM} Pellets

2.3 Results and Discussion

Results for each of the five products tested are presented as compared to their bare soil control tests in the following format: general parameters, TSS/turbidity, photo documentation, and RUSLE information. A discussion comparing the results of the soil amendments to their control condition (jute) is included.

2.3.1 Jute Matting Results

Table 2.1 presents basic data from the jute testing, including total rainfall depth, compaction, and soil loss, comparing it to the bare soil control test performed immediately prior to jute testing. Table 2.2 presents the Cover-factor, with the results from each individual tests using the average method reported alongside the “Overall” results obtained through the regression method. Figure 2.10 offers a turbidity, measured in Nephelometric Turbidity Units (NTU), and TSS comparison to the bare soil control, with bare soil represented by the solid line and jute by the dashed line, and Figure 2.11 presents photo documentation. Test 2 demonstrated much higher than normal rainfall because of one outlier gage at the 4 and 6 in./hr. The K-factor was 0.28.

TABLE 2.1: Jute Matting Data Summary

Parameter	Bare Soil	Test 1	Test 2	Test 3
Rainfall Depth, in. (cm)	4.1 (10.4)	3.9 (9.9)	4.6 (11.7)	4.3 (10.9)
Percent Compaction (%)	77.2	88.6	77.0	87.9
Moisture Content (%)	24.4	23.7	22.4	16.3
2 in./hr Soil Loss, lb (kg)	21.6 (9.8)	3.7 (1.7)	2.1 (1.0)	5.3 (2.4)
4 in./hr Soil Loss, lb (kg)	704 (319)	119 (54)	175 (79)	109 (50)
6 in./hr Soil Loss, lb (kg)	1,386 (629)	419 (190)	1,009 (458)	736 (334)

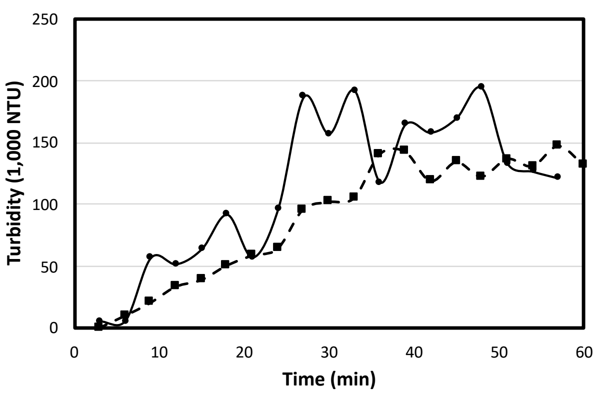

(a) Turbidity

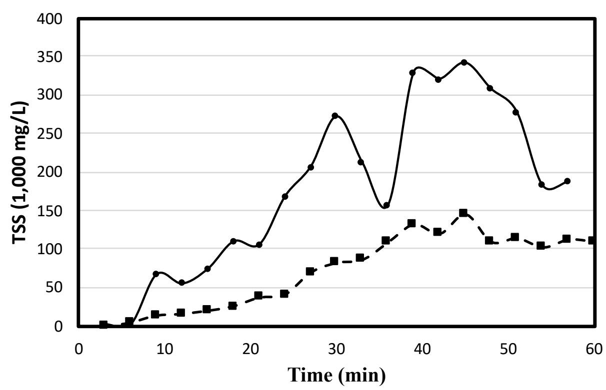

(b) TSS

FIGURE 2.10: Jute Matting Turbidity and TSS Summary

TABLE 2.2: C-Factor Jute Matting

Test 1	0.29
Test 2	0.44
Test 3	0.37
Overall	0.35
Standard Deviation	0.08

(a) Prior to testing (b) Post-testing

FIGURE 2.11: Jute Matting Photos

The jute matting reduced TSS and turbidity in runoff as compared to the control and reduced overall sediment loss. However, the degree was less as with the other rolled erosion control products tested with the rainfall simulator. C-factors were for other RECPs tested were 0.05, 0.14, and 0.12 for Curlex I®, S150®, and ECX-2™, respectively (Faulkner 2020). Rills were observed forming under the matting during testing, while the matting adhered to other portions of the soil appearing to help keep it in place. The jute results provide a benchmark for the PAM and gypsum results.

2.3.2 ProMatrix™ Engineered Fiber Matrix™ Results

ProMatrix™ EFM™ results are presented below. Table 2.3 presents the main results including soil loss results, Table 2.4 presents C-factor information, Figure 2.12 presents a TSS and turbidity comparison, again with the solid line representing the bare soil, and Figure 2.13 presents photos of the plot before and after testing. The K-factor was 0.37.

TABLE 2.3: ProMatrix™ EFM™ Data Summary

Parameter	Bare Soil	Test 1	Test 2	Test 3
Rainfall Depth, in.(cm)	3.7 (9.4)	4.1(10.4)	3.7 (9.4)	3.4 (8.6)
Percent Compaction (%)	83.6	81.7	77.0	80.4
Moisture Content (%)	20.3	19.8	22.4	17.3
2 in./hr Soil Loss, lb (kg)	66.8 (30.3)	0.1 (0.1)	0.0 (0.0)	0.8 (0.4)
4 in./hr Soil Loss, lb(kg)	1,035 (469)	221 (100)	120 (55)	55 (25)
6 in./hr Soil Loss, lb (kg)	1,283 (582)	1,000 (454)	673 (305)	713 (323)

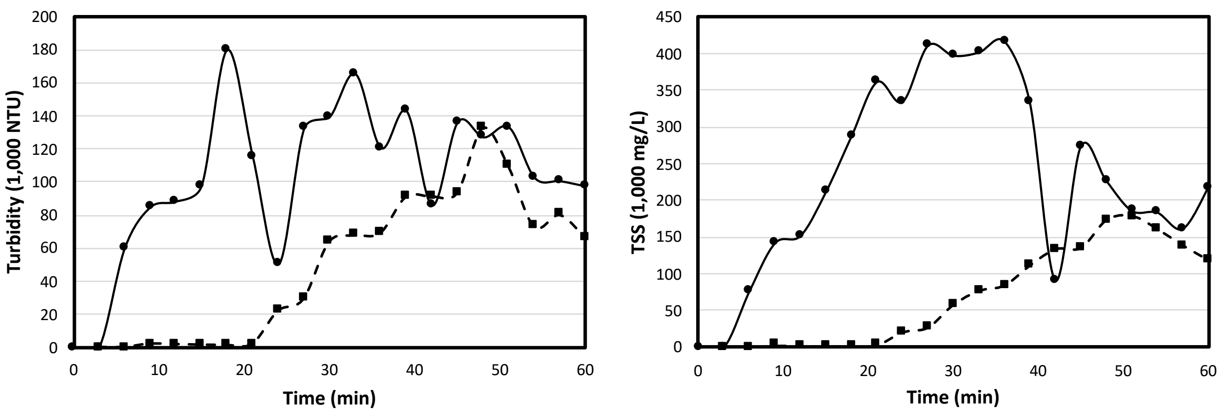

(a) Turbidity (b) TSS

FIGURE 2.12: ProMatrix™ EFM™ Turbidity and TSS Summary

TABLE 2.4: C-Factor ProMatrix™ EFM™ Summary

Test 1	0.41
Test 2	0.32
Test 3	0.36
Overall	0.42
Standard Deviation	0.04

(a) Prior to testing (b) Post-testing

FIGURE 2.13: ProMatrix^{TM} EFM^{TM} Photos

The EFM^{TM} reduced TSS and turbidity as compared to the control, but the effect was greatly reduced or eliminated during the 6 in./hr (15.2 cm/hr) simulation. It can also be seen from Table 2.4 that the magnitude of the soil loss difference decreased in the 6 in./hr (15.2 cm/hr) portion of the test. This is the portion of the simulation where the rills seen in Figure 2.13(b) began to form and the mulch began to detach from the soil in large quantities. The performance of this hydro mulch was comparable but slightly improved over other hydro mulches tested, with a C-factor of 0.42 compared to an average C-factor of 0.51 for all other prior hydro mulches. The failure at 6 in./hr (15.2 cm/hr) was typical of previous mulches tested.

2.3.3 PAM Results

The results shown in Tables 2.5 and 2.6 include results from the fourth trial where PAM was installed utilizing the soft-armoring technique. The photos in Figure 2.15 appear similar to the jute photos in Figure 2.11 because the jute matting is the primary visual feature of the installation – the PAM itself is not visible from an appreciable distance underneath the matting. The PAM tests displayed high variability in measured rainfall. Variability will be discussed later. The K-factor was 0.26.

TABLE 2.5: PAM Data Summary

Parameter	Bare Soil	Test 1	Test 2	Test 3	Test 4
Rainfall Depth, in. (cm)	3.8 (9.7)	4.1 (10.4)	3.6 (9.1)	3.3 (8.4)	4.6 (11.7)
Percent Compaction (%)	80.1	85.2	77.7	77.0	79.2
Moisture Content (%)	14.8	20.5	18.0	22.4	18.3
2 in./hr Soil Loss, lb (kg)	62.7 (28.4)	0.0 (0.0)	0.0 (0.0)	0.0 (0.0)	0.0 (0.0)
4 in./hr Soil Loss, lb (kg)	667 (303)	130 (59)	139	69	121
6 in./hr Soil Loss, lb (kg)	1,022 (464)	1,176 (533)	1,095 (497)	581 (264)	564 (256)

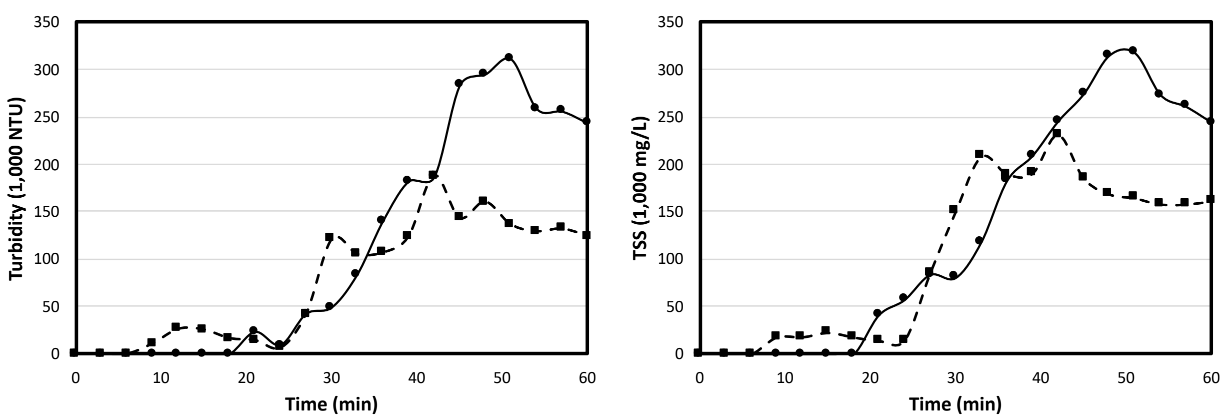

(a) Turbidity (b) TSS

FIGURE 2.14: PAM Turbidity and TSS Summary

TABLE 2.6: C-Factor PAM Summary

Test 1	0.62
Test 2	0.78
Test 3	0.33
Test 4	0.34
Overall (First 3)	0.45
Standard Deviation (All)	0.22

(a) Prior to testing (b) Post-testing

FIGURE 2.15: PAM Test Photos

2.3.4 Gypsum Results

Table 2.7 presents a summary of the basic gypsum data and Table 2.8 presents the C-factor information. Gypsum with jute substantially reduced TSS and turbidity as depicted in Figure 2.16 with the solid line representing the bare soil data and the dashed line representing gypsum. The post-testing photos in Figure 2.17, as compared to those in Figures 2.10 and 2.14, indicate qualitatively improved performance and reduced soil loss. It was noted, as with PAM, that when using soil conditioners, care must be taken between tests to remove at least several inches of soil from the plot before rebuilding. It is possible that gypsum had accumulated in the soil by the third test despite large quantities of soil removal, resulting in improved sediment loss. Gypsum also displayed variability in measured rainfall. The K-factor was 0.24.

TABLE 2.7: Gypsum Data Summary

Parameter	Bare Soil	Test 1	Test 2	Test 3
Rainfall Depth, in. (cm)	4.3 (10.9)	3.4 (8.6)	3.7 (9.4)	4.0 (10.2)
Percent Compaction (%)	79.5	81.5	73.5	90.2
Moisture Content (%)	16.7	16.7	17.1	19.2
2 in./hr Soil Loss, lb (kg)	13.8 (6.3)	1.8 (0.8)	2.0 (0.9)	0.7 (0.3)
4 in./hr Soil Loss, lb (kg)	629 (285)	33.5 (1.4)	10.2 (4.6)	13.7 (6.2)
6 in./hr Soil Loss, lb (kg)	1234 (560)	246 (112)	119 (90)	72 (33)

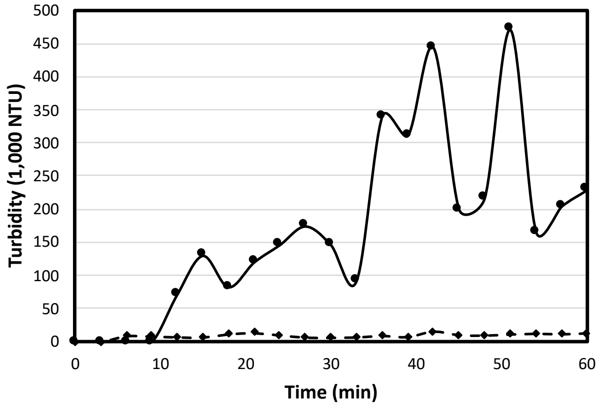

(a) Turbidity

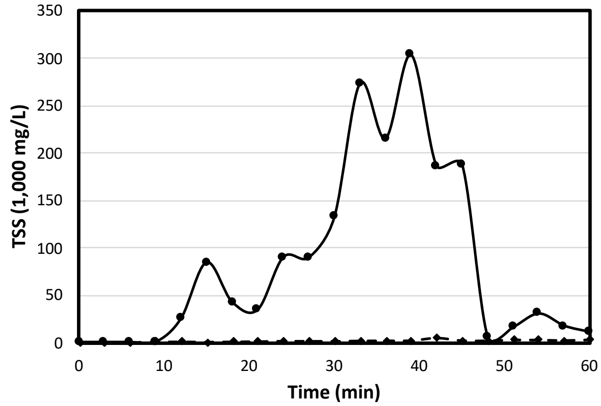

(b) TSS

FIGURE 2.16: Gypsum TSS and Turbidity

TABLE 2.8: C-Factor Gypsum Summary

Test 1	0.23
Test 2	0.08
Test 3	0.05
Overall	0.12
Standard Deviation	0.09

(a) Prior to testing

(b) Post-testing

FIGURE 2.17: Gypsum Test Photos

2.3.5 EarthGuard™ EDGE™ Pellet Results

Table 2.9 presents summary data info for the EarthGuard™ Edge™ pellet testing, Table 2.10 presents C-factor information, Figure 2.18 presents a TSS and turbidity comparison to the bare soil, represented by the solid line, and Figure 2.19 presents before and after photos of testing. The pellets are marketed as a hydro mulch in pelletized form, an easier application method for the same performance as the hydraulically applied mulch of the same name. During the 6 in./hr intensity, the pellets experienced an average of 480 lb (263 kg) of sediment loss, whereas the ProMatrix™ hydro mulch experienced much more loss (786 lb [357kg]) at that intensity. The C-factor demonstrated a modest improvement over the other hydro mulches as well, and Figure 2.16(b) shows fewer catastrophic rills than Figure 2.10(b). It is suspected that, because the fibers are pelletized, that they contain a higher amount of binder than traditional, loose hydro mulches. As per a conversation with an EarthGuard™ sales rep, the binder is also intended to be a soil conditioner, improving soil structure and infiltration and aiding vegetation establishment. Therefore, it is possible that the chemicals in the binder aided in soil retention, even though the coverage area was sparse. The K-factor was 0.24.

TABLE 2.9: EDGE™ Pellets Data Summary

Parameter	Bare Soil	Test 1	Test 2	Test 3
Rainfall Depth, in. (cm)	3.8 (9.7)	3.5 (8.9)	3.9 (9.9)	3.8 (9.7)
Percent Compaction (%)	78.3	91.8	81.7	81.5
Moisture Content (%)	18.7	18.5	17.0	20.7
2 in./hr Soil Loss, lb (kg)	17.6 (8.0)	21.8 (9.9)	9.2 (4.2)	1.2 (0.5)
4 in./hr Soil Loss, lb (kg)	353 (160)	149 (68)	93 (42)	118 (53)
6 in./hr Soil Loss, lb (kg)	1,237 (561)	328 (149)	521 (236)	589 (267)

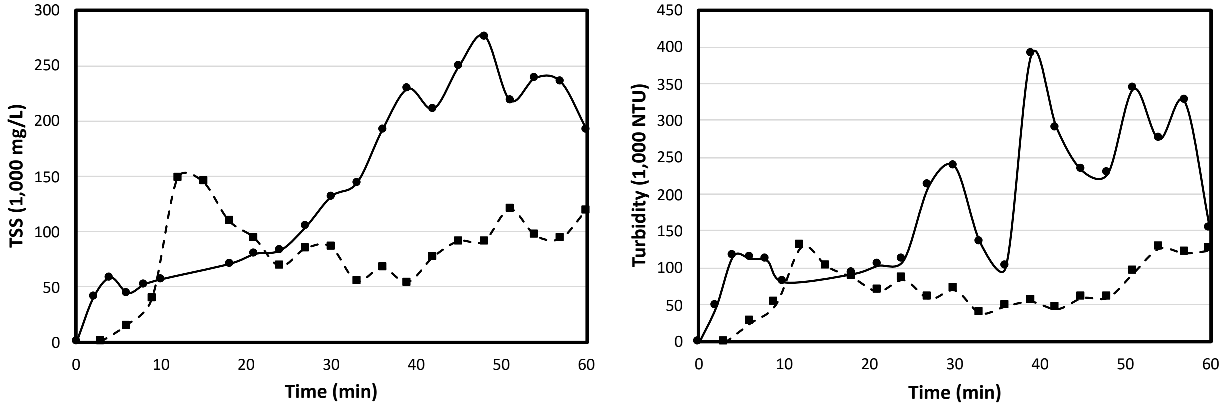

(a) Turbidity (b) TSS

FIGURE 2.18: EDGE^{TM} Pellets TSS and Turbidity

TABLE 2.10: C-Factor Pellets Summary

Test 1	0.38
Test 2	0.38
Test 3	0.45
Overall	0.46
Standard Deviation	0.04

(a) Prior to testing (b) Post-testing

FIGURE 2.19: EDGE^{TM} Pellets Test Photos

2.3.6 Comparison of Soil Amendments

The following section summarizes and compares the soil amendment tests: the jute control, the PAM with jute, and the gypsum with jute. Table 2.11 shows key collected data and Figure 2.20 presents water quality information and a summary of runoff volume.

TABLE 2.11: Comparison Data Summary

Parameter Summary – Average over 3 Tests	Jute	PAM with Jute	PAM Soft-Armoring	Gypsum with Jute
Rainfall Depth, in. (cm)	4.3 (10.9)	3.6 (9.1)	4.6 (11.7)	3.7 (9.4)
Percent Compaction (%)	84.5	80.0	79.2	81.7
Moisture Content (%)	20.8	20.3	18.3	17.7
2 in./hr Soil Loss, lb (kg)	3.7 (1.7)	0.0 (0.0)	0.0 (0.0)	1.5 (0.7)
4 in./hr Soil Loss, lb (kg)	134 (60)	112 (51)	121 (55)	19 (7)
6 in./hr Soil Loss, lb (kg)	721 (327)	951 (431)	564 (256)	145 (66)

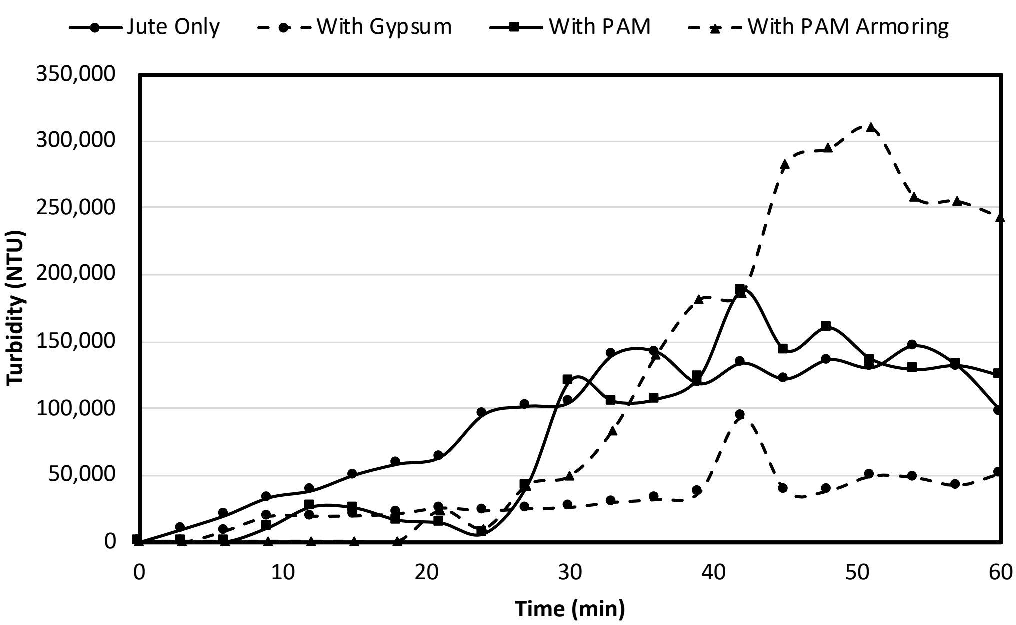

(a) Turbidity Summary

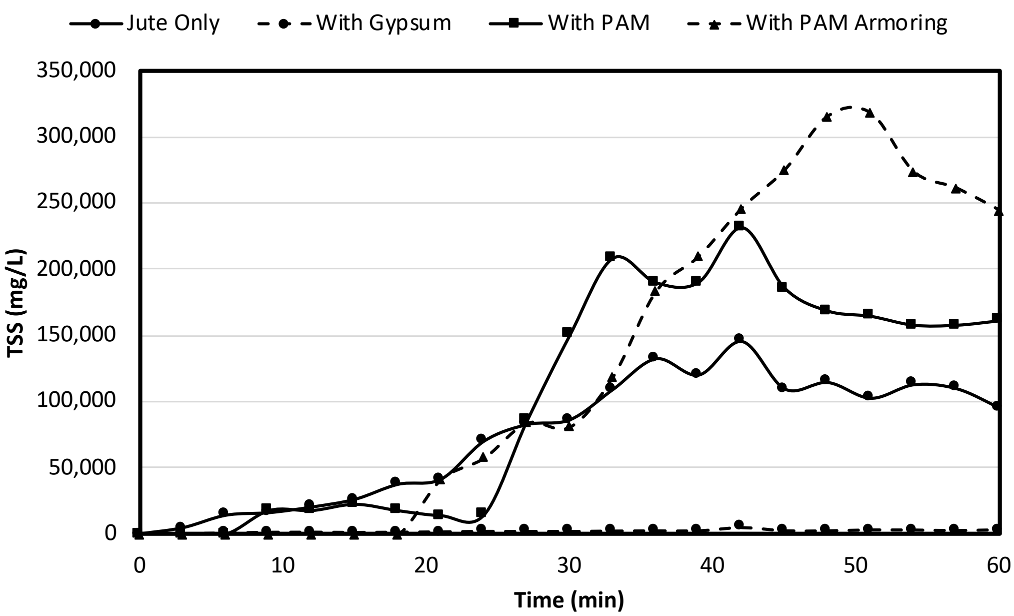

(b) TSS Summary

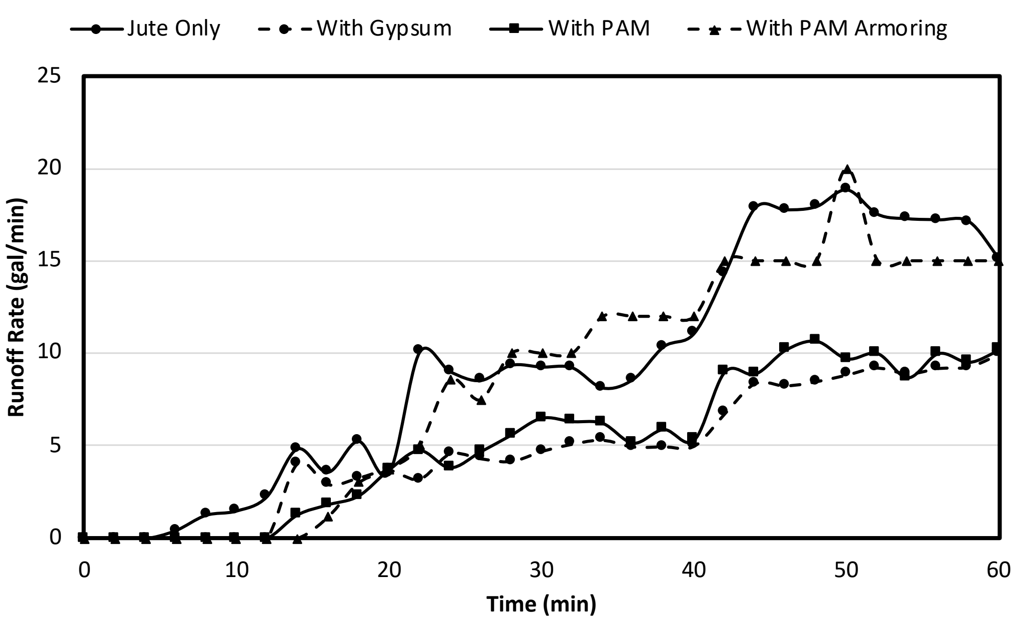

(c) Runoff Volume Summary

FIGURE 2.20: Water Quality and Runoff Comparison, Soil Amendments

Gypsum and PAM both reduced runoff more than the jute throughout the test. Both products are marketed as improving infiltration, and based on the results both products were successful at doing so.

The gypsum demonstrated the best water quality of all three conditions as evidenced by significantly lower turbidity and very significantly lower TSS than jute. The PAM exhibited lower turbidity than jute only during the first half of testing. However, turbidity climbed after about the halfway point and was comparable to the jute for the rest of the test. Similarly, PAM exhibited lower TSS than the jute only during the 2 in./hr (5.1 cm/hr) simulation, but actually exhibited a higher average than the jute only for the remainder of the test. The PAM with soft armoring technique appeared to perform better than the PAM-on-soil from a water quality standpoint for the 2 in./hr (5.1 cm/hr) simulation, but then performed worse than the PAM-on-soil and jute for the 6 in./hr (15.2 cm/hr) simulation. These results suggest that the protection PAM offered at the low intensity gave way quickly when the intensity increased, possibly causing flocculated, heavy soil particles to become dislodged and appear in large quantities in the runoff. The effects were more pronounced when PAM was not applied directly to soil. It is important to note that all PAM water samples demonstrated a high degree of flocculation. However, samples brought back to the lab were agitated just prior to analysis in order to obtain a representative specimen. Settling time of the sediment was not measured. Thus, there may be an important aspect of runoff quality improvement due to PAM, namely, improved settling time of sediment in the runoff, that was not captured in these results.

While PAM had an overall higher C-factor than gypsum, at the 2 in./hr level it reduced sediment loss significantly more than both the control condition and the gypsum, the only product to produce no soil loss whatsoever at that intensity. As PAM becomes wet, the polymer chains unfold and form a protective coating over the soil. Gypsum by contrast simply dissolves into the soil and reacts with the minerals. Thus, while overall PAM performed worse than the gypsum, at the 2 in./hr level it appeared to be performing as intended and prevented substantial sediment loss. It seems that as the soil became oversaturated after the 2 in./hr test, PAM's protective coating failed and it began to exhibit catastrophic soil loss. Soil loss from PAM was so similar to the bare soil condition at these intensities that formal analysis was required to ascertain whether soil loss was statistically significantly different. The *p*-values indicated in Table 2.12 indicate that for these intensities, PAM did not significantly improve sediment loss. Furthermore, the C-factor was greater than the jute alone. While surprising, this is not necessarily unprecedented. Ai-Ping 2011 found that as PAM application rate increased, soil loss and soil concentration in runoff increased as well. Similarly, Babcock and McLaughlin 2013 found that adding PAM to straw increased sediment loss as compared to straw alone. Tumsavas and Kara 2011 found an ideal PAM application rate that was lower than the maximum application rate tested. Ai-Ping posits that the seal formed on the soil led to a decrease in permeability and a corresponding increase in runoff and detachment. They also note that increased water viscosity at the soil surface can increase hydraulic drag and carry away more particles. When PAM's seal is performing properly, it protects soil from these effects. However, if the seal becomes compromised, these effects become active and rapid deterioration can occur. Inadequate contact time prior to wetting may prevent PAM from forming a complete seal, and the PAM in this study had minimal contact time with soil before testing. A conversation with the manufacturer revealed that pre-wetting the soil to activate the polymer would have been advisable, and that using a higher application rate for the design intensity would have also aided in forming a proper seal. McLaughlin et. al 2014 note that steep grades or high rainfall can flush PAM from slopes, and both are used in ASTM D6459. Any of these variables could have compromised PAM's seal and led to its breakdown. It is probable that PAM performs better under different conditions, but the parameters of the D6459 simply reveal the limits of its performance.

TABLE 2.12: Statistical Summary Comparing PAM to Jute

Standard Deviation 4 in./hr (lb)	38
Average Soil Loss 4 in./hr (lb)	112
T-Statistic 4 in./hr	0.00
p-value 4 in./hr	0.50
Standard Deviation 6 in./hr (lb)	300
Average Soil Loss 6 in./hr (lb)	749
T-Statistic 6 in./hr	0.47
p-value 6 in./hr	0.36

2.4 SMALL SCALE GYPSUM TESTING

Gypsum is a soft mineral composed of calcium sulfate, $CaSO_4$, bonded with water. It is used in the agricultural industry as a fertilizer and is a component of many materials such as plaster and drywall. Typically, gypsum is mined but it may also be produced as a by-product of coal power plant production (flue-gas or synthetic gypsum) or a by-product of phosphate fertilizer production (phosphogypsum). Gypsum has been used in agriculture for over two centuries as a fertilizer– it is a source of sulfur and calcium, and the calcium additionally counteracts the toxic action of aluminum on plant roots (Chen and Dick 2011). Gypsum is also relied upon in agriculture to improve soil structure, improve infiltration, and reduce sediment loss through erosion (Fisk 2019). However, gypsum has not been explored much for soil management in the construction industry despite its low cost and wide availability. It was decided as the final product in Phase I to test gypsum with jute as an erosion control product for potential use in construction.

Following the work of Przepiora et. al 1997 who tested gypsum for use in sediment basins, two gypsum products were considered for large-scale ASTM testing. Agricultural gypsum, or calcium sulfate dihydrate, has the formula $CaSO_4*2H_2O$ and is marketed for use in agriculture. Molding plaster, or calcium sulfate hemihydrate, has the formula $CaSO_4*0.5H_2O$ and is marketed for use in materials. A third type of gypsum, phosphogypsum, which is a by-product of phosphorous fertilizer production, was not considered for use due to radioactive pollution concerns (EPA 2021).

2.4.2 Methods

First, a modified jar test was performed to determine which product promoted greater flocculation. Three beakers were filled with 8.45 oz (250 mL) of water and 1.7 oz (50 g) of soil each. This soil-to-water ratio approximated a common soil ratio suggested by average TSS/turbidity found in previous tests. Gypsum was added to two of the beakers at a rate of 0.10 oz (2.8 g) each, and one beaker contained no gypsum. The gypsum dosage was designed to approximate the dosage applied to the plot minus an allowance for some remaining on the plot. After mixing for five minutes, the solutions were allowed to settle. Photos and turbidity measurements were taken after 5, 10, and 20 minutes of settling. Turbidity samples were drawn from the top of the solutions. Three iterations of the test were performed.

Next, two small scale plots were constructed measuring 1.75 ft by 3.75 ft by 3.5 in. (53.3cm by 114.3cm by 7.6 cm). Each plot was hand compacted with three in. of the same loam soil used for large-scale testing. The plots were placed on the large-scale 3:1 slope to mimic the same angle, and they were fitted with a funnel and bin to catch rainfall. A single rain gage was placed near the plots to measure rainfall. One plot was treated with agricultural gypsum and the other with molding plaster. The gypsum was applied by hand at a rate of 2,677 lb/ac (3,000 kg/ha) and then jute matting was placed on top and secured with shortened sod staples. Figure 2.21 illustrates the testing setup. The storm simulation was run for one hour in the same manner prescribed in the ASTM standard and used throughout this thesis. Three iterations of the test were performed.

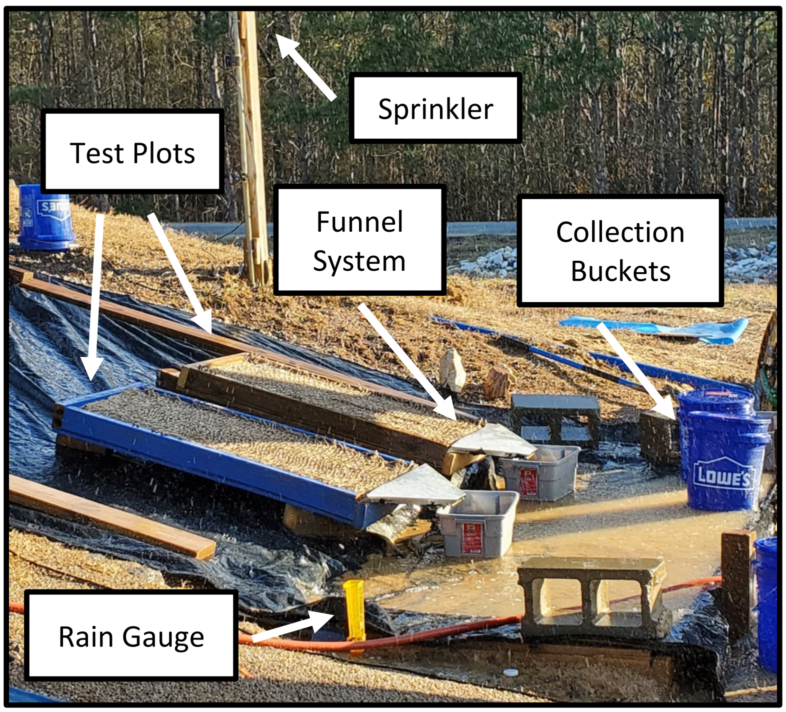

FIGURE 2.21: Small Scale Testing Setup for Gypsum

2.4.3 Results

Results of the modified jar test and small-scale simulation are presented in the following discussion as well as the final product decision.

2.4.3.1 Jar Testing Results

Table 2.13 summarizes the modified jar test results. Notably, the gypsum increased the turbidity as compared to the control, which was the opposite of expected. This could be due to the gypsum itself contributing to more turbidity. In both turbidity and settling time, the agricultural gypsum performed more ideally than the plaster, settling faster and reducing turbidity more. This contradicts the results of Przepiora et. al 1997 who found that the plaster promoted settling more than the agricultural gypsum. The primary difference could be the soil used. The Przepiora used soil with a higher clay concentration than used here, and as with other flocculants, behavior may differ based on soil type.

Table 2.13: Modified Jar Test Turbidity Results

Treatment	Avg. Initial	Avg. 5 min	Avg. 10 min	Avg. 20 min
Control (NTU)	131,563	150	121	51.0
Agricultural (NTU)	138,682	273	152	75.7
Plaster (NTU)	130,467	403	218	119

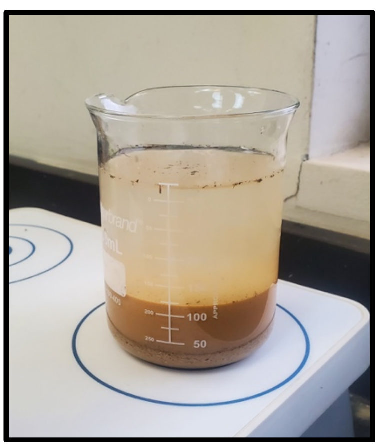

(a) Control 5 min

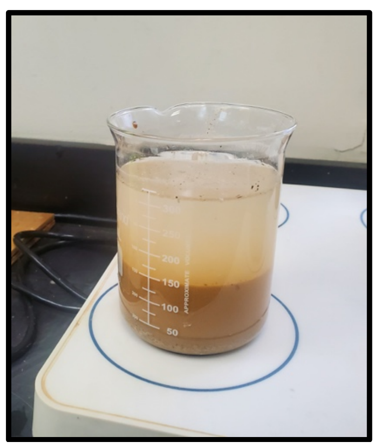

(b) Agricultural 5 min

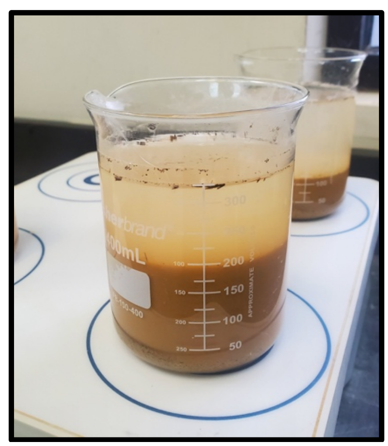

(c) Plaster 5 min

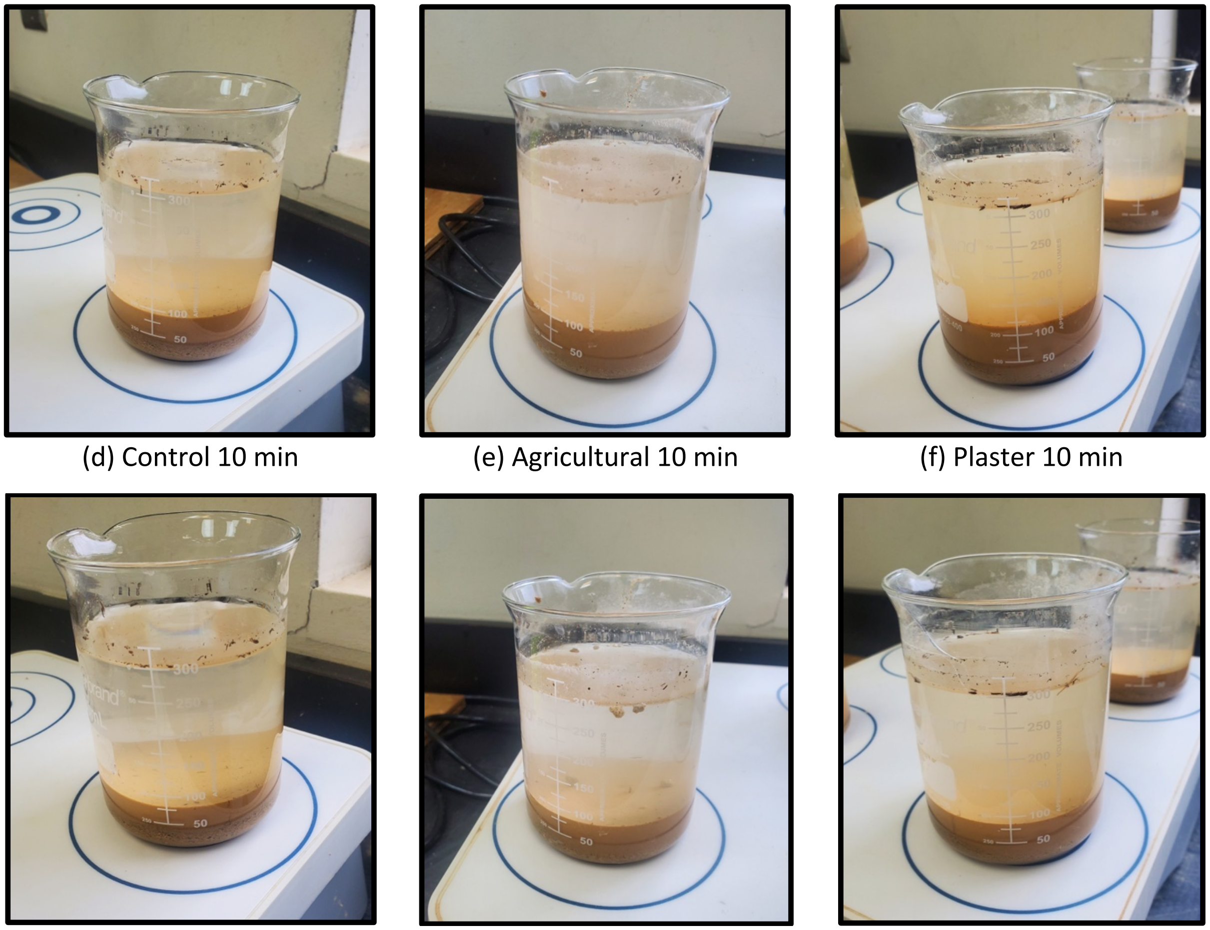

(d) Control 10 min (e) Agricultural 10 min (f) Plaster 10 min

(g) Control 20 min (h) Agricultural 20 min (i) Plaster 20 min

FIGURE 2.22: Modified Jar Test Example Images

2.3.4.2 Small Scale Rainfall Simulation Results

Table 2.14 summarizes the results for the small-scale rainfall simulation for both gypsum products. The agricultural gypsum resulted in less sediment loss, less total runoff, and lower average turbidity and average TSS as depicted in Figure 2.23 than the plaster. Figure 2.24 displays photo documentation during testing. Little change was observed in the appearance of the bench scale simulators during the test. However, while re-dressing the plots between tests it was observed that the soil in the plot treated with agricultural gypsum was noticeably wetter and heavier than the soil in the plot treated with molding plaster, suggesting that the agricultural plot exhibited higher infiltration.

TABLE 2.14: Small Scale Simulator Results, Gypsum

Parameter	Test 1		Test 2		Test 3	
	Ag.	**Plaster**	**Ag.**	**Plaster**	**Ag.**	**Plaster**
Rainfall Depth, in. (cm)	2.9 (7.4)		2.7 (6.9)		3.0 (7.6)	
Total Sediment Loss, oz (kg)	59.0 (1.7)	145.0 (4.1)	139.8 (4.0)	172.6 (4.9)	163.8 (4.6)	166.6 (4.7)
Total Runoff, gal (L)	4.6 (17.4)	7.6 (28.8)	7.2 (27.3)	8.3 (31.4)	8.2 (31.0)	8.5 (32.2)
Average Turbidity 6 in./hr (NTU)	4,936	9,734	6,971	7,320	6,021	6,405
Average TSS 6 in./hr (mg/L)	409	563	390	424	403	464

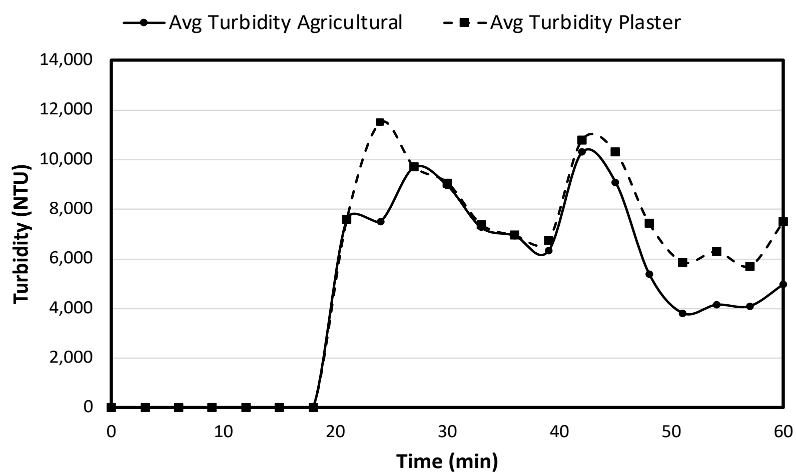

(a) Turbidity Summary

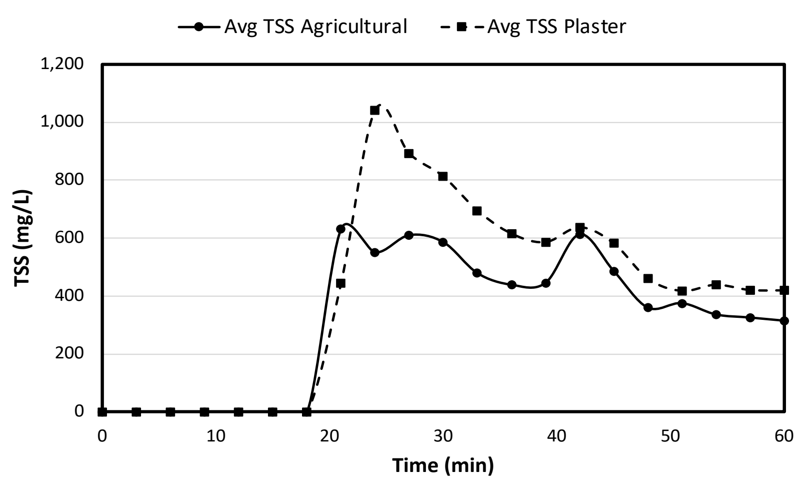

(b) TSS Summary

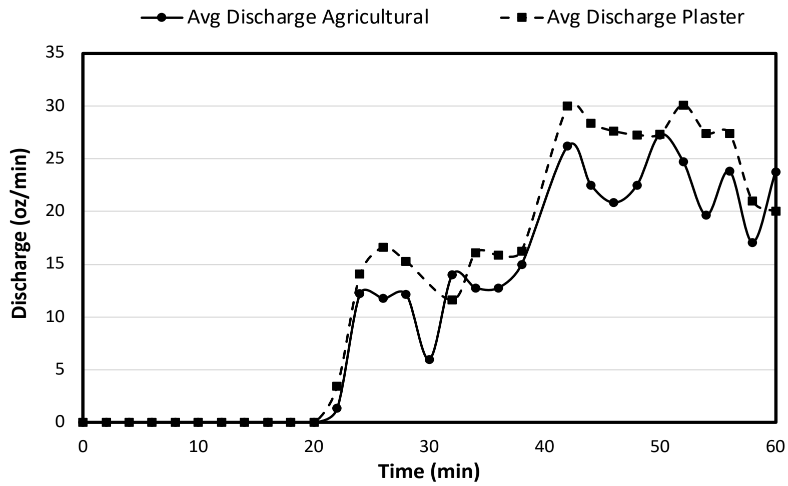

(c) Runoff Volume Summary

FIGURE 2.23: Water Quality and Runoff Comparison, Gypsum Types

(a) Pre-test plot agricultural gypsum

(b) Pre-test plot molding plaster

(c) Post-test plot agricultural gypsum

(d) Post-test plot molding plaster

FIGURE 2.24: Visual Comparison, Bench Scale Gypsum Plots

Because the agricultural gypsum resulted in lower turbidity and faster settling time in the modified jar tests, and less sediment loss, less runoff, and lower turbidity and TSS during the small-scale rainfall simulation than the molding plaster, it was decided to use the agricultural gypsum for in full-scale ASTM D6459 testing as part of Phase I.

2.5 BARE SOIL CONTROL DATA

After Phase I testing was complete, it was desired to review and analyze all results, including those obtained prior to the work of this thesis (Faulkner 2020). The goal was to make full use of Phase I data and to uncover any useful patterns or insights. The first task was compiling and reviewing all bare soil control data. The purpose was to both ascertain the consistency of the control and to possibly offer information that could be used as a proxy for a control in a future informal, quick product test not intended for reporting. Accurate bare soil tests are essential in determining accurate C-factors for products. However they are also highly labor intensive to conduct and may not be worthwhile to run if a test is ever desired that is not intended for a full product evaluation.

For the five bare soil tests performed in this thesis, the average K-factor was found to be 0.27. For the prior six bare soil tests (excluding straw because it was conducted on a slightly different soil type), the average K-factor was 0.28, and the overall standard deviation was 0.05, all indicating consistency in the K-factor. However, sediment loss, turbidity, TSS, and runoff displayed high variation. The standard deviations for sediment loss were up to 25% of the average, for turbidity they were up to 62% of the average, for TSS they were up to 57% of the average, and for runoff they were up to 69% of the average. It is expected to have high variability on a large-scale simulator because the extent of any differences that might occur on a small scale are magnified, so to some extent the standard deviations are not necessarily unanticipated. In addition, these factors are not normalized by the R-factor, which accounts for variability in actual measured rainfall from the design rainfall. This normalization is the reason that K-factor can be very consistent while individual results are much less so. This also illustrates the advantage in using RUSLE to analyze rainfall data – the reported C-factor is accurate despite inevitable variances in individual test conditions. However, if narrower variability in sediment loss, turbidity, TSS, and runoff are desired in the future, factors that may help include effective stockpile management to ensure consistent soil properties, assigning the same undergraduates to perform the same tasks during each test to ensure consistent methods, and possibly narrowing the acceptable window in tolerated deviations compaction and moisture readings before testing. Figure 2.25 presents the box-and-whisker plots.

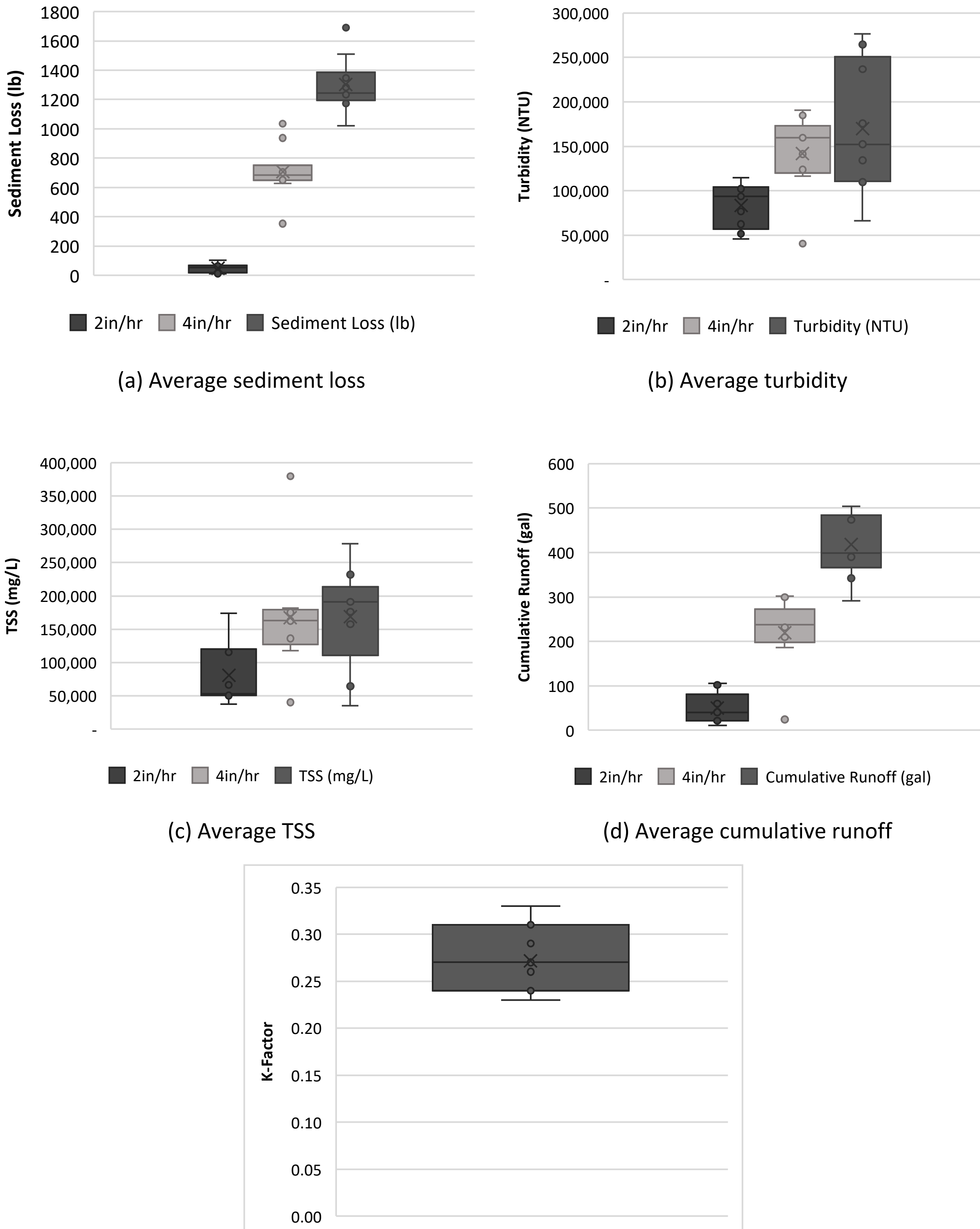

(a) Average sediment loss

(b) Average turbidity

(c) Average TSS

(d) Average cumulative runoff

(e) Average K-factor

FIGURE 2.25: Bare Soil Metrics Distribution

2.6 COMPARISON TO PREVIOUS PHASE I RESULTS

In this section, the five products tested as part of this thesis are compared with the results of 11 previous products tested as part of Phase I. Conclusions are then drawn regarding product comparison. The complete list of products tested as part of Phase I is as follows: loose wheat straw, crimped wheat straw, wheat straw with tackifier, Curlex I® blanket by American Excelsior®, S150® blanket by EroNet™, ECX-2™ blanket by East Coast Erosion Control, Soil Cover with Tack hydro mulch by Profile Products LLC, TerraWood™ with Tacking Agent 3® hydro mulch, EcoFibre™ hydro mulch by Triton Environmental, ProMatrix™ hydro mulch by Profile, EarthGuard™ EDGE™ pellets by Terra Novo, jute, gypsum with jute, and PAM with jute. The straw tests were conducted prior to the full adoption of the ASTM procedure. One difference was the soil type – it was tested on a sandy loam instead of a loam. The other was the data measuring procedure – rainfall and sediment data was only available for the overall test, not for the discretized intensities. This made calculation of C-factors for the intermediate intensities impossible, so only a soil loss ratio (SLR) was found. In the following comparisons of C-factor, therefore, the straw tests were eliminated.

2.6.1 Overall Product Performance at 2 in./hr (5.1 cm/hr)

When all products testing during Phase I, including products tested before the work of this thesis, were compared, it was observed that the C-factors at the 2 in./hr (5.1 cm/hr) were very similar. An ANOVA was performed to determine whether the C-factors at that level indeed statistically differed among the products. Table 2.15 presents the results. As evidenced, at the 95% confidence level, the C-factor at the 2 in./hr (5.1 cm/hr) simulation did not statistically differ among products, with a *p*-value of 0.16. The average C-factor among all products at this level was 0.03. This implies that both the hydro mulches and soil amendments were as effective as the high-end erosion control blankets in protecting the slope from erosion at that intensity. The 2 in./hr (5.1 cm/hr) intensity is approximately the 5-year storm in Auburn, Alabama, the location of testing (NOAA Atlas 14), situated in one of the states which receive the highest precipitation rates in the country. Therefore, under some temporary or low-intensity design circumstances, from purely a performance standpoint, hydro mulches and soil amendments prevented as much sediment loss as erosion control blankets.

TABLE 2.15: ANOVA Overall Results

2 in./hr		**4 in./hr**	
F-stat	1.66	F-stat	14.89
p-value	0.16	*p*-value	$1.37\text{x}10^{-7}$

2.6.2 Hydro Mulch Differences

Performance among products began to differ at the 4 in./hr (10.2 cm/hr) level. An ANOVA for the 4 in./hr (10.2 cm/hr) tests revealed a significant difference between means of C-factors of each product at the 95% confidence level, with a *p*-value of $1.37\text{x}10^{-7}$. To determine where the difference occurred, the hydro mulches were isolated for an ANOVA, and at the 95% confidence level it was found that their C-factors significantly differed from the rest of the products, as seen in the left-hand column of Table 2.16, with a *p*-value of 0.01. However, after eliminating the ProMatrix™ and EarthGuard™ EDGE™ which appeared to have a much lower C-factor than the others, the significance disappeared at the 95% level, with the *p*-value increasing to 0.35. Mulch product performance did not significantly differ at the 6 in./hr (15.2 cm/hr) level for a 95% confidence level either, with a *p*-value of 0.36. Thus, among hydro mulch products were tested ranging from Type 1 through Type 5, the significant performance difference found was the improved performance of the ProMatrix™ which is a Type 4, and the EDGE™ which is a Type 5, at 4 in./hr (10.2 cm/hr), which was to be expected, but these higher-end products did not deliver at the highest intensity.

TABLE 2.16: ANOVA Mulch Results

Mulches 4 in./hr (10.2 cm/hr)		Mulches 4 in./hr (10.2 cm/hr) Without ProMatrix™ and EDGE™		Mulches 6 in./hr (15.2 cm/hr)	
F-stat	6.87	F-stat	5.14	F-stat	2.3
p-value	0.01	p-value	0.35	p-value	0.12

2.6.3 Performance Compared to Published Standards

Table 2.17 lists the maximum allowable C-factor for the product type that the HECP belongs to, taken from the ECTC HECP specs, and the published C-factor from either the manufacturer or the ECTC specs. The average C-factor for each intensity and the total C-factor for the product calculated using the regression method from this testing are presented as well. The values that meet the manufacturer published guidelines are highlighted in italics. As evidenced, four of the five mulches met the manufacturer published data during the 2 in./hr (5.1 cm/hr) simulation, and only two out of five met them overall. While the EDGE™ appeared to fall the shortest of its minimum standard, it tested as the highest performing product during the forceful 6 in./hr (15.2 cm/hr) portion. This is because the qualifications for the Type 5 category are the most stringent and it would have passed if it had been marketed as a Type 2 product. The pellets are included in the HECP analysis because they are marketed as the equivalent product for the traditionally applied hydro mulch of its same name.

TABLE 2.17: HECP C-Factor Comparison

Product Category	Type 1 (Soil Cover)	Type 2 (Eco-Fibre™)	Type 2 (Terra Wood™)	Type 4 (ProMatrix™)	Type 5 (EarthGuard™ EDGE™ Pellets)
Max Allowable C-Factor	0.75	0.50	0.50	0.10	0.02
Published C-Factor	Discontinued	0.55*	0.50*	0.05**	0.01**
Tested C-Factor, 2 in./hr	*0.02*	*0.02*	*0.05*	*0.00*	0.13
Tested C-Factor, 4 in./hr	*0.47*	*0.47*	0.62	0.17	0.29
Tested C-Factor, 6 in./hr	*0.45*	*0.55*	0.54	0.44	0.42
Overall C- Factor using Regression	*0.46*	*0.55*	0.53	0.42	0.46

Note: * = Information from manufacturer ** = Information from ECTC

There is some opacity surrounding testing method in manufacturer data for HECPs. The ECTC language reads "Acceptable large-scale test methods may include ASTM D6459, or other independent testing deemed acceptable by the engineer". One manufacturer indicated that large-scale testing was conducted at Utah Water Research Laboratory (UWRL), who tests on a 4 ft by 20 ft (1.2m by 9.1m) plot containing 12 in. (30.5 cm) matrix of sandy loam soil at varying rainfall intensities and varying tilting slopes at only a 70% of Proctor optimal for one hour (Utah Water Resources). The SCDOT approves the D6459, the Utah State Protocol, which is 5 in./hr (12.7 cm/hr) at a 2.5:1 slope for 60 minutes, or the TTI Protocol, which is a 2:1 slope at 3.5 in./hr (8.9 cm/hr) for 3-30 minute periods, to be substituted for ASTM D6459. While these standards are similar, dimensions of test plot substantially affect results due to the development of erosion patterns permitted by the length, and these are not always specified. The New England Transportation Consortium cites the difficulty of finding ASTM D6459 labs as the reason for not utilizing it to verify products (Long and Demars 2004). The Consortium suggests that, due to the economic infeasibility of constructing and operating large-scale rainfall simulators, the best thing for industry stakeholders is to just utilize whatever lab is most readily available to them, regardless of parameter details.

Tables 2.18 and 2.19 compare the RECP and straw results to industry results. The RECP manufacturer data is taken either from the manufacturer or from the ECTC specs. The maximum C-factor requirements are listed as designated by the product's Type. The Curlex I ® was a Type 2C made of excelsior fiber, the ECX-2™ was a Type 2D made of a double-net excelsior, the S150® Type 3B was made of a double-layer straw, and the jute matting, a heavy, open-weave mat, was not classified. C-factor values which meet the minimum requirements are highlighted in italics. While no products met the requirements overall, the raw magnitude of discrepancy was much smaller than that of some of the HECPs. The published straw data is taken from a comparable study performed at TRI/Environmental in 2013, the other GSI-accredited ASTM D6459 laboratory. The straw data compares SLR rather than C-factor, a comparable metric. The obtained SLRs closely match the TRI 2013 study.

TABLE 2.18: RECP C-Factor Comparison

Product	Curlex I®	ECX-2™	S150®	Jute
Max Allowable C-Factor	0.01	0.05	0.10	N/A
Published C-Factor	0.018**	0.04**	0.118*	N/A
Tested C-Factor, 2 in./hr	*0.02*	*0.03*	*0.05*	0.02
Tested C-Factor, 4 in./hr	0.04	0.10	*0.11*	0.19
Tested C-Factor, 6 in./hr	0.05	0.12	0.14	0.37
Overall C- Factor using RUSLE	0.05	0.12	0.14	0.35

Note: * = Information from manufacturer ** = Information from ECTC

TABLE 2.19: Straw Soil Loss Ratio Comparison

Product Type	Loose Straw	Straw with Tack	Crimped Straw
Published C-Factor	0.06-.0.20*	0.17**	0.34**
Tested Soil Loss Ratio	0.21	0.14	0.26

Note: * = Information from Virginia Transportation Research Council
** = Information from TRI/Environmental

2.6.4 Soil Amendment Performance

Since PAM and gypsum have no published C-factor that could be identified, and are less commonly used products, it was desired to compare their performance to the more popularly categorized ECPs. Based on visual inspection of the data, the PAM and hydro mulches displayed similar C-factors to each other, and the gypsum and RECPs (excluding jute) displayed similar C-factors to each other. A simple two-tailed T-test was performed to determine any differences between the means at the 4 in./hr (10.2 cm/hr) and 6 in./hr (15.2 cm/hr) iterations, since at the 2 in./hr (5.1 cm/hr) iteration all products had already been shown to be identical. For the PAM and hydro mulches, the *p*-value tested as significant at the 95% significance level as seen in Table 2.20. The difference disappeared at the 6 in./hr (15.2 cm/hr) level. Thus, PAM performed better than hydro mulches at 4 in./hr (10.2 cm/hr) with a C-factor of 0.20 versus 0.40. For the gypsum and RECP comparison presented in Table 2.21, neither T-test yielded significant results at the 95% level, indicating that gypsum with jute performed comparably from an erosion control standpoint to standard erosion control blankets.

TABLE 2.20: PAM vs. Mulch T-Test Results

4 in./hr (10.2 cm/hr)		6 in./hr (15.2 cm/hr)	
T-stat	2.08	T-stat	-0.50
p-value	0.05	*p*-value	0.62

TABLE 2.21: PAM vs. Mulch T-Test Results

4 in./hr (10.2 cm/hr)		6 in./hr (15.2 cm/hr)	
T-stat	-1.68	T-stat	0.23
p-value	0.12	*p*-value	0.82

2.6.5 Cover Factor and SLR

Cover factor and soil loss ratio (SLR) are often used interchangeably in rainfall simulation. The SLR is calculated as the proportion of soil loss from a treatment condition to soil loss at a control condition. Often, the soil loss ratio is the only parameter reported. The C-factor is different in that it incorporates the soil loss ratio plus more information about environmental conditions into its reflection of how the described practice impacts soil loss, as described in Equation 2.5. Using the C-factor rather than the SLR for reporting rainfall simulation results has the added benefit of being weighted by the observed rainfall amount on each test, ameliorating the effect of variability in rainfall on deviations in performance. C-factor is also weighted by the simulator geometry (LS-factor) and the soil conditions (K-factor). Thus while C-factor did change with storm intensity based on the erosion control product's interactions with the test environment, it can theoretically be interpreted as being more broadly applicable to more situations than SLR. Table 2.22 presents comparisons of the average SLR in each test to the overall C-Factor as determined with the regression method. If the values differed, a simple two-tailed T-Test was performed between the SLRs for each individual test and the C-factors for each individual test, to determine whether the means were the same. The list of *p*-values for these cases confirms that none were low enough to conclude that the means differed at the 95% level. While some pairs of means appear very different, such as the jute, the small *n* for each category (*n* = 3 for all except for PAM with *n* = 4) and the variability still rendered the difference non-significant. Thus, in this analysis, SLR and C-factor can be said to describe soil loss performance in a comparable manner, and additionally, the SLR from the straw may be compared to the C-factors obtained for the other products with more confidence.

Table 2.22: SLR vs. C-Factor

Products	SLR	C-Factor	p-value
Straws			
Loose Straw	0.21	N/A	N/A
Crimped Straw	0.26	N/A	N/A
Straw with Tack	0.14	N/A	N/A
RECPS			
Curlex I®	0.05	0.05	——
ECX-2™	0.12	0.12	----
S150®	0.14	0.14	----
Jute	0.41	0.35	0.70
HECPs			
Soil Cover	0.49	0.46	0.54
Eco-Fibre™	0.55	0.55	----
TerraWood™	0.55	0.54	0.59
ProMatrix™	0.39	0.38	0.83
EDGE™ Pellets	0.38	0.38	----
Soil Amendments			
PAM + Jute	0.55	0.45	0.81
Gypsum + Jute	0.09	0.12	0.76

2.7 DIFFERENCES IN METHODS FOR CALCULATING C-FACTOR

The average method and the regression method for calculating C-factor can produce slightly different results. In addition, results can vary with which R-factor input is used. In this report the theoretically optimal R-factor obtained in calibration testing of 182.02 is used for the regression method in calculating overall C-factor. The actual measured R-factor for the test is used in the average method in calculating C-factor for each individual intensity. This measured R-factor does not exactly align with the theoretical R-factor due to variations in measured rainfall in each test. Therefore, either R-factor could be used with either method. According to

Sprague 2018, who uses ASTM D6459 at TRI Environmental, Inc. to evaluate erosion control products using the regression method, the advantage to using the theoretical R-factor in the regression method is that it allows inter-product comparison at the same point in the storm event. Therefore, for the regression method, reporting the C-factor at the same point each time (R=182.02) does indeed yield the best benchmark for comparison. For the average method, measured average soil loss is used for the A-factor in the RUSLE equation and this can vary with measured rainfall. Therefore, since measured soil loss depends on testing conditions, A-factor should be paired with the actual observed testing conditions, or actual observed R-factor, when calculating results. Table 2.23 presents C-factors as obtained from different methods. It includes a column that describes the C-factor as a result of averaging the C-factors of the individual tests. This is a slightly different method than taking the overall global average, although as evidenced and as expected it yields very similar results with the exception of PAM. Differences that arose between the average method using the theoretical versus measured R-factor are due to differences between these metrics. Differences that arose between R-factor inputs within the same method illustrate the importance of using the most applicable one. In each case where the average and regression methods differed, with the exception of PAM, the average method using the measured R-factor was closer to the regression method than the average method using the theoretical R-factor, confirming that measured R is preferable to use in this case. In fact, this is the technique used in calculating C-factor for the individual tests. In the two products which displayed the greatest differences, that is the ProMatrix^{TM} and EDGE^{TM}, the differences were likely due to having one outliers on reported rainfall. The presence of outlier was confirmed by comparing the data point to the first quartile of all rainfall measurements in this thesis. On occasions with very low measured rainfall, the flexible hose that delivered water from the pump to the simulators was replaced with a new line which increased pressure to the system and alleviated subsequent low measurements.

Since C-factor varied with intensity, the C-factor as reported from the regression method is likely a more desirable indicator of product performance than the C-factor as reported from the average method. In fact, the regression method already makes use of the average method because it relies on the averages of each individual test to build its model. It therefore already incorporates all averages obtained in the three product tests. It furthermore benchmarks to the theoretical R-factor, which as already stated compensates for differences that occurred between design and measured rainfall. By contrast, the C-factor as obtained from the average method is the more correct indicator of product performance on that particular series of tests. The inconsistency in all PAM results in Table 2.23 is almost certainly due to unreliability in performance between tests– test 2 had a 6 in./hr C-factor of 0.78, much higher than the minimum test of 0.33. The problems with PAM testing have been discussed previously. It is also possible that some residual PAM was left on the test plot which reduced the final C-factor reading, although the amount would have been marginal.

TABLE 2.23: C-Factor Method Comparison with Different R-Factors

Products	Average Method, Theoretical R	Average Method, Measured R	Average of Individual Tests Method	Regression Method, Theoretical R	Regression Method, Measured R
Soil Amendments					
PAM with Jute	0.49	0.51	0.57	0.45	0.43
Gypsum with Jute	0.09	0.10	0.12	0.12	0.12
RECPS					
Curlex I®	0.05	0.05	0.05	0.05	0.06
ECX-2™	0.12	0.12	0.12	0.12	0.12
S150®	0.14	0.14	0.14	0.14	0.15
Jute	0.41	0.37	0.37	0.35	0.39
HECPs					
Soil Cover	0.46	0.45	0.45	0.45	0.45
Eco-Fibre™	0.55	0.55	0.55	0.56	0.56
TerraWood™	0.54	0.54	0.54	0.53	0.53
ProMatrix™	0.33	0.37	0.37	0.42	0.36
EDGE™ Pellets	0.33	0.40	0.40	0.42	0.42

2.8 CONCLUSION

This chapter reviews the work done as part of Phase I testing. It includes an overview of the ASTM D6459 method used at the Stormwater Research Facility and an overview of the products used and their installation. It also includes an overview of the small-scale gypsum testing performed to aid in product selection. It compiled bare soil data to determine any consistencies or inconsistencies. It was found that while the K-factor was very consistent, sediment loss, turbidity, TSS, and runoff varied considerably, likely due to not being tied to a normalized R-factor. The chapter also includes a comparison of these results' C-factors to C-factors obtained during all previous Phase I testing (Faulkner 2020) in order to draw conclusions about how overall product types performed in comparison with one another, and how products within the same product type performed as compared with one another. Results suggest that jute matting performed worse than other RECPs, that PAM as applied in this study prevented significant sediment loss at 2 in./hr but then began to fail in a statistically identical fashion to the hydro mulches, that gypsum as applied in this study performed similarly to the RECPs (excluding jute), that the EDGE™ pellets performed well even though the coverage area appeared less than that of traditional HECPs and that the Type 4 and 5 hydro mulches improved sediment loss at 4 in./hr but all hydro mulches failed at 6 in./hr. Finally, the chapter compares C-factor calculation methods including the use of the two R-factors and concluded that the C-factor as reported with the regression method is the best indicator of product performance as compared to other ASTM D6459 tests, but that the C-factor as calculated with the average method is the best indicator of product performance as obtained on that particular test.

CHAPTER 3: PAM RESIDUAL TESTING

3.1 INTRODUCTION

This chapter presents the detection method and results for residual PAM analysis in runoff from the ASTM D6459 simulator. The following introductory section reviews relevant literature to aqueous detection of PAM in construction stormwater. It details PAM's interaction with soil, discusses its potential impacts on the environment, and surveys residual detection methods available.

3.1.1 Effects on Soil and Environment

PAM carries many benefits related to soil stabilization and erosion control. It was first used in agriculture in the USA, where it was shown to reduce soil loss and increase infiltration (Lentz 2015, Trout et. al 1995, Peterson et. al 2007). PAM also acts as a flocculant when added upstream of sediment basins, reducing turbidity by up to 88% (Trout et. al 1995) and total suspended solids (TSS) by up to 75% (Peterson et. al 2007). As a flocculant, PAM bonds with the slightly charged fine clay fraction of soil (McLaughlin et. al 2007) which increases these small particles' weight and stability (Flangan et. al 2003) and therefore settleability. As a soil amendment, the slightly charged PAM molecule increases hydraulic conductivity as well as infiltration (Xiong et. al 2018), resulting in decreased runoff. The polymer chains unfold when wet forming a protective seal on the soil. In addition, PAM contributes to coarse aggregate stability when it penetrates into void spaces, increasing mean weight diameter of the coarse fraction thereby increasing stability (Levy and Miller 1999).

While PAM has numerous benefits, excessive quantities in runoff may be undesirable. PAM is demonstrated to be very safe for aquatic life, such as minnows, trout, and mussels

(Herth et. al 2015, Seybold 1994, Buczek et. al 2017). Toxicity does vary by product and exposure time however, with LC_{50}, or concentration resulting in 50% fatality of the sample, was as low as 14.1 mg/L for a 96-hr exposure to water fleas (Biem and Biem 1994). Even with a high LC_{50} typical with most organisms such as over 1,000 mg/L, the metric fails to capture any health effects on the sample, nor does it account for concentrations with death rates lower than 50%. A principal concern for any flocculant application is the effect on water viscosity. For PAM, viscosity noticeably increases at concentrations starting at 50 mg/L, which can pose a challenge to small aquatic life. PAM may also flocculate food sources and reduce the density of algae species (Weston 2009). It degrades at a rate of 10% per year in soil (Entry et. al 2002) due mostly to ultraviolet exposure, and degradation can lead to more of the release of monomer amide (AMD), the toxic component which does not adsorb (Guezennec et. al 2015), than was originally present (Xiong et. al 2015). Finally, heavy metal ions such as Chromium (IV) have been demonstrated to adsorb to PAM molecules. While this benefits downstream water quality, it also leads to possible accumulation of heavy metal pollution in soil (Wisniewska et. al 2018). PAM has also been shown to absorb organic pollutants from animal-based agriculture such as coliform (Sojka and Entry 2000), again benefitting downstream water quality but having an unknown effect on soil. Thus, while PAM is typically safe and has multiple environmental benefits, very high or prolonged doses in runoff should generally be avoided. Therefore, it is important to ensure that PAM concentrations in stormwater runoff leaving construction sites are low, which require methods for testing PAM residuals.

3.1.2 Residual Detection

The best detection method for aqueous PAM depends upon the application scenario and especially upon possible interference sources. Table 3.1 summarizes the primary detection methods and their suitability for construction stormwater. Most were developed for the wastewater treatment industry. Detection methods fall into four broad categories: (1) chemical (N-Bromination), (2) physical (viscosity measurement, flocculation), (3) chemical-physical (polarography), and (4) special methods (such as radioactive tagging). The turbidimetric method (Kang et. al 2014) was developed specifically for detection at construction sites, but it yielded inconsistent results when attempted for this study due to probable interference from the retention pond source water. This method detects concentration in soil samples by diluting them with deionized water, centrifuging, dosing with Hyamine, and reading the turbidity of the supernatant. The samples obtained in this study are already a combination of soil and water from the retention pond which has much different properties than deionized water, including conductivity and organic matter content. The impurities are thought to interact with the Hyamine, rendering results invalid. Indeed, the sediment and water impurities were the primary challenge in finding a suitable detection method.

TABLE 3.1: Detection Methods and Construction Suitability

Method	Procedure Overview	Suitability for Construction Stormwater?
Radioactive Tagging (Lu and Wu 2003)	PAM is labeled with C-14 or Tritium	Small scale detection and sensitive to tagging unwanted material
Total Organic Carbon (TOC) (Lu and Wu 2003)	Very popular method where PAM is analyzed as carbon. It is decomposed and then measured as TOC	Inappropriate for any amount of organic matter (OM) or inorganic carbon ions
Colloid Titration (Mocchiutti and Zaruttini 2007)	Titrate with a cationic indicator such as Polydiallyldimethylammonium using a color indicator and/or spectrometry	Good candidate
Turbidimetric (Kang et. al 2014)	Change in turbidity (NTU) before and after reaction with a suspension agent correlates with dosage	Possibly subject to OM interference
Flocculation Measurement (Lu and Wu 2003)	Measure speed of settling flocs by transmittance change	Subject to OM interference
Viscosity Measurement (Jung et. al 2016)	Surface tension angle and viscosity (using a Brookfield viscometer) correlate to dosage	Small scale samples are taken and highly sensitive
Size Exclusion Chromatography (SEC)(Lu et. al 2003)	Polymer gel column filters PAM from interferences	Good candidate
Spectrometry (Momami and Ormeci 2014)	Absorbance or emittance spectra correlated with dosage	Selected for use
Amide Hydrolysis with Ammonia Detection (Lu and Wu 2003)	Hydrolysis releases ammonia from the PAM chain and is detected by a number of methods	Prohibitive equipment and expertise for application. Subject to OM interference
N-Bromination (Lu and Wu 2003)	A unique method using a series of reaction with bromine to create a starch that is passed through spectrometer	Subject to OM interference. Prohibitive equipment for application
Polarography (Betso and McLean 1976)	Current response vs. voltage are obtained at different PAM doses	Prohibitive materials and equipment for application

When looking specifically at construction and rainfall simulators, only a few small-scale, low-intensity projects have attempted to detect concentrations of PAM in runoff. A study by McLaughlin et. al 2014 used 3.3 ft by 1.6 ft (100cm by 50 cm) plots at 5% slope and a rainfall intensity of 3.3 in./hr) (8.3 cm/hr) in conjunction with ultra-high performing erosion control blankets and found runoff concentrations on the order of 6-17 mg/L, although it is unclear whether this was measured in the runoff or in the captured sediment. Sadeghi et. al 2016 used plots of 5.4 ft^2 (0.5 m^2) at a 20% slope and a rainfall intensity of 2.8 in./hr (7.2 cm/hr) and found concentrations around 10 mg/L, using a spectroscopic method similar to the one used in this study.

3.2 MEANS AND METHODS

PAM was applied to the ASTM D6459 slope with jute matting at a rate of 25 lb/ac (28 kg/ha) as advised in a manufacturer statement (APS 2002) and tested in accordance with ASTM D6459 procedures. The same 8 oz. (0.23 L) runoff samples used for TSS/turbidity were also analyzed for residual concentration. Later, samples from the ProMatrix™ hydromulch and the EarthGuard™ EDGE™ pellets were analyzed for residual concentration.

3.2.1 Residual Analysis

This study aimed to select a detection method based on four main criteria: (1) free from organic matter interference, (2) robust to high sediment concentrations, (3) displaying a high upper detection limit, and (4) accessible for others in the construction industry. The concern over organic matter interference was due to the fact that the source water for testing was a small retention pond containing algae and other aquatic life. The concern over sediment concentrations stemmed from the fact that the runoff samples from the ASTM D6459 simulator typically contain high amounts of soil and the soil must not interfere with measuring methods. The concern over detection limit was that some methods are highly sensitive and can only detect very small concentrations, which may not be adequate for the quantities anticipated. Lastly, the concern over accessibility was that the method be replicable to other site conditions such as varying soils and water sources so that others may easily adapt it for further construction research.

The spectroscopic method following Momami and Ormeci 2004 was selected for use as the detection method in this study. This method fulfills the stated research objectives: (1) it is not sensitive to organics, (2) sediment interference can be eliminated through centrifuging, (3) it can detect higher concentrations if needed, and (4) it may be adapted to varying site conditions such as different soil types, sediment concentrations, or water properties. In this method, solutions of PAM at known concentrations were passed through a UV-Visible spectrum spectrometer and absorbance was measured from 200 nm to 750 nm, the breadth of the ultraviolet and visible spectrum. A regression relationship was then established between PAM concentration and absorbance at 200 nm from these calibration samples. The 200 nm was specifically selected for comparison because it represented the greatest magnitude of difference between samples as per the example of Momami and Ormeci. The concentration from an unknown sample could then be estimated from its measured absorbance using the regression relationship. Calibration samples were prepared with source water and PAM at concentrations of 120, 90, 60, 40, 20, and 0 mg/L. Absorbance at 200 nm was plotted and a linear relationship obtained with an R^2 value of 0.99. Figure 3.1 illustrates absorbance curves at these values and also plots absorbance vs. concentration at 200 nm. The regression equation obtained from Figure 3.1 was used to estimate concentration of test samples by using measured absorbance and solving for concentration.

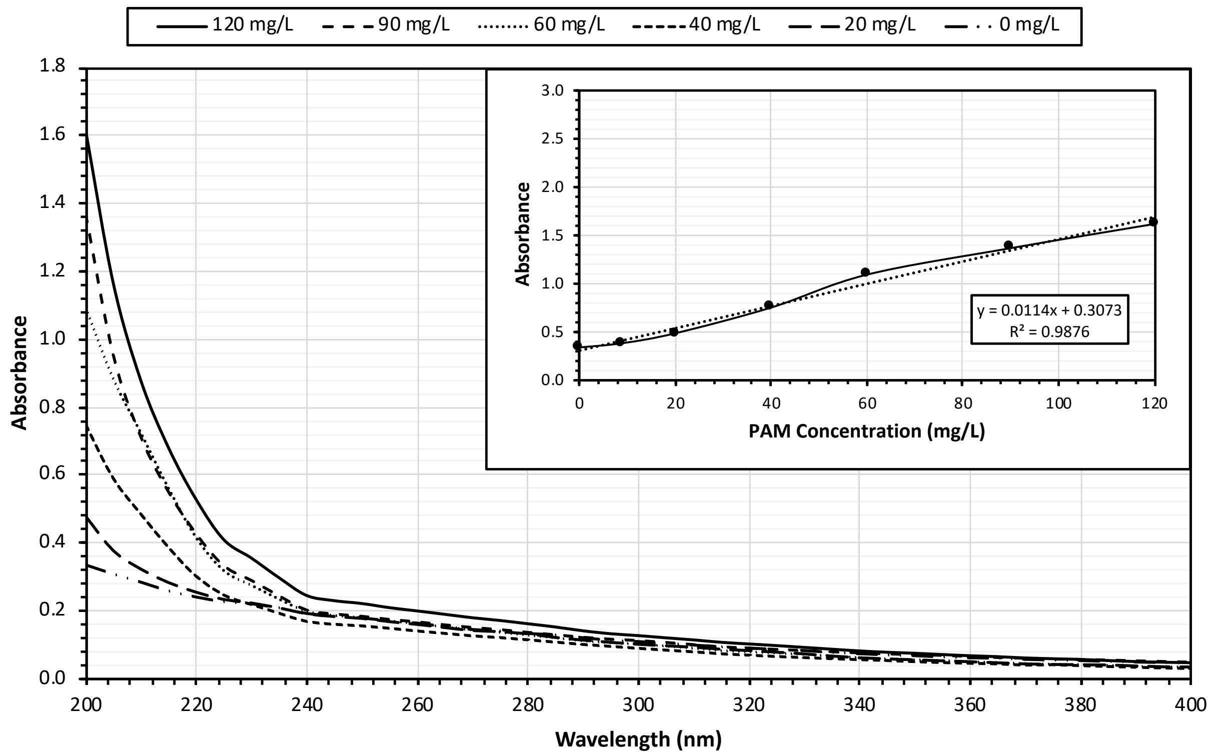

FIGURE 3.1: Calibration Curves

3.3.2 Validity Analysis

Centrifuging was used to remove sediment from runoff samples from the ASTM plot, isolating the runoff, before spectrometer analysis. Samples were centrifuged at 1,200 relative centrifugal force (RCF) for 10 minutes to remove sediment and then only the supernatant was run through the spectrometer. Figure 3.2 depicts the centrifuging process.

(a) Eppendorf machine (b) Sediment removal post-centrifuge

FIGURE 3.2: Centrifuging

The following two paragraphs address the validity of the results with centrifuging. The first concern is that soil removal must be complete for accurate PAM detection, in other words, there should be no soil interference remaining after centrifuging. To determine if residual soil interference affected results, turbidities were compared between calibration samples and supernatant of field samples. The average turbidity of 56 field samples was 8.6 NTU with a standard deviation of 4.2, and the average turbidity of nine calibration samples was 8.4 NTU with a standard deviation of 2.3. There was a weak correlation between concentration and turbidity, with a correlation coefficient of -0.3, suggesting that the flocculant tended to reduce background turbidity but not consistently. A simple T-test between the calibration and field samples yielded a T-statistic of 0.87 and a corresponding p-value of 0.39. Because there is not sufficient evidence that the turbidities of the field samples and the calibration samples differed at the 95% confidence level, it is not believed that soil interference was a concern in the analysis. Removing soil interference is a significant advantage of this method because some samples were so sediment-laden that they contained up to one-part soil per four parts solution by weight.

The second concern that the centrifuging process may remove some PAM from solution along with the soil, artificially reducing its measured concentration. To determine if centrifuging removed PAM from the supernatant, a solution was prepared with 100 mg/L PAM and deionized water, and its absorbance read at 200 nm in the spectrometer. Then the sample was centrifuged and the supernatant was read again. A simple T-test between the raw and centrifuged samples yielded a T-statistic of 2.78 and a corresponding *p*-value of 0.12. Thus, at the 95% confidence level, there was not sufficient evidence that the means between the centrifuged and raw samples differed and therefore it is not believed that centrifuging PAM out of solution was a concern.

A reading at 2 mg/L was added to the blank calibration solutions to determine whether a detection limit might be valid at that level. A simple T-test between the means of the absorbances at 200 nm of the 0 mg/L and the 2 mg/L sample yielded a t-statistic of 8.83 and a corresponding *p*-value of $4.5E^{-4}$. It can be concluded that the detection limit of this method was very reliably at maximum 2 mg/L. Only one sample reading of 52 was below this limit.

3.3 RESULTS AND DISCUSSION

This section reviews and discusses the primary PAM-on-soil method results, the PAM-on-matting (“soft-armoring”) results, and results from residual testing of two hydro mulch products not part of the original scope but investigated due to strong visual evidence of polymer in the runoff.

3.3.1 Primary Testing

The average estimated concentration over the three trials is plotted in Figure 3.3. The first recorded absorbance value corresponds to observance of first runoff. An increase in concentration occurred immediately after first runoff was observed at approximately 12-15 minutes into the test, too large to be measured using the absorbance values constructed during calibration without extrapolation. The concentration was extrapolated at nearly 200 mg/L during trial 3. There was a subsequent decrease in concentration until about halfway through the test or minute 30, when concentration appeared to steadily fluctuate between 20-60 mg/L. The phenomenon of high initial concentration echoed the first flush effect, where the first appearance of stormwater runoff contains the highest concentration of contaminants washed away from the ground surface. Then, as runoff persisted, concentration decreased. Furthermore, the first runoff/high concentration points corresponded to a period of no observed sediment loss. Figure 3.4 compares average PAM concentration to average TSS, a metric used as a proxy for sediment loss, throughout the test. As PAM concentration decreased and the slope lost its protective coating, sediment loss increased.

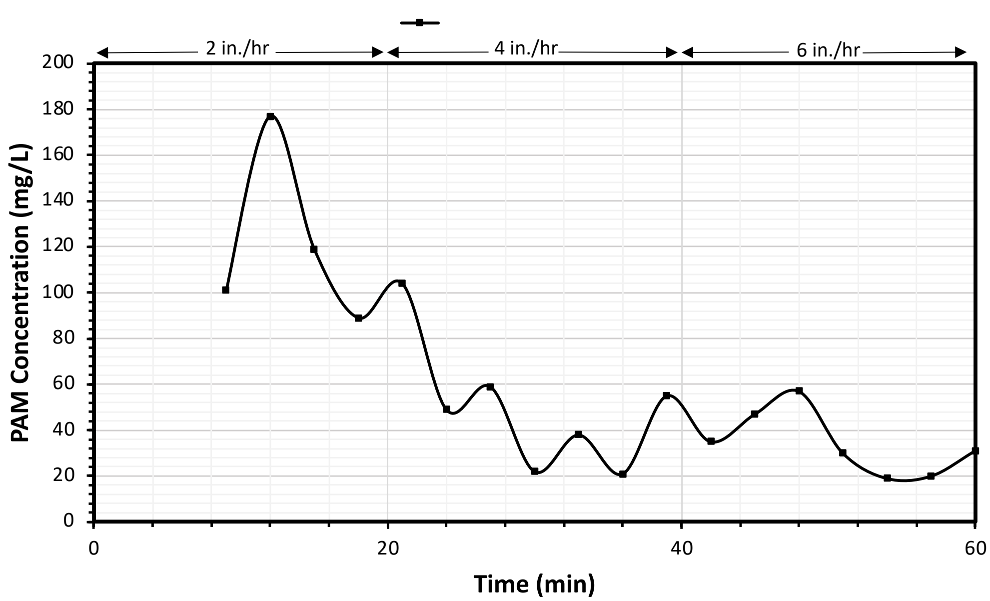

FIGURE 3.3: Estimated PAM Concentration over Time

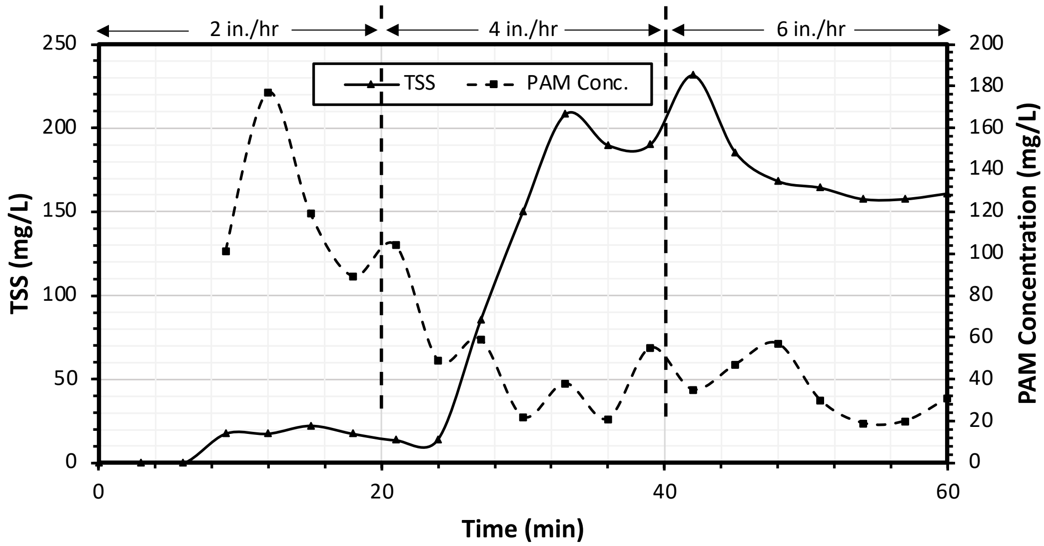

FIGURE 3.4: PAM Concentration vs. TSS

Twelve out of 52 samples displayed high (>100 mg/L) concentrations. Visual observations during testing confirmed the likely presence of high PAM concentrations. Sediment-laden runoff from the plot during PAM testing had a noticeably frothy, soap-like quality, documented in Figure 3.5. Residue clung to surfaces and equipment after draining and heavy bubbles formed at the surface. These features were highly unusual in runoff and clearly indicated presence of some foreign substance. The blank PAM solutions prepared for calibration also displayed a thin, soapy film when agitated and tended to form slight lather at the surface, although to a much lower extent that the highly disturbed runoff.

Because sediment loss in this experiment was so high, it was likely that a high percentage of the applied polymer bonded to the soil ended up in the runoff. An expected concentration could be hypothesized based on total runoff volume generated from each test and amount of PAM applied to each test. Table 3.2 displays the amount of PAM applied, the runoff generated from the test, and the PAM concentration expected if all PAM washed into the runoff. It also provides an estimate of the percentage of PAM from each test that appeared in runoff, as opposed to remaining in the soil, by dividing the observed concentration by the expected concentration anticipated if all PAM washed into the runoff. As evidenced from the table, roughly half on average of product appeared in runoff.

TABLE 3.2: Runoff and Expected Concentration If All PAM Appeared in Runoff

Parameter	Test 1	Test 2	Test 3	Avg.
PAM applied to slope, g (oz.)	84 (3.0)	84 (3.0)	84 (3.0)	84 (3.0)
Total runoff from test, L (gal)	687 (181)	787 (208)	935 (247)	803 (212)
Expected concentration if all PAM (100% runoff) appeared in runoff, mg/L	122	107	90	106
Actual average concentration from test, mg/L	55	52	61	56
Percent of applied product observed in runoff	45%	49%	68%	54%

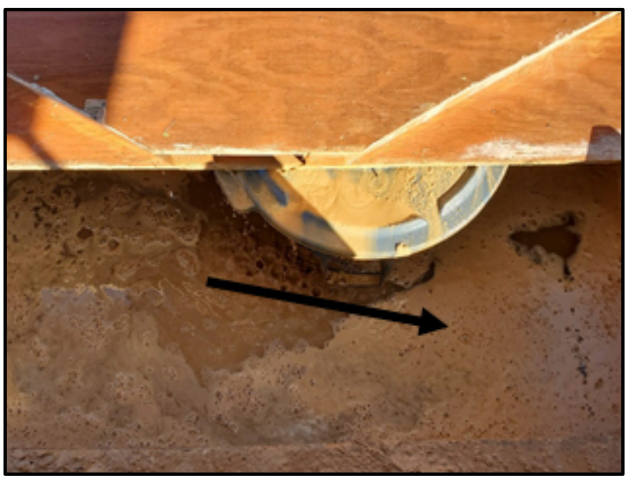

(a) Runoff after 6 in./hr test with suds at water surface

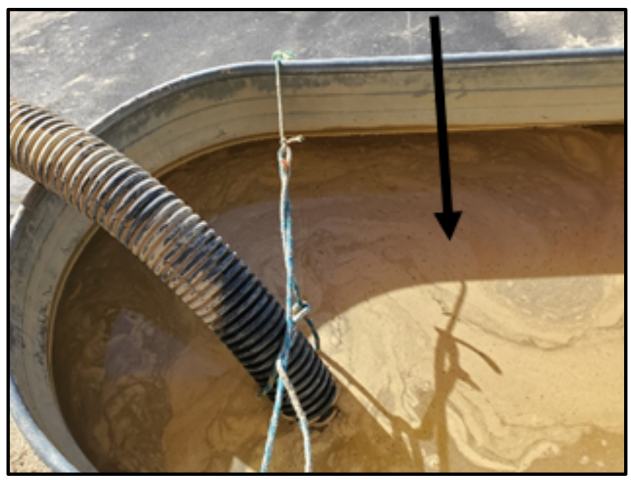

(b) Runoff funneled from 4 in./hr simulation with soapy film

(c) Residue remains after draining runoff

FIGURE 3.5: Evidence of High Concentrations in Plot Runoff

Several explanations exist for the higher concentrations found than in the two previous studies. As discussed previously, there were several factors that compromised the integrity of the ability for PAM to form a complete seal on the test plot. Low contact time, lack of pre-wetting, and an intense storm on a steep slope all may have contributed. In fact, the total intensity called for over the 1-hr D6459 simulation represents approximately the 500-yr storm in the testing location of central Alabama (NOAA Atlas 14). Also as discussed previously, in hindsight the application rate was likely suboptimal. PAM dosing is much more difficult to do on slopes than on, for example, sedimentation basins. Even with jar testing, conditions such as soil type, slope, rainfall, and more can interact in such ways that make exact optimal dosing sometimes difficult. By contrast, in the sedimentation basin example, typical doses are low (1-5 mg/L) (McLaughlin et. al 2016), based on design volume (Johnson et. al 2015), and introduced in ways to maximize mixing, thus making ideal dosing easier. When these factors compromise the protective seal, PAM's impact on soil infiltration and water viscosity can lead to increased erosion, and indeed in these experiments PAM increased sediment loss as compared to the control. Since the other two studies experienced effective PAM performance, most of the PAM probably remained on the plot in its seal rather than deteriorating and washing off as it did here. Therefore, the high concentrations are likely the result of poor performance.

3.3.2 Soft Armoring Testing

The soft-armoring application was evaluated to determine if altering the application technique could ameliorate the effects of the high residual concentration. Figure 3.6 compares the average concentration in the first three trials (PAM on soil) to the concentration observed in the fourth trial (PAM on matting). The PAM on matting, like the PAM on soil, displayed the highest concentration right after first observed runoff due to the “first flush” effect. However, there was a noticeable absence of high (>100 mg/L) concentrations, and concentrations up until minute 50 were consistently lower than the direct-to-soil technique. It is possible that when PAM percolated to the soil from the matting, it was released into the soil/runoff matrix at a more prolonged, sustained rate. However, concentrations from minute 50 to the end of the test were higher than the direct-to-soil technique. It is possible that by that point in the test, the direct-to-soil PAM had become depleted and so began to read lower concentrations. A more robust analysis could be performed with a triplicate test of the alternative technique. Further analysis could run longer tests or multiple tests in succession to see if either application method leads to sustained concentrations over time and whether the total discharge differs after taking time into account. Overall, it is not immediately clear which method may be more desirable, because although the PAM on matting avoided the high (>100mg/L) concentrations, it may also lead to more sustained concentrations.

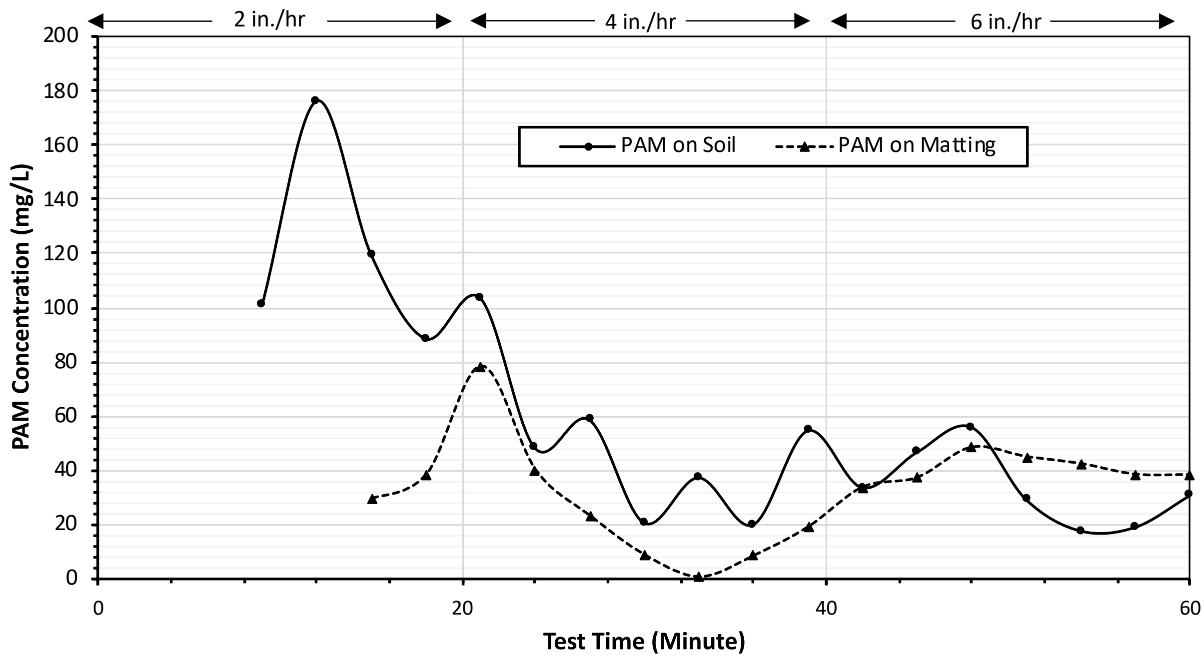

FIGURE 3.6: PAM Concentration Comparison Between Techniques

3.3.3 Mulch Testing

Many mulches utilize PAM or other polymers as binders, and there is a potential that excess binder could appear in runoff when these products are exposed to rain events. The spectroscopic method cannot be used to detect excess binder concentration in runoff because binder formulas are proprietary and thus reliable calibration samples cannot be created. However, some preliminary results can shed light on whether detecting excess polymer binder concentrations in mulch or other products should be a worthwhile avenue for future research.

Samples from the two hydro mulches tested as part of the work of this thesis were centrifuged and placed in the spectrometer. The ProMatrix^{TM} by Profile is a hydraulically applied hydro mulch with a guar-based binder. Guar is a traditional popular binding agent and is biologically derived (Wood 2014). The EarthGuard^{TM} EDGE^{TM} pellets were also examined. EDGE^{TM} contains a PAM-based binder with sodium acrylate, a polymer with similar impacts on soil properties as PAM (Chen et. al 2016). Similar visual phenomena to the PAM runoff were observed and are depicted in Figure 3.7. A high degree of froth formation occurred with the ProMatrix™ guar-based mulch runoff, and a moderate degree of froth formation along with a soapy film was observed with the EDGE™ PAM-acrylate-based runoff. Figure 3.8 depicts absorbance curves of the ProMatrix™ and pellets, respectively. While no conclusion can be made as to the exact concentration of the products due to a lack of knowledge of the precise composition, elevated absorbance levels as compared to the absorbance spectra of the 0 mg/L blank sample given in Figure 3.1 suggest the presence of PAM or other polymers in the runoff. These preliminary results indicate that excess binder concentration in runoff from mulches used in erosion control is a concern and certainly one that merits further investigation.

(a) Hydromulch residue on pump (ProMatrix™) (b) Bubble formation in basin (EDGE™)

(c) Froth formation in runoff (ProMatrix™)

(d) Froth remains after pumping runoff (ProMatrix™)

FIGURE 3.7: Visual Runoff Observations from Mulches with Binders

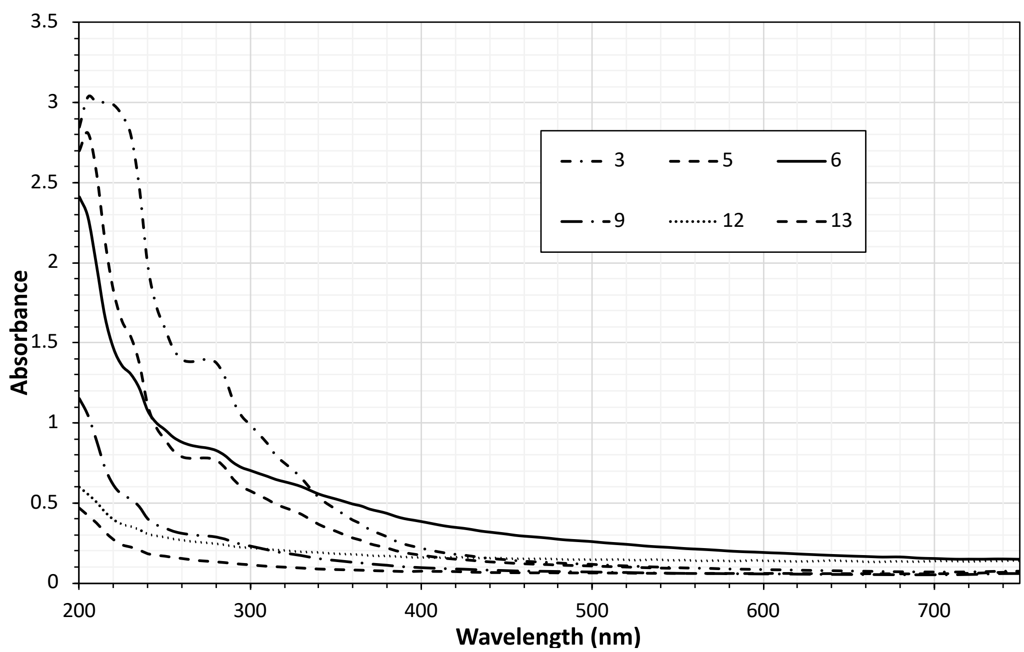

(a) ProMatrix™

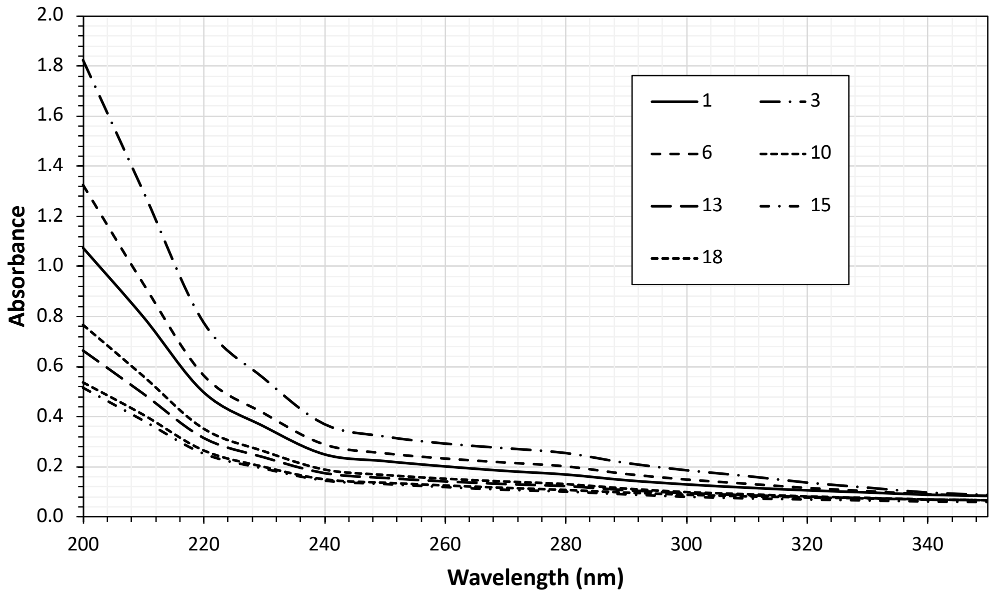

(b) EDGE™ Pellets

FIGURE 3.8: Absorbance Curves of Mulches

3.4 CONCLUSION

In summary, residual concentrations of PAM with jute, tested on the ASTM D6459 rainfall simulator, were determined using UV-Visible spectroscopy. This experiment represented the first large-scale residual testing of the product. The samples were centrifuged to remove soil interference. High (>100mg/L) concentrations were detected especially at first runoff. As concentrations decreased, soil loss increased. The high concentrations may be attributable to a variety of factors related to decreased PAM performance. More testing is recommended for erosion control products containing appreciable amounts of biopolymer or inorganic polymer since evidence supports residual binder concentrations in runoff.

CHAPTER 4: NEW RAINFALL SIMULATOR CONSTRUCTION

4.1 INTRODUCTION

This chapter presents information relevant to the work of construction the additional rainfall simulators as called for in Phase II. This introduction reviews literature related to Alabama soils, effects of soil properties and slopes on erosivity, and rainfall simulator calibration methods. Then design elements for the new simulators are discussed, including spatial dimensions, sprinklers, water supply, and electrical system. The soil selection process is reviewed, including results and final soil selections. Finally, all accomplished construction tasks are documented.

4.1.1 Soil Types in Alabama

The state of Alabama is divided into six different soil areas, each featuring a more prominent soil type (Mitchell 2008). Figure 4.1 depicts the soil types geographically across the state. The uppermost portions of the state are designated Limestone Valleys and Uplands and derive from weathered limestone. Huntsville and portions of Birmingham are located in this region. The surface layer is usually gravelly silt loam. The higher elevation regions descend from sandstone or shale deposits and are named the Appalachian Plateau. The topsoil is silty loam and remainder of the Birmingham area is situated in this region. The Appalachian Plateau gives way to the Piedmont Plateau, descended from granite, hornblende, and mica. The top layer of this soil is usually a silty loam. The Coastal Plain, consisting of remnants of fluvial or marine deposits, features sandy loam topsoil and covers the largest geographic area of the state, including Mobile and Tuscaloosa. The Blackland Prairie region, so-called because of the dark color of the topsoil, is clayey. Montgomery is situated in this region. The Major Floodplains and

Terraces lie along Alabama’s rivers and feature soil formed by the nearby alluvial deposits, the topsoil of which may be sandy loam or silty clay loam. Finally, the Coastal Marshes and Beaches lie along the Mobile River and the coast. They occur at or only slightly above sea level and may contain a variety of conditions. They are typically poorly drained and mucky.

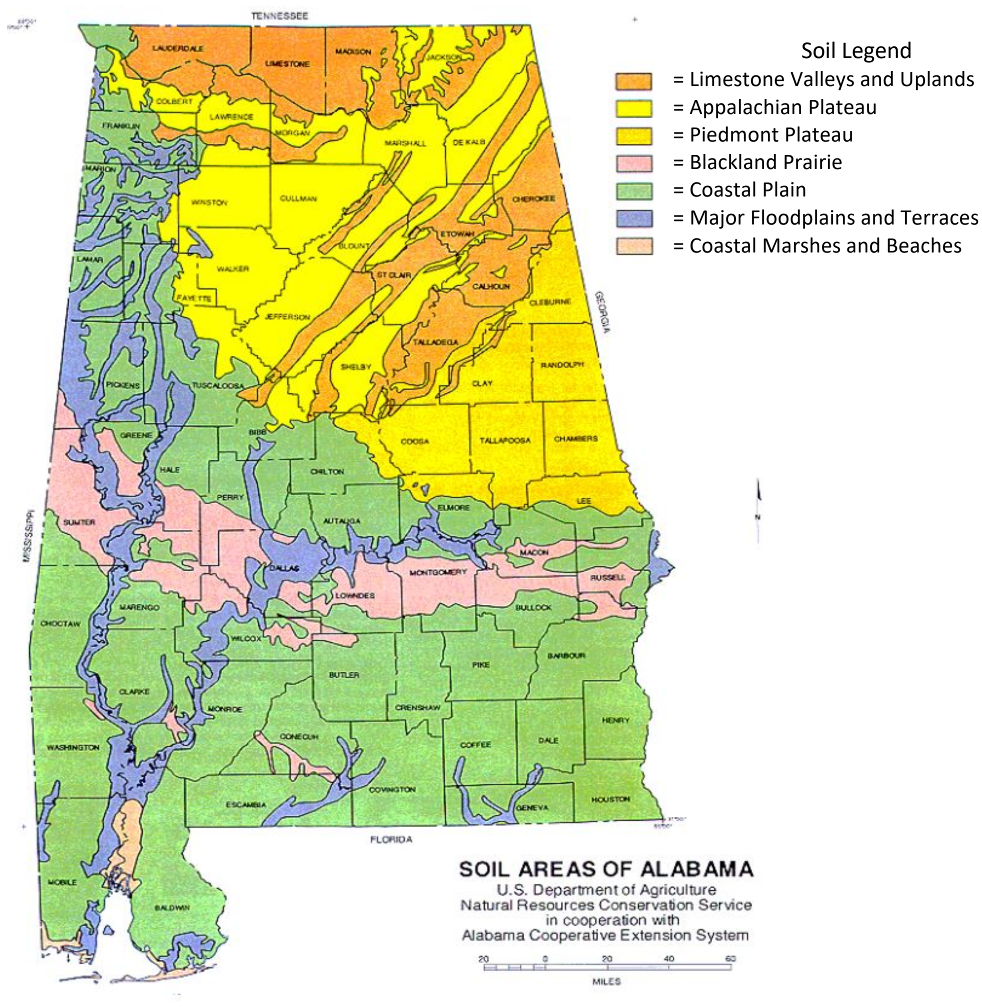

FIGURE 4.1: Soil Map of Alabama (Mitchell 2008)

The official state soil of Alabama is the Bama Soil, recommended by the Professional Soil Classifiers Association of Alabama, the Alabama Soil and Water Conservation Committee, and the Alabama Association of Conservation Districts in 1996 and adopted by the legislature the following year (Bama series 2014). Bama soil occurs in the Coastal Plain region and is yellow red and slightly acidic. The soil type of the Ap and E horizons - the layers that comprise the topsoil - are fine sandy loam (United States Department of Agriculture [USDA] 1998)

Table 4.1 summarizes the soil areas in Alabama according to the USDA, the soil types occurring in those areas, and significant considerations of each. The upcoming Phase II ASTM D6459 testing on different soil types will yield helpful information for different areas of the state. The data from the sand will most closely apply to the southern area of the state including Mobile. The data from the loam will most closely apply to the Bama soil found in much of the state. The data from the clay will most closely apply to the soil in the Blackland Prairie including Montgomery. A lack of knowledge on how erosion control products perform throughout the diverse soils of Alabama was a primary motivation for ALDOT's sponsorship of Phase II, so understanding which results are most relevant for which regions is important.

TABLE 4.1: Alabama Soil Regions (USDA 1998)

USDA Soil Region	USDA Topsoil Classification	Significant Notes
Limestone Valleys and Uplands	Gravely silt loam	Huntsville, some of Birmingham
Appalachian Plateau	Silty Loam	Birmingham, Hoover
Piedmont Plateau	Silty Loam	Eastern part of state
Blackland Prairie	Clay	Montgomery, "Black Belt"
Coastal Plain	Sandy Loam	Central and South, Bama Soil
Major Floodplains and Terraces	Sandy Loam or Silty Clay Loam	Along rivers
Coastal Marshes and Beaches	Varies	Small areas

4.1.2 Erosivity on Different Soil Types

Various studies have sought to determine which soil property has the greatest influence on a soil's erosion potential. A Jacobs et. al (2011) study of streambed erosion used a flume which generated flow at the surface of a bed of various soil types. The study found that cohesion as measured by plasticity index had the most significant effect on erosion as compared with factors such as shear strength or water content, with more cohesive soils exhibiting most resistance to erosion. The strong relationship between plasticity index and erosion corroborated two earlier studies from 1959 and 1995. A rainfall simulator study on 20 soils by Verhaegen (1984) found a positive correlation between erosion losses and sand content and a negative correlation between aggregate stability (WSA), water content at saturation, cohesion as measured during experimentation with a handheld Torvane, and silt content. Luk (1979) studied wash and splash erosion using a rainfall simulator on four soils and three gradients from 3 to 30 degrees. The soil properties of wet aggregate stability and organic carbon content were the strongest predictors of erosion. Sand and clay content were only sometimes significant predictors. Organic carbon not only absorbs water, but it also causes soil to be more aggregate-stable. This is one reason that compost is a widely used soil amendment, since as it breaks down it adds organic carbon to the soil underneath. Sodium content has been shown by Singer et al (1982) to adversely affect soil erodibility due to its ability to disperse organic matter, through experiments with the same soils at different sodic contents. A study by Ekwue (1990) confirmed that organic matter reduced aggregate breakdown and splash detachment. Sand and clay content either displayed insignificant correlation or correlated at lower p-values than the organic matter. Sand is often associated with greater erosion and clay with less. A rainfall simulator study by Ekwue and Harrilal (2010) measured erosion on three different soil types and found that the soil with the least sediment loss was neither the sandiest (a sandy loam) nor the clayeyist (a clay), but the soil in between – a clay loam. The authors suggest that its clay content at 30.6% was enough to produce the cohesion required to resist erosion, while still allowing enough sand content to promote adequate infiltration. A study of streambank erosion by Wynn and Mostaghimi (2006) confirmed that soils with the widest range of grain size standard deviations, especially those containing substantial percentages of both sand and fines, displayed the highest critical shear stress, a parameter directly inversely proportional to streambank erosion rate. The authors suggest that fine particles fill in the voids of the larger particles, which shields them from the hydraulic forces responsible for erosion.

The K-factor nomograph illustrates some of the most important soil properties for erosion, and also illustrates the reason for inconsistent results in the literature for sand and clay. K-factor in RUSLE is commonly determined through a nomograph (Renard 1991), even though a different method was used in this study. The factors significant to erosivity in the nomograph are percent silt, percent sand, organic matter content, soil structure, and permeability. All other things equal, an increase in silt results in higher erosivity, an increase in organic matter results in lower erosivity, and an increase in permeability results in lower erosivity. An increase in sand content leads to an increase in erosivity and the effect may be compounded depending on the overall soil structure. However, an increase in sand content is also typically associated with higher permeability which may offset the increase in erosivity. Clay content is not captured directly in the nomograph, but if the soil texture on the whole is fine, erosivity decreases. At the same time, clay is associated with decreased permeability which increases erosivity again. Thus, the precise effects of sand and clay may be complicated by soil properties generally associated with each. The nomograph may be seen in Figure 4.2

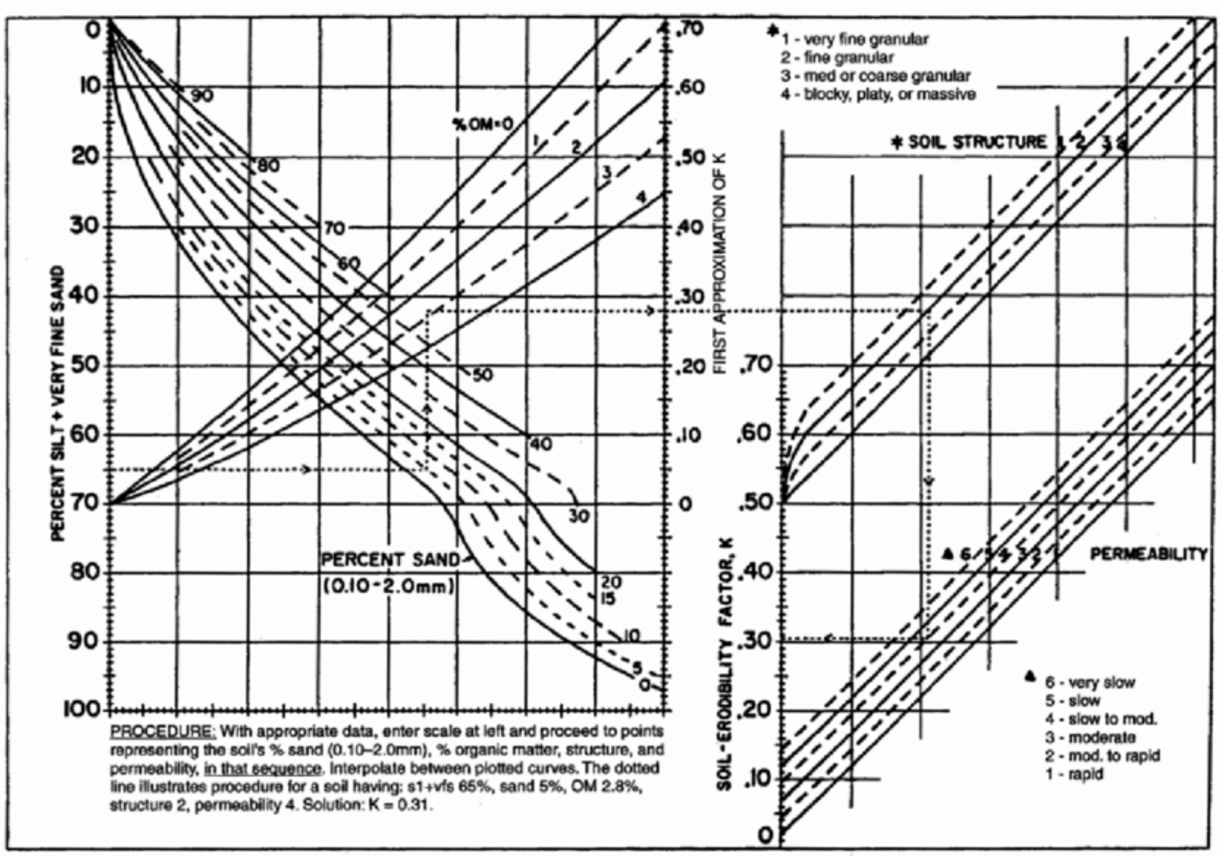

FIGURE 4.2: K-Factor Nomograph for RUSLE (USDA 1991)

Bryan (2000) points out that interrill and rill erosion may interact with soils differently due to their differing hydraulic processes. Interrill processes are propelled by raindrop energy, and soil detachment occurs in this stage. Raindrop energy can profoundly affect overland flow hydraulics, which at beginning stages, is usually supercritical with depths that vary greatly and may frequently be discontinuous. Soil surface properties are most important in shaping the erosive processes in interrill erosion. These properties include clay mineralology, aggregate stability, and presence of gravel. Clay mineralogy was shown to impact erodibility in a rainfall simulator study on 19 soils by Stern et al (1991). Soils with even small amounts of smectite, the expandable clay mineral notorious for swelling, displayed more soil loss than soils that were only kaolinite or illite. Aggregate stability may be influenced by cementing agents in the soil such as humic acids, electrostatic bonding among clay particles, electrolytes, diffuse double layer charges, microbial muscilage, minerals, frost action, compaction and shrinkage. Rill erosion, by contrast, is mostly impervious to raindrop energy since it occurs over concentrated flow whose depth protects the soil from rain impact. Most studies have linked hydrologic processes, rather than soil properties, to the development of rill erosion. High shear velocity of flow, high stream power (energy dissipation of the flowing water against the surface, a function of slope and volumetric flow rate), and high Froude number are hydrologic variables associated with greater rill erosion.

Just as soil properties affect erosion, erosion can in turn affect soil properties. Hydrologic groups are used in hydrologic modeling and designate soils from classes A-D based on their runoff potential and capacity to hold water. Larson et al (1985) evaluated the effect of soil removal through erosion on upper limit water capacity and available water capacity and found that both tended to decrease with increasing soil removed. The effect was sometimes so pronounced that it caused soils to change hydrologic groups. Soil downslope of an eroded area can become enriched with increased clay content, increased nutrient content, and increased organic matter (Kuhn 2007) due to selective transport of fine particles in erosion. Simultaneously, the upslope portions experiencing erosion have shown decreased clay content (Du and Walling 2011), decreased nutrient content, and decreased organic matter (Heckrath et. al 2005).

In summary, the expectations regarding erosion on the sand, loam, and clay soils in the new Phase II simulators may not be absolutely straightforward. The precise expected erosivity of the sand, loam, and clay soils according to RUSLE could be predicted by the K-factor nomograph as seen in Figure 4.2 if all soil properties in the nomograph were measured. In the literature, cohesion (PI) appeared to be the strongest predictor of erosion, but clay mineralogy, organic carbon content, and aggregate stability also played a role which were not measured for the Phase II simulators. Sand and clay content were sometimes significant in the literature but sometimes not. Sand particles are heaviest and create more void space to increase infiltration, but they lack cohesion. Clay particles are the most erodible due to small size and result in low permeability, but display high cohesion. Silt particles are most erodible, and soils containing many sizes offer greater erosion protection. The complication is illustrated by the offsetting effects of particle size versus other typically associated soil properties in the K-factor nomograph.

4.1.3 Erosivity on Different Slopes

Intuitively, an increase in slope leads to greater erosion due to an increase in water velocity over the area, causing increased soil particle detachment and decreased infiltration. However, to what degree erosion may be expected to increase, which types of erosion may be expected and when, the combinatory effects of slope, soil properties, and hydrologic properties, and the existence of any potential critical thresholds are all debated in the literature.

This study uses the RUSLE equation, which presents a commonly accepted mathematical relationship between slope and expected soil loss. The relationship differentiates between slopes less than and greater than 9% and soil loss is modeled as a linear function of the sine of the slope angle. These relationships have already been described in Equations 2.6 - 2.10. However, a Liu et al (1994) used 19 large-scale plots using three different soils in China at slopes ranging from 8.3 to 53.4 percent in combination with natural rain events to study soil loss. The study found a divergence in soil loss patterns starting at around 25% grade and proposed a new relationship denoted in Equation 4.1 that holds for grades above 25%:

$$S = 21.91 sin\theta - 0.96 \qquad (4.1)$$

Noting that the RUSLE equation was not developed using data from steep grades, Nearing (1997) proposed a slope factor relationship to be used for any slope, depicted in Equation 4.2, that both closely approximates the RUSLE and incorporates the Liu et al. (1994) data for steeper slopes:

$$S = -1.5 + \frac{17}{1 + \exp\left(2.3 - 6.2 sin\theta\right)} \qquad (4.2)$$

A Fu et al (2011) rainfall simulator study of steep, short (50 cm) slopes from 9 to 100 percent found an increasing soil loss with slope up until a maximum of 58%, followed by a decrease. The authors explain that runoff also began to decrease after a maximum slope value, which may help explain the decrease in sediment loss.

Use of either of these formulas in this study would have increased *S*, thereby increasing the LS-factor, thereby decreasing K-factor calculated from the control test. The higher LS-factor and lower K-factor would offset one another in the RUSLE calculations so it is difficult to predict the net impact. To determine the precise effects, Equation 4.3 was applied to obtain an updated *S*. With a 3:1 slope equivalent to 18.48 degrees, the new *S* from the Liu et. al study would increase from 5.361 to 5.967. The new LS-factor would increase from 2.86 to 3.21. Table 4.2 presents the resulting impacts on C-factor. While the K-factor always decreased, the reported C-factors as reported to two significant figures either did not change or changed by a maximum of 0.01. Even though the updated method for finding *S* may be more accurate, the impact on final results was negligible. The new *S* as calculated by the Nearing 1997 method was 5.560, and so can be expected to make an even smaller impact.

TABLE 4.2: S-Factor Method (Liu et. al) and Impact on C-Factor

	Old *K*	New *K*	Old *C*, Average	New *C*, Average	Old *C*, Regression	New *C*, Regression
Jute	0.27	0.24	0.37	0.37	0.35	0.35
Gypsum	0.22	0.20	0.10	0.11	0.12	0.12
PAM	0.26	0.23	0.51	0.51	0.45	0.45
ProMatrix™	0.38	0.34	0.37	0.37	0.42	0.42
EDGE™ Pellets	0.23	0.20	0.40	0.41	0.46	0.46
Soil Cover	0.33	0.30	0.46	0.45	0.45	0.46
Eco-Fibre™	0.29	0.26	0.55	0.55	0.56	0.56
TerraWood™	0.31	0.28	0.54	0.53	0.53	0.53
Curlex I®	0.23	0.21	0.05	0.05	0.05	0.05
ECX-2™	0.24	0.22	0.12	0.13	0.12	0.12
S-150®	0.27	0.24	0.14	0.14	0.14	0.14

The same Ekwue and Harrilal (2010) rainfall simulator study referenced in the previous section also tested erosion on different slopes. The authors measured infiltration, runoff, and soil loss from a sandy loam, a clay loam, and a clay on grades of 9, 15, 21, and 30 percent. By contrast with the findings detailed in the previous paragraph, they found nearly linear relationships between each parameter and slope percentage for each soil type, indicating that erosion increased at a constant rate with each percentage increase in slope rather than suggesting the existence of any critical threshold. In their study on a silty clay loam, Grosh and Jarrett (1994) used a rainfall simulator to test slopes ranging from 5 to 85 percent in grade and also found that soil loss increased linearly with increasing grade up to 85%. A flume simulation on 6 gradients ranging from 3.5 to 46.6 percent, and flow discharges from 0.07 to 0.76 gal/min (0.25 to 2.9 L/s) performed by Zhang et al (2002) found that the impact of slope on erosion, measured by detachment rate, increased with increasing slope. More specifically, the following relationship given by Equation 4.3 was obtained

$$D_c = 5.43 * 10^6 q^{2.04} S^{1.27} \quad (4.3)$$

Where D_c is the detachment rate in kg/(s*m^2), q is the flow discharge and S is the slope percentage. Flow velocity was impacted by both slope gradient and flow discharge, among others. The combined effect was found to be as in Equation 4.4

$$D_c = 6.20 * V^{4.12} \quad (4.4)$$

Where V is flow velocity in m/s. Thus, erosion was found to be related to both slope and velocity through a power relationship.

Quansah (1981) studied erosion in terms of detachment, measured by taking the mass of soil present on splash guards that lined soil trays subject to rainfall simulations. The study examined sand, clay loam and clay and considered the effects of soil, rainfall intensity, and slope ranging from 0 to 14 percent. An ANOVA found that the soil, slope, and the interaction between soil and slope were significant with a p-value of 0.001. As found previously, the clay loam exhibited the least detachment, likely because it contained the most variety of soil particles, the clay exhibited the second least since it was most cohesive, and the sands exhibited the most detachment. However, the significance of the interaction term indicates that the degree of increase in detachment as slope increased did vary with soil type, although the magnitude of the change was small. The clay exhibited the greatest magnitude of increase in detachment with slope, with an exponent of 0.27, and the sand the least with an exponent of 0.13. The Ekwue and Harrilal (2010) study also found differential effects of slope when combined with soil properties. The slope effect on soil loss was greatest with the sandiest soil and least with the clayeyer soil, whereas the effect of runoff on soil loss was greatest with the clayeyest soil and about equal for the other two soils.

4.1.4 Rainfall Simulator Calibration Methods

Rainfall simulator calibration refers to the process of determining and adjusting the major parameters of the droplet output in order to better ensure comparability across studies and verify conformance to design. These parameters include rainfall intensity, uniformity, drop size distribution, and kinetic energy. Rainfall intensity and uniformity may be determined by installing and monitoring a series of rain gages over the test area. Drop size distribution and kinetic energy are more difficult to ascertain, and a variety of methods have been introduced to establish them.

The primary method to determine uniformity is the Christiansen's Uniformity Coefficient (CUC), introduced in 1942, which is utilized in this study. It is described by Equation 4.5

$$CUC = 100 * (1 - \frac{\sum_{i=1}^{n} |x_i - \mu|}{\sum_{i=1}^{n} x_i}) \qquad (4.5)$$

Where *n* is the number of reading instruments placed on the rainfall distribution area where each instrument theoretically represents a geographically equal area of rainfall. The CUC weights the readings at each of these equal areas by the overall mean. Maroufpoor et. al 2010 describe other methods used. The results from the assorted methods vary with field conditions, especially with wind speed, and it is unclear whether they provide significantly different results than the CUC. Wilcox and Swales 1947 utilized standard deviation in their calculation of uniformity, given in Equation 4.6

$$U = 100 * (1 - \frac{\sigma}{\mu}) \qquad (4.6)$$

Where *U* represents uniformity. Hart and Reynolds 1965 utilized Equation 4.7 based on numerically integrating the normal distribution function with uniformity between 0.7 and 1.0

$$CU = 100 * (1 - \frac{0.798\sigma}{\mu}) \qquad (4.7)$$

Other researchers utilized either only the lowest or highest quarter of observations in their calculations to capture the most variable portions of the data.

The oldest drop size distribution test utilizes a stain method instead, whereby a filter paper treated with dye is placed in the rainfall, and the resulting colored drops that form on the paper may be measured and counted (Best 1950). Another early test was the flour pan test, developed by Wilson Bentley in1904 and adapted by Laws and Parsons 1943. The test calls for one 1 in. (2.5 cm) deep, screeded pans of flour to be exposed in the rain or rainfall simulation briefly, with the theory that the pellets formed in the dough correspond roughly to the sizes of the raindrops that made them. In the oil method, described by Eigel and Moore 1983, STP and mineral oil are mixed to form a low density, high-viscosity suspension which envelops any raindrops that come into contact with its surface, allowing them to retain their size and shape. The drops are then photographed and counted. More recent research, however, has employed disdrometers, or instruments designed specifically to measure drop size, instead of manual means. Disdrometers are available that operate by optics, displacement, or acoustics (Chowdry et. al 2017). Singh et. al 1999 employed computer visual analysis to digitally capture drop size diameter, and Elbasit et. al 2010 used piezoelectric sensors which translated acoustic vibrations generated by the raindrop into voltage signals. A common disdrometer is the Laser Precipitation Monitor (LPM) (Lanzinger et. al 2006). LPMs and other optical disdrometers typically measure the duration of blocked light on a diode as corresponding to the diameter of a raindrop, as the drop passes through a steady beam of light (Johannsen et. al 2020, King et. al 2010).

Once drop size distribution is obtained, total kinetic energy can be calculated. Calculations convert raindrop size to raindrop mass, and then use fall height to calculate velocity. Aggregating the results over each raindrop absorbed over the duration of the simulation into the basic kinetic energy relationship $KE = 1/2mv^2$ yields the total kinetic energy. Different methods of predicting terminal velocity from drop size, which may depend on fluid properties such as viscosity and metrological variables such as air temperature and pressure, are primarily responsible for the differences in the literature for kinetic energy predictions (van Dijk 2002). Typically, the kinetic energy obtained from rainfall simulation is lower than that of natural rain (Dunkerly 2008) by up to half (Marcos et. al 2000) due to higher variability of drop size in simulation and tendency to an overall smaller drop size distribution. To compensate, researchers sometimes increase intensity to beyond what is normal for their geographic area, or simply conduct an experiment knowing that erosivity at the given intensity will be lower than a comparable naturally occurring rain event (Kuhn 2007). Increasing intensity may be a problematic approach because it entails a corresponding increase in overland flow, which may inadvertently impact observed erosion patterns. Perhaps this is one motivation for the unusually high intensity called for in ASTM D6459. Kinetic energy of natural events across the world only varies only slightly by region, and always tapers as the event continues due to ponding and increasing ground flow (Kathiravelu et. al 2014).

4.2 DESIGN ELEMENTS

The following section outlines select design elements for the Phase II rainfall simulators. The placement and construction of the sprinkler system was essentially copied from the existing Phase I simulator to minimize calibration. This section details the following aspects: spatial features and dimensions, sprinkler configuration, water supply, and electrical components.

4.2.1 Spatial Features and Dimensions

The Phase II simulators are situated in the new 7-acre expansion area of the Auburn University Stormwater Research Facility, and their precise locations are illustrated in Figure 4.3. To aid in initial earthmoving and grading, the spatial dimensions of the plots were entered into AUTO-CAD. In keeping with the existing simulator design, the eight side sprinklers were placed five ft (1.5 m) from the edge of their corresponding plots with four equally spaced on either side of the plot. One additional sprinkler was placed at the top of the plot and one at the bottom, both ten ft (3.1 m) from the edge of the plot. Plots were placed in pairs, with one sand, one clay, and one loam pair on each grade (3:1 and 4:1). Each pair of plots shares one row of four sprinkler risers to conserve lumber costs and space. Between every other plot, 16 ft (4.9 m) of space was left in order to allow passage of the skid steer, giving each plot equipment access for easier rebuilding between tests. It was decided to pursue wind curtains with supports made out of used telephone poles, which are sturdy and available for free from the local power distributor. Figure 4.4 depicts a CAD drawing of the 3:1 slopes. The blue dots represent sprinkler risers, the yellow rectangle represents the skid steer with accurate dimensions, the blue squares represent the catch basins at the base of the slopes, and the brown dots represent proposed wind curtain support locations.

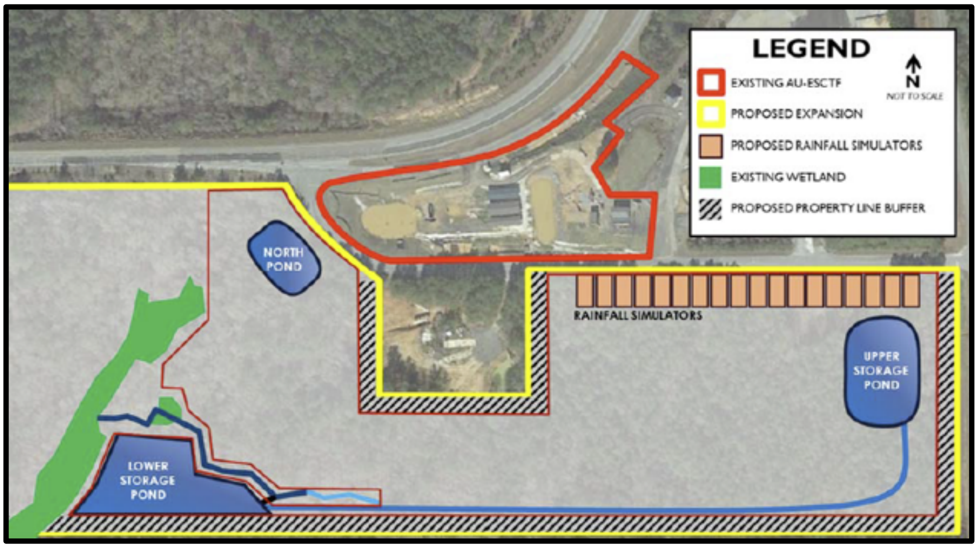

FIGURE 4.3: AU-Stormwater Research Facility Expansion Proposal with Rainfall Simulator (Perez et. al 2019)

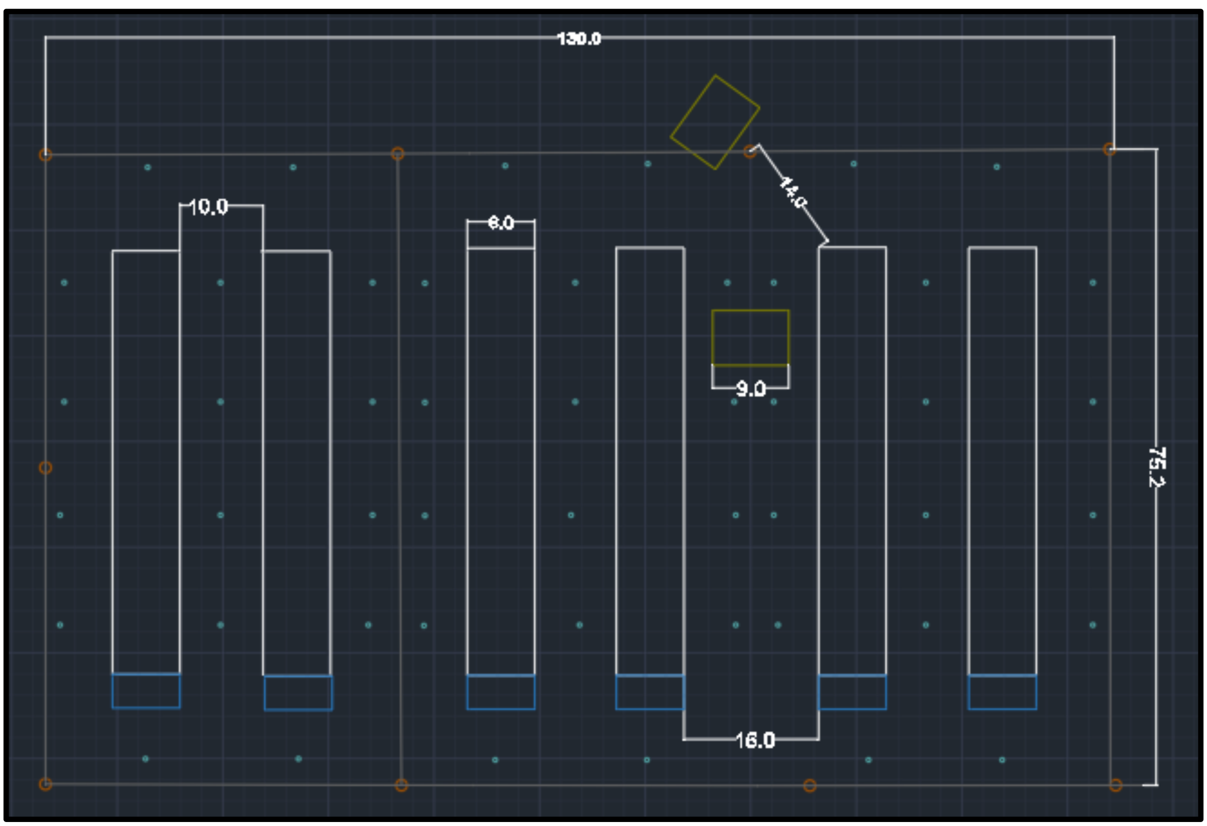

FIGURE 4.4: Plan View Layout of 3:1 Slopes

4.2.2 Sprinkler Configuration

As in the previous design, Nelson Irrigation sprinklers were used for the water droplet distribution. The S-S3000PC 190-degree circle spinner was selected in consultation with the Nelson representative as the updated equivalent of the existing parts, and the same #21 turquoise nozzle and 6 psi pressure regulator were paired with it. A supply tree made of 0.75 in. (1.9 cm) galvanized steel pipe was connected to create a total of 15 ft (4.6 m) of fall height for the sprinklers. The galvanized apparatus included a 0-100 psi pressure gage, and the base connected to 0.75 in. (1.9 cm) rubber hose which connected to the water supply. Ten sprinklers were required per plot, as arranged in Figure 4.4 above. Rather than assembling 120 sprinklers to be in place permanently around every single plot, it was decided to make them portable to save on cost and time. To this end, only two full sets of sprinklers (twenty) were actually assembled and strapped to two full sets (twenty) of 4 in. by 4 in. (10.2 cm by 10.2 cm) lumber posts. To make the assembly portable, permanent 4 in. by 4 in. (10.2 cm by 10.2 cm) PVC sleeves were placed in augured holes in the ground at the location of each sprinkler around each plot, plumbed, and compacted around with fine gravel. The sleeves extended about a foot (0.3 m) above grade. Posts may be slid in and out of the permanent PVC sleeves as needed and sprinklers moved with them. Figure 4.5 depicts the sprinkler head assembly and sleeve design.

(a) Sprinkler head assembly

(b) Permanent PVC sleeves plus 4x4 post example (with temporary red caps)

FIGURE 4.5: Sprinkler Head and Sleeve Design

4.2.3 Water Supply

The first plot was constructed with permanent underground 3 in. (7.6 cm) PVC pipe surrounding the perimeter as water supply, with a stub out to connect to a 3 in. (7.6 cm) flexible hose attached to a high-pressure pump. Five stub outs from underground connected to the 0.75 in. (1.9 cm) flexible hose delivering water to the sprinklers. It was with this assembly that preliminary calibration was established. However, a new plan for the remainder of the plots was developed with the motivation to simplify water delivery and save on material costs and labor. This system will consist of a high-pressure pump at the upper storage pond depicted in Figure 4.3 and one permanent underground PVC delivery pipe running at the base of all simulators. Twelve stub outs, one at the base of each plot, will allow sprinklers to connect to the delivery pipe via long runs of 0.75 in. (1.9 cm) flexible hose. Shutoff valves at each plot will serve to contain water supply to only the plot in operation. The shutoff valve will then allow pressure relief into the lower storage pond post testing.

This system was modeled in EPANET 2.0 in order to properly gage whether the current high-pressure pump in use at the facility was the correct size for the new system. The model is illustrated in Figure 4.6. Each sprinkler was modeled as a node with base demand 1.87 gpm (6.97 L/m) as obtained from Nelson Irrigation, the sprinkler manufacturer. The hour-long rainfall simulation was then modeled as pattern with 1x base demand for 20 minutes, 2x base demand for 20 minutes, and then 3x base demand for 20 minutes. The operation of any plot can be modeled by opening and shutting the shutoff valves in the model depicted by the butterfly symbols. The pipes were modeled with their correct lengths and dimensions, and elevations for each node and pipe as well as the reservoir and outfall were obtained with the Total Station. The pump curve corresponding to the existing (currently used) NorthStar high-pressure pump was obtained from the manufacturer and input into the model.

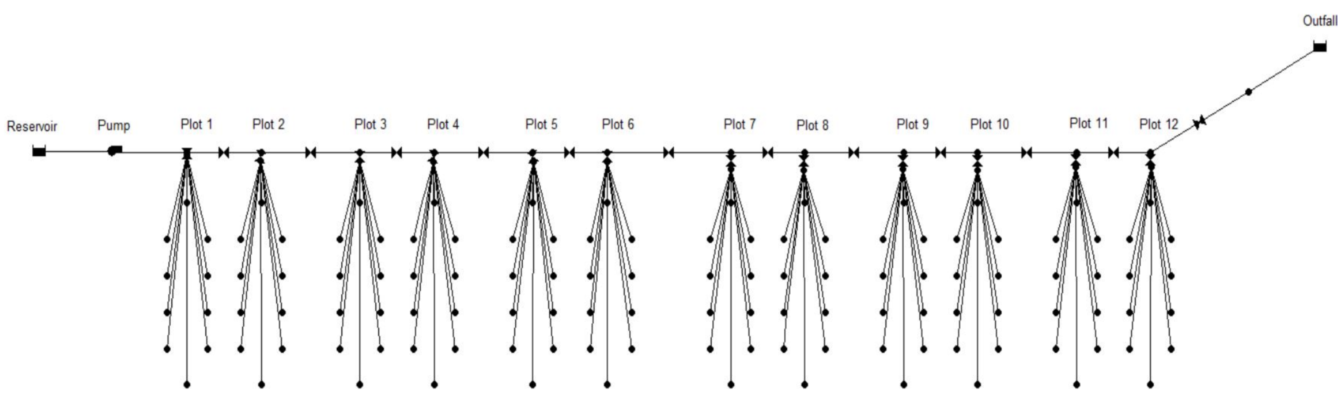

FIGURE 4.6: EPANET 2.0 Model of Rainfall Simulators

Model calibration was performed by adjusting pipe roughness values, selecting the head loss formula used, varying the emission coefficient for each sprinkler, and varying loss coefficients at bends and valves. The goal of calibration was to model the successful operation of Plot 1, with nodes showing the approximate pressure ranges observed in the field during preliminary calibration. The Hazen-Williams head loss formula was selected as the best fit, and roughness values selected were 150 for PVC pipe, 140 for flexible rubber and 120 for galvanized steel (Rossman 2000). Loss coefficients in pipes ranged from 0 to 7 depending on expected number of bends and were set to 0.2 for all gate valves. After trial-and-error, an emission coefficient of 1.15 was selected for each sprinkler node, representing a modest variation of output at each sprinkler with available pressure. Pressures in the model were extremely sensitive to emission coefficient values, were slightly sensitive to head loss formula used, and were not sensitive at all to roughness values or loss coefficients.

Pressures as obtained in the model for Plots 1 and 12 (plots closest to and furthest from the water source) are given in Table 4.3 for each rainfall intensity. To verify proper operation of Plot 12 when it was "turned on", it was confirmed that no demand interfered with the model from inactive sprinklers, that flow was shut off to inoperable areas, and that flow was properly channeled through the main supply pipe. Node 1 represents the sprinkler at the lowest elevation and Node 6 represents the sprinkler at the top of the slopes, at the highest elevation. Pressure decreased in the system as elevation increased. The pressure drop in the model was greater than the pressure drop observed during preliminary calibration. The drop observed during calibration was between 2-6 psi, but the drop predicted in the model was up to 13 psi. This is not a concern provided that enough pressure remains in each sprinkler for its successful operation. However, if during calibration, less rainfall is observed at the top of the slope, measures should be taken to increase pressure to the top sprinklers. The measure suggested here is to increase the diameter of the flexible hose. The new design calls for the supply to the base of each sprinkler from each plot's primary water hook-up to consist of a 0.75 in. (1.9 cm) rubberized hose, whereas the previous design delivered supply to the base of each sprinkler connecting using a 3 in. (7.6 cm) PVC pipe. If rainfall at the top of the new slopes is too sparse, a larger diameter hose could aid in water delivery. To illustrate, when the diameter of the final delivery line was changed from 0.75 in. (1.9 cm) to 3 in. (7.6 cm) in the EPANET model for Plot 1, the pressure drop from low to high elevation shrunk to around 3-5 psi as seen in Table 4.4. Another observation of note is that pressures at Plot 12 were slightly higher in the model than at Plot 1, despite utilizing an additional 234 ft (71 m) of delivery pipe. The reason is likely that Plot 12 is 2.6 ft (0.8 m) lower in elevation than Plot 1. Thus, it is not predicted that there will be any concerns regarding pump suitability for the longer plot reaches, and the existing pump is likely satisfactory.

TABLE 4.3: Pressures at Sprinklers as Designed (EPANET 2.0)

Plot 1 Pressures						**Plot 12 Pressures**					
2 in./hr		**4 in./hr**		**6 in./hr**		**2 in./hr**		**4 in./hr**		**6 in./hr**	
Node	psi	Node	psi	Node	psi	Node	psi	Node	psi	Node	psi
1	57.4	1	46.5	1	34.6	1	60.4	1	51.5	1	42.9
2	54.5	2	43.2	2	31.0	2	57.8	2	48.5	2	39.6
3	52.0	3	40.6	3	28.3	3	55.2	3	45.7	3	36.6
4	49.8	4	38.2	4	25.8	4	52.8	4	43.1	4	33.8
5	47.6	5	35.9	5	23.5	5	50.5	5	40.7	5	31.3
6	44.6	6	32.6	6	20.2	6	47.5	6	37.3	6	27.6
7	47.6	7	35.9	7	23.5	7	50.5	7	40.7	7	31.3
8	49.8	8	38.2	8	25.8	8	52.8	8	43.1	8	33.8
9	52.0	9	40.6	9	28.3	9	55.2	9	45.7	9	36.6
10	54.5	10	43.2	10	31.0	10	57.8	10	48.5	10	39.6

TABLE 4.4: Pressures at Sprinklers with Increased Supply Diameter (3 in.)

2 in./hr		4 in./hr		6 in./hr	
Node	psi	Node	psi	Node	psi
1	62.7	1	54.2	1	46.0
2	62.2	2	53.7	2	45.5
3	61.1	3	52.6	3	44.3
4	60.0	4	51.5	4	43.3
5	59.0	5	50.5	5	42.3
6	58.9	6	49.9	6	41.7
7	59.0	7	50.5	7	42.3
8	60.0	8	51.5	8	43.3
9	61.1	9	52.6	9	44.3
10	62.2	10	53.7	10	45.5

4.2.4 Electrical Components

As in the existing simulator, the new sprinklers turn on and off via the use of solenoid valves. With the portable design of the new sprinklers, a portable electrical system was required to supply power to the solenoids. For this, a single control box was constructed and wired with ten receptacles for 7-wire trailer hitch plugs. Three toggle switches located at the bottom of the box control the solenoids to the three sprinklers located on each riser. The control box can be moved from plot to plot, and the male ends of the 7-wire trailer plugs were wired to the sprinklers, which can be plugged in and unplugged. Figure 4.7 depicts the portable control box.

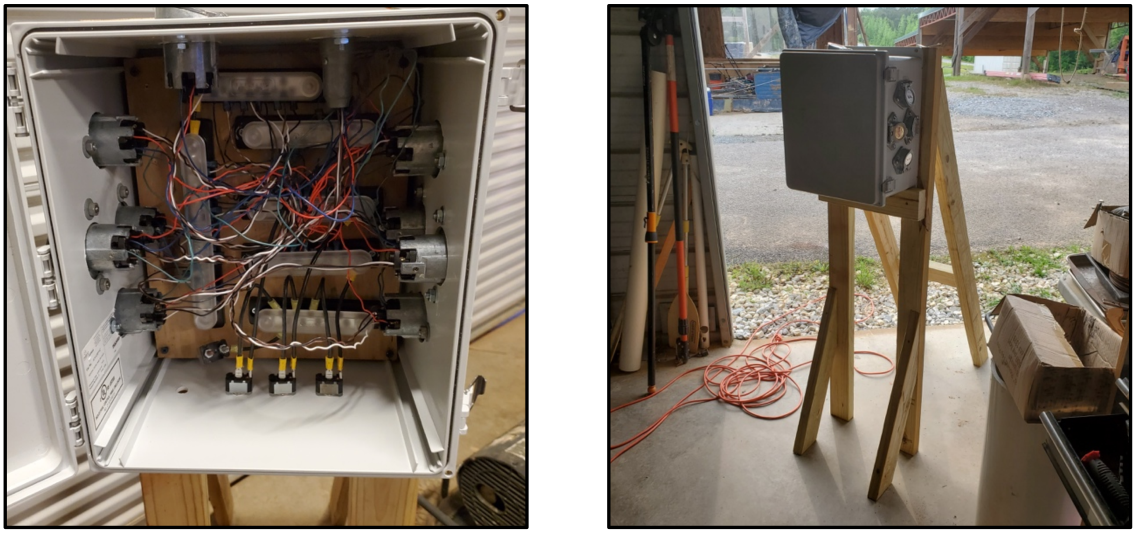

FIGURE 4.7: Electrical Controls

4.3 SOIL SELECTION AND DATA

This section details the extensive soil selection process and includes brief results of all soils tested.

4.3.1 Selection Criteria and Testing Process

The ASTM D6459 standard permits three soil types: sand, loam, and clay. ASTM D6459 defines each soil type with a grain size distribution and plasticity range as reproduced in Table 4.5. The standard provides no references to outside classification systems such as USGS – it solely relies on the criteria listed in Table 4.5. Soil sources were sought which conformed to each of the three categories listed in the standard. Sources investigated included local borrow pits, local trucking company stockpiles, and local construction sites. Figure 4.8 presents all geographical locations in the state of Alabama plus Columbus, Georgia from which samples were taken for this project, marked with stars. In total, twenty-six samples were processed over eleven separate sites in nine locations. The period of investigation last approximately one year.

During that time, when stockpiles remained active, new samples were taken after six months to capture any changes in composition that may have occurred. In such cases the most recent data is presented.

TABLE 4.5: Typical Grain Sizes and Plasticities (ASTM D6459).

Particle size (mm)	Sand	Loam	Clay
D_{100} (mm)	$25 > D_{100} > 3.0$	$10 > D_{100} > 0.3$	$3.0 > D_{100} > 0.02$
D_{85} (mm)	$4.0 > D_{85} > 0.8$	$0.8 > D_{85} > 0.08$	$0.08 > D_{85} > 0.003$
D_{50} (mm)	$0.9 > D_{50} > 0.2$	$0.15 > D_{50} > 0.015$	$0.015 > D_{50} > 0.0008$
D_{15} (mm)	$0.3 > D_{15} > 0.01$	$0.03 > D_{15} > 0.001$	$D_{15} < 0.002$
Plasticity Index	N/A (nonplastic)	$2 < PI < 8$	$10 < PI$

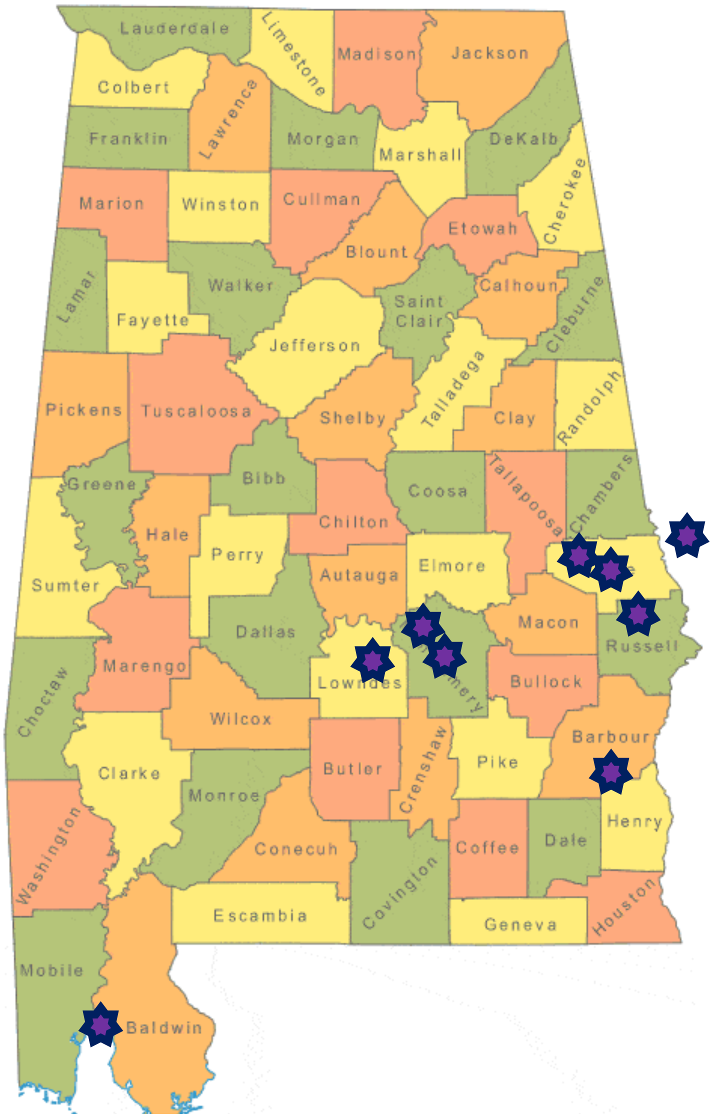

FIGURE 4.8: Regions of Soil Sampling (Geology.com)

The soil analysis procedure was as follows. First, all samples, except the silica and masonry sand samples, underwent a wet sieve on the No. 200 sieve. Typically, 3.5 oz (100g) of sample was used. The sample was saturated with water and the excess was poured into the No. 200 sieve. The sample was continuously rinsed and the water decanted onto the sieve until the water became clear. The No. 200 sieve was rinsed as well. Then, the remaining sample plus the sieve were oven dried, and the mass remaining from both the sample and from the matter retained on the No. 200 were taken as the coarse fraction of the sample. Second, this coarse fraction was subjected to a dry sieve analysis according to *ASTM C136 Standard Test Method for Sieve Analysis of Fine and Coarse Aggregates* (ASTM 2014). From both the wet and dry sieve processes, a grain size distribution (GSD) of the fraction of the sample coarser than 0.003 in. (0.075mm) (fines) could be obtained. If this initial GSD potentially matched up with the ASTM standard given in Table 4.5, the analysis continued. Typically, the wet and dry sieve were both repeated a minimum of twice, unless a clear initial finding eliminated the sample from contention, for example if the D_{100} was clearly too small.

For samples with a potential initial fit, the third step was a hydrometer analysis on the fraction passing No. 200 following *ASTM D7928 Standard Test Method for Particle-Size Distribution (Gradation) of Fine-Grained Soils Using the Sedimentation (Hydrometer) Analysis* (ASTM 2017). Typically, at least two repetitions of the hydrometer analysis were performed. Concurrent with the hydrometer analysis, the fourth step was finding the liquid limit, plastic limit, and plasticity index using *ASTM D4318 Standard Test Methods for Liquid Limit, Plastic Limit, and Plasticity Index of Soils* (ASTM 2019). Again, typically a minimum of two repetitions of the plasticity index test were performed per sample. After hydrometer analysis was complete, the grain size distribution was plotted alongside the ASTM distribution for the soil type it most closely matched. The goal was to obtain a soil whose GSD fit within the upper and lower bounds of the ASTM GSD, and whose plasticity index fell within the bounds presented. Figure 4.9 presents photos of the hydrometer and Casagrande tests.

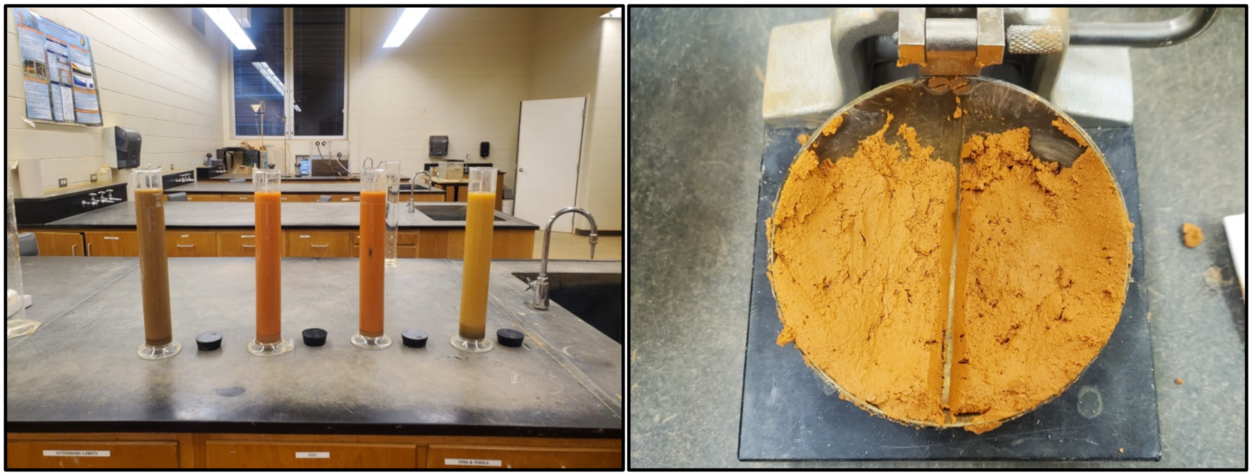

(a) Hydrometer Tests (b) Casagrande Liquid Limit Test

FIGURE 4.9: Soil Testing Examples

Only if soils met all GSD and plasticity criteria were they considered for the final analysis step, the standard Proctor compaction test conforming to *ASTM D698 Standard Test Methods for Laboratory Compaction Characteristics of Soil Using Standard Effort (12,400ft-lbf/ft^3(600 kN-m/m^3))* (ASTM 2012). The Proctor was performed on the final accepted soil for use in each category of sand, loam, and clay. The purpose was to find the soils' maximum dry density for use in percent compaction calculations during future testing and to be able to provide a benchmark for compaction during slope construction. Photos of the final soils selected for sand, clay, and loam after extrusion from the Proctor mold are presented in Figure 4.10. Six data points were collected to construct the curve for each soil.

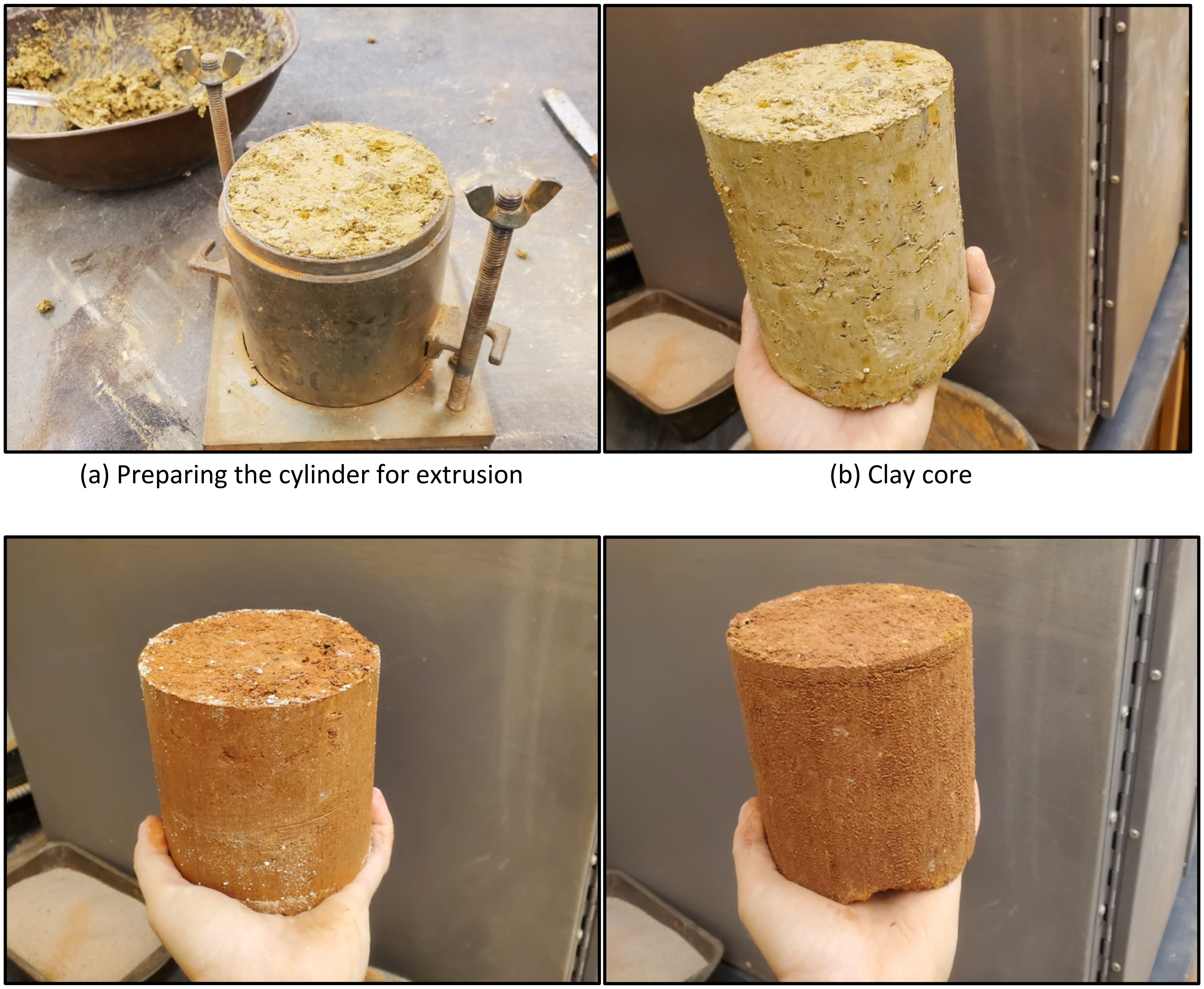

(a) Preparing the cylinder for extrusion
(b) Clay core
(c) Loam core
(d) Sand core

FIGURE 4.10: Proctor Compaction

In addition to matching the ASTM standard, the GSD was used to classify each soil according to the USDA Soil Texture Triangle. The Triangle classifies soils relative to three categories of soil particle size: Sand as defined by particles with diameters ranging from 0.08in. to 0.002 in. (2mm to 0.0625 mm), silt between 0.002 in. and 0.00008 in. (0.0625 mm and 0.002mm), and clay less than 0.00008 in. (0.002mm) (USDA 2012). Each classification is defined by the percentage of sand, silt, or clay particles that comprise it. The Soil Texture Triangle is shown in Figure 4.11.

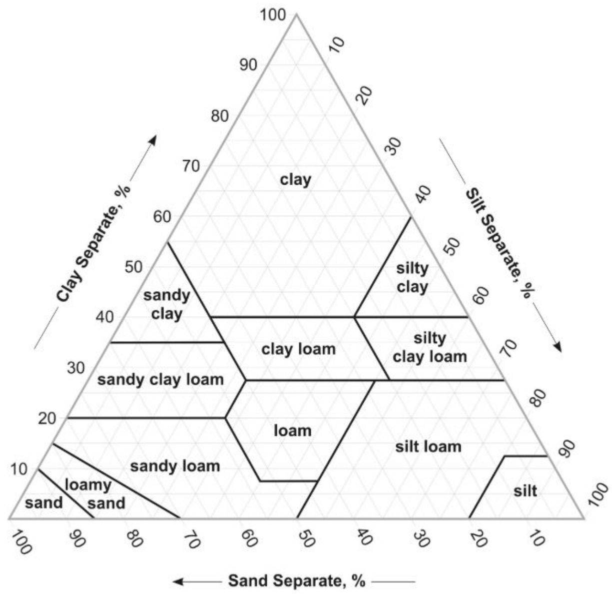

FIGURE 4.11: Soil Texture Triangle (USDA 2012)

4.3.2 Sand Testing and Results

Seven samples were tested for potential sand fit. Three samples were from the coastal plains soils region of Alabama: one sample was from a borrow pit in the Mobile area and two, one with a slightly more red color and one slightly more tan, from a pit in the Dothan area. The rest were artificial: one a milled silica product from the US Silica plant in Hurtsboro, one a concrete sand from Thompson Carriers in Opelika, and two different sandy materials from M and M Trucking in Auburn. One additional sample originally tested for loam fit the sand GSD, but contained too much plasticity to qualify. Because samples were difficult to find locally, and ultimately the sample that did work was expensive to truck, a masonry sand/topsoil blend from M and M was considered but ultimately rejected due to a potential plasticity concern. The mixture had been designed to fit the sand GSD criteria with a ±16% margin of error for both components during field mixing. Ultimately, only the red-hued sample from the Dothan area both fit the GSD and tested as non-plastic and so was selected for use. Figure 4.12 presents the results for the sand testing, showing the GSD as compared with the ASTM standard and listing the USDA classification and plasticity index. The ASTM upper and lower bounds are depicted by dashed lines and the soil GSD is depicted by the solid line. Also presented in Figure 4.13 are photos demonstrating the failure of the selected soil at the plastic limit test, verifying the soil's nonplasticity, and presented in Figure 4.14 is the soil's Proctor compaction curve.

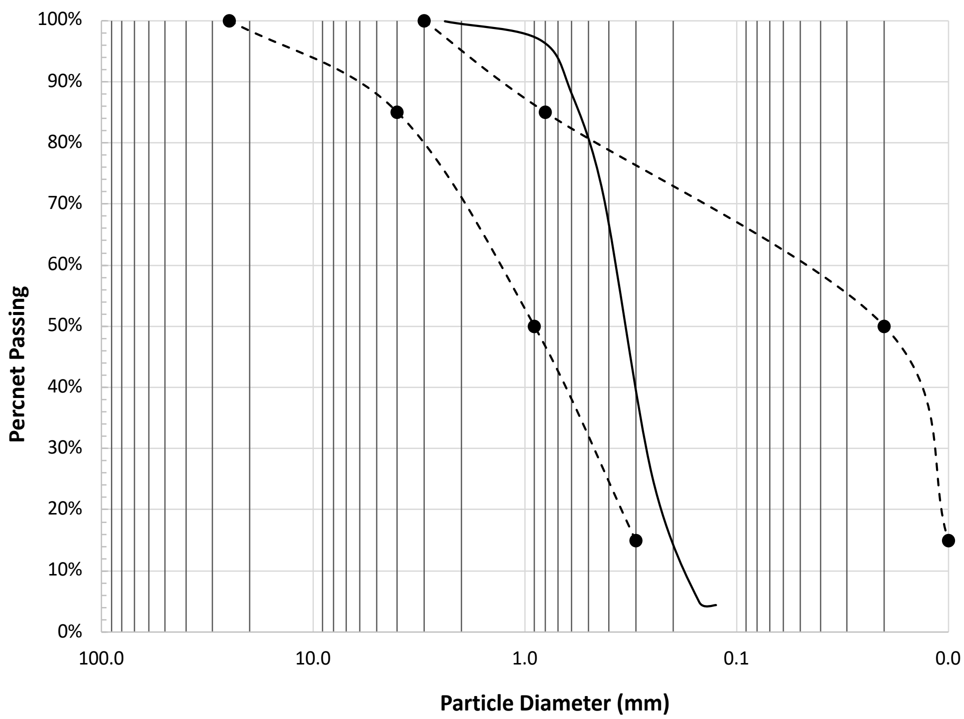

(a) GSD Thompson Sand
USDA: Sand
Plasticity: Nonplastic

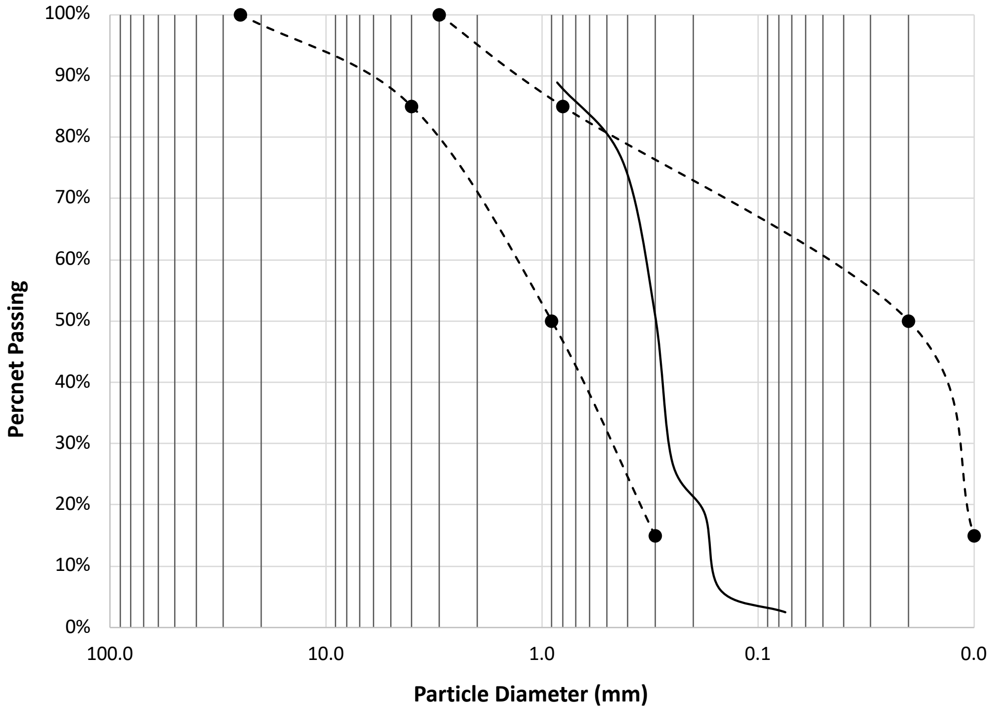

(b) GSD M and M Tan Sand
USDA: Sand
Plasticity: Nonplastic

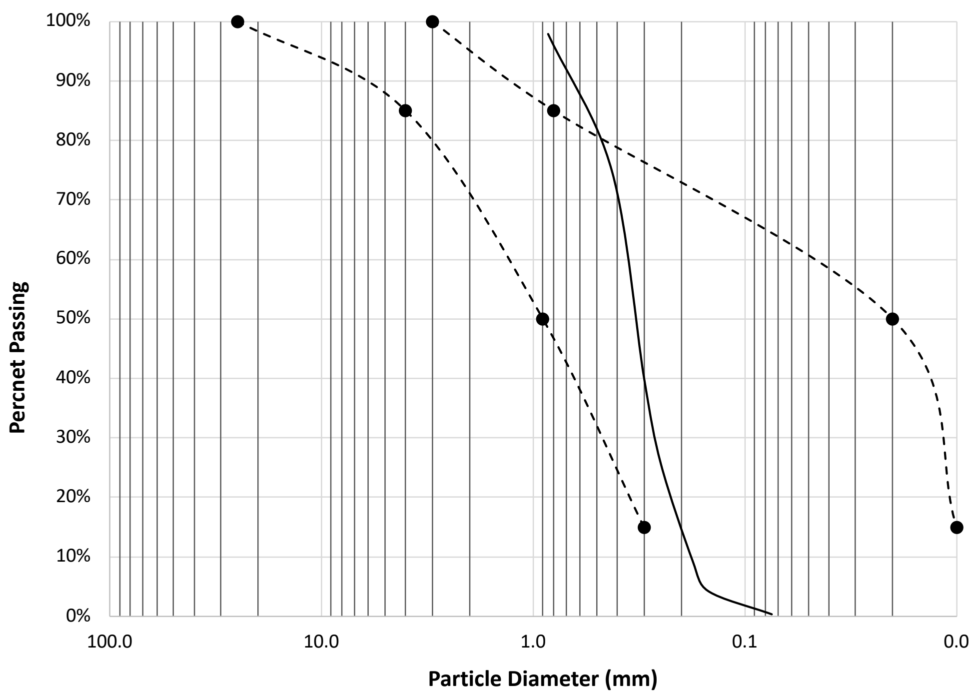

(c) GSD M and M White Sand
USDA: Sand
Plasticity: Nonplastic

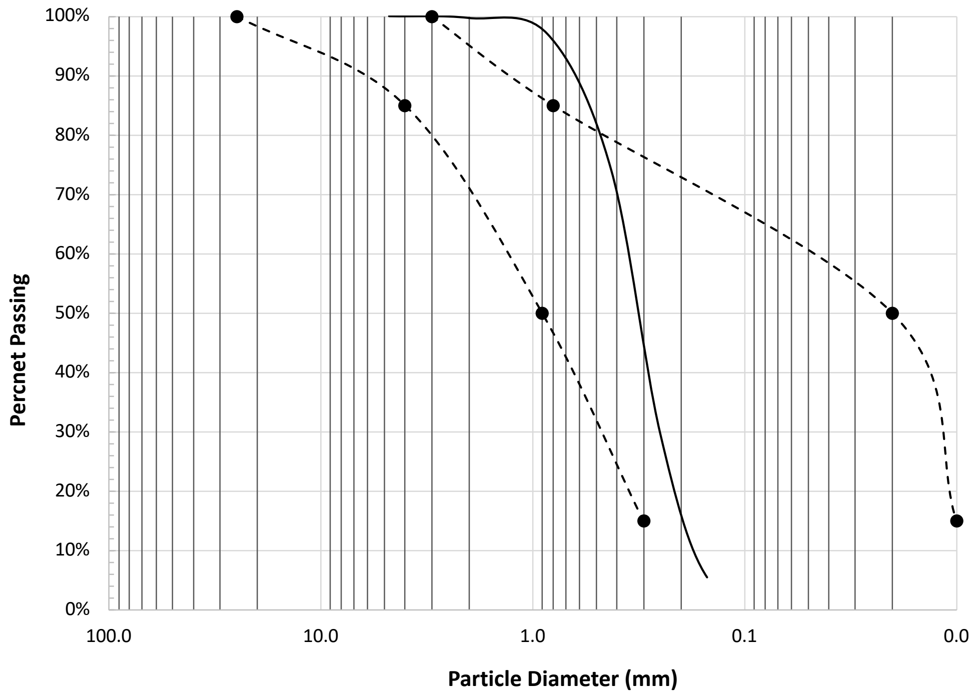

(d) GSD Mobile Sand
USDA: Sand
Plasticity: Nonplastic

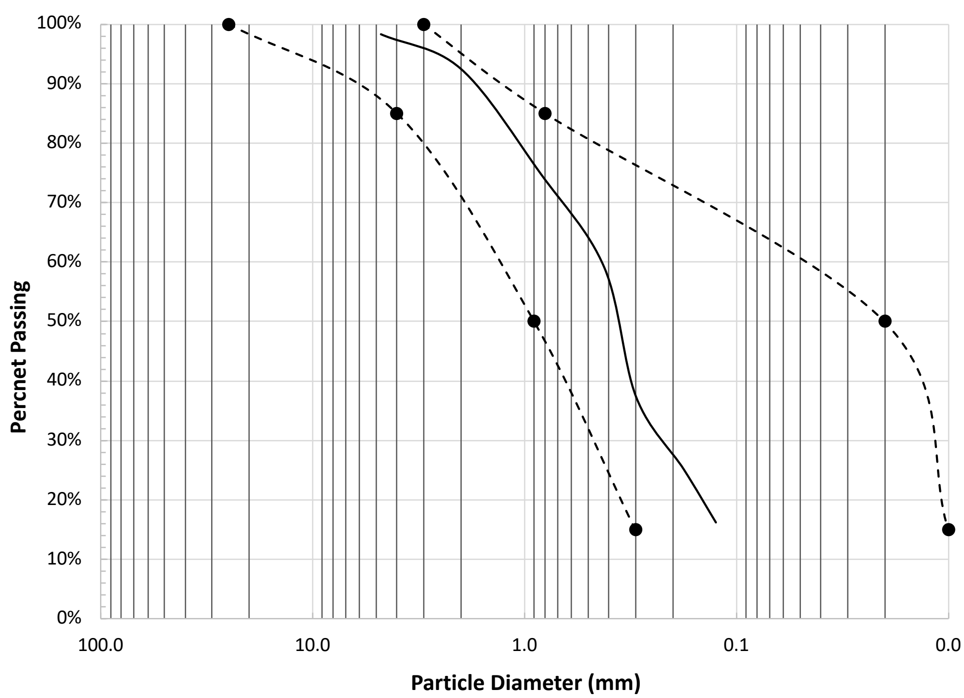

(e) Dothan Area Tan Sand
USDA: Sand or loamy sand
Plasticity: Nonplastic

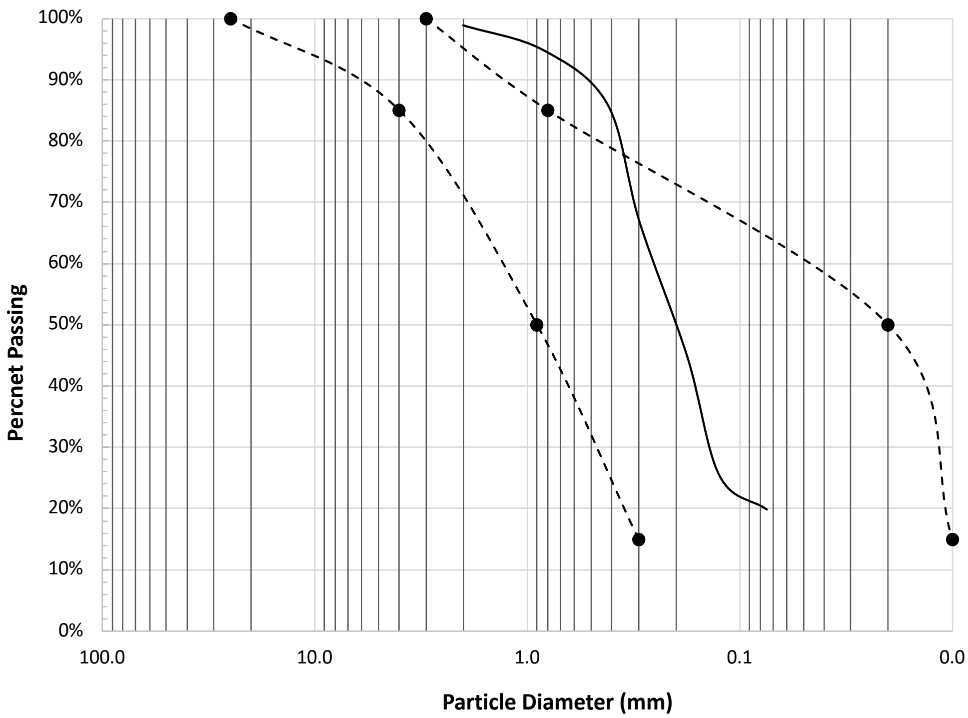

(f) Dothan Area Red Sand
USDA: Sand or loamy sand
Plasticity: Nonplastic

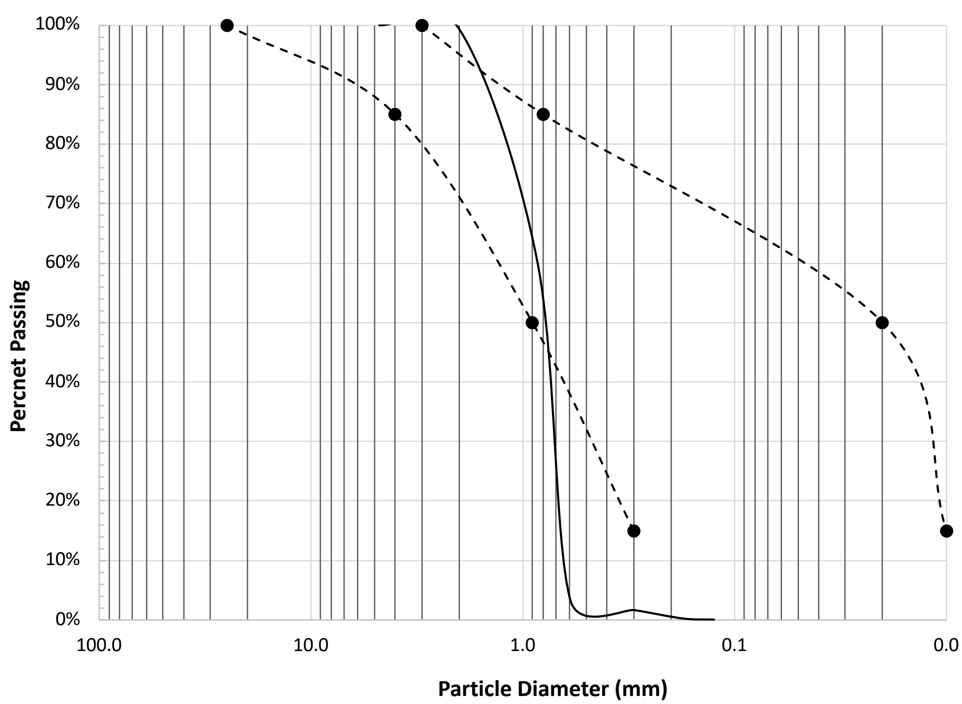

(g) US Silica Sand
USDA: Sand
Plasticity: Nonplastic

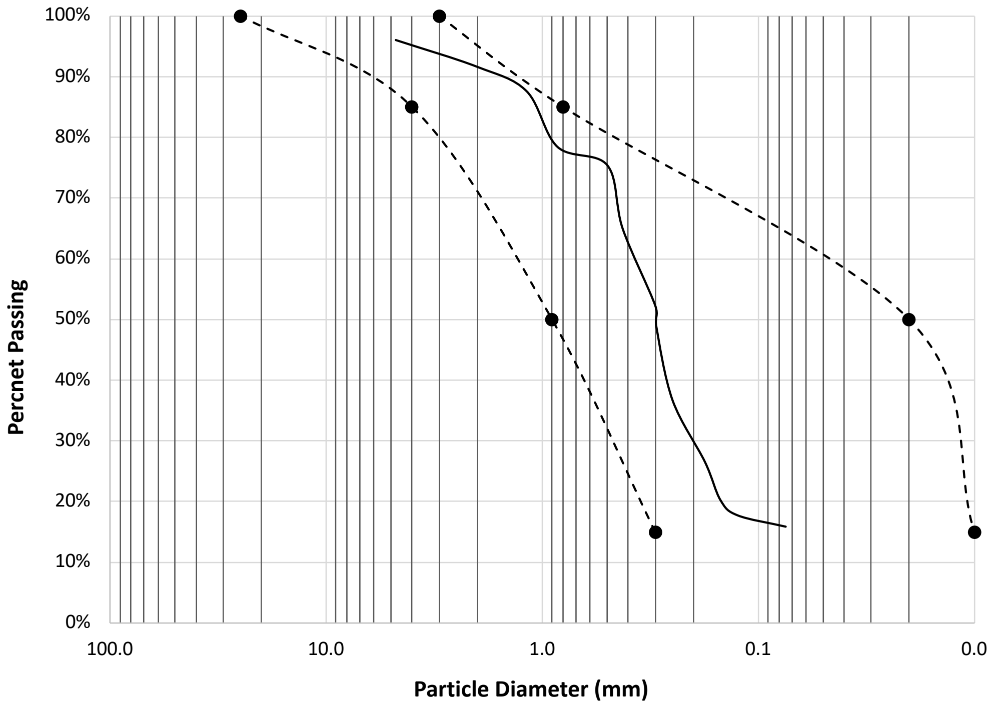

(h) Sand/Topsoil Blend
USDA: Sand
Plasticity: 3

FIGURE 4.12: Soil Testing Results for Sands

(a) Drier soil crumbled (b) Wetter soil smeared

FIGURE 4.13: Plasticity Failure Demonstration

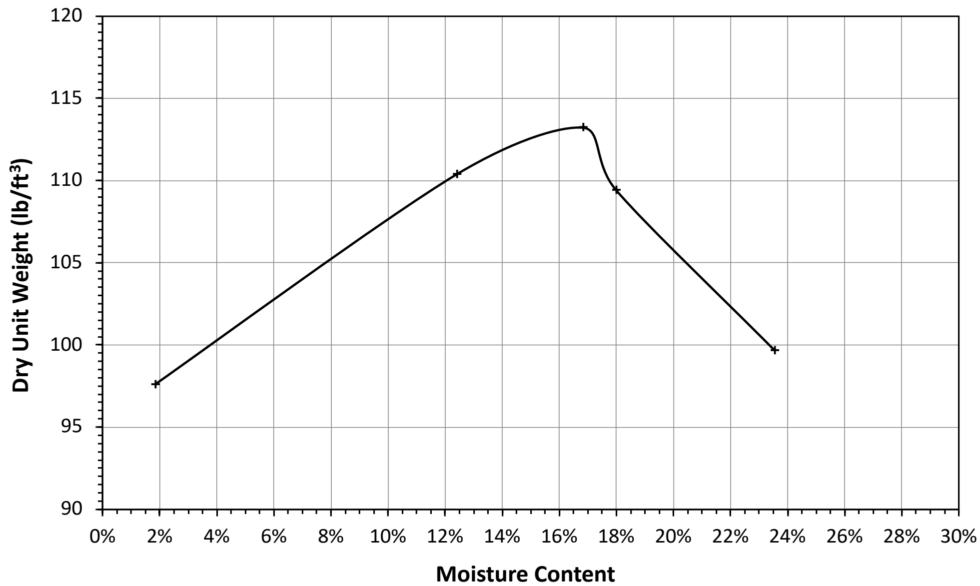

FIGURE 4.14: Proctor Compaction Curve, Sand (Max Dry Unit Weight 133.2 pcf)

4.3.3. Loam Testing and Results

Fifteen sample were tested for loam fit, most in the immediate area surrounding the AU-Stormwater Research Facility. Two samples were obtained from borrow sources less than three miles from the facility, one from a construction site in Lee County, two from Columbus, Georgia, two from borrow sources south of Montgomery, three from the facility expansion construction, and five from a trucking company in Auburn. Two primary problems were encountered when pursuing a loam source: either soils in the area typically classified as a sandy loam, with one or more parameters fitting just slightly outside of requirements, or soils tested as highly colloidal and failed to obtain a D_{15} during hydrometer analysis. The detection limit of the hydrometer test is 0.00008 in. (0.002mm), so samples whose D_{15} fell below that threshold were impossible to reliably classify without more sophisticated measures. Even if a D_{15} were obtained the minimum D_{15} requirement for loam is 0.00004 in. (0.001mm) so these soils would have failed the ASTM criteria regardless. One sample from Columbus met the GSD for loam but tested slightly too plastic, and one sample from local carrier Thompson Trucking met the GSD but was not plastic enough. Another soil matched closely but was not immediately selected due to a high presence of gravel. During the window of soil testing, the AU-Stormwater Research Facility underwent an expansion, a portion of which accommodated the new construction of Phase II of the *ALDOT Rainfall Simulator* project. Two excavated strata were sampled during construction, one in the dam area and one from spoils from a retention pond. The sample from the dam area tested as loam but was not set aside due to lack of quantity. Later, after earthmoving was complete and plot construction was set to commence on the plots for Phase II, samples were taken in situ from the new rainfall simulator areas. Five replicates were taken from the area and all fit the ASTM loam criteria. Thus, it was decided to leave the soil in place for the loam plots. Spoil material from the plot construction, namely from re-grading, plot excavation, and basin excavation, was set aside in stockpiles for later use in testing. Figure 4.15 presents the loam testing results in the same style as Figure 4.12, and Figure 4.16 presents the compaction curve.

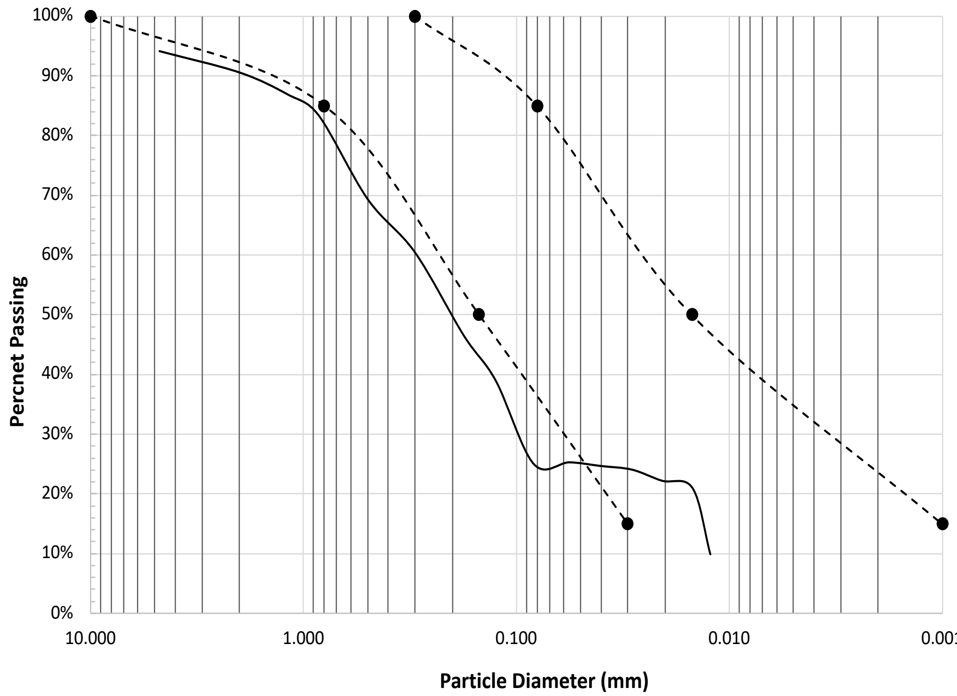

(a) M and M Trucking Tan Stockpile
USDA: Sandy clay loam
Plasticity: Not tested

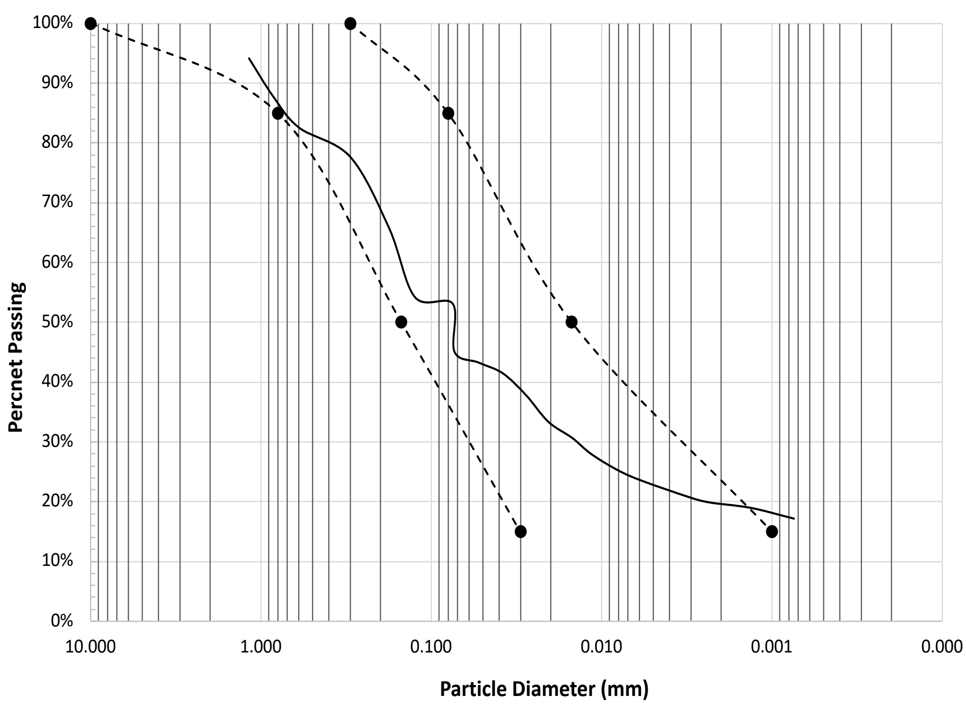

(b) M and M Trucking Red Stockpile
USDA: Sandy Loam
Plasticity: Not tested

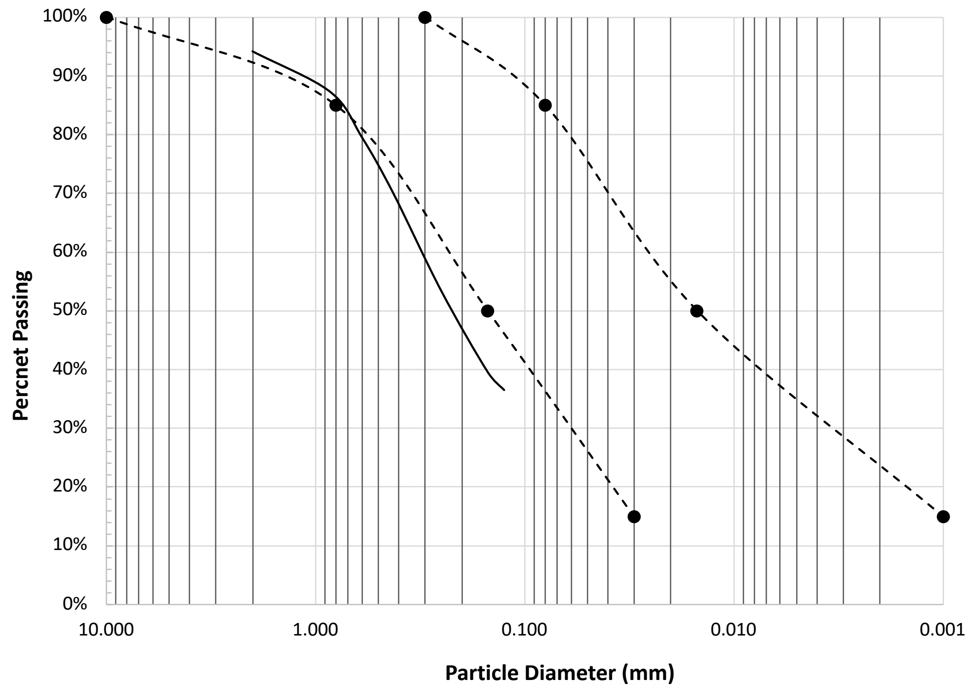

(c) M and M Trucking Stockpile No. 1
USDA: Not known
Plasticity: Not tested

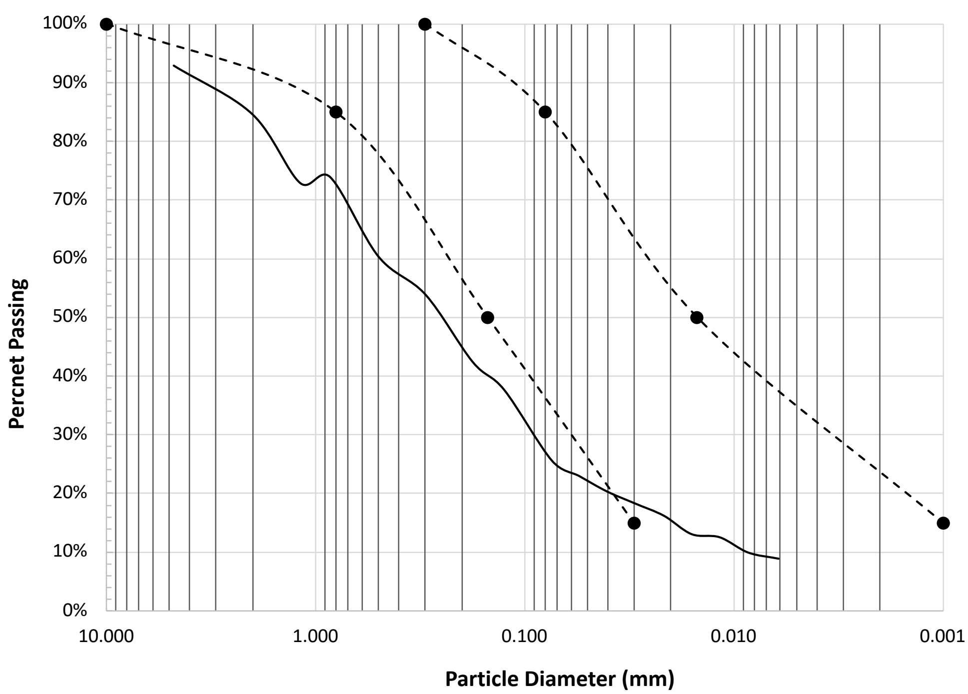

(d) M and M Trucking Stockpile No. 3
USDA: Sandy Loam
Plasticity: 3

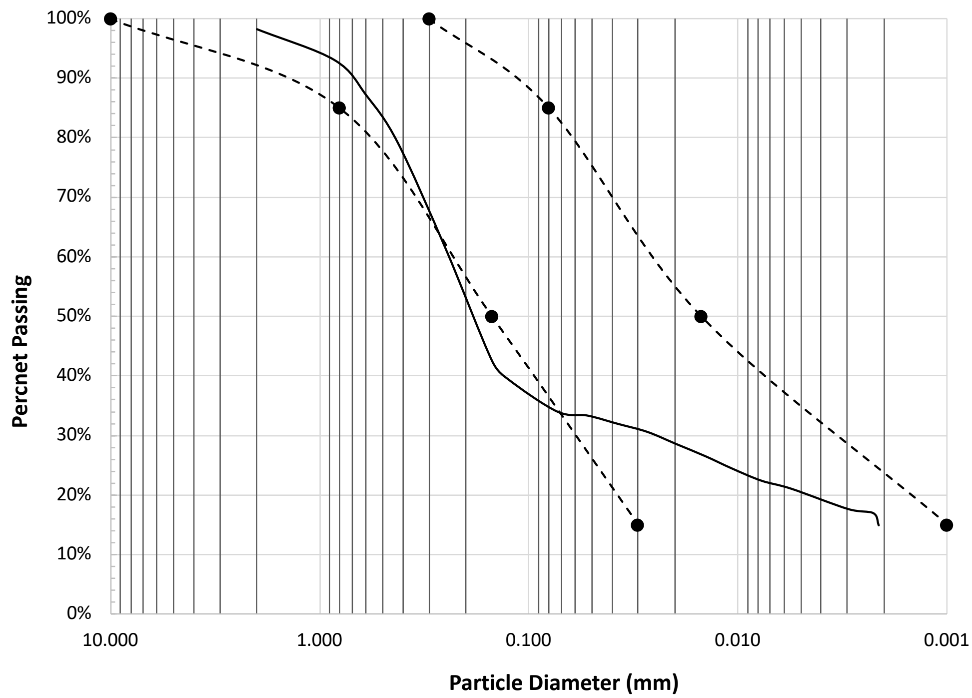

(e) M and M Trucking Stockpile No. 4
USDA: Sandy Loam
Plasticity: Not tested

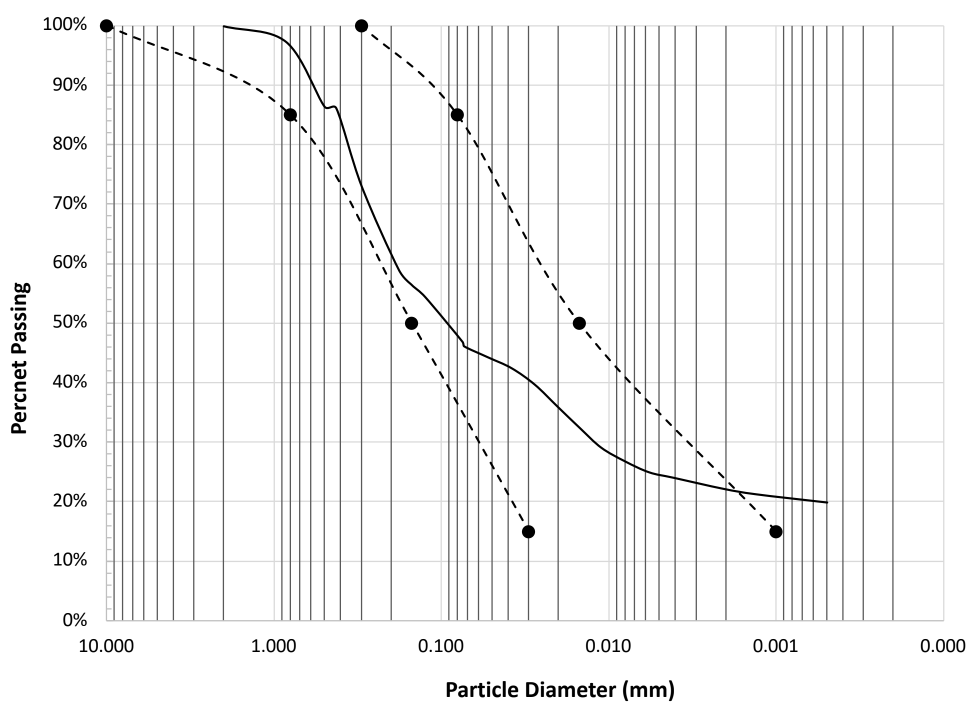

(f) Pro-South Excavation Tan Sample
USDA: Sandy clay loam
Plasticity: Not tested

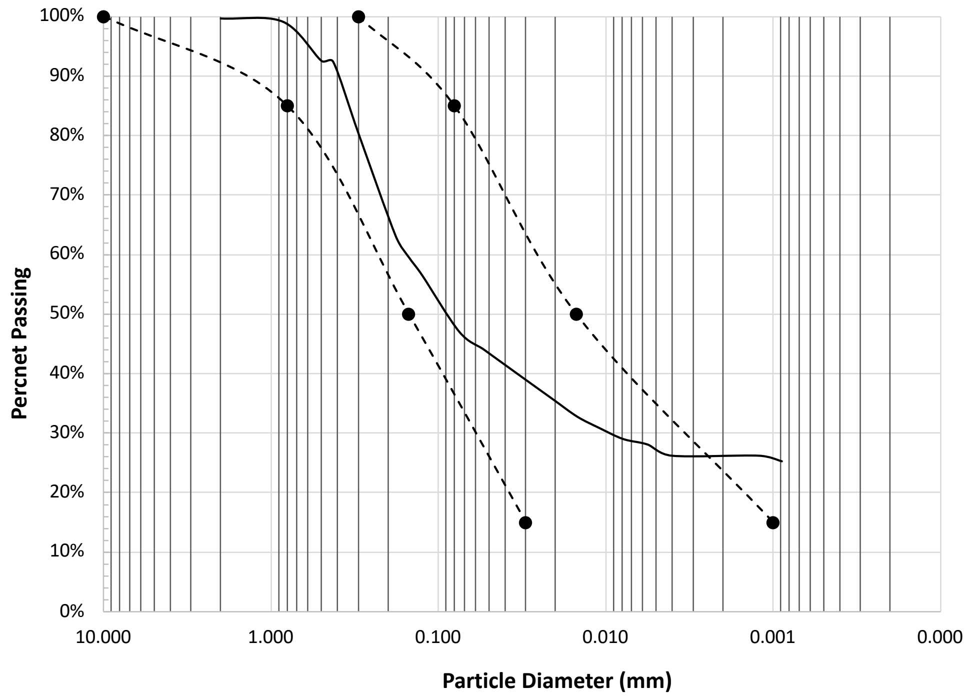

(g) Pro-South Excavation Red Sample
USDA: Sandy clay loam
Plasticity: 5

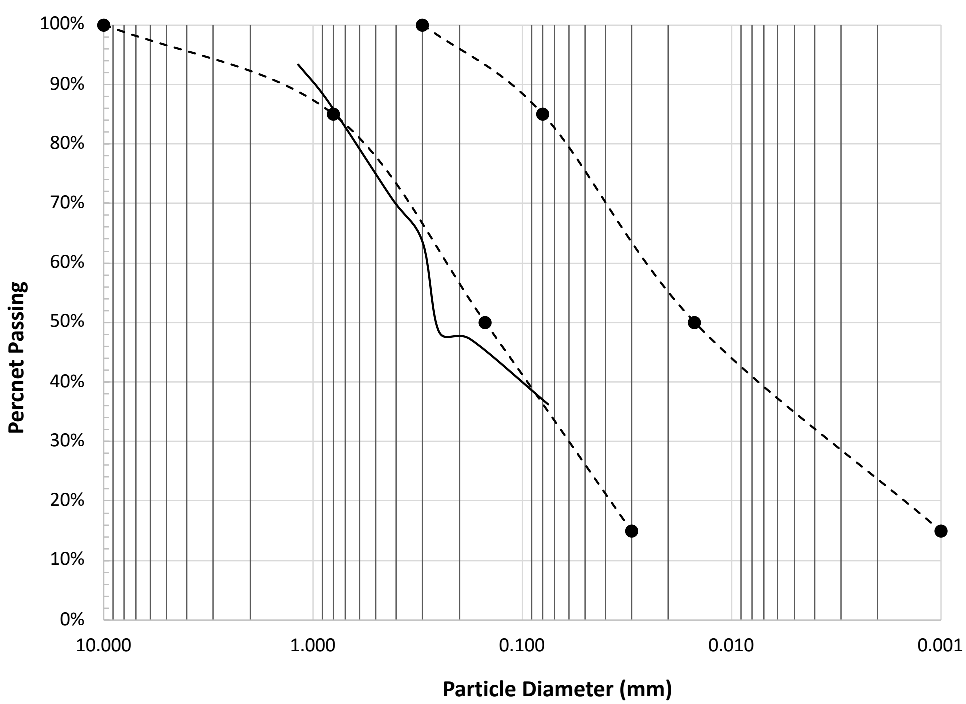

(h) Lee Road, Columbus
USDA: Not known
Plasticity: Not tested

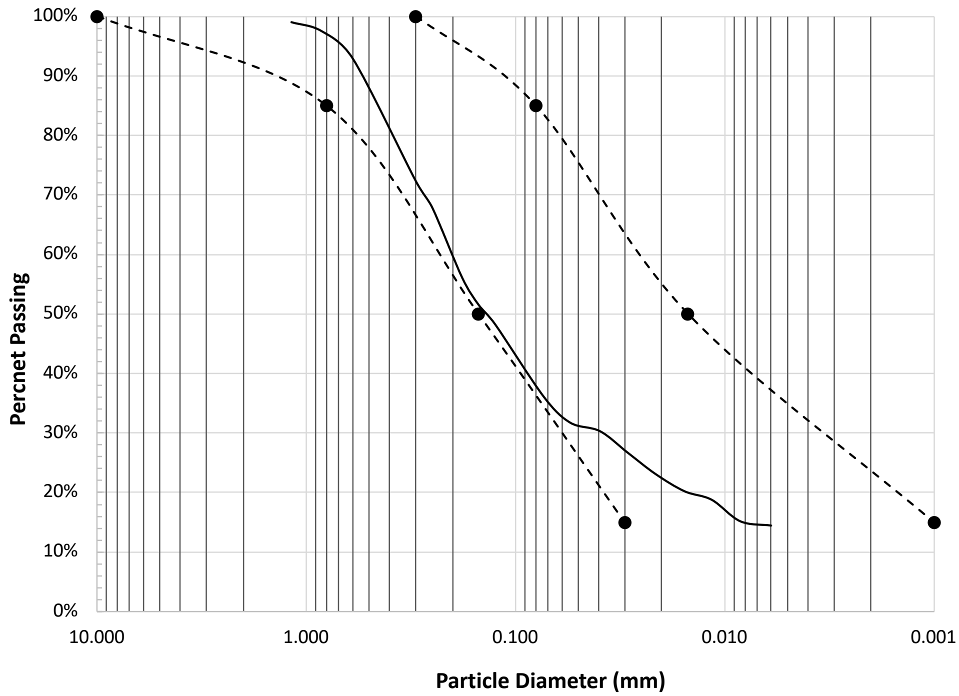

(i) Red Clay, Columbus
USDA: Silt loam
Plasticity: 9

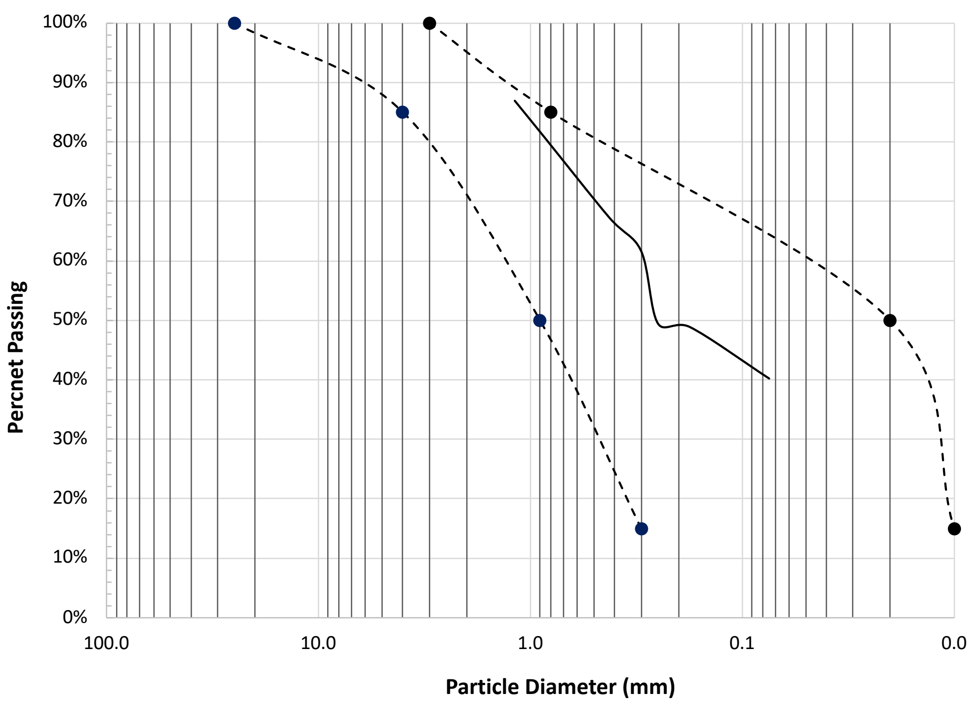

(j) Thompson Stockpile
USDA: Silt loam
Plasticity: 0

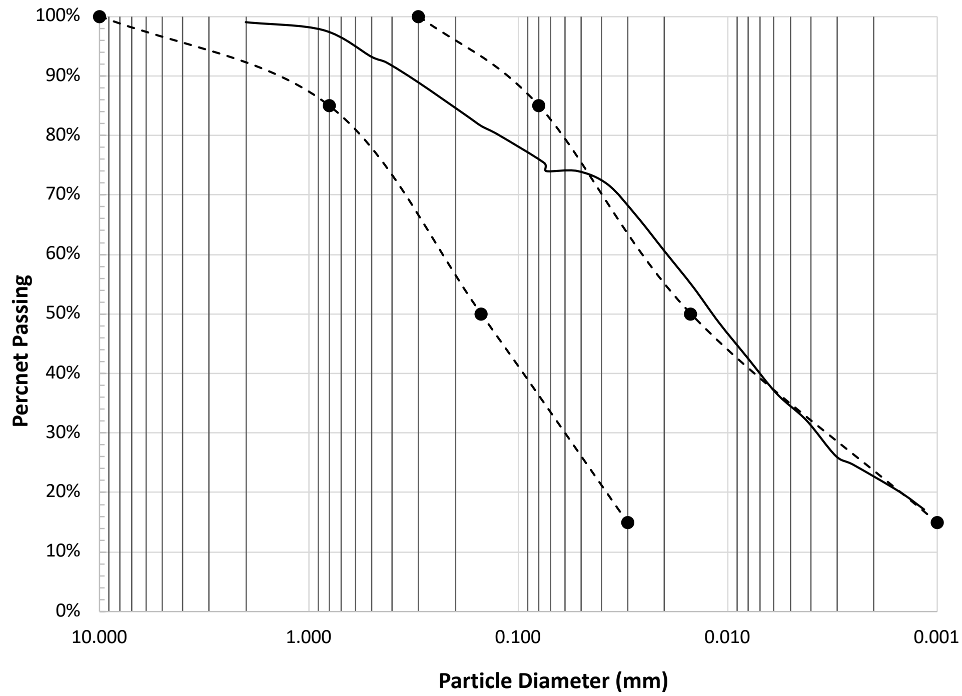

(k) Thompson Borrow Source
USDA: Silt loam
Plasticity: 5

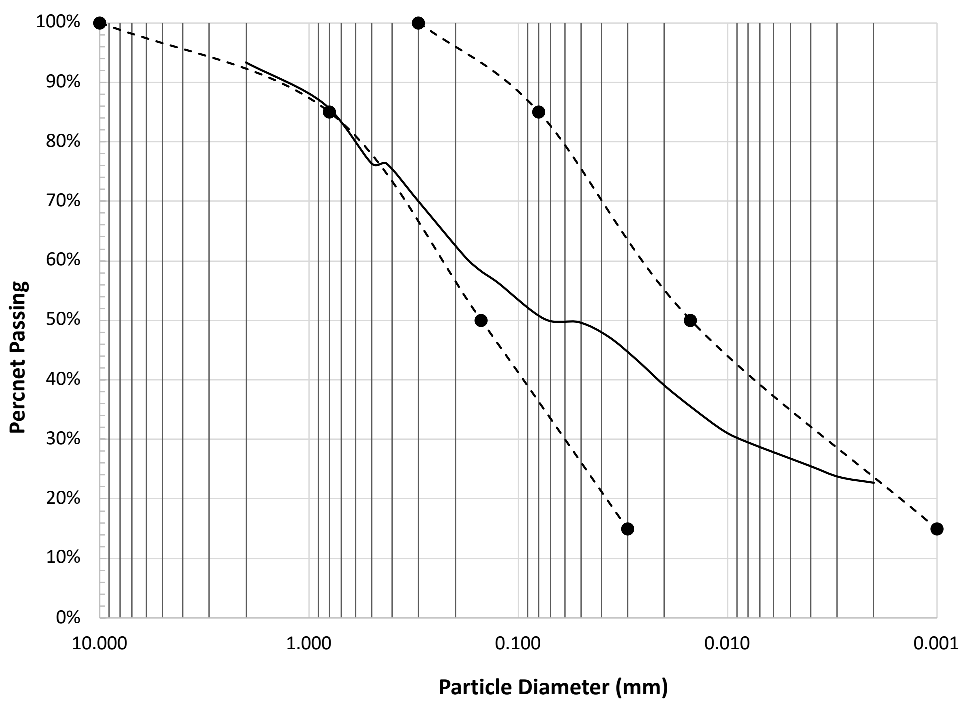

(l) Budweiser Site
USDA: Sandy clay loam
Plasticity: 7

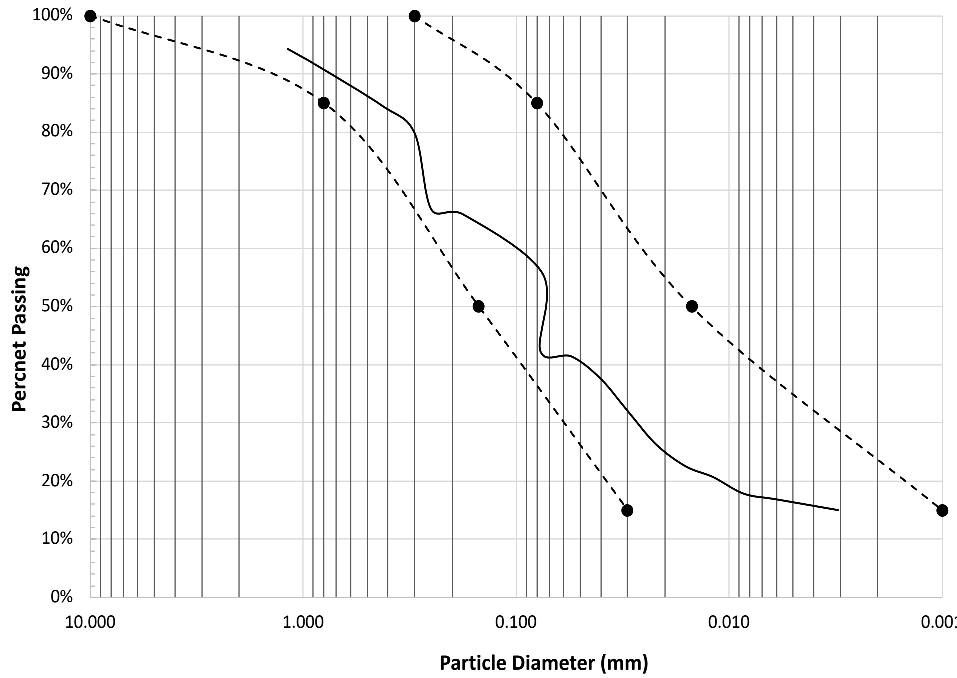

(m) Facility Expansion Dam
USDA: Sandy loam
Plasticity: 8

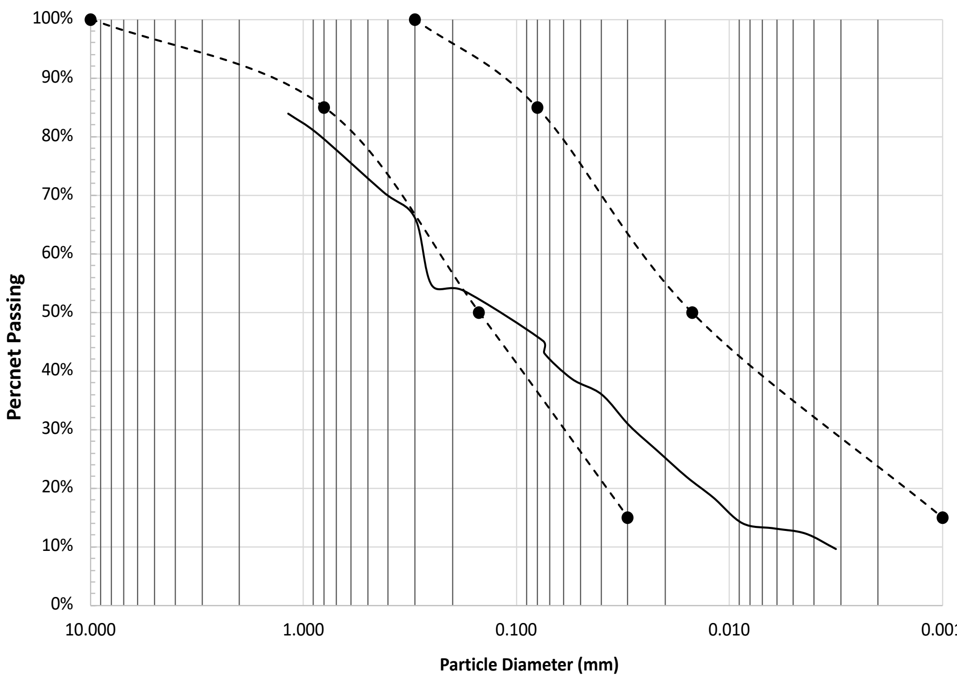

(n) Facility Expansion Retention Pond
USDA: Sandy loam
Plasticity: Not known

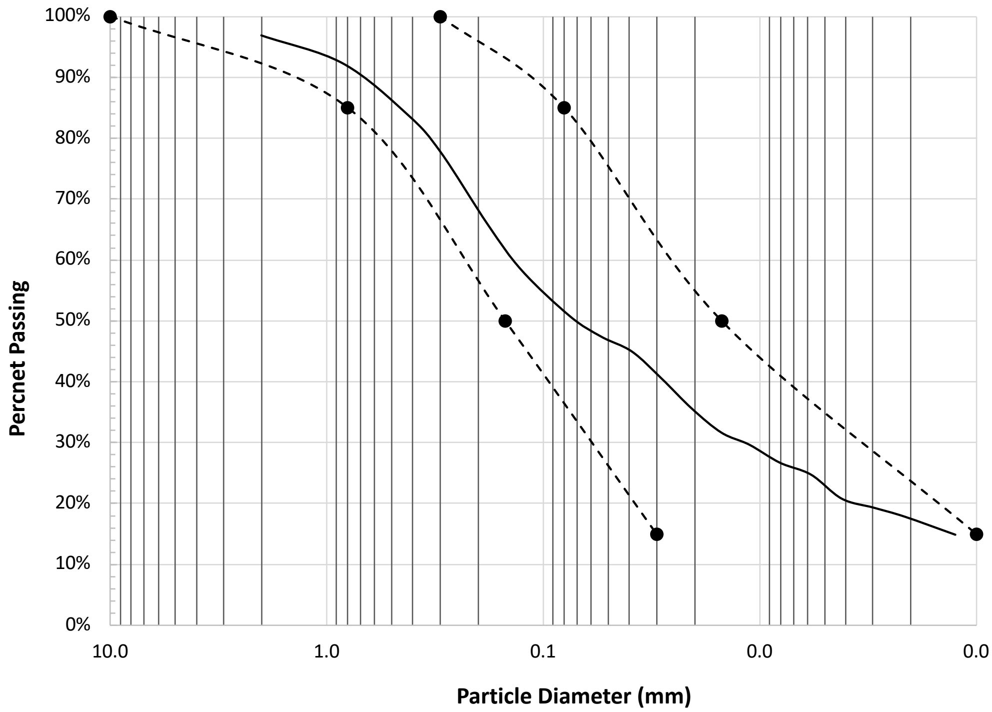

(o) In Situ Sample from Facility (Upper area plot 5)
USDA: Loam
Plasticity: 8

FIGURE 4.15: Soil Testing Results for Loams

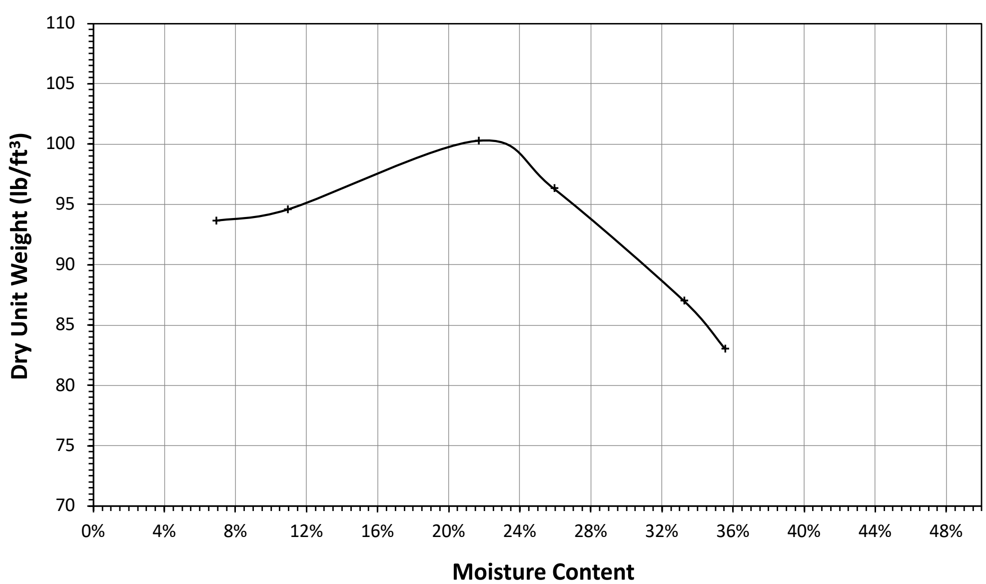

FIGURE 4.16: Proctor Compaction Curve, Loam (Max Dry Unit Weight: 100.3 pcf)

4.3.4. Clay Testing Results

Three samples were tested for potential clay fit. All were from the Blackland Prairie soils region of Alabama, from sites close to the Montgomery area. All were highly plastic, and the soil selected was from the grey-white vein that runs throughout the Blackland Prairie region known as “prairie”. Because all soils were so fine grained, three repetitions of the hydrometer test were performed for each. Figure 4.17 presents the clay testing results. Figure 4.18 presents the Proctor compaction curve.

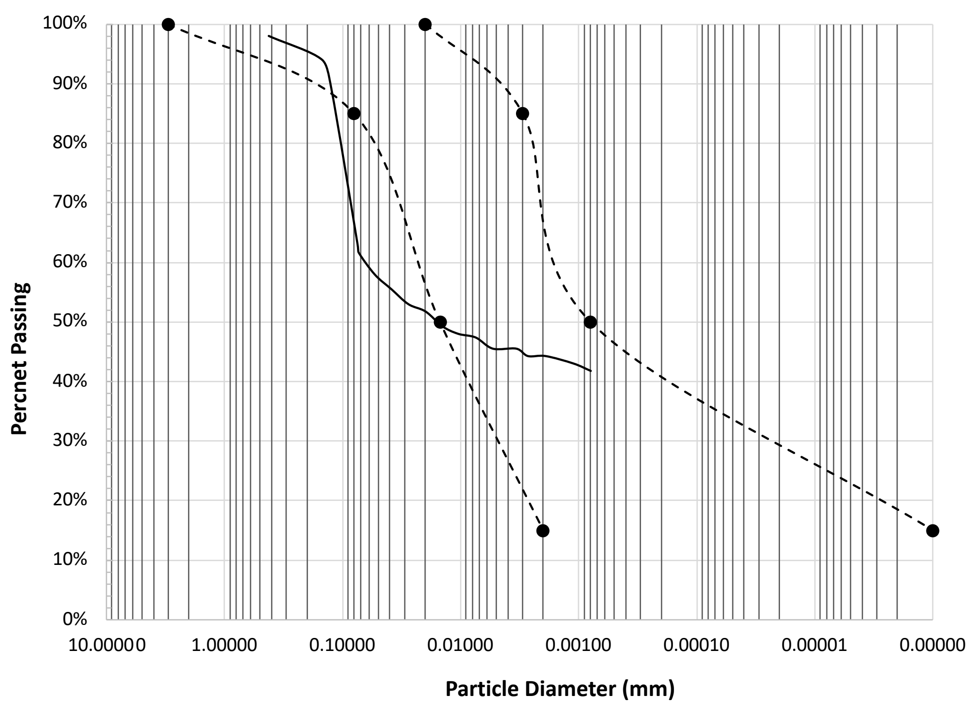

(a) Holly Henley Site Clay
USDA: Clay
Plasticity: 40

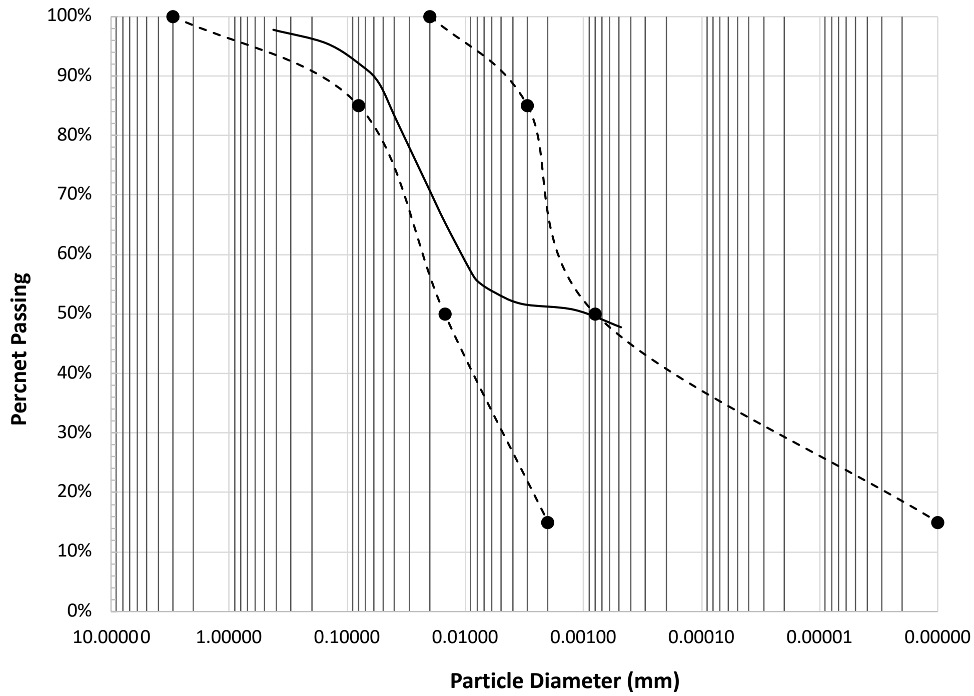

(b) Stone Martin Site Clay
USDA: Clay
Plasticity: 40

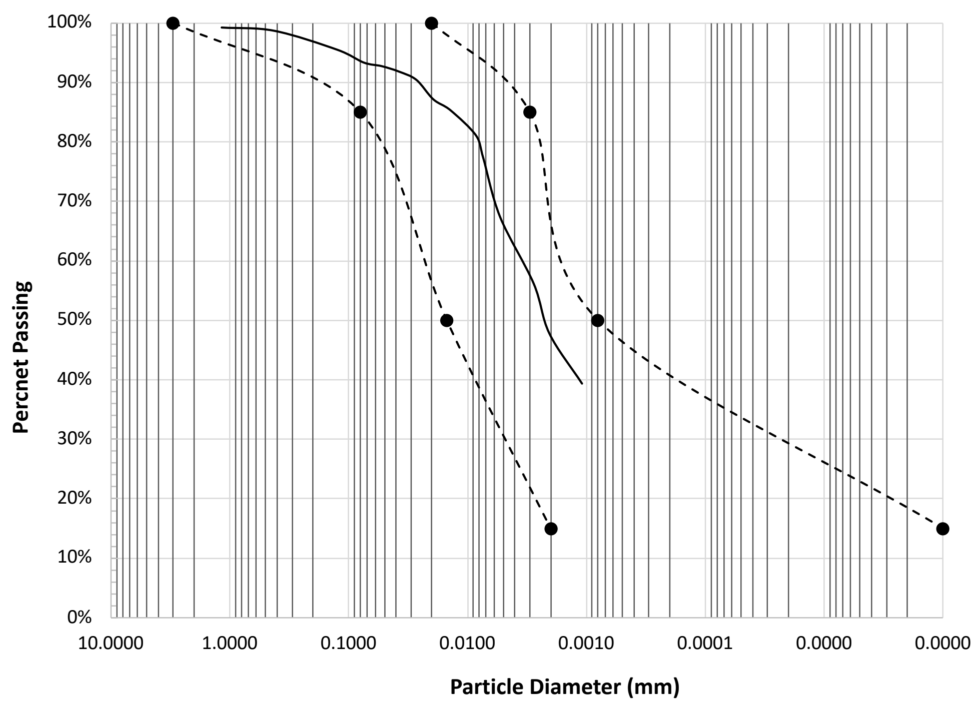

(c) Stone Martin Site Prairie
USDA: Silty Clay/Clay Border
Plasticity: 23

FIGURE 4.17: Soil Testing Results for Clays

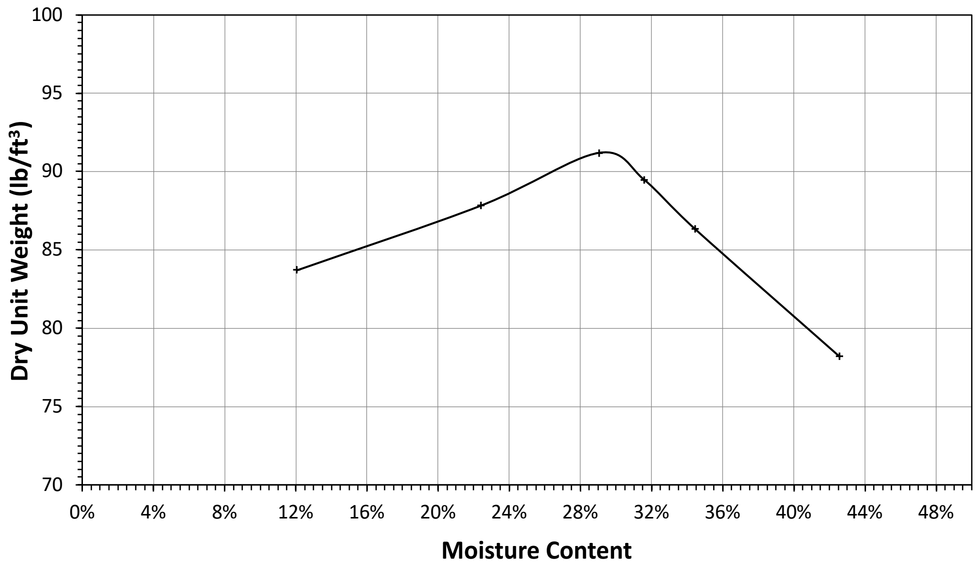

FIGURE 4.18: Proctor Compaction Curve, Clay (Max Dry Unit Weight: 92.0 pcf)

4.4 CONSTRUCTION METHODS AND RESULTS

This section describes the construction process for the Phase II simulators and all progress that was made as part of the work of this thesis.

Earthmoving commenced at the AU-Stormwater Research Facility expansion area in July 2020 under the direction of Dr. Mike Perez, Dr. Wesley Donald, and Blake Whitman. After initial earthmoving was complete, simulator construction could commence, but the degree of outstanding Phase I tasks prohibited focusing on construction exclusively until March 2021. It was decided to focus on completion of one trial plot, referred to as Plot 1, before proceeding with the remaining eleven. This “trial plot” allowed best methods and processes to be identified before replication. Indeed, several major design parameters and processes were altered after lessons learned on the trial plot. The flow chart presented in Figure 4.19 was created to aid in sequencing construction tasks on Plot 1, from earthmoving to preliminary calibration. Plumbing tasks are listed in blue, soils tasks in pink, electrical tasks in yellow and sprinkler assembly tasks in grey.

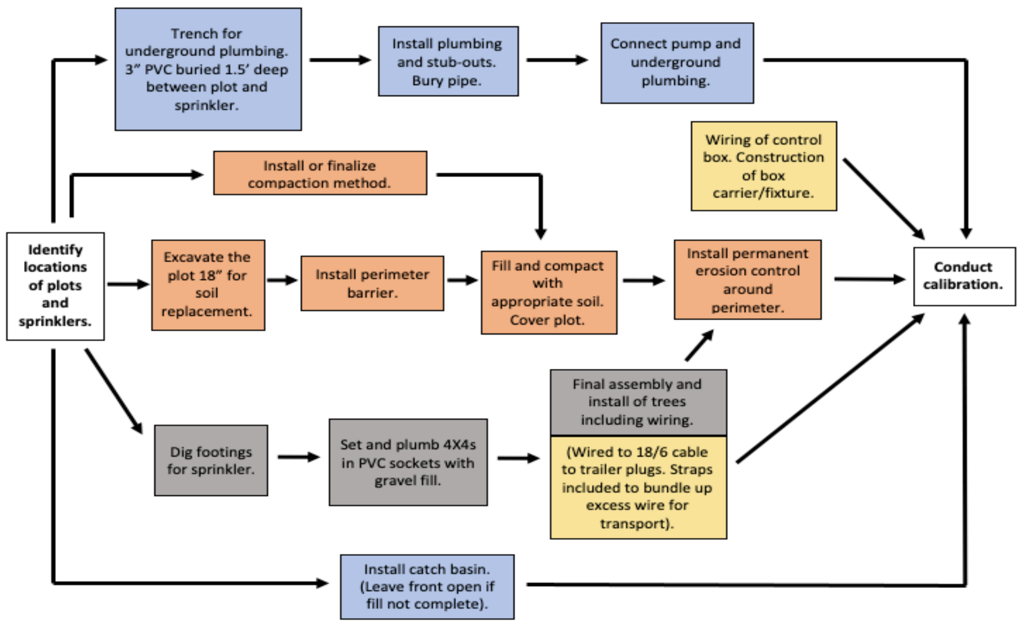

FIGURE 4.19: Construction Tasks Flow Chart, Plot 1

For Plot 1, the underground plumbing was installed prior to plot excavation. The footings and PVC sleeves were also dug and installed for the sprinklers around all plots, because extra labor was available and the task was not predicted to interfere with later tasks. Figure 4.20 shows a run of underground plumbing on Plot 1 and a CAD detail of the stub outs.

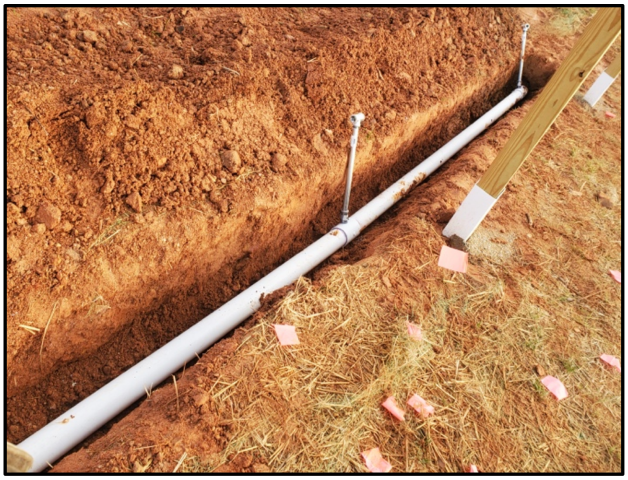

(a) Underground plumbing plot 1

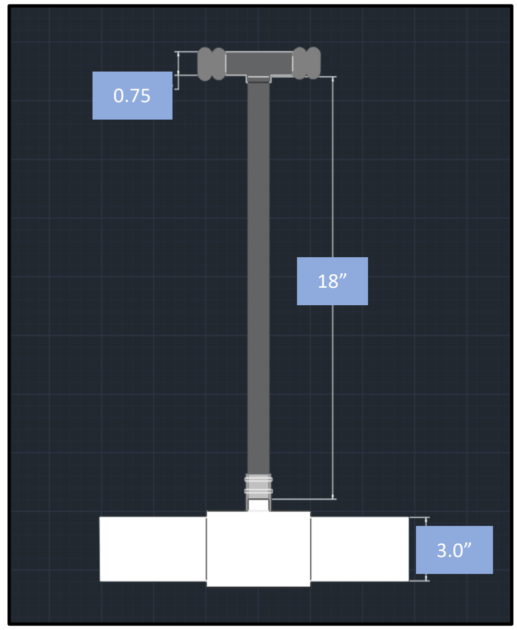

(b) Stub out detail

FIGURE 4.20: Plumbing Detail

Excavation began after backfilling the plumbing. For Plot 1, a builder’s level was used to mark correct elevations on stakes along the plot boundary. Rough excavation was performed with a mini excavator, then fine grading was done by hand to a level of 18” below correct grade. For the trial plot, barriers composed of plywood and landscape edging were placed at the correct grade at the plot boundary to demarcate the soil matrix. Clay soil was then introduced with a skid steer in three – 6 in. (15.2 cm) lifts, graded with the excavator and then by hand after dumping, and compacted with a plate compactor after each lift. After the plot was complete, the side slopes were stabilized against erosion with a seed and fertilizer mixture formulated for the soil along with erosion control blankets. A 750-gallon (2,839 liter) plastic tub was installed below-grade for the catch basin. Figure 4.21 depicts the process.

(a) Plot excavated and ready for fill

(b) Earth ramp for skid steer

(c) Distributing soil after a lift

(d) Compaction after first lift

(e) Finished first plot, lower view

(f) Finished first plot, upper view

FIGURE 4.21: Plot 1 Construction Process

Figure 4.22 illustrates the process for construction of a later plot, one of the 4:1 sand plots.

(a) Installing the second lift

(b) Spreading the soil

(c) Compacting the final lift

(d) Finished plot

FIGURE 4.2*2*: Sand Plot Construction Process

For the loam plots, where the soil was left in place, approximately 18 in. (45.7cm) of soil was tilled with the excavator and rocks and organic debris removed by hand. Then the tilled soil was raked and compacted with a plate compactor. Final grade was typically approximately 6 in. (15.2cm) too low at the top of the plots and a few inches too high at the bottom, likely due to erosion since earthmoving a year prior. Therefore, prior to compaction of the in-situ soil, soil was removed from the bottom of the slopes, and additional soil was added at the low locations taken from spoil piles from adjacent plot's excavation. The demarcation boards were placed by excavating the sides of the plot with the mini excavator, placing the boards with stakes at the proper heights, and backfilling. After lessons learned from the trial plot, for the remaining plots the plywood board method of demarcating the boundaries was replaced with a series of 2x12 boards held together with wood gusset plates for the purposes of additional rigidity, strength, and ease of maintaining proper dimensions. Additionally, the builder's level method was replaced with the total station for increased accuracy of dimensions and elevations. Figure 4.23 illustrates a loam plot undergoing initial preparation and also a panorama of all six 4:1 plots. In total, final earthmoving was completed on all six 4:1 plots as part of the work of this thesis including excavation, boundary demarcation, soil placement and compaction. Permanent erosion stabilization of side slopes was achieved on four plots, and three catch basin and French drain systems were installed.

(a) Loam plot undergoing grading (b) 4:1 Plots – panorama during construction

FIGURE 4.23: Loam Plots and All 4:1 Plots

After a heavy rain, the catch basin in Plot 1 experienced tank flotation, a phenomenon where excess pore pressure in the surrounding soil causes an underground tank to rise out of the ground. It was thought that excessive runoff from the impervious area above the rainfall simulators, an area of approximately 180,000 ft^2 (16,723 m^2), contributed to the problem, so a small diversion channel and berm was constructed at the top of the simulator area covering approximately 400 linear feet (123 m) and draining into the upper retention pond. Later, immediately after a rainstorm, heavy flow was observed running over the rip rap channel into the upper retention pond, indicating that the diversion channel was effectively diverting runoff. In addition, to counteract any possible expansive potential of the soil, the floated tank was removed and a French drain system installed around its base with #57 stone, heavy-duty geotextile fabric, and 6 in. (15.2 cm) perforated pipe. The pipe was encased by the stone approximately two feet (0.6 m) below the lip of the basin and the whole assembly wrapped with the fabric. A 6 in. (15.2 cm) base layer of gravel was added underneath the basin and fabric, and the drain daylighted to grade approximately 30 ft (9.1 m) from the basin. Later, after running the simulator for approximately an hour and a half during a calibration run, flow was observed from the drain, indicating that the drain was effectively diverting runoff. It is believed therefore that these two measures have solved the flotation problem. Figure 4.24 illustrates the problem and solution.

(a) Tank flotation (b) Flow from daylight of French drain

FIGURE 4.24: Basin Flotation and French Drain Flow

Permanent funnel boards for sampling and portable basin covers were created for each individual plot, as can be seen in Figure 4.25. A compaction setup was devised for re-compacting slopes after testing and rebuilding, since the ASTM standard allows only a drum roller for this task. A cradle attachment for the skid steer was ordered that can hold a trailer winch. The skid steer and winch may then be situated the top of the slope to tow the four feet (1.2m) turf roller up and down the slope, as was done on the existing rainfall simulator. The setup was intended to be an improvement over the system on the existing simulator due to the portability. Figure 4.26 displays the setup.

(a) Funnel board (b) Basin cover

FIGURE 4.25: Funnel Boards and Basin Covers

FIGURE 4.26: Compaction Setup

4.5 PRELIMINARY CALIBRATION METHODS AND RESULTS

Preliminary calibration was performed on Plot 1. Even though the water delivery configuration was changed after Plot 1 construction, the permanent underground plumbing supply already installed on the plot was still utilized in order to obtain a benchmark and to identify any potential problems. Calibration efforts were hampered by water supply problems in the upper retention pond. The pond began to display infiltration problems, failing to hold sufficient water to operate testing, especially with other high-volume demand from neighboring research projects. In some cases, water was pumped from the lower retention pond several hundred feet away through a series of hoses and pumps, but this turned out to be an untenable long-term solution due to too much head demand on the pumps and insufficient intermediate holding capacity. As required by the ASTM standard, three types of data were collected: intensity, uniformity, and drop size distribution.

4.5.1 Intensity and Uniformity

To obtain intensity and uniformity, five rounds of simulations were run with 15 minutes at each intensity (2, 4, and 6, in./hr [5.1, 10.2, and 15.2 cm/hr]). A series of 20 rain gages were installed on the plot, sectioning the plot into a grid of 20 equally divided areas. Figure 4.27 shows the rain gage configuration. Intensity was simply calculated as the average amount of rain measured in each gage at the end of each 15-minute period multiplied by four. Pressure readings were also taken at each sprinkler riser during each simulation. Uniformity was measured by the Christensen Uniformity Coefficient (CUC), denoted by Equation 4.5. While not ideal, the CUC was above 70%, the minimum typically accepted threshold, and greater than in some studies (for example, Kavian et. al 2019). Thus, the uniformity was considered to be satisfactory - however, it was much less than previously obtained uniformity in the calibration for the existing plot. The intensity displayed more variability than desired. Previously obtained standard deviations were less than 0.10 in. (0.25 cm) and the current results obviously surpass this. Thus, the simulators require additional verification going forward. Table 4.6 presents the data and compares it to the previously obtained results for the existing simulator.

(a) Layout for calibration (b) With additional center row

FIGURE 4.27: Rain Gage Layout for Plot 1 Calibration

TABLE 4.6: Preliminary Calibration Data, Intensity and Uniformity

Current Results					
Avg. Intensity, in./hr (cm/hr)		**Standard Deviations, in./hr (cm/hr)**		**Christiansen Uniformity Coefficient**	
2 in./hr	2.4 (6.1)	**2 in./hr**	0.32 (0.81)	**2 in./hr**	70.6
4 in./hr	3.9 (9.9)	**4 in./hr**	0.48 (1.22)	**4 in./hr**	77.1
6 in./hr	5.8 (14.7)	**6 in./hr**	0.60 (1.52)	**6 in./hr**	71.0
Previous Results					
Avg. Intensity, in./hr (cm/hr)		**Standard Deviations, in./hr (cm/hr)**		**Christiansen Uniformity Coefficient**	
2 in./hr	2.1 (5.3)	**2 in./hr**	0.04 (0.10)	**2 in./hr**	85.7
4 in./hr	4.1 (10.4)	**4 in./hr**	0.06 (0.15)	**4 in./hr**	87.5
6 in./hr	6.1 (15.5)	**6 in./hr**	0.07 (0.18)	**6 in./hr**	87.5

To gain more insight into why the intensity data may be variable, pressure readings were correlated with intensity for each of the five simulations. Depending on the amount of surface head available in the pond, pressure readings differed. For the last two rounds the throttle on the pump was turned up or down to determine whether power to the system influenced pressure and rain gage readings. A correlation coefficient was obtained relating pressure and intensity. Table 4.7 presents the results. As evidenced, no correlation was found between pressure in the system and intensity due to the high correlation coefficients with inconsistent signs. This is likely due to the action of the 6 psi pressure regulators at each sprinkler. At the range of pressures tested here, they probably maintained a constant pressure at the sprinkler heads despite differences in pressure in the pipe, which is what they are designed to do. Minor irregularity was observed when surface head to the pump was very low but was difficult to quantify. To aid in future data collection, an additional row of rain gages was added down the center of the plot. See Figure 4.27.

TABLE 4.7: Correlation Between Pressure and Intensity

2 in./hr (5.1 cm/hr)	-0.84
4 in./hr (10.2 cm/hr)	0.50
6 in./hr (15.2 cm/hr)	-0.31
Overall	-0.50

4.5.2 Drop Size Distribution and Energy

For drop size distribution, the flour pan method was used as called for in the ASTM standard. In this method, regular, all-purpose flour was placed in a 10 in. (25.4 cm) aluminum pie pan and struck off to make a level surface. The pans were exposed to the rainfall in the simulation for four seconds. One sample was taken at the top third of the slope, one in the middle, and one at the bottom third of the slope for each of the three intensities, for a total of nine samples. The flour was allowed to air dry overnight and then the pellets formed by the water were sifted out and oven-dried at 212°F (100° C) for two hours. The hardened pellets were then run through a standard dry sieve analysis to separate by size, and then the number of pellets on each individual sieve was counted and weighed. Figure 4.27 illustrates the lab analysis. Data processing for the flour pan test was as follows. Average mass per drop was obtained by dividing the total weight on the sieve by the number of drops in Equation 4.8

$$Mass\ per\ Drop = \frac{Total\ Drops}{Total\ Mass} \qquad (4.8)$$

Mass ratio for each sieve size was then be determined with Equation 4.9

$$M_R = (0.038) * \ln\left(W_{avg}\right) + 1 \qquad (4.9)$$

The average diameter is then given in Equation 4.10

$$D_{avg} = \sqrt[3]{\frac{6}{\pi} * W_{avg} * M_R} \qquad (4.10)$$

An adjusted pellet weight was found by multiplying the total weight on each sieve by its mass ratio, and an adjusted mass percentage was found by dividing adjusted pellet weight on each sieve by the aggregate adjusted pellet weight. Fall velocity was determined using the regression relationship in Equation 4.11, depicting the relationship between size and velocity at a height of 15 ft (4.6 m)

$$y = -0.1667x^2 + 1.8235x + 2.8602 \quad (4.11)$$

Where *x* represents raindrop size in mm and *y* represents fall velocity in m/s. For the final energy calculation, total rainfall mass was found by multiplying each intensity by the test plot area by the density of water. Then, the weight of rainfall on each sieve could be found by multiplying the total rainfall mass by the adjusted mass percentage. With this information, kinetic energy of each sieve is available from the standard kinetic energy equation in Equation 4.12

$$KE = \frac{1}{2}mv^2 \qquad (4.12)$$

Total kinetic energy, or *E* in the RUSLE equation, was then determined by applying Equation 4.13, with inputs in US standard units, to each sieve and summing the results for all sieves. This *E* is the number to be used in RUSLE calculations during future product testing on the simulators.

$$E = \frac{KE}{\frac{Plot\ Area}{43560}} \quad (4.13)$$

Table 4.8 presents the raindrop size and fall velocities and Figure 4.29 presents the size distribution per intensity in chart form. According to the ASTM standard, no more than 10% of drops should be smaller than 0.04 in. (1.0 mm) and no more than 10% greater than 0.24 in. (6.0 mm). As evidenced by Table 4.8, the drop size distribution meets this ASTM criteria and so can be said to be satisfactory. The table also compares drop size results to previous results. The new results show a more equal distribution of drop sizes in the 2 in./hr (5.1cm/hr) and 4 in./hr (10.2cm/hr) intensities but a more concentrated distribution than previous in the 6 in./hr (15.2 cm/hr). Table 4.9 presents energy information and compares it to the results of the existing rainfall simulator. The goal was to obtain an *E* similar to the one obtained previously. As evidenced, the energy in the 6 in./hr (15.2 cm/hr) data was substantially higher than previously recorded. This is mathematically related to the more concentrated drop size distribution at a higher diameter than the previous results. It is not believed that excess pressure or wind may have contributed, although it certainly could have been the case. It is also not known how much of a deviation is acceptable, or how accurate the first results were. The previous calibration had only been run once, and therefore a measure of variability or accuracy was not possible. Going forward it is recommended to re-do the flour pan test for at least the 6 in./hr (15.2 cm/hr) intensity. It is also advised to repeat the entire flour pan test at least a few times to gain information on the typical variability of this test.

FIGURE 4.28: Flour Pan Testing

TABLE 4.8: Raindrop Size and Velocity

Current Results			Previous Results		
2 in/hr (5.1 cm/hr)			**2 in/hr (5.1 cm/hr)**		
Average Drop Size in. (mm)	**Mass Percentage**	**Fall Velocity ft/s (m/s)**	**Average Drop Size in. (mm)**	**Mass Percentage**	**Fall Velocity ft/s (m/s)**
0.20 (5.0)	6%	25.6 (7.8)	0.24 (6.1)	4%	25.6 (7.8)
0.13 (3.3)	29%	23.3 (7.1)	0.15 (3.8)	55%	24.2 (7.4)
0.09 (2.3)	8%	20.3 (6.2)	0.09 (2.5)	10%	20.9 (6.4)
0.07 (1.8)	33%	18.5 (5.6)	0.07 (1.8)	19%	18.4 (5.6)
0.05 (1.2)	12%	15.7 (4.8)	0.05 (1.2)	9%	15.8 (4.8)
0.04 (1.0)	12%	15.0 (4.6)	0.04 (0.9)	2%	14.4 (4.4)
4 in/hr (10.2 cm/hr)			**4 in/hr (10.2 cm/hr)**		
Average Drop Size in. (mm)	**Mass Percentage**	**Fall Velocity ft/s (m/s)**	**Average Drop Size in. (mm)**	**Mass Percentage**	**Fall Velocity ft/s (m/s)**
0.25 (6.4)	9%	25.3 (7.7)	0.21 (5.3)	10%	25.7 (7.8)
0.13 (3.2)	31%	22.8 (6.9)	0.14 (3.5)	61%	23.7 (7.2)
0.10 (2.5)	14%	21.0 (6.4)	0.10 (2.6)	8%	21.2 (6.5)
0.07 (1.8)	31%	18.2 (5.5)	0.08 (2.00	11%	19.1 (5.8)
0.05 (1.2)	10%	15.8 (4.8)	0.05 (1.2)	7%	15.8 (4.8)
0.04 (0.9)	5%	14.4 (4.4)	0.04 (0.9)	3%	14.3 (4.4)
6 in/hr (15.2 cm/hr)			**6 in/hr (15.2 cm/hr)**		
Average Drop Size in. (mm)	**Mass Percentage**	**Fall Velocity ft/s (m/s)**	**Average Drop Size in. (mm)**	**Mass Percentage**	**Fall Velocity ft/s (m/s)**
0.23 (5.8)	3%	25.7 (7.8)	0.23 (5.8)	9%	25.7 (7.7)
0.14 (3.6)	60%	23.9 (7.3)	0.15 (3.7)	46%	23.9 (7.3)
0.10 (2.5)	13%	21.0 (6.4)	0.09 (2.3)	46%	20.2 (6.2)
0.07 (1.8)	16%	18.3 (5.6)	0.07 (1.8)	16%	18.2 (5.5)
0.06 (1.6)	6%	16.8 (5.1)	0.05 (1.6)	17%	17.4 (5.3)
0.04 (1.0)	12%	15.0 (4.6)	0.04 (1.0)	3%	14.6 (4.5)

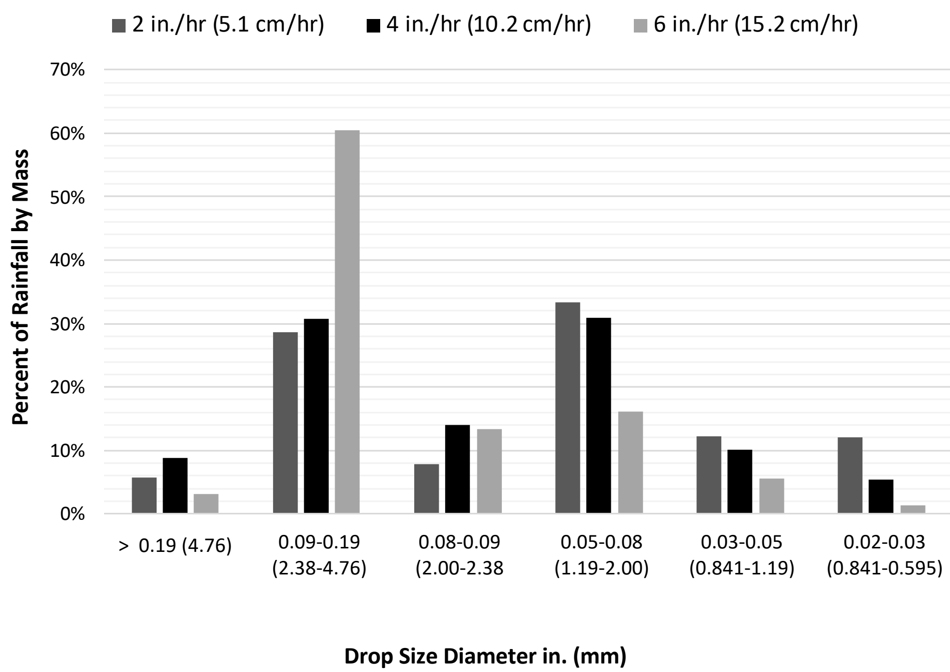

FIGURE 4.29: Drop Size Distribution and Intensity

TABLE 4.9: Storm Energy, Compared to Previous Results of Phase I Rainfall Simulator

Rainfall Intensity	2 in./hr (5.1 cm/hr)	4 in./hr (10.2 cm/hr)	6 in./hr (15.2 cm/hr)	Total
Kinetic Energy Rainfall ft-lbf (kJ) Current	6,826 (9.3)	14,377 (19.5)	76,862 (104.2)	98,065 (133.0)
Kinetic Energy Rainfall ft-lbf (kJ) Previous	8,729 (11.8)	17,704 (24.0)	24,266 (32.9)	50,699 (68.7)
Total Energy *E* ft-tonf/acre (MJ/ha) Current	465 (3.12)	979 (6.56)	5,231 (35.1)	6,675 (44.8)
Total Energy *E* ft-tonf/acre (MJ/ha) Previous	594 (3.99)	1,205 (8.09)	1,652 (11.1)	3,451 (23.2)

4.6 CONCLUSION

In total, construction progress on the Phase II rainfall simulators consisted of the following: a literature review to guide applicability and results interpretation, design using CAD of the layout, dimensions, and elevations, design using EPANET 2.0 of the new delivery system, testing and selection of the correct soils, earthmoving and grading to construct the 4:1 plots including correct and compacted soils, assembly of two sets of portable sprinklers with receivers on each plot, creation of the electrical control system, side slope stabilization, installation of 3 catch basins and French drains, and installation of several funnel boards and basin covers.

CHAPTER 5: CONCLUSIONS AND FUTURE DIRECTIONS

5.1 INTRODUCTION

This thesis carries on the work of the large-scale rainfall simulation efforts at the Auburn University Stormwater Research Facility. The initial goal was twofold: to complete all previously funded erosion control product testing on the current ASTM D6459 rainfall simulator (wrap up Phase I of *Evaluation of ALDOT Erosion Control Practices using Rainfall Simulation*), and to construct and calibrate new additional ASTM D6459 rainfall simulators of different soil types and slopes for future testing (begin Phase II). A third goal was added along the way: to conduct residual testing for polyacrylamide in testing runoff. The results of this work have strong implications and good lessons learned for the Stormwater Research Facility's future research in Phase II and beyond, so attention is paid in this chapter to implications and future directions.

5.2 SUMMARY

The objective of this research project was to assess erosion control product and practice performance using ASTM D6459 rainfall simulation. The objectives were accomplished by conducting the tasks described below.

Five products were evaluated on the existing ASTM D6459 slope with loam soil. First, jute matting was tested, installed with the reverse trenching technique, and stapled with a 6 in. (15.2 cm) seam overlap in the middle of the plot. Then, ProMatrix™ Engineered Fiber Matrix™, a bonded fiber hydro mulch. It was applied at a rate of 3,000 lb/ac (3,363 kg/ha) at a reduced water-to-fiber ratio as advertised by the manufacturer. It performed slightly better than the three other hydro mulches previously tested on the plot. Next, Applied Polymer Systems Silt Stop 712 Polyacrylamide was tested. It was applied directly to the soil at a rate of 25 lb/ac (28 kg/ha) and covered with jute matting. The PAM with jute did not perform statistically significantly different than the jute alone during the 4.in/hr (10.2 cm/hr) and 6 in/.hr (15.2 cm/hr) simulations but performed far superior in the 2.in/hr (5.1 cm/hr) simulation. It is believed that the protective seal washed off under the heightened intensity and the soil lost any protection it had, but the protection it provided prior to that point was effective.

The last two products intended to be tested, another hydro mulch and a Miscanthus mulch, were unable to be obtained and so a list of innovative products was brought to the ALDOT advisory committee for selection. Gypsum, a soil amendment used in agriculture for nutrient enrichment, soil structure improvement, and soil loss prevention, was selected. Other erosion control research has used different types of gypsum, so the two most promising, calcium sulfate dihydrate and calcium sulfate hemihydrate, were subjected to small scale and modified jar testing to determine which one performed optimally on the loam soil. Calcium sulfate dihydrate, or agricultural gypsum, resulted in less turbidity and soil loss and was selected for large scale testing. It was applied at a rate of 4,461 lb/ac (5,000 kg/ha) with the jute matting and resulted in significantly less soil loss than the jute matting alone. Also selected were EarthGuard™ EDGE™ pellets, a dry, pelletized form of the hydro mulch of the same name designed to expand when wet. The pellets were spread onto the soil surface at a rate of 3,000 lb/ac (3,363 kg/ha) and performed slightly better than other hydro mulches tested which were applied in the traditional manner with water. It is thought that the additional binder enhanced infiltration and soil structure enough to improve its erosion control performance on the loam soil.

After Phase I product testing was finished, all results were compiled and analyzed. C-factor results were aggregated with the C-factors and SLRs obtained in all previous Phase I testing to adequately compare performance of various product types tested. It was found that gypsum with jute performed comparably to erosion control blankets, that PAM with jute performed comparably to hydro mulches with both displaying large failures at high intensities, that HECP performance did not vary substantially by product at the 6 in./hr (15.2 cm.hr) intensity but that the two higher grade products performed somewhat better at the 4 in./hr (10.2 cm/hr) intensity, and that all products performed statistically identically at 2 in./hr (5.1 cm/hr). Most products failed to meet their minimum ECTC required C-factors at the 6 in./hr (15.2 cm/hr) intensity and overall. It was also found that SLR and C-factor described soil loss performance approximately identically for the straw. When all bare soil tests were summarized and compared, the K-factor obtained across all tests was consistent and displayed a low standard deviation, whereas TSS, turbidity, and runoff displayed high variability since these results were not normalized to observed rainfall. A comparison of C-factor calculation methods indicated that C-factor reported with the regression method and the theoretical R-factor was the most reliable reporting metric for product comparisons, whereas the C-factor reported with the average method and the measured R-factor most closely reflected test-specific product performance and captured any potential deviations in measured rainfall from the design.

Residual testing was desired for the PAM with jute test to determine if PAM appeared in the runoff. After evaluating aqueous detection methods, a detection method was selected whereby the sample was centrifuged to remove soil and the supernatant placed in a spectrometer, which read absorbance of the sample from 200 nm to 750 nm, the UV-visible spectrum. To find PAM concentration, blank samples using the pond source water were prepared with PAM solutions at known concentrations. The absorbance at 200 nm was then plotted and a linear regression of high R^2 was obtained. The absorbance of each sample at 200nm could then be compared to the regression and PAM concentration estimated. Tests were performed to verify that centrifuging removed all soil interference from the PAM solution, and that centrifuging did not remove a substantial amount of PAM from solution. Detected PAM concentrations were much higher than expected, over 100 mg/L for the first detected runoff. Concentrations were highest at first runoff and decreased over the test period, similar to a first flush effect. Visual observations such as excessive bubbles in the runoff confirmed the presence of a high amount of foreign substance. When PAM was installed on top of the jute matting in the soft-armoring technique, the initial spike in high (>100 mg/L) concentrations disappeared. Runoff from the ProMatrix™ hydro mulch and the EarthGuard™ pellets was also run through the spectrometer, but no firm conclusions could be drawn because the proprietary nature of the binder renders constructing reliable calibration curves difficult. However, absorbances comparable to the highest PAM absorbances were detected along with similar, if not more severe, visual runoff observations such as froth or surface film.

New construction commenced on 12 additional rainfall simulators, covering two different slopes (4:1 and 3:1) and three different soil types (clay, sand, and loam as defined in the ASTM D6459 standard). A model was made in CAD of the simulator area, and land clearing and initial earthmoving were executed under the direction of the Stormwater Research Facility staff. Soil testing was used to identify candidates for the clay, sand, and loam soils for building the plots. Twenty-six samples were taken over 11 different sites, including borrow pits, construction sites, and local contractor stockpiles. Each sample underwent the same process, typically repeated twice. First, a wet sieve analysis was performed followed by a dry sieve on the resulting coarse fraction. If the soil still proved a promising fit to the standard, hydrometer analysis and liquid/plastic limit tests were performed. For the final three soils selected, Proctor compaction was performed to aid in verifying compaction during construction and to be used in future testing. Ultimately, a sand was identified from Newville, AL, a clay from Montgomery, AL, and a loam from in situ testing at the location of the new simulators. The first two soils were trucked in and the last was tilled and left in place, with construction spoils stockpiled for future testing.

Sprinkler design including dimensions and parts were imitated from the existing simulator to minimize calibration. However, other components were redesigned to be portable to save on time and material costs. The sprinkler posts were designed to slide in and out of a series of permanent, in-ground sleeves. A single electrical control box was built with plugs that could accommodate the two sets of sprinklers as they are moved from plot to plot. The compaction method was changed from a permanent support to a portable winch basket attachment for the skid steer. The water delivery was re-designed from a permanent underground system around the perimeter of each plot that hooked up to a portable flex-hose, to a permanent underground supply running only along the base of every plot, with hookups at each plot and the sprinkler flexible hoses attaching to the hookups. This portable system has not been constructed; however, it has been modeled in EPANET 2.0 to verify the size and capacity of the supply pump and pipes. Each plot has its own permanent, underground catch basin with a 750-gal (2,839 L) capacity supported by a French drain system. Each plot required extensive re-grading by the time actual construction commenced to reach accurate elevations and dimensions. In total, the six 3:1 plots were constructed over the course of this thesis, with four out of the six side slopes stabilized with seed/fertilizer and ECBs, three basins with drains constructed for those six plots, and two full sets of ten sprinklers each assembled and installed. Finally, a preliminary calibration was conducted on the first plot. Five fifteen-minute iterations of the 2, 4, and 6 in./hr (5.1, 10.2, 15.2 cm/hr) simulations were run with 20 rain gages to evaluate intensity and uniformity. A series of flour pan tests was also conducted to evaluate drop size distribution and plot kinetic energy. Water supply problems in the upper pond prevented more calibration from being conducted, but initial results can guide future calibration efforts once the permanent underground supply/portable hookups are constructed.

5.3 IMPLICATIONS AND FUTURE DIRECTIONS

This section presents some broader significances of the work presented in this thesis. It outlines the significance of Phase I testing to overall rainfall simulation literature, discusses future recommendations for rainfall simulation testing at the facility, recaps the implications of the PAM residual results, details recommendations for Phase II progress especially with regards to calibration, methods, and variability, and finally discusses a new ASTM rainfall simulation standard, released during the writing of this thesis, while reaffirming the continued relevance of the D6459.

5.3.1 Phase I Testing Contributions to Literature

The primary benefit of Phase I testing is that the tests were conducted on a large-scale, standardized rainfall simulator. One of the chief shortcomings identified in rainfall simulation research is the lack of a consistent, replicable, accepted methodological standard (Grismer

2012) and the ensuing lack of comparability among results (Ries et. al 2009). Virtually every rainfall simulation study available utilizes different parameters, and the possible variations include: style of drop formation, pressure in the system, simulation intensity and time, drop size distribution, uniformity, fall height, dimensions of plot, slope of plot, soil type and compaction, depth of soil bed, method of calibration, and method of assessing soil loss and overall performance (Yakubu and Yusop 2016). When experiments yield varying results, such methodological variations mean that pinpointing the source of the differences is difficult and validating results not possible. Thus, standardization of parameters would better ensure comparability. There are only two accepted standards for rainfall simulation design by ASTM International –but at the time this research was conducted only one of them, the ASTM D6459 *Standard Test Method for Determination of Rolled Erosion Control Product (RECP) Performance in Protecting Hillslopes from Rainfall-Induced Erosion*, was to full field scale and labeled as acceptable for establishing design parameters. Auburn University operates only one of two accredited ASTM D6459 labs in the country by the Geosynthetic Institute (GSI).

Such large-scale studies (Clopper at. 2001, Li et. al 2013, Faucette et. al 2009, Tauer et. al 2008) can more realistically mimic erosion patterns found in the field than small-scale studies can, even though small-scale studies are much more abundantly available. Rill erosion begins to form when the shear stress of the flow exceeds the shear stress of the soil (Lei et. al 2008). A rainfall simulation study of a silty clay by Yao et. al 2008 found that rill initiation began between 6.2-22.3 ft (1.9-6.8 m) from the top of the plot depending on slope. Lal 1994 recommends a minimum of 16.4 ft (5m) for adequate rill development, preferentially 32.8 feet (10m). Thus, plot lengths shorter than that range may not develop realistic erosion patterns and the results may not be transferrable to the field. Indeed, erosion control testing on small-scale plots has been shown to overpredict product performance, generating greater reduction in sediment loss and more favorable C-factors, than identically calibrated field-scale plots. In a study comparing small (2 ft by 4 ft [0.61 m by 1.2 m]), medium (4 ft by 8 ft [1.2m by 2.4m]) and large (8 ft by 40 ft [2.4m by 12.2m]) rainfall simulator plots performed by Ricks 2020, the small plot under-predicted theoretical soil loss from the RUSLE equation by 80%, the medium plot by 40%, and the large plot by 13%. Furthermore, when used to test hydro mulch products, the small plots produced C-factors that were an average 35% lower than the ones obtained from the large plot. Similarly, a study by Sprague and Nelson 2009 which correlated the performance of RECPs on bench-scale ASTM D7101 with full-scale ASTM D6459 found that the C-factors obtained in the small-scale test were consistently lower than those obtained in the large-scale test.

The storm prescribed by the ASTM D6459 standard is another advantage of the Phase I testing results. Most rainfall simulator studies use intensities that far exceed what is typically found in nature and the intensities achieved in this study are no exception. However, the ASTM D6459 intensity increases over the course of the simulation. While the nature of the ASTM D6459 storm has been the subject of much criticism, it is an advantage in this thesis because it can uncover the scenarios where products behave similarly, and where product performance begins to significantly diverge. The results have particular significance when it comes to product selection for various design scenarios, especially selection of hydro mulches. Performance of hydro mulches was found to be equal to that of high-performing RECPs at the lowest intensity, but performance diverged at higher intensities and the hydro mulches began to catastrophically fail. Performance within hydro mulches at the higher intensities differed at the 4 in./hr (10.2

cm/hr) intensity for two products but all deteriorated the same at 6 in./hr (15.2 cm/hr). The comparison of soil amendments with traditional erosion control products over increasing intensities offered a valuable comparison as well. Soil amendments are used less often in construction erosion control than traditional products and are typically studied as stand-alone experiments in rainfall simulation literature without a side-by-side evaluation to other products. This renders an accurate comparison to other products difficult, but by testing both product types side-by-side on a standardized rainfall simulator, a confident comparison may be made. When combined with previous results from Phase I (Faulkner 2020), it can be seen that PAM with jute performed similar to the hydro mulches at higher intensities, and gypsum with jute compared similar to the RECPs at the higher intensities. At the lowest intensity (2 in./hr [5.1 cm/hr]), all products tested as part of Phase I both during and prior to this thesis, including straw mulch variations, performed identically as evaluated with ANOVA. Thus, product quality differentiation in terms of sediment loss only becomes relevant as design storms increase in intensity.

5.3.2 Phase I Testing: Lessons Learned for Phase II

The conclusion of Phase I testing included two soil amendment products, and the possibility remains open that such amendments may be tested as part of Phase II or in the future. Two key pieces of advice for future rainfall simulator research arose out of the work of this thesis regarding future soil amendment testing. First, to ensure robust testing, it is essential to eliminate residual product interference between tests by removing contaminated soil. Otherwise, the product may build up on the plot and generate a compounding affect which will artificially carry over into the next test. To illustrate, the runoff from the bare soil control performed after the PAM analysis was observed to display characteristics indicating that it still contained some residual PAM (film, bubbles), even after extensive attempted removal of contaminated soil and rinsing of the plot, necessitation even more soil removal after the fact. The new ASTM D8298 *Standard Test Method for Determination of Erosion Control Products (ECP) Performance in Protecting Slopes from Continuous Rainfall-Induced Erosion Using a Tilted Bed Slope* (ASTM 2020) specifically states that when testing soil amendments, all soil from the test plot must be completely removed and replaced. The removal recommendation for future testing should entail removing a substantial portion of the soil from the plot after the test is complete and before tilling begins, up to several inches. The soil should be replaced with fresh soil shaken from the stockpile. This will represent more of a drain on the stockpile than the other products tested, and stockpile management should be planned accordingly.

The second recommendation is to test more than one application rate of soil amendments. Previous rainfall simulation studies of PAM, gypsum, or both tested a minimum of two and up to eight application rates (for example, Babcock and McLaughlin 2013, Sadeghi et. al 2016, Tumsavas and Kara 2011, Ai-Ping et. al 2010, Lee et. al 2010, Yu et. al 2003, Kebede et. al 2020). This study utilized only one application rate of PAM and one application rate of gypsum due to time and funding restrictions. To be consistent with the literature, future research should consider allocating enough time and funding at the outset to accommodate testing at least two application rates of soil amendment products. The motivation for testing different rates is that performance varies with application rate due to complex interactions of soil properties, geography, and rain event properties. While manufacturer recommendations are always followed, some products (like gypsum) do not have a manufacturer recommendation if they are not made exclusively for the erosion and sediment control industry. Other amendments (like PAM) may have demonstrated ranges of effectiveness. Since the nature of the large-scale ASTM D6459 simulator is much more labor intensive to operate than the series of bench-scale studies cited in this paragraph, it is inherently more challenging to conduct more tests. Therefore, a plan should be made at the outset to accommodate the additional resources needed to test various rates.

The following recommendations apply to testing more generally. The variability in measured rainfall during Phase I testing is the primary shortcoming of the work of this thesis. The C-factor obtained from the regression method takes rainfall variability into account and is reported in this thesis with high confidence. However, the C-factor as reported with the average method deviated some from the regression C-factor when rainfall varied to any appreciable extent. This makes results look inconsistent, and regardless, rainfall should be match design as much as possible to maintain conformance with certification. Myriad factors could have been at play and should be addressed before Phase II testing commences. First, the simulators should be carefully calibrated. The ASTM standard calls for re-calibration yearly, but it is not known if this was ever performed on the simulator used in Phase I. It is recommended to follow calibration procedures at least yearly and more often if time permits. The reason is that Phase II will have many more simulators where many more complications could occur. Also, the pump will be used more frequently and may be more susceptible to wear and problems especially since it has surpassed its fifth year of service at the time of this writing. and pumps and hoses maintained for consistent rainfall. Along those lines, variation could have been possibly ameliorated by cleaning out the pump impeller and more consistently ensuring that flexible hoses were not distended from constant pressure. In fact, after the conclusion of Phase I testing, the pump impeller was cleaned and pump performance notably increased. However, it was not known to attempt this prior. Several months passed between the previous Phase I work and the commencement of this thesis, during which time the simulator was used for a different research project. It is possible that the pump became clogged in that time due to low water levels or that breaks occurred in the wind curtains that were not present previously. The existing wind curtains contain gaps and do not extend high enough to capture the drops as they form, rendering them less effective. It is highly recommended to install the wind curtains before Phase II testing begins, and to ensure that there are few gaps in the system and that coverage extends above the level of the sprinkler heads. It was furthermore discovered that the flexible supply hose could become distended over frequent use or if pressure was left in the system. After each fresh flex hose was installed, rainfall performance improved. It is possible that pressure was accidentally left in the system too often and affected rainfall performance between replacements.

Bare soil results were shown to be consistent with K-factor, which corrects for rainfall variation, but not for the other metrics (turbidity, TSS, and runoff volume). While this is not a main concern, it would be beneficial for these metrics to be more consistent since they are used as benchmarks for each individual product test. While no measure can guarantee more consistency due to the rainfall variability aspect, it is suggested to maintain effective stockpile management in order to ensure that soil properties remain the same. This task will require constant monitoring and maintenance of stockpiles because the stockpiles currently at the facility are expected to serve future testing for years in the future. Vegetative stabilization has begun on the loam and clay, but ensuring that vegetative stabilization becomes complete and stabilizing the sand are essential tasks moving forward. In addition, it is suggested to assign the same undergraduate assistants to data collection and processing tasks. This will require additional coordination since workers have variable schedules, so having multiple workers competent in each task is helpful, along with possible practice only lab sessions.

It was noted that the literature contains updated methods to calculate the S-factor from RUSLE based on recent research on steep slopes. However, when the new equations were incorporated into Phase I data, the higher S-factor and lower K-factor offset one another, leading to no substantive changes in reported C-factor to two significant figures. Therefore, the existing method is likely adequate.

5.3.3 PAM Residual Analysis Implications

Residual PAM detection in this thesis found high (>100 mg/L) concentrations of PAM in runoff from the ASTM D6459 simulator. The concentrations were much higher than those found in the two previous bench-scale studies, and many measured concentrations exceeded the threshold at which PAM begins to increase water viscosity. While initially this appears to be cause for alarm, it is thought that the intensity of the simulation, the erodible nature of the soil, a possible sub-optimal application rate, and the lack of pre-wetting to activate the polymer all may have played a role. This was the first large-scale study conducted on residual PAM, and further large-scale studies are needed at different application rates, different application methods, and at various slopes, intensities, and soil types.

Further large-scale studies are also merited for any erosion control product that contains biopolymers or inorganic polymers. Both visual and spectroscopic observations of runoff from ProMatrix™ and EarthGuard™ EDGE™ pellets suggested greatly elevated concentrations of binder in the runoff, even though exact quantification was impossible due to the proprietary nature of the binders. Further evaluation is needed in order to determine exact concentrations in mulches using methods that do not require a calibration relationship. This evaluation should include a review of any potential environmental concerns of the particular polymer, if known, to assess whether the concentrations pose a concern for receiving waters.

5.3.4 Phase II Recommendations

As a result of observations during construction, the following may be helpful for the implementation of Phase II testing. Full calibration is the next task due when construction is complete. The preliminary calibration was difficult due to the water source problem and due to the necessity of waiting on wind velocity to die down to acceptable testing standard. The results obtained were less than acceptably consistent. The measured rainfall displayed a high standard deviation, higher than previously recorded, and the measured energy differed from that previously measured on the existing plot although the exact degree of acceptable deviation in this metric is not known. To aid in future calibration, it is recommended to proceed with the wind curtain design and installation before final calibration is attempted, to ensure no wind interference with results, with the curtains extending above the height of the sprinkler heads. The planned improvement in the upper retention pond will aid in maintaining constant and sufficient head on the pump and will almost certainly help with consistency, so final calibration should be conducted after this repair is complete. If variability continues to be unacceptable, it is suggested to thoroughly clean the inside of each sprinkler assembly including pipes and nozzles, and to ensure the cleanliness of all other plumbing, since some dirt acquired during construction may lead to intermittent clogging. If any flexible hose is used, care must be taken to release pressure after use in order to prevent swelling and a corresponding decrease in system pressure. The impeller on the pump must be maintained free of obstructions, which has proven a challenge thus far in the sediment-laden and debris-containing supply ponds. It is highly recommended to create a rock bed for the intake to rest on to prevent sediment entrapment. It is also highly recommended to filter water used for priming the pump, since small debris may inadvertently be introduced directly into the pump during priming.

The catch basins selected contain a smooth bottom with several indentations. It can be easy to slip on the bottom of the basins when wet, and sediment can build up in the indentations. It is suggested to cover the bottom of each basin with a rough plastic or resin that can fill the voids and provide slip resistance. In the trial plot basin, concrete was placed in the indentations and the entire bottom was then sealed with commercial roofing tar. It will be seen when testing commences whether this is an adequate solution or whether other alternatives should be explored. A short tub of about 32 gal (121L) capacity was ordered to capture runoff from the first two intensities, but it still needs to be determined whether a larger capacity tub is needed. The French drains around the catch basins should be kept clear of equipment, since they are buried shallowly towards their termination. It is highly recommended to use the tracked skid steer when attempting to maneuver in between plots. The tire skid steer is wider and more difficult to maneuver, and the pressure of the tires tends to push soil around and potentially move the post sleeves. It may not be possible to maneuver the tracked skid steer sideways between plots, but even by remaining facing uphill the tracked skid steer can still provide replacement soil to each adjacent plot.

5.3.5 New ASTM Rainfall Simulation Standard

Since the time of this research, in 2020, a new rainfall simulation standard was released, ASTM D8298 *Standard Test Method for Determination of Erosion Control Products (ECP) Performance in Protecting Slopes from Continuous Rainfall-Induced Erosion Using a Tilted Bed Slope*. The standard allows for a one-hour simulation at either 4.0 or 5.0 inches per hour, at a slope of either 2.5:1 or 4:1, on the same soil types as the D6459, with minimum dimensions of 16.4ft x 3.3 ft x 1 ft. The standard appears to address one primary shortcoming of the D6459 - it is written to be applicable to all types of erosion control products, not just RECPs. In practice, ASTM D6459 labs, both certified and not certified, including the one used in this thesis, evaluate types of erosion control products beyond RECPs simply because it is the only standard available for product comparison. It is not believed such application of the standard to be problematic – the new D8298 also applies the similar test conditions, conditions that are very similar to the D6459, to all ECP types without any specification in parameters adaptations to different products. The only apparent difference is that the new standard contains additional wording to explicitly ensure the controlled application of the different types of products. For example, minimum installation standards for hydro mulches are stated at length, and it specifies to remove all soil from the plot when additives are used. The D8298 allows for two types of rainfall intensities, one less severe and one more severe, staying constant throughout the test. Thus, the new standard may be more favorable to hydro mulch evaluation, which as evidenced in this study exhibit lower C-factors at under less extreme circumstances. The smaller size may make it more accessible to operate, but still be large enough to be considered “larger-scale”. The new standard is problematic in that it allows for variation of parameters within the test, the very thing that a standard should eliminate. It also does not eliminate the most criticized aspect of the D6459, which is the severity of the storm, and it is possible that the minimum size may not allow for full rill development in all cases. However, it is encouraging to see a more accessible rainfall simulation standard on the market, and it is hoped that labs which were not able to modify to ASTM D6459 will be able to modify to this new standard, thus promoting uniformity and replicability in the field.

REFERENCES

Ai-Ping, Want, Fa-Hu Li, and Sheng-Min Yang. 2011. "Effect of polyacrylamide application on runoff, erosion, and soil nutrient loss under simulated rainfall." *Pedosphere, 21*(5), 628-638.

Akbarzadeh, A., Mehrjardi, R. T., Refahi, H. G., Rouhipour, H., & Gorji, M. 2009. "Application of soil conditioners and man-made erosion control materials to reduce erosion risk on sloping lands." *African Journal of Plant Science*, *3*(4), 074-084.

Alabama Deparment of Archives and History. 2014. "Official symbols and emblems of Alabama: Official Alabama soil: Bama soil series." Accessed May 2020. <archives.alabama.gov/emblems/st_soil.html>.

Anderson, Curt. 2021. "Florida manatee deaths soar as polluted water kills seagrass." *The Associated Press, October 27, 2021.*

Applied Polymer Systems, INC. 2002. "Technical guidance for the use of Polyacrylamides (PAM) and PAM blends for soil erosion control and storm water clarification." Accessed June 2020.<https://www.siltstop.com/pictures/9-30-05%20APS%20Tech%20PAM.pdf>.

Assouline, S, El Idrissi, and E Persoons. 1997. "Modelling the physical characteristics of simulated rainfall: a comparison with natural rainfall." *Journal of Hydrology, 196*(1-4), 336-347.

ASTM International. 2010. "Standard Test Method for Density of Soil in Place by the Drive-Cylinder Method". West Conshohocken, PA, 1-7.

ASTM International. 2017. "Standard Test Method for Determination of Erosion Control Product (ECP) Ability to Encourage Seed Germination and Plant Growth Under Bench-Scale Conditions." West Conshokocken, PA, 1-5.

ASTM International. 2017. "Standard Test Method for Determination of Turbidity Above 1 Turbidity Unit (TU) in Static Mode." West Conshohocken, PA, 1-22.

ASTM International. 2013. "Standard Test Method for Filterable Matter (Total Dissolved Solids) and Nonfilterable Matter (Total Suspended Solids) in Water." West Conshohocken, PA, 1-9.

ASTM International. 2012. "Standard Test Method for Laboratory Compaction Characteristics of Soil Using Standard Effort (12,400 ft-lbf/ft^3 (600 kN-m/m^3))." West Conshohocken, PA, 1-13.

ASTM International. 2019. “Standard Test Method for Liquid Limit, Plastic Limit, and Plasticity Index of Soils.” West Conshohocken, PA, 1-10.

ASTM International. 2017. “Standard Test Method for Particle-Size Distribution (Gradation) of Fine-Grained Soils Using the Sedimentation (Hydrometer) Analysis.” West Conshohocken, PA, 1-25.

ASTM International. 2017. “Standard Test Method of Rolled Erosion Control Product (RECPs) Performance in Protecting Hillslopes from Rainfall Induced Erosion.” West Conshohocken, PA, 1-20.

ASTM International. 2014. “Standard Test Method for Sieve Analysis of Fine and Coarse Aggregates.” West Conshohocken, PA, 1-5.

ASTM International. 2020. “Standard Test Method for Determination of Erosion Control Products (ECP) Performance in Protecting Slopes from Continuous Rainfall-Induced Erosion Using a Tilted Bed Slope.” West Conshohocken, PA, 1-15.

Babcock, D. L. and R. A. McLaughlin. 2013. “Erosion control effectiveness of straw, hydromulch, and polyacrylamide in a rainfall simulator.” *Journal of Soil and Water Conservation, 68*(3), 221-227.

Beim, AA and AM Beim. 1994. “Comparative ecological – toxicological data on determination of maximum permissible concentrations (mpc) for several flocculants.” *Environmental Technology, 15*(2), 195-198.

Ben-Hur, M., R. Stern, A. J. van der Merwe, and I. Shainberg. 1992. “Slope and gypsum effects on infiltration and erodibility of dispersive and nondispersive soils.” *Soil Science Society of America Journal 56*, 1571-1576.

Best, A. C. 1950. “The size distribution of raindrops.” *Quarterly Journal of the Meteorological Society, 76*(327), 16-36.

Betso, S. R., & McLean, J. D. 1976. “Determination of acrylamide monomer by differential pulse polarography.” *Analytical Chemistry, 48*(4), 766-770.

Boxel, van J. 1998. “Numerical model for the fall speed of raindrops in a rainfall simulator.” *I. C. E. Special Report, 1*, 77-85.

Bryan, Rorke B. 2000. “Soil erodibility and processes of water erosion on hillslope.” *Geomorphology, 32*, 385-415.

Bubenzer, G. D. 1979. “Inventory of rainfall simulators.” *Proceedings of the Rainfall Simulator Workshop, Tuscon, Arizona*, 120-130.

Buczek, Sean B., W. Cope, W. G., McLaughlin, R. A., & Kwak, T. J. 2017. “Acute toxicity of polyacrylamide flocculants to early life stages of freshwater mussels.” *Environmental Toxicology and Chemistry, 36*(10), 2715-2721.

Chen, Liming, and Warren A. Dick. 2011. “Gypsum as an agricultural amendment, Bulletin 945.” *The Ohio State University*.

Chouksey, Arpit, Vinit Lambey, Bhaskar R. Nikam, Shiv Prasad Aggarwal and Subashisa Dutta. 2017. “Hydrological modelling using a rainfall simulator over an experimental hillslope plot.” *Hydrology, 4(*17).

Chowdhury, Md. Enayet, Md. Azijul Islam, Dr. Mohammad Shariful Islam, Md. Safin Shahriar and Tahsina Alam. 2017. “Design, operation, and performance evaluation of a portable perforated steel tray rainfall simulator.” *Proceedings of 14th Global Engineering and Technology Conference,* Vol. 63.

Clopper, Paul, Michael Vielleux, and Anthony Johnson. 2001. “Quantifying the performance of hillslope erosion control best management practices.” In *Bridging the Gap: Meeting the World’s Water and Environmental Resource Challenges*, 1-10.

Deng, Y., Dixon, J. B., & White, G. N. 2006. “Adsorption of polyacrylamide on smectite, illite, and kaolinite.” *Soil Science Society of America, 70*(1).

Du, P. and D. E. Walling. 2011. “Using 137Cs measurements to investigate the influence of erosion and soil redistribution on soil properties.” *Applied Radiation and Isotopes, 69*(5), 717-726.

Dunkerley, David. 2008. “Rain event properties in nature and in rainfall simulation experiments: A comparative review with recommendations for increasingly systematic study and reporting.” *Hydrological Processes*, 22, 4415-4435.

Eigel, J. D. and I. D. Moore. 1983. “A simplified technique for measuring raindrop size and distribution.” *Transactions of the ASAE, 26*(4), 1079-1084.

Ekwue, E. I. 1990. “Effect of organic matter on splash detachment and the processes involved.” *Earth Surface Processes and Landforms, 15*, 175-181.

Ekwue, E. I., A. Harrilal. 2010. “Effect of soil type, peat, slope, compaction effort and their interactions on infiltration, runoff and raindrop erosion of some Trinidadian soils.” *Biosystems Engineering, 105*, 112-118.

Elbasit, M. A. M., C. S. P. Ojha, Z. Ahmed, H. Yasuda, A. Salmi, and F. Ahmed. 2015. “Rain microstructure and erosivity relationships under pressurized rainfall simulator.” *Journal of Hydrologic Engineering, 20*(6), C6015001.

Elbasit, Abd, Mohamed AM, Hiroshi Yasuda, Atte Salmi, and Hisao Anyoji. 2010. “Characterization of rainfall generated by dripper-type rainfall simulator using piezoelectric transducers and its impact on splash soil erosion.” *Earth Surface Processes and Landforms, 35*(4), 466-475.

Entry, James A., R. E. Sojka, Maribeth Watwood, and Craig Ross. 2002. “Polyacrylamide preparations for protection of water quality threatened by agricultural runoff contaminants.” *Environmental Pollution, 120*(2), 191-200.

Erosion Control Technology Council. n.d. “Fact sheet: Hydraulic Erosion Control Products.” Accessed July 2021. <https://www.ectc.org/assets/docs/HECPDocs/ectc_Y20_HECP%20EPA%20Fact%20Sheet%20FINAL.pdf>.

Erosion Control Technology Council. 2018-2019. “Product Selection Based Upon ECTC Specification Categories.” Accessed August 2021. <https://www.ectc.org/product-selection-by-category>.

Erosion Control Technology Council. 2018-2019. “Product Selection Based Upon RECP Specification Categories.” Accessed August 2021. <https://www.ectc.org/product-selection-recp>.

Faucette, L. B., C. F. Jordan, L. M. Risse, M. Cabrera, D.C. Coleman, and L.T. West. 2008. “Evaluation of stormwater from compost and conventional erosion control practices in construction activities.” *Journal of Soil and Water Conservation, 60*(6), 288-297.

Faucette, L. B., Scholl, B., Beighley, R. E., and Governo, J. 2009. “Large-scale performance and design for construction activity erosion control best management practices.” *Journal of Environmental Quality*, *38*(3), 1248-1254.

Faulkner, Brian. 2020. “Evaluation of erosion control practices under large-scale rainfall simulation following ASTM D6459 standard test methods.” Master’s thesis. <http://hdl.handle.net/10415/7187>.

Fisk, Susan V. 2019. “Gypsum as an agricultural product.” *Soil Science Society of America*. Accessed 11 August 2021. https://www.soils.org/news/science-news/gypsum-agricultural-product/.

Flangan, D. C., Norton, L. D., Peterson, J. R., & Chaudhari, K. 2003. “Using polyacrylamide to control erosion on agricultural and disturbed soils in rainfed areas.” *Journal of Soil and Water Conservation*, *58*, 301-311.

Fu, Suhua, Baoyuan Liu, Heping Liu, and Li Xu. 2011. “The effect of slope on interrill erosion at short slopes.” *Catena, 84*, 29-34.

Geosynthetic Institute. n.d. “List of Accredited Laboratories and Their Accredited Test Methods.” Accessed August 2021. <https://geosynthetic-institute.org/gai/methlist/d6459.html>.

Grismer, Mark E. 2012. “Standards vary in studies using rainfall simulators to evaluate erosion.” *California Agriculture, 66*(3), 102-107.

Grosh, J.L, and A. R. Jarrett. 1994. “Interrill erosion and runoff on very steep slopes.” *Transactions of the American Society of Agricultural and Biological Engineers, 37*(4), 1127-1133.

Guezennec, A. G., Michael, C., Bru, K., Touze, S., Desroche, N., Minf, I., & Motelica-Heino, M. 2015. “Transfer and degradation of polyacrylamide-based flocculants in hydrosystems: A review.” *Environmental Science and Pollution Research*, *22*, 6390-6406.

Gypsoil. 2021. “Sulfate over winter.” Accessed August 2021. <http://www.gypsoil.com/news-and-events/sulfate-over-winter>.

The Haw River Assembly. 2020. “River Issues.” Accessed April 2020. <http://hawriver.org/river-issues/chatham-park/.

He, Xiuban, and Huang, Zhanbin. 2001. “Zeolite application for enhancing water infiltration and retention in loess soil.” *Resources, Conservation, and Recycling, 34*(1), 45-52.

Heckrath, G., J. Djurhuus, T. A. Quine, K. Van Oost, G. Govers. And Y. Zhang. 2005. “Tillage erosion and its effect on soil properties and crop yield in Denmark.” *Journal of Environmental Quality, 34*, 312-324.

Herth, Gregor, Gunnar Schornick, and Fredric L. Bucholz. 2015. “Polyacrylamides and poly(acrylic acids).” *Ullmann’s Encyclopedia of Industrial Chemistry*, 1-16.

Illinois Environmental Protection Agency. 2002. “What is Phase II of the NPDES Storm Water Management Program?” *Authority of the State of Illinois*. Accessed August 2021. <http://www.epa.state.il.us/small-business/phase-two/phase-two.pdf>.

Jacobs, Walter, Pierre Le Hir, Walther Van Kesteren, and Philippe Cann. 2011. “Erosion threshold of sand-mud mixtures.” *Continental Shelf Research, 31*, S14-S25.

Johannsen, Lisbeth Lolk, Nives Zamboon, Peter Strauss, Tomas Dostal, Martin Neumann, David Zumr, Thomas A. Cochrane, Gunter Bloschl, and Andreas Klik. 2020. “Comparison of three types of laser optical disdrometers under natural rainfall conditions.” *Hydrological Sciences Journal, 65*(4), 524-535.

Johnson, Joanne. 2015. “Development of best management practices for turbidity control during rainfall events at highway construction sites using polyacrylamide.” Dissertation. <http://scholarworks.uark.edu/etd/1065>

Jung, J., Jang, J., & Ahn, J. 2016. “Characterization of a polyacrylamide solution used for remediation of petroleum contaminated soils.” *Materials, 9*(1), 16.

Kang, J., King, S. E., McLaughlin, R. A., & Wiseman, J. D. 2014. “Flocculated sediment and runoff quality improvement by polyacrylamide.” *Transactions of the American Society of Agricultural and Biological Engineers, 57*(3), 861-867.

Kathiravelu, Gopinath, Terry Lucke, Richard White, and Peter W B Nichols. 2014. “Review on design requirements of a rainfall simulator for urban stormwater studies.” In *Proceedings of the 2014 Stormwater Queensland Conference, Townsville, Australia*, 6-8.

Kato, H., Y. Onda, Y. Tanaka, and M. Asano. 2009. “Field measurement of infiltration rate using an oscillating nozzle rainfall simulator in the cold, semiarid grassland of Mongolia.” *Catena, 76*(3), 173-181.

Kavian, Ataollah, Maziar Mohammadi, Artemi Cerda, Moghadaseh Fallah and Leila Gholami. 2019. “Calibration of the SARI portable rainfall simulator for field and laboratory experiments.” *Hydrological Sciences Journal, 64*(3), 350-360.

Kidane, Desale, and Binyam Alemu. 2015. “The effect of upstream land use practices on soil erosion and sedimentation in the Upper Blue Nile basin, Ethiopia.” *Research Journal of Agriculture and Environmental Management*, *4*(2), 55-68. Available at http://www.apexjournal.org.

King, B. A., T. W. Winward, and D. L. Bjorneberg. 2010. “Laser precipitation monitor for measurement of drop size and velocity of moving spray-plate sprinklers.” *Applied Engineering in Agriculture, 26*(2), 263-271.

Kontchou, Julios A., Milen Nachev, and Bernd Sures. 2021. “Ecotoxicological effects of traffic-related metal sediment pollution in Lumbriculus variegatus and Gammarus sp.” *Environmental Pollution, 286*(B), 115884.

Kuhn, Nikolaus J. 2007. “Erodibility of soil and organic matter: Interdependence of organic matter resistance to interrill erosion.” *Earth Surface Processes and Landforms, 32*, 794-802.

Lal, Rattan. 1994. *Soil Erosion Research Methods*. Boca Raton, Florida: CRC Press.

Lanzinger, Eckhard, Manfred Theel, and Herbert Windolph. 2006. “Rainfall amount and intensity measured by the thies laser precipitaiton monitor.” *TECO-2006, Geneva, Switzerland*, 4-6.

Larson, W. E., T. E. Fenton, E. L. Skidmore, and C. M. Benbrook. 1985. “Effects of soil erosion on soil properties as related to crop productivity and classification.” *Soil Erosion and Crop Productivity.*

Lassu, Tamas, Manuel Seeger, Piet Peters and Saskia D. Keestra. 2015. “The Wageningen rainfall simulator: Set-up and calibration of an indoor nozzle-type rainfall simulator for erosion studies.” *Land Degradation and Development, 26*, 604-612.

Laws, J. Otis, and Donald A. Parsons. 1943. “The relation of raindrop size to intensity.” *Transactions of the American Geophysical Union*, 452-460.

Lee, S. S., C. J. Gantzer, A. L. Thompson, and S. H. Anderson. 2010. “Polyacrylamide and gypsum amendments for erosion and runoff control on two soil series.” *Soil and Water Conservation Society*, *65*(4), 233-242.

Lei, T. W., Q. W. Zhang, L. J. Yan, J. Zhao, and Y. H. Pan. 2008. “A rational method for estimating erodibility and critical shear stress of an eroding rill.” *Geoderma*, *144*, 628-633.

Lentz, R. D. 2015. “Polyacrylamide and biopolymer effects on flocculation, aggregate stability, and water seepage in a silt loam.” *Geoderma*, *241-242*, 289-294.

Levy, G. J., & Miller, W. P. 1999. “Polyacrylamide adsorption and aggregate stability.” *Soil and Tillage Research, 51*, 121-128.

Li, Ming-Han, Jett McFalls, and Young-jae Yi. 2013. “Comparing erosion control products’ performance results from field and large-scale laboratory testing.” *Indian Geotechnical Journal, 43*(4), 382-387.

Liu, B. Y., M. A. Nearing, L. M. Risse. 1994. “Slope gradient effects for soil loss on steep slopes.” *Transactions of the American Society of Agricultural Engineers, 37*(6), 1835-1840.

Liu, Bo, Xiaolei Wang, Lihua Shi, Xichuan Liu, Zhaojing Kang and Zhentao Chen. 2017. “Research on the fine-scale spatial uniformity of natural rainfall and rainfall from a rainfall simulator with a rotary platform (RSRP).” *Atmosphere, 8*(113), 1-14.

Long, R. P, and K. R. Demars. 2004. "Feasibility study of an erosion control laboratory in new england." *The New England Transportation Consortium*, Technical Report No. NETCR 49.

Lora, Marco, Matteo Camporese, and Paolo Salandin. 2016. "Design and performance of a nozzle-type rainfall simulator for landslide triggering experiments." *Catena*, *140*, 77-89.

Lu, Shaojuan, Zhanli Wang, Yaxian Hu, Baoyuan Liu, and Jun'e Liu. 2008. "Effectiveness and durability of polyacrylamide (PAM) and polysaccharide (Jag C 162) in reducing soil erosion under simulated rainfalls." *Water, 10*(257).

Lu, J., & Wu, L. 2003. "Polyacrylamide quantification methods in soil conservation studies." *Journal of Soil and Water Conservation*, *58*(5), 270-275.

Lu, J., Wu, L., & Gan, J. 2003. "Determination of polyacrylamide in soil waters by size exclusion chromatography." *Journal of Environmental Quality, 32*(5), 1922-1926.

Luk, S. H. 1979. "Effect of soil properties on erosion by wash and splash." *Earth Surface Processes, 4*, 241-255.

Marcos, E., R. Tarrega and E. Luis-Calabuig. 2000. "Comparative analysis of runoff and sediment yield with a rainfall simulator after experimental fire." *Arid Soil Research and Rehabilitation, 14*(3), 293-307.

Maroufpoor, Eisa, Arsalan Faryabi, Houshang Ghamarnia, and Goran Yamin Moshrefi. 2010. "Evaluation of uniformity coefficients for sprinkler irrigation systems under different field conditions in Kurdistan province (northwest of Iran)." *Soil and Water Research, 5*(4), 139-145.

McLaughlin, R., Amoozegar, A., Duckworth, O., & Heitman, J. 2014. "Optimizing soil-polyacrylamide interactions for erosion control at construction sites." *Water Resources Research Institute of the University of North Carolina*. Accessed september 2020. <https://repository.lib.ncsu.edu/bitstream/handle/1840.4/8288/NC-WRRI-441.pdf?sequence=1>.

McLaughlin, R. A., & Bartholomew, N. 2007. "Soil factors influencing suspended sediment flocculation by polyacrylamide." *Soil Science Society of America, 71*(2), 537-544.

McLaughlin, R. A., & Knappe, D. 2015-2016. "Optimizing factors of sediment flocculation in construction site runoff." *North Carolina Department of Transportation Research and Development*. Accessed December 2020. <https://connect.ncdot.gov/projects/research/RNAProjDocs/2015-16%20Final%20Report.pdf>.

Miller, W. P. 1987. “Infiltration and soil loss of three gypsum-amended ultisols under simulated rainfall.” *Soil Science Society of America Journal, 51*, 1314-1320.

Mitchell, Charles C. 2008. “Natural resources conservation services soil areas in Alabama.” *The United States Department of Agriculture.* Accessed September 2020. <nrcs.usda.gov/wps/portal/nrcs/detail/soils/survey/office/ssr7/?cid=nrcs142p2_047868>.

Mocchiutti, P., & Zaruttini, M. 2007. “Key considerations in the determination of polyelectrolyte concentration by the colloidal: titration method.” *Bioresources, 2*(3), 399-407.

Momani, F. A. A., & Ormeci, B. 2014. “Measurement of polyacrylamide polymers in water and wastewater using an in-line UV-Vis spectrophotometer.” *Journal of Environmental Chemical Engineering*, *2*, 765-772.

National Oceanic and Atmospheric Administration. 2017. “NOAA Atlas 14 Point Precipitation Frequency Estimates: Auburn #2.” Accessed July 2021. <https://hdsc.nws.noaa.gov/hdsc/pfds/pfds_map_cont.html>.

National Transportation Product Evaluation Program. (2015). “AASHTO/NTPEP Erosion Control Products User Guide.” Accessed August 2021.”< https://ntpep.transportation.org/wp-content/uploads/sites/66/2020/09/ECP-User-Guide_Feb-2015.pdf>.

Naves, Juan, Jose Anta, Joaquin Suarez, and Jeronimo Puertas. 2020. Development and calibration of a new dripper-based rainfall simulator for large-scale sediment wash-off studies. *Water, 12*(1), 152.

Nearing, M. A. 1997. “A single, continuous function for slope steepness influence on soil loss.” *Soil Science Society of America Journal, 61*, 917-919.

North American Green. 2009. “Material and Performance Specification Sheet. S150 Erosion Control Blanket.” Accessed August 2021. <https://www.brockwhite.com/userfiles/documents/info/nag_s150_spec.pdf>.

Oklahoma State University. 2021. “Roll erosion control practices. Erosion and sediment control for construction sites.” <http://erosioncontrol.okstate.edu/roll-erosion-control-practices-1> Accessed September 2021.

Pall, R., W. T. Dickinson, D. Beals, and R. McGirr. 1983. “Development and calibration of a rainfall simulator.” *Canadian Agricultural Engineering, 25*(2), 181-187.

Paterson, D. G., C. Buhmann, G. M. E. Pienaar, and R. O. Barnard. 2011. “Beneficial effect of palm geotextiles on inter-rill erosion in South African soils and mine dam tailings: a rainfall simulator study.” *South African Journal of Plant and Soil, 28*(3), 181-189.

Perez, Michael A., Wesley N. Donald, and Xing Fang. 2019. “Evaluation of ALDOT erosion control practices using rainfall simulation on various soil types and slope gradients.” *A research proposal submitted to the Alabama Department of Transportation, Montgomery, Alabama.*

Petersen, A. L., A. M. Thompson, C. A. Baxter, J. M. Norman, and A. Roa-Espinosa. 2007. “A new polyacrylamide (PAM) formulation for reducing erosion and phosphorous loss in rainfed agriculture.” *Transactions of the ASCBE, 50*(6), 2091-2101.

Profile Products. 2010. “EcoFibre Hydraulic Mulch – Wood.” Accessed August 2021. <https://tritonenviro.com/download/EROSION%20CONTROL/4)%20Hydraulic%20Erosion%20Control%20Products%20(HECPs)/A)%20Base%20Hydromulch/Wood/Profile%20Products%20-%20EcoFibre.pdf>.

Profile Products. 2010. “Terra-Wood with Tack.” Accessed August 2021. <https://www.cascadegeos.com/userdocs/products/Terra-Wood-Brochure1QS.pdf>.

Przepiora, A., D. Hesterberg, J. E. Parsons, J. W. Gilliam, D. K. Cassel, and W. Faircloth. 1997. “Calcium Sulfate as a flocculant to reduce sedimentation basin water turbidity.” *Journal of Environmental Quality, 26*, 1605-1611.

Quansah, C. 1981. “The effect of soil type, slope, rain intensity and their interactions on splash detachment and transport*.” Journal of Soil Science, 32*, 215-224.

Regmi, T. P., and Thompson, A. L. 2000. “Rainfall simulator for laboratory studies.” *Applied Engineering in Agriculture, 16*, 641-652.

Renard, K. G., G. R. Foster, G. A. Weesies, D. K. McCool, and D. C. Yoder. 1997. “Predicting soil erosion by water: A guide to conservation planning with the Revised Universal Soil Loss Equation (RUSLE).” *The United States Department of Agriculture, Agricultura Handbook No. 703.*

Renard, Kenneth G., George R. Foster, Glenn A. Weesies, and Jeffery P. Porter. 1991. “RUSLE-Revised Universal Soil Loss Equation.” *Journal of Soil and Water Conservation, 46*(1), 30-33.

Rossman, Lewis A. 2000. “EPANET 2 User’s Manual.” *The National Risk Management Research Laboratory, The United States Environmental Protection Agency*, Cincinnati, Ohio. Accessed July 2021. <https://www.microimages.com/documentation/Tutorials/Epanet2UserManual.pdf>.

Ries, Johannes Bernhard, Manuel Seeger, Thomas Iserloh, Stehanie Wistorf, and Wolfgang Fister. 2009. "Calibration of simulated rainfall characteristics for the study of soil erosion on agricultural land." *Soil and Tillage Research, 106*(1), 109-116.

Ricks, Matthew D., Matthew A. Horne, Brian Faulkner, Wesley C. Zech, Xing Fang, Wesley N. Donald, and Michael A. Perez. 2019. "Design of a pressurized rainfall simulator for evaluating performance of erosion control practices." *Water, 11*, 2386.

Ryan, A. Paddy. 1991. "Environmental effects of sediment on New Zealand streams: A review." *New Zealand Journal of Marine and Freshwater Research, 25*(2), 207-221.

Sadeghi, Seyed Hamidreza, Zeinab Hazbavi, Habibollah Younesi, and Nader Bahramifar. 2016. "Trade-off between runoff and sediments from treated erosion plots and polyacrylamide and acrylamide residues." *Catena, 142,* 213-220.

Seybold, C. A. 1994. "Polyacrylamide review: Soil conditioning and environmental fate." *Communications in Soil Science and Plant Analysis, 25*(11-12), 2171-2185.

Singer, Michael J., Peter Janitzsky, and John Blackard. 1982. "The influence of exchangeable sodium percentage on soil erodibility." *Soil Science Society of America Journal*, *46*, 117-121.

Singh, R., N. Panigraphy, and G. Philip. 1999. "Modified rainfall simulator infiltrometer for infiltration, runoff, and erosion studies." *Agricultural Water Management, 41*(3), 167-175.

Slade, R. 2014. "Construction sediment: The greatest threat to water quality." *Hill Country Alliance*. Accessed December 2020. <https://hillcountryalliance.org/wp-content/uploads/2014/06/Construction-sediment.pdf>.

Snell, E. n. d. "Polymer enhanced BMPs for the construction industry." Accessed December 2020. <https://swcssnec.org/wp-content/uploads/Polymer-Enhanced-Best-Management-Practices-for-the-Construction-v2d-1.pdf>.

Sojka, R. E., and J. A. Entry. 2000. "Influence of polyacrylamide application to soil on movement of microorganisms in runoff water." *Environmental Pollution, 108*(3), 405-412.

Soo Lee, Sang, Haleem S. Shah, Yasser M. Awad, Sandeep Kumar, and Yong Sik Ok. 2015. "Synergy effects of biochar and polyacrylamide on plants growth and soil erosion control." *Environmental Earth Sciences, 74,* 2463-2473.

Soo Lee, Sang, Scott X Chang, Yoon-Young Chang, and Yong Sik Ok. 2013. "Commercial versus synthesized polymers for soil erosion control and growth of Chinese cabbage." *SpringerPlus, 2*(534).

Sousa, Silvio Fagundes de, Thiago Augusto Mendes, and Eduardo Queija de Siqueira. 2017. "Development and calibration of a rainfall simulator for hydrological studies." *RBRH, 22.*

South Carolina Department of Transportation. 2011. "Supplemental Technical Specification for Hydraulic Erosion Control Products." Accessed August 2021. <https://www.scdot.org/business/pdf/stormwater/SC-M-815-11.pdf>.

Sprague, C. Joel. 2018. "Large-scale slope erosion testing (ASTM D6459) of LSC Environmental's EarthGuard Fiber Matrix Hydraulically Applied Erosion Control Product (HECP) over loam." *American Association of State Highway and Transportation Officials/National Transportation Product Evaluation Program* Technical Report.

Sprague, C. Joel, Peter Kemp, and James E. Sprague. 2013. "Performance testing of traditional slope erosion controls." Presented at the *International Erosion Control Association*, San Diego, CA, conference 44.

Sprague, C. Joel, and Jarrett Nelson. 2009. "Correlation of bench-scale and large-scale performance testing of RECPs." Presented at the *International Erosion Control Association*, Reno, NV.

Stern, R., M. Ben-Hur, and I. Shainberg. 1991. "Clay mineralogy effect on rain infiltration, seal formation, and soil losses." *Soil Science*, 455-462.

Taucer, P. I., C. L. Munster, B. P. Wilcox, M. K. Owens, and B. P. Mohanty. 2008. "Large-scale rainfall simulation experiments on juniper rangelands." *Transactions of the ASABE, 51*(6), 1951-1961.

Trout, T. J., R. E. Sojka, and R. D. Lentz. 1995. "Polyacrylamide effect on furrow erosion and infiltration." *Transactions of the ASAE, 38*(3), 761-765.

USDA Natural Resources Conservation Service. 1998. "Official Series Description." Accessed May 2020. <web.archive/org/web/20090407074901/http://www2.ftw.nrcs.usda.gov/osd/dat/B/BAMA.html>.

The United States Department of Agriculture Natural Resources Conservation Service. 2012. In *Part 631 National Engineering Handbook* (pp. 3-3).

The United States Department of Agriculture Forest Service. 2006. "Erosion Control Treatment Selection Guide." Accessed August 2021. < https://www.fs.fed.us/t-d/pubs/pdf/hi_res/06771203hi.pdf>.

The United States Environmental Protection Agency. 2008. “The Homebuilders Clean Water Settlement.” Accessed May 2020. < https://www.epa.gov/enforcement/home-builders-clean-water-settlement>.

The United States Environmental Protection Agency. 2004. “Clean Water Act Requirements for Construction Projects in Indian Country.” *Region 9 Clean Water Act Compliance Office*. Accessed July 2020. ,https://nepis.epa.gov/Exe/ZyNET.exe/P1001M4E.TXT?ZyActionD=ZyDocument&Client=EPA&Index=2000+Thru+2005&Docs=&Query=&Time=&EndTime=&SearchMethod=1&TocRestrict=n&Toc=&TocEntry=&QField=&QFieldYear=&QFieldMonth=&QFieldDay=&IntQFieldOp=0&ExtQFieldOp=0&XmlQuery=&File=D%3A%5Czyfiles%5CIndex%20Data%5C00thru05%5CTxt%5C00000016%5CP1001M4E.txt&User=ANONYMOUS&Password=anonymous&SortMethod=h%7C-&MaximumDocuments=1&FuzzyDegree=0&ImageQuality=r75g8/r75g8/x150y150g16/i425&Display=hpfr&DefSeekPage=x&SearchBack=ZyActionL&Back=ZyActionS&BackDesc=Results%20page&MaximumPages=1&ZyEntry=1&SeekPage=x&ZyPURL>.

The United States Environmental Protection Agency. 2021. “Radioactive material from fertilizer production.” Accessed August 2021. <https://www.epa.gov/radtown/radioactive-material-fertilizer-production>.

Theisen, M. S. 1992. “The role of geosynthetics in erosion and sediment control: An overview”. *Geotextiles and Geomembranes, 11*, 535-550.

Tumsavas, Zeynal, and Ali Kara. 2011. “The effect of polyacrylamide (PAM) applications on infiltration, runoff, and soil losses under simulated conditions.” *African Journal of Biotechnology, 10*(15), 2894-2903.

Van Dijk, A. I. J. M., L. A. Bruijnzeel, and C. J. Rosewell. 2002. “Rainfall intensity-kinetic energy relationships: a critical literature appraisal.” *Journal of Hydrology, 261*(1-4), 1-23.

Verhaegen, Th. 1984. “The influence of soil properties on the erodibility of Belgian loamy soils: a study based on rainfall simulation experiments.” *Earth Surface Processes and Landforms, 9*, 499-507.

Weston, D. P., Lentz, R. D., Cahn, M. D., Ogle, R. S., Rothert, A. K., & Lydy, M. J. 2009. “Toxicity of anionic polyacrylamide formulations when used for erosion control in agriculture.” *Journal of Environmental Quality, 38*(1), 238-247.

Wisniewska, M., Fijalkowska, G., & Szewczuk-Karpisz, K. 2018. “The mechanism of anionic polyacrylamide adsorption on the montmorillonite surface in the presence of Cr(VI) ions.” *Chemosphere*, *211,* 524-534.

Wynn, Theresa, and Saied Mostaghimi. 2006. "The effects of vegetation and soil type on streambank erosion, southwestern Virginia, USA." *Journal of the American Water Resources Association*, 69-82.

Xiong, B., Loss, R. D., Shields, D., Pawlik, T., Hochreiter, R., Zydney, A. L., & Kumar, M. 2018. "Polyacrylamide degradation and its implication in environmental systems." *Nature Partner Journals Clean Water, 1*(17), 1-9.

Yakubu, Mahadi Lawan, Zulkifli Yusop and Mohamad Ali Fulazzaky. 2014. "The influence of rain intensity on raindrop diameter and the kinetics of tropical rainfall: Case study of Skudai, Malaysia." *Hydrological Sciences Journal, 61*(5), 944-951.

Yao, C., T. Lei, W. J. Elliot, D. K. McCool, J. Zhao, S. Chen. 2008. "Critical conditions for rill initiation." *Transactions of the ASABE*, *51*(1), 107-114.

Yu, Jian, T. Lei, I. Shainberg, A. I. Mamedov, and G. J. Levy. 2003. "Infiltration and erosion in soils treated with dry PAM and gypsum." *Soil Science Society of America Journal, 67*, 630-636.

Yusuf, K. O., O. O. Oyebode, S. O. Olaoke, S. Omokore, A. K. Iwayemi, and W. A. Adewoye. 2017. "Design and construction of a simple rainfall simulator from locally available materials." *Nigerian Journal of Pure and Applied Sciences, 30*(1), 2394-2946.

Zhang, G. H., B. Y. Liu, M. A. Nearing, C. H. Huang, and K. L. Zhang. 2002. "Soil detachment by shallow flow." *American Society of Agricultural Engineers, 45*(1).

APPENDIX A: CHAPTER 2 SUPPORTING DATA
Example Worksheets
Bare Soil Summary Test Data
Jute Matting Test Data
ProMatrix™ Test Data
PAM Test Data
Gypsum Test Data
EarthGuard™ EDGE™ Pellets Test Data
Bench Scale Gypsum Test Data
Gypsum Jar Test Data

TABLE A.1: Example Moisture and Compaction Worksheet, Bare Soil 10/14/2020

Drive Cylinder Compaction

Sample Location	Top	Middle	Bottom
Height of Soil in Cylinder (in.)	3.5	2.625	2.375
Volume of Soil (in.^{3})	41.28	30.96	28.01
Volume of Soil (ft^3)	0.0239	0.0179	0.0162
Weight of Soil and Cylinder (g)	1597	1374	1273
Weight of Cylinder (g)	570	570	570
Weight of Soil (g)	1027	804	703
Weight of Soil (lb)	2.264	1.773	1.550
Wet Density (lb/ft^3)	94.79	98.94	95.62
Dry Density (lb/ft^3)	76.49	84.95	79.40
Max Dry Density of Test (lb/ft^3)	96	96	96
Compaction (%)	79.68%	88.49%	82.70%
Average Compaction (%)	83.62%		

Moisture

Tare Weight Moist Soil (g)	92	85.0	93.0
Tare Weight Dry Soil (g)	70	71.0	74.0
Moisture Content (%)	23.9%	16.5%	20.4%
Optimal Moisture for Test (%)	20.0%	20.0%	20.0%
Average Moisture Content (%)	20.3%		

TABLE A.2: Example Sediment Loss Analysis Worksheet, Bare Soil 10/14/2020

Parameter	2 in./hr	4 in./hr			6 in./hr		
Settling Time (hr)	24	24	24	24	24	24	24
Total Wet Weight of Sediment (lb)	114.4	675.0	805.2	27.8	738.2	894.6	12.0
Dry Weight (lb)	66.8	485.2	530.9	19.0	687.1	587.2	8.5
Moisture Content (%)	171.22%	139.11%	51.67%	46.05%	107.4%	52.35%	40.94%
Total Dry Weight of Sediment (lb)	66.8	1035.2			1282.8		

TABLE A.3: Example TSS and Turbidity Worksheet, Bare Soil 10/14/2020

Sample ID	Time (min)	Dilution Factor	Turbidity Reading (NTU)	Filter + Crinkle Dish (g)	Dry Filter + Soil + Crinkle Dish (g)	Turbidity (NTU)	TSS (mg/L)
201	0						
202	3						
203	6	76	789	1.3838	3.2968	59964	76520
204	9	101	839	1.3983	4.9412	84739	141716
205	12	101	873	1.3975	5.1900	88173	151700
206	15	126	775	1.3993	6.6939	97650	211784
207	18	201	895	1.3850	8.5739	179895	287556
208	21	201	573	1.3824	10.4211	115173	361548
209	24	251	200	1.3854	9.7448	50200	334376
210	27	251	527	1.3834	11.6600	132277	411064
211	30	251	555	1.3821	11.3194	139305	397492
212	33	201	823	1.3876	11.4344	165423	401872
213	36	201	600	1.3948	11.8235	120600	417148
214	39	201	711	1.3700	9.7037	142911	333348
215	42	201	427	1.3905	3.6591	85827	90744
216	45	251	543	1.3836	8.2189	136293	273412
217	48	201	632	1.3571	7.0268	127032	226788
218	51	251	530	1.3665	6.0121	133030	185824
219	54	201	510	1.3768	5.9619	102510	183404
220	57	151	666	1.3870	5.4145	100566	161100
221	60	151	645	1.3841	6.8122	97395	217124

TABLE A.4: Example Runoff Worksheet, Bare Soil 10/14/2020

Intensity, in./hr	Test Time, min	Time per gallon, sec	Modification Factor	Time per gallon, min	Runoff Rate, gal/min	Runoff, gal	Cumulative Runoff, gal	Runoff (gal)
2	0	0	0.25	0.00	0.00	0.00	0.00	102.0
	2	0	0.25	0.00	0.00	0.00	0.00	
	4	0	0.25	0.00	0.00	0.00	0.00	
	6	20.1	0.25	0.08	0.75	1.49	1.49	
	8	8.73	0.25	0.04	1.72	3.44	4.93	
	10	4.4	0.25	0.02	3.41	6.82	11.75	
	12	1.81	0.25	0.01	8.29	16.57	28.32	
	14	1.91	0.25	0.01	7.85	15.71	44.03	
	16	1.55	0.25	0.01	9.68	19.35	63.38	
	18	1.78	0.25	0.01	8.43	16.85	80.24	
	20	1.38	0.25	0.01	10.87	21.74	101.98	
4	22	4.77	1.00	0.08	12.58	25.16	127.13	301.8
	24	3.31	1.00	0.06	18.13	36.25	163.39	
	26	4.23	1.00	0.07	14.18	28.37	191.76	
	28	3.31	1.00	0.06	18.13	36.25	228.01	
	30	3.43	1.00	0.06	17.49	34.99	263.00	
	32	3.50	1.00	0.06	17.14	34.29	297.28	
	34	3.73	1.00	0.06	16.09	32.17	329.45	
	36	4.55	1.00	0.08	13.19	26.37	355.83	
	38	4.43	1.00	0.07	13.54	27.09	382.91	
	40	5.77	1.00	0.10	10.40	20.80	403.71	
6	42	3.03	1.00	0.05	19.80	39.60	443.32	504.2
	44	3.35	1.00	0.06	17.91	35.82	479.14	
	46	3.33	1.00	0.06	18.02	36.04	515.17	
	48	3.00	1.00	0.05	20.00	40.00	555.17	
	50	3.23	1.00	0.05	18.58	37.15	592.32	
	52	2.97	1.00	0.05	20.20	40.40	632.73	
	54	2.67	1.00	0.04	22.47	44.94	677.67	
	56	3.07	1.00	0.05	19.54	39.09	716.76	
	58	2.78	1.00	0.05	21.58	43.17	759.93	
	60	2.61	1.00	0.04	22.99	45.98	805.90	

TABLE A.5: Bare Soil Data Summary (Thesis Tests Only)

Parameter	Test 1	Test 2	Test 3	Test 4	Test 5	Avg.
Rainfall Depth (in)	3.8	3.7	4.1	3.8	4.3	3.9
Compaction (%)	80.6%	83.6%	77.2%	79.5%	78.3%	79.8
Moisture (%)	24.4%	20.3%	14.8%	16.7%	18.7%	19.0
2 in/hr Soil Loss (lb)	62.7	66.8	21.6	13.8	17.6	36.5
4 in/hr Soil Loss (lb)	667.1	1035.2	704.2	628.6	353.1	677.6
6 in/hr Soil Loss (lb)	1021.6	1282.8	1385.8	1236.5	1233.9	1232.1
k-factor	0.26	0.31	0.27	0.24	0.24	0.26

TABLE A.6: Average TSS and Turbidity, Bare Soil Tests (All Data)

Time (min)	Turbidity (NTU)	TSS (mg/L)
0	1033	530
3	13026	15834
6	17981	28873
9	18668	30870
12	20563	42886
15	37012	58041
18	24068	72839
21	11073	67405
24	27489	82742
27	28894	80028
30	34118	80904
33	25153	83959
36	29615	67199
39	18199	18678
42	28292	55212
45	26440	45887
48	27639	37694
51	21535	37210
54	21146	32750
57	20512	43954
60	1292	662

TABLE A.7: Jute Matting Data Summary

Parameter	Bare Soil	Test 1	Test 2	Test 3
Rainfall Depth (in)	4.1	3.9	4.6	4.3
Percent Compaction (%)	77.2%	88.6%	77.0%	87.9%
Moisture Content (%)	24.4%	23.7%	22.4%	16.3%
2 in/hr Soil Loss (lb)	21.6	3.7	2.1	5.3
4 in/hr Soil Loss (lb)	704.2	118.7	174.7	109.3
6 in/hr Soil Loss (lb)	1,385.8	418.9	1008.5	735.9

TABLE A.8: Jute Matting TSS/Turbidity Summary

Time (min)	Turbidity (NTU)	TSS (mg/L)	Turbidity (NTU)	TSS (mg/L)	Turbidity (NTU)	TSS (mg/L)
3						
6	2607	1772	1710	1552	24870	10706
9	35136	28516	3712	3492	21525	10366
12	33405	20600	10230	7316	56202	20164
15	60878	22672	34164	19396	20604	18938
18	61722	19924	23103	14104	66120	44538
21	71442	26408	29631	19928	74100	66356
24	46592	26880	29427	20844	115666	76628
27	91708	50344	45186	41564	149745	119098
30	90687	77492	62852	64984	150750	106300
33	60915	40864	89587	87300	163614	131536
36	149339	97728	103068	120600	167417	110358
39	110148	94824	146080	171344	169676	132358
42	79797	75892	140562	167828	134536	117946
45	94269	97420	149625	219740	157126	120804
48	66531	86304	169778	158336	129265	84942
51	89270	73632	165072	158276	154365	112646
54	107802	77172	198789	145816	84336	85660
57	98536	66172	149946	184004	191553	89272
60	91982	56628	183513	191964	118590	81694

TABLE A.9: Jute Runoff Data

Test 1			Test 2			Test 3		
Runoff, gal	Cumulative Runoff, gal	Cumulative Runoff, gal	Runoff, gal	Cumulative Runoff, gal	Cumulative Runoff, gal	Runoff, gal	Cumulative Runoff, gal	Cumulative Runoff, gal
0.00	0.00		0.00	0.00		0.00	0.00	
0.00	0.00		0.00	0.00		0.00	0.00	
0.00	0.00		0.00	0.00		0.00	0.00	
2.40	2.40		0.18	0.18		0.00	0.00	
7.38	9.78		0.21	0.40		0.00	0.00	
8.72	18.50	75.39	0.27	0.67	13.92	0.00	0.00	46.96
11.41	29.91		1.25	1.92		0.95	0.95	
19.80	49.71		3.00	4.92		6.32	7.27	
8.24	57.95		3.00	7.92		10.31	17.58	
16.35	74.30		3.00	10.92		12.24	29.82	
1.09	75.39		3.00	13.92		17.14	46.96	
34.09	109.48		6.32	20.23		20.00	66.96	
19.26	128.74		12.00	32.23		22.90	89.86	
16.00	144.74		12.00	44.23		23.30	113.16	
16.17	160.92		13.33	57.56		26.73	139.89	
20.91	181.82	198.37	13.33	70.90	123.14	21.43	161.32	234.85
19.20	201.02		13.33	84.23		22.90	184.22	
16.88	217.90		12.00	96.23		20.00	204.22	
16.60	234.50		15.00	111.23		20.10	224.32	
18.21	252.71		15.00	126.23		29.06	253.38	
21.05	273.76		17.14	143.37		28.44	281.81	
30.53	304.29		20.00	163.37		35.29	317.11	
49.79	354.09		24.00	187.37		33.52	350.63	
50.42	404.51		30.00	217.37		26.20	376.83	
56.60	461.11		24.00	241.37		27.09	403.91	
52.86	513.97	519.73	24.00	265.37	286.23	36.25	440.17	362.92
49.38	563.36		24.00	289.37		31.83	472.00	
48.00	611.36		30.00	319.37		25.75	497.75	
41.67	653.02		30.00	349.37		31.75	529.50	
35.29	688.32		30.00	379.37		37.50	567.00	
29.78	718.09		30.00	409.37		30.77	597.77	

TABLE A.10: ProMatrix™ EFM™ Data Summary

Parameter	Bare Soil	Test 1	Test 2	Test 3
Rainfall Depth (in)	3.7	4.1	3.7	3.4
Percent Compaction (%)	83.6%	81.7%	77.0%	80.4%
Moisture Content (%)	20.3%	19.8%	22.4%	17.3%
2 in/hr Soil Loss (lb)	66.8	0.1	0.0	0.8
4 in/hr Soil Loss (lb)	1,035.2	220.7	120.2	54.9
6 in/hr Soil Loss (lb)	1,282.8	1,000.6	673.4	712.6

TABLE A.11: ProMatrix™ EFM™ TSS/Turbidity Summary

Time (min)	Turbidity (NTU)	TSS (mg/L)	Turbidity (NTU)	TSS (mg/L)	Turbidity (NTU)	TSS (mg/L)
3						
6						
9						
12	4060	6008			2253	3120
15	3880	5296			1486	2544
18	1232	1648	1166	748	1834	3728
21	1132	1428	1090	1384	1542	3440
24	1574	2112	1550	1024	2756	7656
27	36414	31520	20582	17268	8950	15288
30	56323	43504	20094	23356	11206	16188
33	111936	93856	42521	50804	37434	31812
36	104341	88380	55853	75528	43044	68344
39	114048	67052	52217	95824	41514	90688
42	126896	118400	81911	111808	64977	105408
45	85184	90228	75952	129572	113135	180828
48	133408	96272	61206	139800	85768	170012
51	122007	100112	137410	194600	139675	224892
54	99414	106736	116160	182752	113498	245208
57	50434	79332	70195	178512	98252	222704
60	99358	80540	55870	165880	85305	167520

TABLE A.12: PAM Data Summary

Parameter	Bare Soil	Test 1	Test 2	Test 3	Test 4
Rainfall Depth (in)	3.8	4.1	3.6	3.3	4.6
Percent Compaction (%)	80.1%	85.2%	77.7%	77.0%	79.2%
Moisture Content (%)	14.8%	20.5%	18.0%	22.4%	18.3%
2 in/hr Soil Loss (lb)	62.7	0.0	0.0	0.0	0.0
4 in/hr Soil Loss (lb)	667.1	129.7	139.0	68.5	121.3
6 in/hr Soil Loss (lb)	1,021.6	1,176.2	1,094.8	580.5	563.9

TABLE A.13: PAM TSS/Turbidity Summary

Time (min)	Turbidity (NTU)	TSS (mg/L)	Turbidity (NTU)	TSS (mg/L)	Turbidity (NTU)	TSS (mg/L)
3						
6						
9						
12			29100	47436	3680	5700
15			16500	18976	62400	34090
18	21948	35072	15900	18024	38200	14115
21	31977	20084	1940	2288	14700	30350
24	23715	23008	4420	5788	14200	12525
27	5916	22600	5430	7356	7460	13165
30	1948.2	9472	51500	164816	73600	81610
33	83993	114716	82000	229832	196400	106535
36	25172	134392	100933	329296	188800	161400
39	36449	176212	115867	230400	167600	162950
42	42224	215312	154833	241096	173200	114595
45	249228	281476	157667	277856	157200	135295
48	126811	190348	144433	250344	158000	115955
51	161068	116308	167767	300616	152000	88420
54	97963	144972	141400	236912	169600	111530
57	118998	132884	132533	240600	135000	99665
60	151803	157964	120867	243552	122800	71685

TABLE A.14: PAM Runoff Data

Test 1			Test 2			Test 3		
Runoff, gal	Cumulative Runoff, gal	Cumulative Runoff, gal	Runoff, gal	Cumulative Runoff, gal	Cumulative Runoff, gal	Runoff, gal	Cumulative Runoff, gal	Cumulative Runoff, gal
0.00	0.00		0.00	0.00		0.00	0.00	
0.00	0.00		0.00	0.00		0.00	0.00	
0.00	0.00		0.00	0.00		0.00	0.00	
0.00	0.00		0.00	0.00		0.00	0.00	
0.00	0.00		0.00	0.00		0.00	0.00	
0.00	0.00	4.09	0.00	0.00	19.00	0.00	0.00	31.25
0.00	0.00		0.00	0.00		0.00	0.00	
0.81	0.81		3.00	3.00		3.75	3.75	
0.88	1.69		5.00	8.00		5.00	8.75	
1.20	2.89		5.00	13.00		7.50	16.25	
1.20	4.09		6.00	19.00		15.00	31.25	
6.00	10.09		7.50	26.50		15.00	46.25	
2.00	12.09		10.00	36.50		10.91	57.16	
7.50	19.59		8.57	45.07		12.00	69.16	
10.91	30.50		9.23	54.30		13.33	82.49	
12.00	42.50	97.57	12.00	66.30	101.21	15.00	97.49	126.58
10.91	53.41		12.00	78.30		15.00	112.49	
12.00	65.41		13.33	91.64		12.00	124.49	
10.91	76.32		10.00	101.64		10.00	134.49	
12.00	88.32		10.00	111.64		13.33	147.83	
13.33	101.65		8.57	120.21		10.00	157.83	
10.00	111.65		20.00	140.21		24.00	181.83	
13.33	124.99		20.00	160.21		20.00	201.83	
20.00	144.99		17.14	177.35		24.00	225.83	
20.00	164.99		20.00	197.35		24.00	249.83	
17.14	182.13	181.71	17.14	214.49	207.57	24.00	273.83	246.25
20.00	202.13		20.00	234.49		20.00	293.83	
20.00	222.13		17.14	251.64		15.00	308.83	
20.00	242.13		20.00	271.64		20.00	328.83	
20.00	262.13		17.14	288.78		20.00	348.83	
17.14	279.27		20.00	308.78		24.00	372.83	

TABLE A.15: Gypsum Data Summary

Parameter	Bare Soil	Test 1	Test 2	Test 3
Rainfall Depth (in)	4.3	3.4	3.7	4.0
Percent Compaction (%)	79.5	81.5	73.5	90.2
Moisture Content (%)	16.7	16.7	17.1	19.2
2 in/hr Soil Loss	13.8	1.8	2.0	0.7
4 in/hr Soil Loss	628.6	33.5	10.2	13.7
6 in/hr Soil Loss	1233.9	245.5	118.7	71.6

TABLE A.16: Gypsum TSS/Turbidity Summary

Time (min)	Turbidity (NTU)	TSS (mg/L)	Turbidity (NTU)	TSS (mg/L)	Turbidity (NTU)	TSS (mg/L)
3						
6						
9						
12			29100	47436	3680	5700
15			16500	18976	62400	34090
18	21948	35072	15900	18024	38200	14115
21	31977	20084	1940	2288	14700	30350
24	23715	23008	4420	5788	14200	12525
27	5916	22600	5430	7356	7460	13165
30	1948.2	9472	51500	164816	73600	81610
33	83993	114716	82000	229832	196400	106535
36	25172	134392	100933	329296	188800	161400
39	36449	176212	115867	230400	167600	162950
42	42224	215312	154833	241096	173200	114595
45	249228	281476	157667	277856	157200	135295
48	126811	190348	144433	250344	158000	115955
51	161068	116308	167767	300616	152000	88420
54	97963	144972	141400	236912	169600	111530
57	118998	132884	132533	240600	135000	99665
60	151803	157964	120867	243552	122800	71685

TABLE A.17: Gypsum Runoff Data

Test 1			Test 2			Test 3		
Runoff, gal	Cumulative Runoff, gal	Cumulative Runoff, gal	Runoff, gal	Cumulative Runoff, gal	Cumulative Runoff, gal	Runoff, gal	Cumulative Runoff, gal	Cumulative Runoff, gal
0.00	0.00	27.91	0.00	0.00	24.98	0.00	0.00	29.28
0.00	0.00		0.00	0.00		0.00	0.00	
0.00	0.00		0.00	0.00		0.00	0.00	
0.00	0.00		0.00	0.00		0.00	0.00	
0.00	0.00		0.00	0.00		0.00	0.00	
0.00	0.00		0.00	0.00		0.00	0.00	
0.00	0.00		0.00	0.00		0.00	0.00	
5.77	5.77		10.00	10.00		7.14	7.14	
6.25	12.02		5.00	15.00		6.25	13.39	
7.32	19.34		5.00	20.00		7.32	20.71	
8.57	27.91		4.98	24.98		8.57	29.28	
6.82	34.73	94.95	5.61	30.59	88.32	6.82	36.10	94.95
9.09	43.82		9.30	39.89		9.09	45.19	
8.39	52.21		9.16	49.05		8.39	53.58	
8.22	60.43		8.57	57.62		8.22	61.80	
9.84	70.26		8.63	66.25		9.84	71.64	
11.01	81.27		8.63	74.89		11.01	82.65	
10.81	92.08		10.34	85.23		10.81	93.46	
10.26	102.34		9.23	94.46		10.26	103.71	
10.34	112.68		9.16	103.62		10.34	114.06	
10.17	122.85		9.68	113.30		10.17	124.23	
14.46	137.31	223.67	11.65	124.95	158.01	14.46	138.69	225.04
18.46	155.77		13.48	138.43		18.46	157.15	
18.18	173.96		13.19	151.62		18.18	175.33	
18.75	192.71		13.48	165.10		18.75	194.08	
19.67	212.38		13.79	178.90		19.67	213.75	
21.05	233.43		13.33	192.23		21.05	234.80	
20.00	253.43		13.48	205.71		20.00	254.80	
21.05	274.48		13.19	218.90		21.05	275.86	
21.05	295.54		13.64	232.54		21.05	296.91	
23.08	318.61		13.79	246.33		23.08	319.99	

TABLE A.18: EDGE™ Pellets Data Summary

Parameter	Bare Soil	Test 1	Test 2	Test 3
Rainfall Depth (in)	3.8	3.5	3.9	3.8
Percent Compaction (%)	78.3%	91.8%	81.7%	81.5%
Moisture Content (%)	18.7%	18.5%	17.0%	20.7%
2 in/hr Soil Loss (lb)	17.6	21.8	9.2	1.2
4 in/hr Soil Loss (lb)	353.1	148.8	93.2	118.1
6 in/hr Soil Loss (lb)	1,236.5	327.9	521.3	588.7

TABLE A.19: EDGE™ Pellets TSS/Turbidity Summary

Time (min)	Turbidity (NTU)	TSS (mg/L)	Turbidity (NTU)	TSS (mg/L)	Turbidity (NTU)	TSS (mg/L)
3	0	0	0	0	0	0
6	78881	44650	0	0	0	0
9	155373	116610	0	0	0	0
12	163815	129680	52419	92050	172659	223680
15	126630	100860	61408	135620	120399	198640
18	149544	101630	38986	113760	74772	114320
21	128640	95960	32825	153890	46029	32460
24	116379	78660	56459	109320	81405	17080
27	122409	107560	20705	74540	34170	70800
30	124620	127850	31209	109400	56682	21080
33	72561	89370	15554	30080	31155	45440
36	88038	100870	18180	80530	41406	20160
39	101706	88260	37673	52600	26130	20540
42	79797	102690	21715	64930	33969	61960
45	122610	125240	25048	85790	33366	62380
48	83616	68430	36461	49880	62310	154540
51	111957	116230	74033	86380	95877	157920
54	143916	78260	76457	85030	161604	125840
57	135675	78400	86153	94060	141102	107680
60	182709	115880	92819	97190	98490	145060

TABLE A.20: Bench Scale Gypsum Testing Data Summary

Parameter	Test 1		Test 2		Test 3	
	Ag. Gypsum	Plaster	Ag. Gypsum	Plaster	Ag. Gypsum	Plaster
Rainfall Depth (in)	2.9		2.7		3.0	
Total Sediment Loss (g)	59.0	145.0	139.8	172.6	163.8	166.6
Total Runoff (gal)	4.6	7.6	7.2	8.3	8.2	8.5

TABLE A.21: Bench Scale Gypsum TSS and Turbidity Summary

	Average Agricultural Gypsum		Average Moulding Plaster	
Time (min)	Turbidity (NTU)	TSS (mg/L)	Turbidity (NTU)	TSS (mg/L)
3	0	0	0	0
6	0	0	0	0
9	0	0	0	0
12	0	0	0	0
15	0	0	0	0
18	0	0	0	0
21	0	0	0	0
24	7601	632	7601	446
27	7511	551	11503	1043
30	9699	611	9721	893
33	8952	587	9067	814
36	7269	480	7388	696
39	6938	440	6951	616
42	6321	446	6736	587
45	10308	614	10804	639
48	9097	488	10308	583
51	5389	361	7430	462
54	3810	376	5871	419
57	4148	337	6288	440
60	4098	327	5716	422

TABLE A.22: Modified Jar Testing Turbidity Results

	Initial			5 minutes			10 minutes			20 minutes		
	Test 1	Test 2	Test 3	Test 1	Test 2	Test 3	Test 1	Test 2	Test 3	Test 1	Test 2	Test 3
Control (NTU)	119238	123747	151704	192	160	99	100.5	219	43.7	59.6	62.1	31.3
Agricultural (NTU)	119192	125584	171269	290	205	323	134	133	189	77.2	69.8	80.2
Plaster (NTU)	119572	131596	140567	398	437	375	168	183	304	94.8	135	128

TABLE A.23: Complied Bare Soil Metrics

	Sediment Loss (lb)			Turbidity Average (1,000 NTU)			TSS Average (1,000 mg/L)			Cumulative Runoff (gal)		
	2in./hr	4in./hr	6in./hr	2in./hr	4in./hr	6in./hr	2in./hr	4in./hr	6in./hr	2in./hr	4in./hr	6in./hr
Overall Average	49.4	707.3	1,301.7	83.2	141.2	169.7	80.8	167.6	169.1	50.3	219.8	418.4
Standard Deviation	33.3	173.5	179.3	25.1	45.4	74.2	46.2	90.7	76.2	34.8	82.2	72.9

APPENDIX B: CHAPTER 3 SUPPORTING DATA

Calibration Sample Absorbance Data
PAM Absorbance and Concentration Data
Soil Interference Validation Data
Detection Limit Data
PAM Removal Validity Data
ProMatrix^{TM} Absorbance Data
EarthGuard^{TM} EDGE^{TM} Pellet Absorbance Data

TABLE B.1: Calibration Sample Absorbance Data, to 400 nanometers

Wave-length	DI	0 mg/L		20 mg/L		40 mg/L		60 mg/L		90 mg/L		120 mg/L	
200	0.2128	0.553	0.5401	0.6971	0.6909	0.9558	0.9674	1.304	1.3038	1.585	1.5738	1.833	1.8293
205	0.1923	0.5055	0.4935	0.5736	0.5704	0.7772	0.7875	1.0729	1.0749	1.1492	1.1387	1.3612	1.3587
210	0.1768	0.4648	0.455	0.5031	0.5005	0.6578	0.6656	0.8983	0.9003	0.892	0.8817	1.0585	1.0558
215	0.1589	0.4206	0.4123	0.4454	0.4432	0.5435	0.5476	0.7179	0.7193	0.7116	0.7032	0.8421	0.8417
220	0.1405	0.383	0.3768	0.398	0.3969	0.4418	0.4428	0.5561	0.5545	0.5699	0.5609	0.6713	0.6705
225	0.126	0.354	0.3497	0.362	0.361	0.37	0.3752	0.4451	0.4424	0.4602	0.4542	0.5381	0.5385
230	0.1196	0.3425	0.3359	0.345	0.3444	0.3383	0.3387	0.3958	0.393	0.4101	0.4052	0.4772	0.4781
235	0.1112	0.3223	0.3163	0.3223	0.3221	0.3044	0.3041	0.3468	0.3437	0.358	0.3499	0.4114	0.4113
240	0.1	0.2926	0.2897	0.2937	0.2926	0.2695	0.2679	0.3	0.2964	0.3044	0.2969	0.3477	0.348
245	0.0956	0.2816	0.2774	0.2837	0.2779	0.2576	0.2546	0.2822	0.2811	0.2879	0.2815	0.3277	0.3288
250	0.093	0.2724	0.2692	0.2747	0.2706	0.2502	0.2473	0.2728	0.2728	0.2786	0.2724	0.3171	0.3173
255	0.0888	0.261	0.2563	0.2605	0.2573	0.2385	0.2366	0.2598	0.259	0.265	0.2587	0.3011	0.3005
260	0.0851	0.2509	0.2451	0.2477	0.2465	0.2265	0.2251	0.247	0.2466	0.2543	0.2481	0.2877	0.2873
265	0.0814	0.2351	0.2331	0.2342	0.2339	0.2148	0.2152	0.2344	0.2337	0.2417	0.2355	0.274	0.2737
270	0.078	0.2225	0.2217	0.2215	0.2223	0.204	0.2047	0.2221	0.2208	0.2305	0.2242	0.2609	0.2598
275	0.0758	0.2166	0.2143	0.218	0.2151	0.1964	0.1978	0.2133	0.2115	0.2218	0.2162	0.251	0.2491
280	0.0732	0.2068	0.2044	0.209	0.2061	0.1869	0.1891	0.2024	0.2008	0.2104	0.2063	0.2389	0.237
285	0.0699	0.1961	0.2002	0.192	0.1948	0.1766	0.1792	0.1906	0.1897	0.1995	0.1964	0.2257	0.2244
290	0.0656	0.1833	0.1877	0.1799	0.1826	0.1654	0.168	0.1781	0.1763	0.1881	0.1844	0.21	0.2091
295	0.0616	0.1744	0.1732	0.1698	0.1715	0.1557	0.1584	0.1692	0.1657	0.178	0.1753	0.197	0.1968
300	0.0588	0.1684	0.1666	0.1621	0.1624	0.1495	0.1477	0.1638	0.1585	0.1714	0.1684	0.189	0.1882
305	0.056	0.1607	0.1587	0.1546	0.1552	0.1424	0.1384	0.1539	0.1504	0.163	0.16	0.1802	0.1783
310	0.0539	0.1533	0.1512	0.1473	0.1502	0.1353	0.1314	0.1455	0.1419	0.1545	0.1515	0.1719	0.1701
315	0.0528	0.146	0.1461	0.1403	0.1428	0.1285	0.1243	0.1374	0.1337	0.146	0.1446	0.1638	0.162
320	0.0516	0.1412	0.1412	0.135	0.1379	0.1237	0.1186	0.1323	0.129	0.142	0.1382	0.1573	0.1563
325	0.0505	0.1361	0.1361	0.1293	0.1322	0.1188	0.1135	0.1276	0.125	0.1373	0.1335	0.151	0.1507
330	0.0492	0.1313	0.1314	0.1244	0.1243	0.1137	0.1096	0.1215	0.1204	0.1324	0.1292	0.1448	0.1438
335	0.0478	0.1245	0.125	0.1173	0.1158	0.1084	0.1056	0.1154	0.1144	0.1277	0.1243	0.138	0.1372
340	0.0467	0.1196	0.1197	0.1112	0.1093	0.1035	0.1028	0.1099	0.108	0.1233	0.1196	0.1318	0.131
345	0.046	0.1152	0.1156	0.1072	0.1054	0.1006	0.099	0.1057	0.1038	0.1204	0.1153	0.1262	0.1273
350	0.0458	0.1122	0.1138	0.1042	0.1026	0.0973	0.0952	0.1026	0.1009	0.1179	0.1131	0.123	0.1241
355	0.0452	0.1085	0.1088	0.1008	0.0988	0.0943	0.0918	0.0997	0.0978	0.1151	0.1103	0.1187	0.1197
360	0.0444	0.1057	0.105	0.0972	0.0956	0.0915	0.0888	0.0963	0.0934	0.1115	0.1061	0.1148	0.1151
365	0.0442	0.1053	0.1028	0.0944	0.0917	0.09	0.0864	0.0934	0.0907	0.1081	0.1028	0.1123	0.1116
370	0.0429	0.0997	0.0987	0.0894	0.0875	0.0847	0.0818	0.0886	0.0867	0.1039	0.0999	0.1084	0.1055
375	0.0421	0.0978	0.0952	0.0869	0.0851	0.0843	0.0828	0.0855	0.0845	0.1013	0.0963	0.1055	0.1021
380	0.0414	0.0956	0.0929	0.0857	0.083	0.0801	0.0802	0.0826	0.0841	0.0996	0.0943	0.1026	0.0995

385	0.0405	0.0915	0.0905	0.0825	0.0835	0.0779	0.0756	0.0792	0.081	0.0979	0.0906	0.0984	0.0954
390	0.04	0.0901	0.087	0.0796	0.0795	0.0753	0.0727	0.077	0.0759	0.0951	0.0877	0.0945	0.0922
395	0.0399	0.0886	0.0851	0.0776	0.0762	0.0734	0.0701	0.0762	0.0739	0.0924	0.0861	0.0919	0.0907
400	0.0399	0.0859	0.0843	0.0779	0.0749	0.0718	0.0684	0.0758	0.073	0.0897	0.085	0.0904	0.0894

TABLE B.2: PAM Absorbance Readings and Concentrations

	Test 1		**Test 2**		**Test 3**		**Average PAM (mg/L)**	**Test 4**	
Min.	**Absorbance**	**PAM (mg/L)**	**Absorbance**	**PAM (mg/L)**	**Absorbance**	**PAM (mg/L)**		**Absorbance**	**PAM (mg/L)**
0									
3									
6									
9			1.0424	160	1.8778	354	257		
12			2.0875	403	2.5512	511	457		
15	1.7147	317	1.6966	312	1.5716	283	304	0.65245	29
18	1.4084	245	1.3042	221	1.2553	210	225	0.75460	38
21	1.3823	239	1.1772	192	1.9107	362	264	0.88465	78
24	0.6202	62	0.8791	122	1.0971	173	119	0.77195	40
27	1.5482	278	0.5656	49	0.8321	111	146	0.58025	23
30	0.8293	111	0.4729	28	0.3687	4	48	0.41825	9
33	0.8724	121	0.5345	42	0.8232	109	91	0.32660	1
36	0.6805	76	0.553	47	0.3973	10	44	0.41415	8
39	0.7666	96	0.6201	62	1.4329	251	136	0.53455	19
42	0.7391	90	0.6649	73	0.7067	82	82	0.58540	34
45	0.8804	123	1.1911	195	0.4701	27	115	0.74015	37
48	0.8002	104	0.751	93	1.3196	225	141	0.86655	48
51	0.7	81	0.7696	97	0.4816	30	69	0.82645	45
54	0.5336	42	0.6084	59	0.4202	16	39	0.79905	42
57	0.643	67	0.6592	71	0.2938	0	46	0.75300	38
60	0.8707	120	0.674	75	0.4512	23	73	0.75260	38

TABLE B.3: Soil Interference Validation Data

Turbidity of Centrifuged Field Samples (NTU)		Turbidity of Calibration Samples (NTU)
6.6	16.2	7.79
11.5	7.74	6.95
6.16	9.97	8.48
7.36	13.1	7.49
14.5	8.78	5.49
13.6	18.1	12.3
7.1	7.24	8.47
7.63	4.86	6.55
5.4	4.86	12.1
10.9	3.76	
14.2	5.67	
9.99	6.81	
5.2	4.83	
6	2.23	
6.87	5.39	
7.59	5.66	
5.76	5.78	
7.92	4.84	
6.13	12.2	
6.94	7.55	
8.38	7.64	
12.1	14.3	
26.4	8.32	
13.7	8.75	
11.6	9.63	
8.92	6.41	
7.67	6.14	
3.75	6.72	

TABLE B.4: Detection Limit Data

Corrected 2 mg/L Absorbance at 200nm		
0.5088	0.5011	0.502

TABLE B.5: PAM Removal Validity Data

Corrected Centrifuged Absorbance at 200nm		
0.6327	0.6337	0.6140
Corrected Uncentrifuged Absorbance at 200nm		
0.6166	0.6109	0.6412

TABLE B.6: ProMatrix™ Sample Absorbance Data, to 400 nanometers

Wave-length	DI	Sample #3		Sample #5		Sample #6	Sample #9		Sample #12		Sample #12	
200	0.1939	2.8492	2.8461	2.7016	2.696	2.4121	1.1488	1.1493	0.6026	0.5917	0.4521	0.4851
205	0.1747	3.0387	3.0333	2.8121	2.8076	2.2867	1.0465	1.0467	0.5569	0.5498	0.4097	0.4368
210	0.163	3.0071	2.9997	2.5648	2.5613	1.9868	0.8888	0.8907	0.5063	0.5036	0.3644	0.3881
215	0.1496	2.999	3.0048	2.1348	2.1371	1.6622	0.7178	0.7189	0.443	0.4431	0.3091	0.3294
220	0.1357	2.9861	2.9889	1.8213	1.8216	1.4647	0.61	0.6108	0.3987	0.3916	0.2637	0.2802
225	0.1235	2.9224	2.9212	1.6336	1.6336	1.3569	0.5511	0.5517	0.3698	0.3617	0.2325	0.2458
230	0.119	2.8034	2.8043	1.5384	1.5393	1.3054	0.5238	0.5245	0.3557	0.3521	0.2187	0.2326
235	0.1119	2.4787	2.4787	1.3736	1.3741	1.2181	0.4772	0.4777	0.3355	0.3327	0.2018	0.2131
240	0.1013	1.9871	1.9875	1.1085	1.1075	1.0754	0.401	0.4011	0.3054	0.3076	0.1793	0.188
245	0.0966	1.7319	1.7323	0.9696	0.9703	1.0003	0.3639	0.3638	0.291	0.2991	0.1702	0.1781
250	0.0939	1.5941	1.5939	0.8952	0.8956	0.9574	0.3441	0.344	0.2834	0.2903	0.1648	0.1723
255	0.0895	1.4628	1.4623	0.8239	0.8247	0.9095	0.3232	0.3231	0.2733	0.2777	0.1562	0.1641
260	0.0861	1.3976	1.3967	0.7866	0.7869	0.8788	0.3104	0.3105	0.2666	0.2709	0.1498	0.1579
265	0.0819	1.3835	1.3826	0.7772	0.7769	0.86	0.3023	0.3023	0.2615	0.2602	0.1431	0.1502
270	0.0779	1.392	1.3905	0.7786	0.7785	0.8493	0.2972	0.2973	0.259	0.2523	0.1374	0.1436
275	0.0757	1.3986	1.3967	0.7797	0.779	0.8416	0.2941	0.2938	0.2554	0.2474	0.1339	0.1396
280	0.0732	1.3787	1.3767	0.7658	0.7658	0.8268	0.2881	0.2877	0.2495	0.2424	0.1299	0.1356
285	0.0709	1.2917	1.2895	0.7207	0.7206	0.7964	0.2758	0.2753	0.2409	0.2378	0.1256	0.1311
290	0.0678	1.1413	1.1397	0.647	0.6465	0.7511	0.2565	0.256	0.2303	0.2287	0.1201	0.1252
295	0.065	1.044	1.0429	0.5998	0.599	0.7199	0.2417	0.241	0.223	0.2241	0.1156	0.1203
300	0.0631	0.9905	0.9888	0.5734	0.5731	0.7017	0.2319	0.2311	0.22	0.2223	0.1124	0.1165
305	0.0609	0.9326	0.9309	0.5465	0.5464	0.6828	0.2203	0.2196	0.2145	0.2176	0.1083	0.1107
310	0.0593	0.8739	0.8723	0.5201	0.5205	0.665	0.2084	0.2081	0.2125	0.2116	0.1044	0.106
315	0.058	0.7978	0.7965	0.4897	0.4899	0.6452	0.1961	0.196	0.2061	0.2082	0.1011	0.1038
320	0.0569	0.7509	0.7507	0.4693	0.4696	0.6312	0.1879	0.1882	0.2059	0.2032	0.0978	0.1016
325	0.0558	0.7071	0.706	0.4503	0.4499	0.6172	0.1802	0.1802	0.1989	0.1997	0.0955	0.0987
330	0.0543	0.6568	0.6558	0.4275	0.4262	0.6003	0.1723	0.172	0.1935	0.1978	0.093	0.0954
335	0.0528	0.5939	0.5929	0.3962	0.3947	0.5774	0.1618	0.1622	0.1932	0.194	0.0898	0.0914
340	0.0515	0.5369	0.5361	0.3647	0.3643	0.5546	0.153	0.1533	0.1912	0.1931	0.0875	0.0883

345	0.0506	0.4969	0.496	0.3414	0.3414	0.5378	0.1466	0.1469	0.1853	0.1893	0.0858	0.0868
350	0.0498	0.4635	0.4627	0.3217	0.322	0.5233	0.1415	0.1415	0.1854	0.1831	0.0841	0.0853
355	0.0491	0.4282	0.4277	0.2994	0.2997	0.5078	0.1361	0.136	0.1842	0.1793	0.0824	0.0845
360	0.0481	0.3945	0.3944	0.2789	0.2794	0.4916	0.1303	0.1304	0.1824	0.178	0.0812	0.083
365	0.0474	0.3704	0.37	0.2649	0.2643	0.4793	0.1261	0.1264	0.1775	0.1773	0.0801	0.0811
370	0.0466	0.3343	0.3332	0.2432	0.2426	0.4594	0.1199	0.1202	0.1712	0.1732	0.0775	0.0798
375	0.0456	0.3126	0.3116	0.2301	0.2296	0.4468	0.1158	0.1162	0.1715	0.169	0.0758	0.0782
380	0.0451	0.291	0.2902	0.2175	0.2166	0.4334	0.1118	0.1119	0.1747	0.1659	0.0748	0.0765
385	0.0442	0.264	0.2637	0.2008	0.1996	0.4151	0.1063	0.1066	0.1716	0.1627	0.0731	0.0749
390	0.0435	0.2442	0.2449	0.1882	0.187	0.4009	0.1021	0.1026	0.1672	0.1607	0.0712	0.0734
395	0.0433	0.2309	0.2316	0.1799	0.1787	0.3916	0.0995	0.0996	0.1628	0.1596	0.0705	0.0753
400	0.0433	0.2187	0.219	0.1724	0.171	0.3824	0.097	0.097	0.1613	0.1608	0.0703	0.0789

TABLE B.7: EarthGuard^{TM} EDGE^{TM} Pellet Sample Absorbance Data, to 400 nanometers

Wave-length	DI	Sample #1		Sample #3		Sample #6		Sample #10		Sample #13		Sample #15	
200	0.0865	1.0731	1.0744	1.8218	1.8239	1.3235	1.325	0.767	0.7675	0.664	0.6672	0.5129	0.5151
210	0.071	0.7971	0.7976	1.2973	1.2978	0.9295	0.9299	0.5638	0.5613	0.4905	0.4951	0.3833	0.3837
220	0.0602	0.4956	0.4965	0.7742	0.7737	0.5646	0.564	0.3537	0.3521	0.3148	0.317	0.2517	0.2522
230	0.0545	0.3597	0.3594	0.5512	0.5509	0.4134	0.4133	0.2629	0.2633	0.2379	0.2394	0.1928	0.1927
240	0.0494	0.2486	0.248	0.3686	0.3688	0.2897	0.2889	0.1902	0.1903	0.175	0.1757	0.1454	0.1448
250	0.0477	0.2215	0.2212	0.3196	0.3195	0.2553	0.2533	0.1685	0.169	0.1562	0.1563	0.1314	0.1314
260	0.0453	0.2	0.2003	0.291	0.2911	0.234	0.2324	0.154	0.1535	0.1423	0.1425	0.1193	0.1196
270	0.0423	0.1821	0.1821	0.2725	0.2727	0.2177	0.2172	0.1428	0.1424	0.1321	0.1313	0.1086	0.1087
280	0.0414	0.1677	0.1676	0.2532	0.2537	0.2026	0.202	0.1326	0.1324	0.1256	0.122	0.1012	0.1016
290	0.0403	0.1449	0.1448	0.2136	0.2135	0.1716	0.1718	0.1146	0.1141	0.1073	0.107	0.0902	0.0905
300	0.0385	0.1285	0.1278	0.1853	0.1839	0.1497	0.1495	0.1007	0.1002	0.0957	0.0952	0.0811	0.0805
310	0.0379	0.116	0.1146	0.1625	0.1607	0.133	0.1328	0.0929	0.0911	0.0872	0.0869	0.0747	0.0741
320	0.0386	0.1054	0.1037	0.1362	0.1345	0.1164	0.1158	0.0833	0.0831	0.081	0.0809	0.0705	0.0698
330	0.0377	0.0968	0.0953	0.1156	0.1149	0.1037	0.1033	0.0776	0.077	0.0763	0.0749	0.0666	0.0657
340	0.037	0.0878	0.086	0.0958	0.0953	0.0908	0.0907	0.0716	0.0706	0.0708	0.0693	0.0626	0.0612
350	0.0371	0.0835	0.0817	0.0861	0.0862	0.0852	0.0843	0.0688	0.0671	0.0679	0.0665	0.0608	0.0594
360	0.0369	0.0799	0.0779	0.0783	0.0785	0.0798	0.0793	0.0659	0.0644	0.0645	0.0641	0.059	0.0577
370	0.0367	0.0755	0.0741	0.0716	0.072	0.0745	0.0743	0.063	0.0613	0.0614	0.0613	0.0566	0.0562
380	0.036	0.0718	0.0712	0.0661	0.0659	0.0697	0.0697	0.0598	0.0586	0.0584	0.0582	0.0538	0.0542
390	0.0356	0.0676	0.0678	0.0596	0.059	0.0641	0.0642	0.0576	0.0545	0.0546	0.0546	0.0513	0.0515
400	0.0358	0.066	0.0663	0.056	0.0557	0.0611	0.0614	0.0531	0.052	0.0529	0.0526	0.0503	0.0502

APPENDIX C: CHAPTER 4 SUPPORTING DATA

Final Sand Soil Testing Results
Final Clay Soil Testing Results
Sample Final Loam Soil Testing Results
Plot 1 Construction Compaction Results
Preliminary Intensity/Uniformity Results
Flour Pan Data

TABLE C.1: Sand Wet Sieve Analysis Results

Analysis #1		Analysis #2	
Original Mass (g)	200.0	**Original Mass (g)**	200.0
Dry Mass (g)	166.8	**Dry Mass (g)**	160.03
Fines (g)	33.2	**Fines (g)**	39.97
Percent Fines	17%	**Percent Fines**	20%

TABLE C.2: Sand Dry Sieve Analysis Results

		Analysis #1					Analysis #2				
Sieve No.	Size (mm)	Mass Sieve (g)	Mass Sieve Plus Soil (g)	Mass of Soil (g)	% of Original	% Passing	Mass Sieve (g)	Mass Sieve Plus Soil (g)	Mass of Soil (g)	% of Original	% Passing
4	4.760	608.7	610.40	1.7	0.8%	99.2%	608.6	610.90	2.3	1.1%	98.9%
10	2.000	487.9	501.40	13.5	6.8%	92.4%	488.2	496.30	8.1	4.1%	94.8%
20	0.841	412.7	428.50	15.8	7.9%	84.5%	412.8	430.50	17.7	8.8%	86.0%
40	0.420	464.1	495.80	31.7	15.9%	68.7%	464.2	502.60	38.4	19.2%	66.8%
50	0.297	363.1	399.10	36.0	18.0%	50.7%	363.3	407.40	44.1	22.1%	44.7%
80	0.177	487.9	525.60	37.7	18.9%	31.8%	487.8	526.60	38.8	19.4%	25.3%
120	0.125	309.6	323.60	14.0	7.0%	24.8%	309.6	320.60	11.0	5.5%	19.8%
200	0.075	500.7	510.80	10.1	5.1%	19.8%	500.4	507.80	7.4	3.7%	16.1%
Pan	0.000	357.3	358.00	0.7	0.3%	19.4%	357.4	357.80	0.4	0.2%	15.9%
Sum				161.2					168.2		
% Fines Missed in Wet Sieve				1.8%					1.2%		
% Lost in Dry Sieve				0.73%					0.84%		

TABLE C.3: Proctor Compaction Results, Sand

Compacted Soil - Sample No.	1		2		3		4		5		6	
Weight Container (g)	14.7	14.7	14.8	14.8	14.8	14.0	14.9	14.4	14.2	14.8	14.7	14.7
Moist Sample Weight (g)	62.6	79.4	54.2	56.6	65.4	70.6	72.2	83.1	89.3	67.5	74.6	72.3
Dry Sample Weight (g)	61.9	78.0	50.7	52.8	59.7	64.5	63.9	73.3	77.7	59.6	63.5	61.1
W = Moisture Content (%)	1.5	2.1	9.7	9.9	12.8	12.0	17.0	16.7	18.2	17.8	22.9	24.1
Average Moisture Content (%)	1.8%		9.8%		12.4%		16.8%		18.0%		23.5%	
Weight of Mold (g)	4274		4271		4271		4271		4272		4272	
Weight of Compacted Soil & Mold (g)	5777		5857		6147		6271		6224		6134	
Weight of Wet Soil in Mold (g)	1503		1586		1876		2000		1952		1862	
Moist Unit Weight (lb/ft^3)	99.4		104.9		124.1		132.3		129.1		123.2	
Dry Unit Weight of Compaction (lb/ft^3)	97.6		95.5		110.4		113.2		109.4		99.7	

TABLE C.4: Clay Wet Sieve Analysis Results

Analysis #1		Analysis #2	
Original Mass (g)	100.0	Original Mass (g)	100.0
Dry Mass (g)	7.84	Dry Mass (g)	4.74
Fines (g)	92.16	Fines (g)	95.26
Percent Fines	92%	Percent Fines	95%

TABLE C.5: Clay Dry Sieve Analysis Results

		Analysis #1					Analysis #2				
Sieve No.	Size (mm)	Mass Sieve (g)	Mass Sieve Plus Soil (g)	Mass of Soil (g)	% of Original	% Passing	Mass Sieve (g)	Mass Sieve Plus Soil (g)	Mass of Soil (g)	% of Original	% Passing
16	**1.180**	498.6	499.1	0.5	0.5%	99.5%	498.4	499.1	0.7	0.7%	99.3%
40	**0.425**						463.9	465.2	1.3	1.3%	98.0%
80	**0.180**	487.7	490.2	2.5	2.5%	97.0%	309.4	313.3	3.9	3.9%	94.1%
200	**0.075**	499.6	501.6	2.0	2.0%	95.0%	500.1	502.4	2.3	2.3%	91.8%
Pan	**0.000**	356.6	356.7	0.1	0.1%	94.9%	356.7	356.8	0.1	0.1%	91.7%
Sum				5.1					8.3		
% Fines Missed in Wet Sieve				0.1%					0.1%		
% Lost in Dry Sieve				7.06%					5.87%		

TABLE C.6: Hydrometer Test #1 Clay

Meniscus Corr. (cm)	1	Temperature Corr. (cm)	1	Mass (g)	50.0	
Viscosity (p)	**0.009775**	**Specific Gravity**	**2.7**	**Temperature (Celcius)**	**21**	
Time (s)	**Reading**	**Corrected Reading Meniscus + Temperature**	**Mass Percent Finer**	**Effective Depth (L)**	**Particle Diameter**	**Percent Finer of Total**
15	53	51.0	102.0	7.9309	0.07326	97%
30	52	50.0	100.0	8.095	0.05234	95%
60	52	50.0	100.0	8.095	0.03701	95%
120	51.5	49.5	99.0	8.17705	0.02630	94%
240	50	48.0	96.0	8.4232	0.01887	91%
480	49	47.0	94.0	8.5873	0.01347	90%
900	46	44.0	88.0	9.0796	0.01012	84%
1800	44	42.0	84.0	9.4078	0.00728	80%
7200	36	34.0	68.0	10.7206	0.00388	65%
21600	29	27.0	54.0	11.8693	0.00236	51%
28800	26	24.0	48.0	12.3616	0.00208	46%
86400	21	19.0	38.0	13.1821	0.00124	36%

TABLE C.7: Hydrometer Test #2 Clay

Meniscus Corr. (cm)	1	Temperature Corr. (cm)	-1	Mass (g)	50.0	
Viscosity (p)	0.009775	Specific Gravity	2.7	Temperature (Celcius)	21	
Time (s)	Reading	Corrected Reading Meniscus + Temperature	Mass Percent Finer	Effective Depth (L)	Particle Diameter	Percent Finer of Total
15	52	52.0	104.0	7.7668	0.072507	96%
30	51	49.0	98.0	8.2591	0.05287	90%
60	50	48.0	96.0	8.4232	0.037754	88%
120	49	47.0	94.0	8.5873	0.026955	87%
240	47	45.0	90.0	8.9155	0.019421	83%
480	46	44.0	88.0	9.0796	0.013859	81%
1320	44.5	42.5	85.0	9.32575	0.00847	78%
1800	42.5	40.5	81.0	9.65395	0.007379	75%
3600	40	38.0	76.0	10.0642	0.005328	70%
14400	35	33.0	66.0	10.8847	0.00277	61%
28800	29	27.0	54.0	11.8693	0.002046	50%
108000	25	23.0	46.0	12.5257	0.001085	42%

TABLE C.8: Hydrometer Test #3 Clay

Meniscus Corr. (cm)	1	Temperature Corr. (cm)	0	Mass (g)	50.0	
Viscosity (p)	0.00958	Specific Gravity	2.7	Temperature (Celcius)	22	
Time (s)	Reading	Corrected Reading Meniscus + Temperature	Mass Percent Finer	Effective Depth (L)	Particle Diameter	Percent Finer of Total
15	47	46.0	92.0	8.7514	0.076194	35%
30	45	44.0	88.0	9.0796	0.054878	33%
60	41	40.0	80.0	9.736	0.040183	30%
120	38	37.0	74.0	10.2283	0.029123	28%
240	35	34.0	68.0	10.7206	0.021083	26%
480	34	33.0	66.0	10.8847	0.015022	25%
900	33	32.0	64.0	11.0488	0.011053	24%
1800	32	31.0	62.0	11.2129	0.007873	23%
16200	31	30.0	60.0	11.377	0.002644	23%
72000	30	29.0	58.0	11.5411	0.001263	22%

TABLE C.9: Casagrande Tests, Clay

Tin #	Tin Weight (g)	Tin Plus Moist Soil (g)	Tin Plus Dry Soil (g)	Mass Moist Soil (g)	Mass Dry Soil (g)	Moisture Content	No of Blows
Test 1-1	14.7	31.01	25.73	16.31	11.03	48%	18
Test 1-2	13.95	31.96	26.35	18.01	12.4	45%	26
Test 1-3	14.04	29.74	25.46	15.7	11.42	37%	45
Test 2-1	14.76	27.87	23.63	13.11	8.87	48%	13
Test 2-2	14.50	29.27	24.44	14.77	9.94	49%	29
Test 2-3	14.68	24.8	21.58	10.12	6.9	47%	38

TABLE C.10: Plastic Limit Tests, Clay

Tin #	Tin Weight (g)	Tin Plus Moist Soil (g)	Tin Plus Dry Soil (g)	Mass Moist Soil (g)	Mass Dry Soil (g)	Moisture Content
Test 1-1	14.09	26.94	24.37	12.85	10.28	25%
Test 1-2	14.67	22.83	21.28	8.16	6.61	23%
Test 1-3	14.53	25.1	22.95	10.57	8.42	26%
Test 2-1	14.7	24.37	22.56	9.67	7.86	23%
Test 2-2	14.81	26.83	24.57	12.02	9.76	23%
Test 2-3	14.54	22.07	20.68	7.53	6.14	23%

TABLE C.11: Loams Wet Sieve Analysis Results

Analysis #1 (Sample 1)		Analysis #1 (Sample 2)	
Original Mass (g)	100.0	**Original Mass (g)**	100.0
Dry Mass (g)	52.18	**Dry Mass (g)**	52.95
Fines (g)	47.82	**Fines (g)**	47.05
Percent Fines	48%	**Percent Fines**	47%

TABLE C.12: Loams Dry Sieve Analysis Results

		SAMPLE #1					SAMPLE #2				
Sieve No.	**Size (mm)**	**Mass Sieve (g)**	**Mass Sieve Plus Soil (g)**	**Mass of Soil (g)**	**% of Original**	**% Passing**	**Mass Sieve (g)**	**Mass Sieve Plus Soil (g)**	**Mass of Soil (g)**	**% of Original**	**% Passing**
8	2.350	479.6	485.6	6.0	6.0%	94.0%	479.1	481.9	2.8	2.8%	97.2%
16	1.180	498.5	502.4	3.9	3.9%	90.1%	498.5	502.2	3.7	3.7%	93.5%
35	0.500	464.0	475.6	11.6	11.6%	78.5%					
50	0.300	363.0	368.6	5.6	5.6%	72.9%	389.0	402.0	13.0	13.0%	80.5%
80	0.180	487.7	498.2	10.5	10.5%	62.4%	487.8	506.5	18.7	18.7%	61.8%
120	0.125	309.4	316.6	7.2	7.2%	55.2%	309.4	316.7	7.3	7.3%	54.5%
200	0.075	499.8	506.2	6.4	6.4%	48.8%	500.0	507.0	7.0	7.0%	47.5%
Pan	0.000	356.8	357.1	0.3	0.3%	48.5%	357.3	358.1	0.8	0.8%	46.7%
Sum				51.5					53.3		
% Fines Missed in Wet Sieve				0.6%					1.7%		
% Lost in Dry Sieve				-1.32%					0.66%		

TABLE C.13: Hydrometer Test, Loam Sample #1

Meniscus Corr. (cm)	1	Temperature Corr. (cm)	1	Mass (g)	50.0	
Viscosity (p)	0.009775	Specific Gravity	2.7	Temperature (Celcius)	21	
Time (s)	Reading	Corrected Reading Meniscus + Temperature	Mass Percent Finer	Effective Depth (L)	Particle Diameter	Percent Finer of Total
15	53	51.0	102.0	7.9309	0.073269	49%
30	51	49.0	98.0	8.2591	0.05287	47%
60	50	48.0	96.0	8.4232	0.037754	46%
120	45	43.0	86.0	9.2437	0.027966	41%
240	42	40.0	80.0	9.736	0.020295	38%
480	36	34.0	68.0	10.7206	0.015059	33%
900	33	31.0	62.0	11.2129	0.011247	30%
1800	29	27.0	54.0	11.8693	0.008182	26%
7200	25	23.0	46.0	12.5257	0.004203	22%
21600	22	20.0	40.0	13.018	0.002474	19%
28800	20	18.0	36.0	13.3462	0.002169	17%
86400	18	16.0	32.0	13.6744	0.001268	15%

TABLE C.14: Hydrometer Test, Loam Sample #2

Meniscus Corr. (cm)	1	Temperature Corr. (cm)	1	Mass (g)	50.0	
Viscosity (p)	0.009775	Specific Gravity	2.7	Temperature (Celcius)	21	
Time (s)	**Reading**	**Corrected Reading Meniscus + Temperature**	**Mass Percent Finer**	**Effective Depth (L)**	**Particle Diameter**	**Percent Finer of Total**
15	51	49.0	98.0	8.2591	0.07477	46%
30	50	48.0	96.0	8.4232	0.053393	45%
60	48	46.0	92.0	8.7514	0.038483	43%
120	45	43.0	86.0	9.2437	0.027966	40%
240	41	39.0	78.0	9.9001	0.020465	37%
480	38	36.0	72.0	10.3924	0.014827	34%
900	35	33.0	66.0	10.8847	0.011081	31%
1800	32	30.0	60.0	11.377	0.008011	28%
3600	29	27.0	54.0	11.8693	0.005786	25%
7200	26.5	24.5	49.0	12.27955	0.004161	23%
14400	24.5	22.5	45.0	12.60775	0.002982	21%
28800	23	21.0	42.0	12.8539	0.002129	20%
86400	20.5	18.5	37.0	13.26415	0.001248	17%
172800	19	17.0	34.0	13.5103	0.000891	16%

TABLE C.15: Casagrande Tests, Loams

Tin #	Tin Weight (g)	Tin Plus Moist Soil (g)	Tin Plus Dry Soil (g)	Mass Moist Soil (g)	Mass Dry Soil (g)	Moisture Content	No of Blows
Test 1-1	14.86	27.2	23.78	12.34	8.92	38%	12
Test 1-2	13.94	25.84	22.89	11.9	8.95	33%	24
Test 1-3	13.95	26.28	23.56	12.33	9.61	28%	43
Test 2-1	14.79	26.37	22.78	11.58	7.99	45%	14
Test 2-2	14.64	26.93	23.48	12.29	8.84	39%	28
Test 2-3	14.69	26.39	23.42	11.7	8.73	34%	40

TABLE C.16: Plastic Limit Tests, Loams

Tin #	Tin Weight (g)	Tin Plus Moist Soil (g)	Tin Plus Dry Soil (g)	Mass Moist Soil (g)	Mass Dry Soil (g)	Moisture Content
Test 1-1	14.74	22.41	20.6	7.67	5.86	31%
Test 1-2	14.61	22.36	20.49	7.75	5.88	32%
Test 1-3	14.54	22.27	20.49	7.73	5.95	30%
Test 2-1	14.06	23.74	21.85	9.68	7.79	24%
Test 2-2	14.64	21.25	19.90	6.61	5.26	26%
Test 2-3	14.67	24.8	22.79	10.13	8.12	25%

TABLE C.17: Plot 1 Compaction Results, Post-Construction

Sample Location	Top	Middle	Bottom
Height of Soil in Cylinder (in.)	2.00	2.25	2.625
Volume of Soil (in.^{3})	23.59	26.53	30.96
Volume of Soil (ft^3)	0.0136	0.0154	0.0179
Weight of Soil and Cylinder (g)	1262.2	1273.8	1385.2
Weight of Cylinder (g)	570	570	570
Weight of Soil (g)	692.2	703.8	815.2
Weight of Soil (lb)	1.526	1.552	1.797
Wet Density (lb/ft^3)	111.80	101.04	100.32
Dry Density (lb/ft^3)	94.26	85.49	84.62
Max Dry Density of Test (lb/ft^3)	92	92	92
Compaction (%)	102.46%	92.92%	91.98%
Average Compaction (%)	95.78%		
Moisture			
Tare Weight Moist Soil (g)	106.4	102.2	113.2
Tare Weight Dry Soil (g)	86.6	83.6	92.2
Moisture Content (%)	18.6%	18.2%	18.6%
Optimal Moisture for Test (%)	29.5%	29.5%	29.5%
Average Moisture Content (%)	18.5%		

TABLE C.18: 2 in./hr Intensity Data, Plot 1

Rain Gauge Number	Test 1	Test 2	Test 3	Test 4	Test 5 (6 in./hr)
1	1.0	0.5	0.4	0.7	1.6
2	0.6	0.3	0.7	0.8	1.3
3	0.6	0.4	0.5	0.5	1.4
4	0.8	0.8	1.0	1	1.3
5	0.9	0.5	0.7	0.7	1.5
6	0.9	0.6	0.4	0.6	1.9
7	1.2	0.3	0.6	0.7	1.7
8	0.6	0.5	0.5	0.4	2.0
9	0.8	0.4	0.7	0.5	1.7
10	0.5	0.5	0.7	0.8	2.1
11	0.8	0.5	0.4	0.8	1.8
12	0.6	0.6	0.4	0.6	1.5
13	0.7	0.4	0.4	0.7	1.8
14	0.9	0.8	0.9	0.9	1.4
15	0.8	0.6	0.8	0.8	1.5
16	0.8	0.2	0.7	0.8	1.7
17	1.0	0.7	0.4	1.0	2.5
18	0.6	0.5	0.6	0.6	2.2
19	1.1	0.6	0.5	1.1	1.5
20	0.4	0.5	0.6	0.4	1.7

TABLE C.19: Pressures, 2 in./hr (psi)

Sprinkler Tree Number	Test 1	Test 2	Test 3	Test 4	Test 5
1	50	48	50	40	28
2	49	46	50	38	28
3	49	46	50	38	30
4	49	43	46	36	30
5	44	44	46	36	34
6	44	44	46	36	28
7	46	46	50	40	32
8	48	46	50	39	30
9	48	47	50	40	30
10	50	48	50	41	32

TABLE C.20: 4 in./hr Intensity Data, Plot 1

Rain Gauge Number	Test 1	Test 2	Test 3	Test 4	Test 5
1	2.1	1.1	1.4	1.9	1.6
2	1.5	1.5	1.0	2.2	2.5
3	1.3	1.0	1.4	1.5	1.7
4	2.4	1.4	2.1	2.4	2.3
5	2.1	1.8	1.6	1.9	3.4
6	2.4	1.3	1.2	1.6	2.4
7	2.6	1.4	1.0	1.6	3.6
8	1.6	1.4	1.3	1.2	2.1
9	2.0	1.5	1.8	1.6	2.4
10	1.8	1.4	2.4	1.6	2.2
11	2.0	1.0	1.7	1.5	2.4
12	1.6	1.1	1.1	1.3	3.4
13	1.7	0.9	1.1	2.2	2.6
14	2.7	1.5	2.2	2.3	3.4
15	1.3	1.6	2.0	1.8	2.9
16	2.1	1.4	1.5	1.7	2.7
17	2.8	0.9	1.3	1.3	2.3
18	1.6	1.4	1.5	1.4	2.4
19	2.4	1.0	1.5	2.0	2.0
20	2.0	1.1	2.4	2.1	2.5

TABLE C.21: Pressures, 4 in./hr (psi)

Sprinkler Tree Number	Test 1	Test 2	Test 3	Test 4	Test 5
1	40	50	50	35	30
2	40	48	48	32	36
3	39	48	44	32	34
4	38	46	44	30	34
5	38	44	44	30	36
6	38	48	46	30	30
7	38	50	48	34	30
8	40	48	48	32	34
9	40	48	50	33	34
10	42	50	50	33	36

TABLE C.22: 6 in./hr Intensity Data, Plot 1

Rain Gauge Number	Test 1	Test 2	Test 3	Test 4	Test 5
1	3.9	2.1	2.7	3.7	3.5
2	3.0	3.5	4.1	1.6	1.7
3	1.7	2.1	2.5	3.0	2.6
4	4.5	2.7	3.8	4.1	4.2
5	4.4	4.0	3.2	4.5	4.8
6	4.2	2.6	2.0	3.0	3.6
7	5.2	2.9	3.5	2.8	1.7
8	3.1	2.6	2.3	2.6	2.7
9	4.3	2.8	2.9	2.4	2.6
10	3.7	3.0	4.3	3.4	3.4
11	3.9	2.3	3.2	3.3	3.0
12	3.4	2.5	2.4	3.9	4.0
13	3.2	2.0	2.0	2.5	3.0
14	5.1	2.8	4.2	4.4	4.1
15	1.2	3.5	3.8	3.6	3.4
16	4.5	2.6	2.7	3.5	3.1
17	5.1	2.6	2.4	1.7	2.9
18	3.3	1.7	1.7	2.5	2.5
19	4.1	1.8	2.7	2.5	2.3
20	4.3	2.3	3.7	3.0	3.2

TABLE C.23: Pressures, 6 in./hr (psi)

Sprinkler Tree Number	Test 1	Test 2	Test 3	Test 4	Test 5
1	29	48	40	32	32
2	27	44	44	28	34
3	24	44	44	28	36
4	26	42	44	26	36
5	26	42	42	26	38
6	24	40	44	27	34
7	26	42	44	30	36
8	28	46	44	28	36
9	28	46	46	29	36
10	30	46	46	31	38

TABLE C.24: 2 in./hr Flour Pan Data

Sieve No.	Sieve Size (mm)	Sieve Weight (g)	Sieve with Pellet Weight (g)	Number of Pellets
#4	4.760	768.4	768.6	2
#8	2.380	477.7	478.1	16
#10	2.000	680.4	680.5	19
#16	1.190	483.6	484.0	152
#20	0.841	633.6	633.7	262
#30	0.595	474.1	474.4	355
Pan	0.000	491.0	491.2	
Total				806

Sieve Size	Sieve Size (mm)	Sieve Weight (g)	Sieve with Pellet Weight (g)	Number of Pellets
#4	4.760	768.5	768.5	0
#8	2.380	477.6	478.4	39
#10	2.000	680.5	680.7	35
#14	1.190	483.6	484.5	338
#20	0.841	633.6	634.1	430
#30	0.595	474.2	474.5	605
Pan	0.000	491.0	491.3	
Total				1447

Sieve Size	Sieve Size (mm)	Sieve Weight (g)	Sieve with Pellet Weight (g)	Number of Pellets
#4	4.760	768.5	768.7	5
#8	2.380	477.7	478.6	64
#10	2.000	680.5	680.8	46
#14	1.190	483.6	484.9	372
#20	0.841	633.6	634.0	454
#30	0.595	474.2	474.6	733
Pan	0.000	491.0	491.2	
Total				1674

TABLE C.25: 4 in./hr Flour Pan Data

Sieve No.	Sieve Size (mm)	Sieve Weight (g)	Sieve with Pellet Weight (g)	Number of Pellets
#4	4.760	768.6	768.7	1
#8	2.380	477.7	478.1	39
#10	2.000	680.6	681.0	53
#16	1.190	424.5	425.4	361
#20	0.841	633.7	634.0	305
#30	0.595	474.1	474.4	501
Pan	0.000	491.2	491.3	
Total				1260

Sieve Size	Sieve Size (mm)	Sieve Weight (g)	Sieve with Pellet Weight (g)	Number of Pellets
#4	4.760	768.4	769.0	4
#8	2.380	477.7	479.3	95
#10	2.000	680.6	681.0	61
#14	1.190	424.4	425.5	379
#20	0.841	633.6	633.9	378
#30	0.595	474.4	474.5	360
Pan	0.000	491.0	491.3	
Total				1277

Sieve Size	Sieve Size (mm)	Sieve Weight (g)	Sieve with Pellet Weight (g)	Number of Pellets
#4	4.760	768.5	768.6	2
#8	2.380	477.7	478.7	66
#10	2.000	680.5	681.1	67
#14	1.190	424.5	425.7	422
#20	0.841	633.7	634.2	515
#30	0.595	474.3	474.5	590
Pan	0.000	491.0	491.3	
Total				1662

TABLE C.26: 6 in./hr Flour Pan Data

Sieve No.	Sieve Size (mm)	Sieve Weight (g)	Sieve with Pellet Weight (g)	Number of Pellets
#4	4.760	601.7	601.8	1
#8	2.380	477.7	482.1	212
#10	2.000	361.2	362.0	106
#16	1.190	483.6	484.9	490
#20	0.841	633.4	634.0	282
#30	0.595	412.9	413.0	482
Pan	0.000	355.6	356.0	
Total				1573

Sieve Size	Sieve Size (mm)	Sieve Weight (g)	Sieve with Pellet Weight (g)	Number of Pellets
#4	4.760	601.6	602.1	5
#8	2.380	477.7	483.1	220
#10	2.000	361.2	362.3	135
#14	1.190	483.7	484.8	400
#20	0.841	633.6	633.9	293
#30	0.595	412.8	412.9	305
Pan	0.000	355.7	356.2	
Total				1358

Sieve Size	Sieve Size (mm)	Sieve Weight (g)	Sieve with Pellet Weight (g)	Number of Pellets
#4	4.760	601.7	601.7	1
#8	2.380	477.7	479.7	103
#10	2.000	361.2	362.0	110
#14	1.190	483.7	484.7	315
#20	0.841	633.6	633.9	225
#30	0.595	412.9	413.0	409
Pan	0.000	355.6	356.0	
Total				1163

TABLE C.27: 2 in./hr Flour Pan Calculations

Sieve No.	Total Mass (g)	Total Drops	Mass per Drop (g)	Mass Ratio	Avg. Diameter (mm)	Adj. Pellet Weight (g)	Adj. Mass %	Fall Velocity (m/s)	Fall Velocity (ft/s)	Incremental Mass (lb)	Kinetic Energy (ft-lb)	Kinetic Energy (ft-tons)	E
#4	0.4	7	57.1429	1.2	5.0	0.4615	0.06	7.81	25.63	2.0	643.5	0.3	44
#8	2.1	119	17.6471	1.1	3.3	2.3291	0.29	7.09	23.27	9.9	2677.9	1.3	182
#10	0.6	100	6.0000	1.1	2.3	0.6409	0.08	6.18	20.27	2.7	558.8	0.3	38
#16	2.6	862	3.0162	1.0	1.8	2.7091	0.33	5.62	18.45	11.5	1957.6	1.0	133
#20	1.0	1146	0.8726	1.0	1.2	0.9948	0.12	4.78	15.70	4.2	520.4	0.3	35
#30	1.0	1693	0.5907	1.0	1.0	0.9800	0.12	4.57	14.99	4.2	467.2	0.2	32

TABLE C.28: 4 in./hr Flour Pan Calculations

Sieve No.	Total Mass (g)	Total Drops	Mass per Drop (g)	Mass Ratio	Avg. Diameter (mm)	Adj. Pellet Weight (g)	Adj. Mass %	Fall Velocity (m/s)	Fall Velocity (ft/s)	Incremental Mass (lb)	Kinetic Energy (ft-lb)	Kinetic Energy (ft-tons)	E
#4	0.8	7	114.2857	1.2	6.4	0.9441	0.09	7.71	25.31	6.0	1936.0	1.0	132
#8	3.0	200	15.0000	1.1	3.2	3.3087	0.31	6.96	22.83	21.2	5522.1	2.8	376
#10	1.4	181	7.7348	1.1	2.5	1.5088	0.14	6.39	20.97	9.7	2125.0	1.1	145
#16	3.2	1162	2.7539	1.0	1.8	3.3232	0.31	5.55	18.22	21.3	3533.6	1.8	241
#20	1.1	1198	0.9182	1.0	1.2	1.0964	0.10	4.81	15.80	7.0	876.0	0.4	60
#30	0.6	1451	0.4135	1.0	0.9	0.5799	0.05	4.39	14.40	3.7	384.7	0.2	26

TABLE C.29: 6 in./hr Flour Pan Calculations

Sieve No.	Total Mass (g)	Total Drops	Mass per Drop (g)	Mass Ratio	Avg. Diameter (mm)	Adj. Pellet Weight (g)	Adj. Mass %	Fall Velocity (m/s)	Fall Velocity (ft/s)	Incremental Mass (lb)	Kinetic Energy (ft-lb)	Kinetic Energy (ft-tons)	E
#4	0.6	7	85.7143	1.1691	5.7629	0.7015	0.03	7.83	25.70	10.0	3289.3	1.6	224
#8	11.8	535	22.0561	1.1176	3.6108	13.1872	0.60	7.27	23.86	187.3	53288.1	26.6	3627
#10	2.7	351	7.6923	1.0775	2.5109	2.9093	0.13	6.39	20.96	41.3	9073.7	4.5	618
#16	3.4	1205	2.8216	1.0394	1.7759	3.5340	0.16	5.57	18.28	50.2	8389.0	4.2	571
#20	1.2	800	1.5000	1.0154	1.4275	1.2185	0.06	5.12	16.81	17.3	2444.8	1.2	166
#30	0.3	1196	0.2508	0.9474	0.7685	0.2842	0.01	4.16	13.66	4.0	376.5	0.2	26

APPENDIX D: MANUFACTURER SPEC SHEETS

Manufacturer Spec Sheets for Erosion Control Products Tested
Spec Sheets for Parts used in Rainfall Simulator Sprinklers

Rolled Jute Mesh Specifications

Subject: Certification Rolled Jute Mesh

Country of Origin: India
Jute mesh is not a native natural resource of America, therefor the product is imported and sold through distribution in the United States.

Description

Jute erosion control mat is woven from spun jute yarns. The mat contains about 65% open area. This completely biodegradable blanket is the solution to environmentally sensitive general erosion control applications requiring up to 6—9 months of functional life.

This letter certifies that our L&M Jute Mesh meets and/or exceeds the specifications listed below. The average laboratory test values for the L&M Jute Mesh are as follows:

Specifications

Material	Jute Mesh
Roll size Roll Area	4' x 225' (width x length) (1.22 m x 68.6 m) 100 SY (83.3 sq.m.)
Open Area	70 - 75%
Mesh size	11mm x 18mm
Water Absorption	>450% of fabric weight
Thickness	0.25 inch (6 mm)
Recommended shear stress	0.45 lbs./sq.ft. (22 N/sq.m)
Recommended flow	6 fps (1.8 m/s)
Recommended slope	3:1
Coverage	100 Square Yards/roll
Roll weight	92 Lbs (+/- 5%) (500 g/m2)
Quantity per Pallet	9 and 12
Country origin	India

Unless otherwise noted, this certification is based on testing conducted by an independent testing laboratory. These test results are no more than one year old when presented to the authorizing agent. L & M Supply Co., Inc. issued this letter of certification to indicate our commitment to providing our customers with a quality product which will meet or exceed the minimum average roll values in accordance with the applicable American Society for Testing and Materials (ASTM) test method.

Respectfully,

Quinten McMillan
L&M Supply Co., Inc.

P.O. Box 640
Willacoochee, GA 31650
Phone: 800-948-7870 Fax: 912-534-6254

Date: 7-1-16

Section 31 25 14.13 – Hydraulically-Applied Erosion Control Engineered Fiber Matrix™

GENERAL

1.01 SUMMARY

1. This section specifies the hydraulically-applied erosion control product ProMatrix™ Engineered Fiber Matrix™ (EFM™). ProMatrix EFM is 100% biodegradable, made in the United States and is composed of 100% recycled, thermally refined (within a pressurized vessel) virgin wood fibers, crimped interlocking biodegradable fibers derived from regenerated plant sources, mineral activators and wetting agents (including high-viscosity colloidal polysaccharides, cross-linked biopolymers, and water absorbents). The EFM is phytosanitized, free from plastic, and when cured forms an intimate bond with the soil surface to create a continuous, porous, absorbent and flexible erosion resistant blanket that allows for rapid germination and accelerated plant growth. The EFM performs as a Bonded Fiber Matrix (BFM) product and may require a 4-24 hour curing period to achieve maximum performance.

2. Related Sections: Other Specification Sections, which directly relate to the work of this Section include, but are not limited to the following:

    1. *Section 01 57 00 – Temporary Erosion and Sediment Control*
    2. *Section 02 24 23 – Chemical Sampling and Analysis of Soils*
    3. *Section 31 00 00 – Earthwork*
    4. *Section 31 91 00 – Planting Preparation*
    5. *Section 32 01 90.16 – Amending Soils*
    6. *Section 32 92 00 – Turf and Grasses*

1.02 SUBMITTALS

1. Product Data: Submit manufacturer's product data and installation instructions. Include required substrate preparation, list of materials and application rate.

2. Certifications: Manufacturer shall submit a letter of certification that the product meets or exceeds all technical and packaging requirements and is made in the U.S.A.

1.03 DELIVERY, STORAGE AND HANDLING

1. Deliver materials and products in UV and weather-resistant factory labeled packages. Store and handle in strict compliance with manufacturer's instructions and recommendations. Protect from damage, weather, excessive temperatures and construction operations.

PRODUCTS

2.01 ACCEPTABLE MANUFACTURER

1. PROFILE Products LLC
   750 Lake Cook Road – Suite 440

Buffalo Grove, IL 60089
International - +1-847-215-1144
United States and Canada – 800-366-1180 (Fax 847-215-0577)
www.profileproducts.com

2.02 MATERIALS

1. The EFM shall be ProMatrix EFM and conform to the following typical property values when uniformly applied at a rate of 3,500 pounds per acre (3,900 kilograms/hectare) under laboratory conditions.

Property	Test Method	Tested Value (English)	Tested Value (SI)
Physical			
Thickness	ASTM D6525[1]	≥ 0.16 inch	≥ 4 mm
Ground Cover	ASTM D6567[1]	≥ 98%	≥ 98%
Water Holding Capacity	ASTM D7367	≥ 1,400%	≥ 1,400%
Material Color	Observed	Green	Green
Performance			
Cover Factor[2]	Large Scale Testing[4]	≤ 0.05	≤ 0.05
% Effectiveness[3]	Large Scale Testing[4]	≥ 95%	≥ 95%
Cure Time	Observed	4 – 24 hours	4 – 24 hours
Vegetation Establishment	ASTM D7322[1]	≥ 600%	≥ 600%
Functional Longevity[5]	ASTM D5338	≤ 12 months	≤ 12 months
Environmental			
Ecotoxicity	EPA 2021.0	48-hr LC_{50} > 100%	48-hr LC_{50} > 100%
Biodegradability	ASTM D5338	Yes	Yes
Certified BioPreferred® Biobased Content	ASTM D6866	97%	97%

1. ASTM test methods developed for Rolled Erosion Control Products and have been modified to accommodate Hydraulically-Applied Erosion Control Products.
2. Cover Factor is calculated as soil loss ratio of treated surface versus an untreated control surface.
3. % Effectiveness = One minus Cover Factor multiplied by 100%.
4. Large scale testing conducted at Utah Water Research Laboratory. For specific testing information please contact a Profile technical service representative at 800-508-8681 (US and Canada) or +1-847-215-1144 (International).
5. Functional Longevity is the estimated time period, based upon ASTM D5338 testing and field observations, that a material can be anticipated to provide erosion control and agronomic benefits as influenced by composition, as well as site-specific conditions, including; but not limited to – temperature, moisture, light conditions, soils, biological activity, vegetative establishment and other environmental factors.

2.03 COMPOSITION

1. All components of the EFM shall be pre-packaged by the Manufacturer to assure both material performance and compliance with the following values. Under no circumstances shall field mixing of components be permitted. No chemical additives with the exception of fertilizer, soil neutralizers and biostimulant materials should be added to this product.

    1. Thermally Processed* (within a pressurized vessel) Virgin Wood Fibers – 77%
       *Heated to a temperature greater than 380 degrees Fahrenheit (193 degrees Celsius) for 5 minutes at a pressure greater than 50 psi (345 kPa)
    2. Wetting agents (including high-viscosity colloidal polysaccharides, cross-linked biopolymers, and water absorbents) – 18%
    3. Crimped Biodegradable Interlocking Fibers derived from regenerated plant sources – 2.5%
    4. Micro-Pore Granules – 2.5%

2.04 PACKAGING

1. Bags: Net Weight – 50 lb (22.7 kg), UV and weather-resistant plastic film
   Pallets: Weather-proof, stretch-wrapped with UV resistant pallet cover
   Pallet Quantity: 40 bags/pallet or 1 ton (909 kg)/pallet

EXECUTION

3.01 SOIL TESTING

1. Soil Samples shall be taken and sent to a third-party, independent lab for analysis and in compliance with Section 02 24 23 – Chemical Sampling and Analysis of Soils, if applicable.

2. The tests shall include analysis and interpretation of results.

3. The soil testing methods used shall be compliant with recognized agronomic testing standards, as outlined in Section 02 24 23, for revegetation of disturbed sites.

4. Soil Analysis shall include results for:

    1. Soil pH
    2. Soluble Salts
    3. Excess Carbonate
    4. Organic Matter
    5. Nutrient readings for:
        1. Nitrogen, Phosphorus, Potassium
        2. Magnesium, Calcium, Sodium, Manganese, Sulfur, Zinc, Copper, Iron, Boron
    6. Cation Exchange Capacity
    7. Percent Base Saturation Sodium

5. ProGanics® BSM, BioPrime™, JumpStart™, Aqua-pHix™ and NeutraLime™ Dry or other amendments shall be specified according to Section 32 01 90.16 – Amending Soils and applied with the hydroseeding slurry at Manufacturer recommended rates based on soil test results.

3.02 VEGETATION SPECIES SELECTION

1. Once soils have been analyzed for agronomic potential and amendment recommendations, selection of suitable plant species for achieving sustainable growth and effective erosion control shall be determined by a qualified seed supplier, consulting professional and/or regulatory agency. Species selection and establishment shall be compliant with Section 32 92 00 – Turf and Grasses, if applicable.

2. Site and project specific information considered for species selection shall include:

    1. Project Location and Planning
        1. Climate
        2. Elevation
        3. Aspect
        4. Slope/Gradient
        5. Permanent or Temporary Planting
        6. Installation Date(s)
    2. Soil Conditions

1. Soil Texture
2. Soil pH
3. Toxicities/Deficiencies noted in the previous section.

3. Site Maintenance Requirements
   1. Mowing
   2. Irrigation
   3. Animal grazing preference
4. Preferred Vegetation
   1. Drought Tolerant
   2. Native Vegetation
   3. Shrub Species
   4. Turf Grasses
   5. Cool Season
   6. Warm Season
   7. Blend of Cool and Warm Season
   8. Legume Species
   9. Cover Crops

3.03 SUBSTRATE AND SEEDBED PREPARATION

1. Examine substrates and conditions where materials will be applied. Apply products to geotechnically stable slopes that have been designed and constructed to divert runoff away from the face of the slope. Do not proceed with installation until satisfactory conditions are established.

2. Depending upon project sequencing and intended application, prepare seedbed in compliance with other specifications under Section 1.01 B

3.04 INSTALLATION

1. Strictly comply with equipment manufacturer's installation instructions and recommendations. Use approved hydroseeding machines with fan-type nozzle (50-degree tip). To achieve optimum soil surface coverage, apply EFM from opposing directions to soil surface. Rough surfaces (rocky terrain, cat tracked and ripped soils) may require higher application rates to achieve 100% cover. Slope interruption devices or water diversion techniques are recommended when slope lengths (3H:1V) exceed 50 feet (15 m). Slope interruption intervals may need to be decreased based on steeper slopes or other site conditions. EFM is not recommended for channels or areas with concentrated water flow unless used in conjunction with a rolled erosion control product designed to accommodate the anticipated hydraulic conditions. Unless approved by the Manufacturer, no chemical additives with the exception of fertilizer, soil neutralizers and biostimulant materials should be added to this product.

2. For Erosion Control and Revegetation: To ensure proper application rates, measure and stake area. For maximum performance, apply EFM in a two-step process*:

   1. *Step One: Apply fertilizer with specified prescriptive agronomic formulations and typically 50% of specified seed mix with a small amount EFM for visual metering. Do not leave seeded surfaces unprotected, especially if precipitation is imminent.*
   2. *Step Two: Mix balance of seed and apply EFM at a rate of 50 lb per 83.3 gallons (22.7 kg/316 liters) of water over freshly seeded surfaces. Confirm loading rates with equipment manufacturer.*

   **Depending upon site conditions EFM may be applied in a one-step process where all components may be mixed together in single tank loads. Consult with Manufacturer for further details.*

Best results and more rapid curing are achieved at temperatures exceeding 60°F (15°C). Curing times may be accelerated in high temperature, low humidity conditions with product applied on dry soils.

3. Mixing: A mechanically agitated hydroseeding machine is strongly recommended:

1. *Fill 1/3 of mechanically agitated hydroseeder with water. Turn pump on for 15 seconds and purge and pre-wet lines. Turn pump off.*
2. *Turn agitator on and load low density materials first (i.e. seed).*
3. *Continue slowly filling tank with water while loading fiber matrix into tank.*
4. *Consult application and loading charts to determine number of bags to be added for desired area and application rate. Mix at a rate of 50 lb per 83.3 gallons (22.7 kg/316 liters).*
5. *All EFM should be completely loaded before water level reaches 75% of the top of tank.*
6. *Top off with water and mix until all fiber is fully broken apart and hydrated (minimum of 10 minutes — increase mixing time when applying in cold conditions). This is very important to fully activate the bonding additives and to obtain proper viscosity.*
7. *Add fertilizer and any other remaining amendments.*
8. *Shut off recirculation valve to minimize potential for air entrainment within the slurry.*
9. *Slow down agitator and start applying with a 50-degree fan tip nozzle.*
10. *Spray in opposing directions for maximum soil coverage.*

11. Application Rates: These application rates are for standard conditions. Designers may wish to increase application rates on rough surfaces.

Slope Gradient / Condition	English	SI
≤ 3H to 1V	3,000 lb/ac	3,400 kg/ha
> 3H to 1V and ≤ 2H to 1V	3,500 lb/ac	3,900 kg/h
> 2H to 1V and ≤ 1H to 1V	4,000 lb/ac	4,500 kg/ha

For additional details including mixing ratios/loading rates for specific machine sizes and visual keys for proper application, please consult Profile® Application Guide for Engineered Fiber Matrix™.

3.05 CLEANING AND PROTECTION

1. Always flush residual slurry from hydraulic seeding/mulching equipment immediately following each application, at the end of each work period or when equipment will be left unattended. Compounds containing residual Urea, Nitrogen, Phosphorus, Potassium and other substances may form and can be hazardous to human health and equipment.

2. Clean spills promptly. Advise owner of methods for protection of treated areas. Do not allow treated areas to be trafficked or subjected to grazing.

3.06 INSPECTION AND MAINTENANCE

1. All inspections and maintenance recommendations shall be conducted by qualified professionals consistent with the owner, engineer/specifier and regulatory entity(s) expectations.

2. Initial inspections shall insure installations are in accordance with the project plans and specifications with material quantities and activities fully documented. Refer to Section 32 92 00 – Turf and Grasses for any additional details.

3. Subsequent inspections shall be conducted at pre-determined time intervals and corrective maintenance activities directed after each significant precipitation or other potentially damaging weather or site event.

Applied Polymer Systems
519 Industrial Drive, Woodstock, GA 30189
www.siltstop.com

APS 700 Series Silt Stop®

Polyacrylamide Erosion Control Powder

APS 700 Series Silt Stop® is a group of soil specific tailored polyacrylamide co-polymer powders for erosion control. They reduce and prevent erosion of fine particles and colloidal clays from soil into stormwater.

Primary Applications

- Mine Tailings and Waste Piles
- Newly cleared Construction or Building Sites
- Road and Highway construction
- Hydroseeding and Water Truck application
- Hand spreading and Ditch placement

Features and Benefits

- Removes solubilized soils and clay from water
- Prevents colloidal solutions in water when applied to the soil surface
- Will reduce soil movement during rain event on moderate slopes
- Binds cationic metals within the soil matrix, reducing solubilization
- Reduces pesticide and fertilizer loss during rain events
- Reduces wind borne dust conditions
- Increases soil permeability and water penetration to shallow plants
- Reduces operational and cleanup costs
- Reduces environmental risk and compliance

Specifications / Compliances

- ANSI/NSF Standard 60 Drinking water treatment chemicals
- 48h or 96h Acute Toxicity Tests (*D. magna*, *P. promelas*, or *O. mykiss*)
- 7 day Chronic Toxicity Tests (*P. promelas* or *C. dubia*)

Packaging

APS 700 Series Silt Stop® is packaged in 50 pound bags

Technical Information

Appearance: White granular powder
Bulk Density: 40-50 lbs./cubic foot
Percent Moisture: 15% maximum
pH 0.5% solution :6-8
Shelf Life: up to 5 years

Note: Dosage-application rates are determined on soil specific testing. Soil polymers and blends should never be used without testing the soil first. Consult your local distributor or send your samples to Applied Polymer Systems, Inc.

Applied Polymer Systems

519 Industrial Drive, Woodstock, GA 30189
www.siltstop.com

Coverage

Soft Armoring application rate (per acre coverage): varies by soil content and grade of slope.

Gentle to Moderate slopes (0 to 4H:1V)

High Clay Content: 10-20 # powder
High Sand Content: 25-50 # powder

Steep slopes (3H:1V to 1H:1V)

High Clay Content: 20-35 # powder
High Sand Content: 45-50 # powder

Hydroseeding application rate (per acre coverage): varies by soil content and grade of slope.

Gentle to Moderate slopes (0 to 4H:1V)

High Clay Content: 10-20 # powder/ 3000 gallons/ acre
High Sand Content: 25-50 # powder/ 3000 gallons/ acre

Steep slopes (3H:1V to 1H:1V)

High Clay Content: 20-35 # powder/ 3000 gallons/ acre
High Sand Content: 40-50 # powder/ 3000 gallons/ acre

Directions for Use

Dry Form - APS Silt Stop® Powder may be applied by hand spreader, mechanical disc, or hand sowing. Slope or ditch application may require artificial support such as straw, or wood fiber mulch to reduce down slope movement. Areas of high water velocity will require benching or tier structuring to reduce velocity. Sheet flow applications are best. APS Silt Stop® Powder may be mixed with dry silica sand to aid in spreading. Ratios of sand to powder will vary in accordance with the type of spreading device used.

Liquid Form - APS Silt Stop® Powder may be applied with hydroseeders, water trucks or other spraying devices. All spraying devices must have a mechanical agitator or mixing apparatus or hydraulic recirculation. **Caution - Do Not** mix powder into a spraying device that does not contain a mixing apparatus.

Mixing - Sprinkle powder into the water with the mixing apparatus operating as the last material to be added to the mix. Three to Five minutes of mixing will be required after the powder is sprinkled into the water. **ADD THE POWDER SLOWLY**-adding the powder to fast will result in clumping resulting in poor performance.

Longer mixing times will create high viscosity solutions possibly causing some types of spray equipment to undergo cavitations.

Caution - Do Not exceed 8 lbs / 1500 gallons as viscosity of the water may damage spraying equipment. (This will treat ½ acre)

Clean-up

Spilled powder should be cleaned up dry as best as possible using broom or vacuum. Extreme slippery conditions will result. In event of skin contact, wash power from skin as soon as possible using soap and water.

Precautions / Limitations

- Prevent inhalation of the powder, use adequate dust mask.
- Clean up spills quickly. Do not use water unless necessary, extremely slippery conditions will result.
- Do not add water to the APS Silt Stop® Powder; add the powder (sprinkle) to the water slowly.
- APS Silt Stop® Powder will remain viable on the soil surface for 60-90 days. Longer viability will occur when applied powder is covered with straw or wood fiber mulch.
- APS 700 Series Silt Stop® powders have been specifically tailored to specific soil types. Soil types in varying geographical areas may require testing. If proper performance of this product is not satisfactory, contact Applied Polymer Systems.

PM-D

PM (Dry Silt Stop Form)

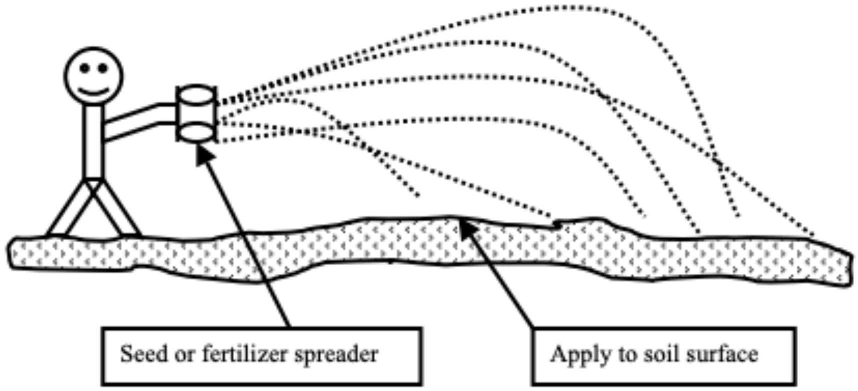

Notes:

1) **Dry Silt Stop shall be applied using a seed or fertilizer spreader or may be mixed with other dry spread additives.**

2) **Dry Silt Stop shall be covered with straw, mulch, matting or jute.**

3) **Application rate shall be 10 pounds/acre but not greater than 25 pounds/acre.**

4) **For use on all slope conditions.**

(All Silt Stop shall be site specific, soil tested achieving 95% NTU reduction or better and must have acute and chronic toxicity testing reports.)

USG Industrial & Specialty Solutions

USG NO. 1 MOULDING PLASTER

SOUTHARD, OK

DESCRIPTION

USG No. 1 Moulding Plaster is a high purity general purpose plaster that can be used in a wide variety of applications including architectural ornamentation and dental use. The physical properties can be varied depending upon the desired end use, while the use consistency can vary from a practical range of 63 lbs. water/100 lbs. of plaster (29 kg water/45 kg plaster) to as high as 70 lbs. water/100 lbs. of plaster (32 kg water/45 kg plaster).

USG No. 1 Moulding Plaster is noncombustible. With a coefficient of thermal conductivity (k) of 0.25 to 4.0 depending on density and additives, USG No. 1 Moulding Plaster can help to provide a high degree of fire resistance. When dry, USG No. 1 Moulding Plaster is electrically nonconductive and makes a good insulating medium.

Please contact your local USG Sales Representative for further assistance for specific use information.

TYPICAL PHYSICAL PROPERTIES

Normal Consistency	63 - 70 lbs. water/100 lbs. product (29 - 32 kg water/45 kg product)
Hand Mix Vicat Set, Target	25 - 35 minutes
% Passing — 50 mesh	99% - 100%
% Passing — 100 mesh	98.5% - 100%
Compressive Strength, One Hour After Set	850 - 1250 psi (5.9 - 8.6 MPa)
Compressive Strength, Dry	1700 – 2500 psi (11.7 - 17.2 MPa)
% Expansion	0.15% - 0.20%

NOTE: The *Typical Physical Properties* in the above table were achieved under controlled laboratory conditions with freshly produced material, results may vary.

MIXING INSTRUCTIONS

MIX PREPARATION

Use potable water at temperatures between 70 °F (21 °C) and 100 °F (38 °C). Because variations in slurry (USG No. 1 Moulding Plaster and water mixture) temperature produce variations in set time, it is important to keep both the USG No. 1 Moulding Plaster and water in a stable temperature environment prior to use. The higher the temperature of the slurry, the shorter the set time. Conversely, the lower the temperature of the slurry, the longer the set time.

Weigh both the USG No. 1 Moulding Plaster and the water prior to use for each mix. The water-to-USG No. 1 Moulding Plaster ratio is critical because it governs the strength and the density of the final cast.

SOAKING

Sift or strew USG No. 1 Moulding Plaster into the water slowly and evenly. Do not drop large amounts of USG No. 1 Moulding Plaster directly into the water as proper soaking of the USG No. 1 Moulding Plaster may not occur. USG No. 1 Moulding Plaster should be fully dispersed in the water prior to mixing. Small batches require less soaking time than large batches. See USG IG503 *Plaster Mixing Procedures* for specific soaking instructions.

MIXING

Mixing USG No. 1 Moulding Plaster slurry is one of the most important steps in producing USG No. 1 Moulding Plaster casts with maximum strength, absorption, hardness and other important properties.

Mechanically mixed slurries develop uniform casts with optimal strengths. USG No. 1 Moulding Plaster can be mechanically mixed through both batch and continuous processes. Proper blade and bucket dimensions are important for obtaining the best batch mix (see USG IG503 *Plaster Mixing Procedures* for details).

Longer mixing times result in higher mold strength and shorter set times.

USG
IT'S YOUR WORLD. BUILD IT.®

POURING

To prevent air entrainment and provide a uniform, smooth surface, careful pouring of USG No. 1 Moulding Plaster slurry is necessary. Agitation/vibration of the filled mold is a further step used to prevent air at or near the mold surface. Whenever possible, USG No. 1 Moulding Plaster slurry should be poured carefully in the deepest area so that the slurry flows evenly across the surface of the case mold.

Pouring a large amount of slurry directly on the face of the case mold may result in slight densification of the USG No. 1 Moulding Plaster mold at the point where it strikes the surface of the case. This produces a hard spot, giving uneven absorption.

DRYING

All casts should be dried as quickly as is safely possible after manufacture so that maximum physical properties can develop. Dry to a constant weight.

The best drying rooms or ovens provide 1) uniform and rapid circulation (minimum of 15-30 fps (4.6-9.1 mps)) of air with no "dead spots" having little or no air movement, 2) equal temperatures throughout the entire area, and 3) provisions for exhausting a portion of the air while replacing it with fresh air. High humidity surrounding the drying room or oven inhibits drying efficiency because the air pulled into the room is incapable of picking up much moisture from the molds.

The maximum temperature at which USG No. 1 Moulding Plaster molds are safe from calcination is 120 °F (49 °C). With substantial free water in the mold, a higher drying temperature can be used without difficulty. As drying progresses, the temperature must be reduced to prevent calcination. Before removing molds from the dryer, the temperature should approach that of the area around the dryer to prevent thermal shock. See IG502 *Drying Plaster Casts* for additional information.

STORAGE AND USE

When properly used, USG No. 1 Moulding Plaster is easy to work with and complies with the federal Labeling of Hazardous Art Materials Act, 12 U.S.C. Section 1277 and ASTM D4236. Keep indoors at temperatures between 65 °F - 75 °F (18 °C - 24 °C) and 45% - 55% RH. Do not stack more than two pallets high. Keep from drafts. Rotate stock. USG No. 1 Moulding Plaster should be used within 6 months of the manufacturing date located on the package. Always follow handling and use directions and safety warnings on the package.

PRODUCT INFORMATION
See usg.com for the most up-to-date product information.

CAUTION
When mixed with water, this material hardens and becomes very hot sometimes quickly. DO NOT attempt to make a cast enclosing any part of the body using this material. Dust from mixing may cause irritation to eyes, skin, nose, throat and upper respiratory tract. Use only in a well-ventilated area, wear a NIOSH/MSHA-approved respirator. Wear eye protection. If eye contact occurs, flush thoroughly with water for 15 minutes. If on skin: Wash with plenty of water. If swallowed and/or irritation persists, call physician. For more information call Product Safety: 800-507-8899 or see the SDS at usg.com
KEEP OUT OF REACH OF CHILDREN.

NOTE
The information in this document is subject to change without notice. USG Corp. and/or its affiliates assume no responsibility for any errors that may inadvertently appear in this document. Consult your USG sales office or representative for information.

NOTICE
We shall not be liable for consequential, incidental or special damages, directly or indirectly sustained, nor for any loss caused by application of these goods not in accordance with current printed instructions or for other than the intended use. Our liability is expressly limited to the replacement of defective goods or a refund of the purchase price, at USG's option, and does not include costs of labor or any other costs associated with material replacement. Any claim shall be deemed waived unless made in writing to us within thirty (30) days from date it was or reasonably should have been discovered.

SAFETY FIRST!
Follow good safety/industrial hygiene practices during installation. Wear appropriate personal protective equipment. Read applicable SDSs and literature before specification and installation.

800 USG.4YOU
800 (874.4968)
usg.com

Manufactured by
United States Gypsum Company
550 West Adams Street
Chicago, IL 60661

IG1857-USA-ENG/rev. 1-20

Printed in U.S.A.

IT'S YOUR WORLD. BUILD IT.®

Pulverized Agricultural Gypsum – USA Gypsum

Description

Spread with “Vicon” type broadcast spreaders or drop spreaders designed for powder.

1. Calcium (Ca): 19%
2. Sulfur (S): 14%
3. Moisture: 4%
4. Calcium Sulfate Dihydrate: 85%
5. pH: 7.25
6. Density per cubic foot: 35 (15.86 kg)
7. Particle size varies from 1/4″ to dust

Uses for Pulverized Gypsum:

1. Agricultural Crops
2. Lawns & Gardens
3. Compost Additive
4. Animal Bedding Additive
5. Poultry Litter Amendment
6. Soil Stabilization & Remediation
7. As a Bulking, Solidification or Stabilization Agent
8. Water Clarifier
9. Industrial Products

EDGE™
EARTHGUARD® PELLETS

Pellet form of top-rated EarthGuard® Fiber Matrix.

For Hydraulic or Dry Application

This patented technology offers extraordinary erosion control protection, exceptional turbidity reduction and quick growth establishment, with fast, easy applications at a great price.

Applied hydraulically, Edge™'s compact and quickly expanding pellet makes it simple to transport, handle, load and compared to other hydraulically applied erosion products, requires approximately 50% less water to install. Possessing a +99.9% erosion control rating, at low application rates, makes it much more economical than other top tiered spray-on and blanket products.

Applied dry, Edge™ eliminates the need for water, concerns of cold weather installations, and site access problems. It's also, great for manual application on smaller sites when a hydraulic application isn't cost effective.

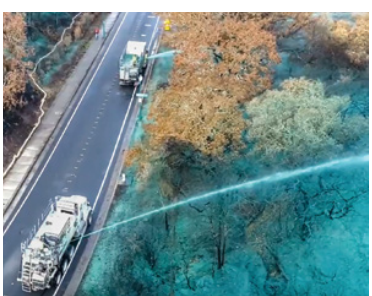

EDGE™ EARTHGUARD® PELLETS

Requires Less:

- Water
- Labor & Time
- Material & Handling
- Application is Not Temperature Dependent

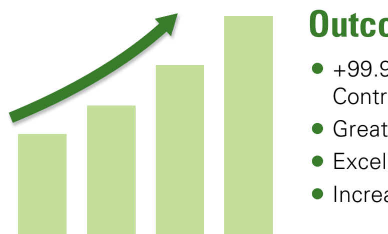

Outcome:

- +99.9% Erosion Control Protection
- Greater Efficiency
- Excellent Results
- Increased Profits

Applied dry in pellet form, Edge™ expands on contact with dew or rainfall, spreading both the fiber and EarthGuard® patented soil stabilizer.

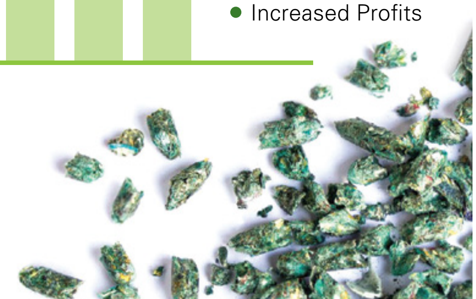

LSC Environmental Products, LLC
www.LSCenv.com • sales@LSCenv.com • 800-800-7671

LSC™

EDGE™ EARTHGUARD® PELLETS

Product Packaging Availability:

Pre-packaged in:

- 50 lb. Bag
- 900 lb. Bulk Sack
- 1000 lb. Bulk Sack

Specialized packaging for aerial bucket capacity is also available.

Shorter pallet height – easy to transport, ability to load full 1 ton pallet on top of hydro-seeder without unpacking.

Standard hydromulch pallet 96" H

Pallet of EDGE 48" H

Information and statements herein are believed to be reliable but are not to be constructed as a warranty or guarantee. Some extreme situations may require higher application rates. LSC Environmental Products, LLC offers no warranties, express or implied. Nothing herein is to be taken as permission to practice any patented invention without a license. Edge™ is a registered trademark of LSC Environmental Products, LLC.

MADE IN THE USA

Application Rates – Hydraulic Application

NORMAL CONDITIONS: Maximum Rainfall of < 20" (480 mm) Before Adequate Vegetative Establishment

	≤ 4 to 1 Slope		3 to 1 Slope		2 to 1 Slope		≥ 1 to 1 Slope	
	Per Acre	Per Ha	Per Acre	Per Ha	Per Acre	Per Ha	Per Acre	Per Ha
Edge™	1500 LB	1690 KG	1800 LB	2020 KG	2000 LB	2245 KG	3000 LB	3355 KG

SEVERE CONDITIONS: Maximum Rainfall of > 20" (480 mm) Before Adequate Vegetative Establishment

	≤ 5 to 1 Slope		4 to 1 Slope		≥ 3 to 1 Slope	
	Per Acre	Per Ha	Per Acre	Per Ha	Per Acre	Per Ha
Edge™	2000 LB	2245 KG	2500 LB	2800 KG	3000 LB	3355 KG

Loading Rates – Hydraulic Application

NORMAL CONDITIONS: Maximum Rainfall of < 20" (480 mm) Before Adequate Vegetative Establishment

Machine Size (gal)	Bags Per Load (50 lb/22.7 kg)	Loads Per Area – Based On Slope							
		≤ 4:1		3:1		2:1		> 2:1	
		per AC	per HA	per AC	per HA	per AC	per HA	per AC	per HA
325	4.5	6.7	16.4	8	19.8	8.9	22	13.3	32.8
550	7.5	4	9.9	4.8	11.9	5.3	13.2	8	19.7
700	9.5	3.2	7.8	3.8	9.4	4.2	10.4	6.3	15.6
800	10.5	2.9	7	3.4	8.5	3.8	9.4	5.7	14.1
1,000	13	2.3	5.7	2.8	6.8	3.1	7.6	4.6	11.4
1,200	16	1.9	4.6	2.3	5.6	2.5	6.2	3.8	9.2
1,500	20	1.5	3.7	1.8	4.4	2	4.9	3	7.4
2,000	27	1.1	2.7	1.3	3.3	1.5	3.7	2.2	5.5
3,000	40	0.8	1.9	0.9	2.2	1	2.5	1.5	3.7
4,000	53	0.6	1.4	0.7	1.7	0.8	1.9	1.1	2.8

SEVERE CONDITIONS: Maximum Rainfall of > 20" (480 mm) Before Adequate Vegetative Establishment

Machine Size (gal)	Bags Per Load (50 lb/22.7 kg)	Loads Per Area – Based On Slope					
		≤ 5:1		4:1		≥ 3:1	
		per AC	per HA	per AC	per HA	per AC	per HA
325	4.5	8.9	22.0	11.1	27.4	13.3	32.8
550	7.5	5.3	13.2	6.7	16.4	8	19.7
700	9.5	4.2	10.4	5.3	13.0	6.3	15.6
800	10.5	3.8	9.4	4.8	11.7	5.7	14.1
1,000	13	3.1	7.6	3.8	9.5	4.6	11.4
1,200	16	2.5	6.2	3.1	7.7	3.8	9.2
1,500	20	2	4.9	2.5	6.2	3	7.4
2,000	27	1.5	3.7	1.9	4.6	2.2	5.5
3,000	40	1	2.5	1.3	3.1	1.5	3.7
4,000	53	0.8	1.9	0.9	2.3	1.1	2.8

Application Rates – Dry Application

	≤ 4 to 1 Slope		3 to 1 Slope		≥ 2 to 1 Slope	
	Per Acre	Per Ha	Per Acre	Per Ha	Per Acre	Per Ha
Edge™	3000 LB	3355 KG	3500 LB	3925 KG	4500 LB	5045 KG

For technical services or to locate your nearest Edge™ dealer:

LSC ENVIRONMENTAL PRODUCTS, LLC™

Call: **1-800-800-7671** • Email: **Sales@LSCenv.com**

Visit LSC online at: **www.LSCenv.com**

LSC Environmental Products, LLC

2183 Pennsylvania Ave., Apalachin, NY 13732

Solutions for the Greener Good

NELSON

WATER APPLICATION SOLUTIONS FOR CENTER PIVOT IRRIGATION

PART-CIRCLE
R3030 ROTATOR*
Black #12651-001
(#40-#50 3NV Nozzle)
Tan #12651-003
(#24-#39 3NV Nozzle)
White #12651-002
(#14-#23 3NV Nozzle)
U3030 included

PART-CIRCLE

NELSON IRRIGATION OFFERS SEVERAL PART-CIRCLE OPTIONS. CHOOSE FROM THE PC-ROTATOR®, PC-SPINNER AND PC-SPRAYHEAD. ALL SPRINKLERS ARE AVAILABLE IN BOTH 3000 SERIES (WITH 3TN NOZZLE) AND 3030 SERIES (WITH 3NV NOZZLE). THE 3030 SERIES UTILIZES THE UNIVERSAL ADAPTER (U3030).

THESE PART-CIRCLE SPRINKLERS CAN BE USED FOR DRY WHEEL TRACK SOLUTIONS, HOSE BOOM APPLICATIONS OR A SIMPLE END OF SYSTEM ADDITION.

FOR PC-ROTATOR: MOUNT ONLY ON A STRAIGHT RIGID DROP OR A HOSE BOOM UTILIZING A TORQUE CLIP AND SIDEFORCE CONTROL FITTING SUCH AS THE IACO HB.

PART-CIRCLE
R3000 ROTATOR*
Black #10843-001
(#40-#50 3TN Nozzle)
Tan #10843-003
(#24-#39 3TN Nozzle)
White # 10843-002
(#14-#23 3TN Nozzle)

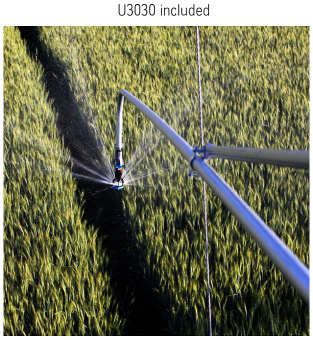

PART-CIRCLE
S3030 SPINNER*
#12650 (U3030 INCLUDED)

PART-CIRCLE
S3000
SPINNER*
#9926-001

PART-CIRCLE
D3030 SPRAY*
#9894-001
(ORDER U3030 BODY
#12381 SEPARATELY)

PART-CIRCLE
D3000
SPRAY*
#9894-001

*Part numbers do not include nozzles or square thread adapters. PC-R3030 and S3030 part numbers include U3030 body. #12381 must be ordered separately for the PC-D3030.

Tel: +1 509.525.7660 / Fax: +1 509.525.7907 / nelsonirrigation.com / info@nelsonirrigation.com

SMART OPTIONS FOR COMMON CHALLENGES

SOLVE WHEEL TRACK PROBLEMS

Excessive water in the wheel tracks can cause slippage of the tires, causing the system to slow down in wet areas and steep slopes — increasing the application depth in relation to other parts of the fields. Deep wheel track ruts are also detrimental to the equipment and harvesting efficiency.

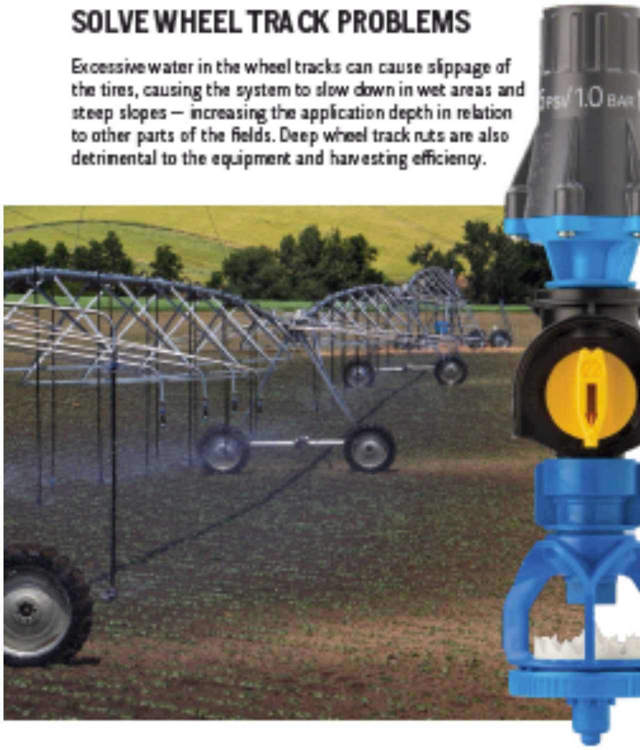

Nelson part circle sprinklers direct the water off of the pivot structure at the towers and away from the wheel track to prevent deep wheel track ruts. Overall field uniformity can be maintained by preventing excessive slippage of the tires, and maintaining a uniform speed of travel.

PC-R3030 ROTATOR®

PERFORMANCE:

- 180° Arc (varies slightly with flow rate)
- Wide Throw
- High Uniformity
- Wind Fighting Pattern

Mount on a rigid drop assembly or IACO Hose Boom Assembly. Go to www.boombacks.com.

Nozzle #	Plate	Min-Max Pressure	Spacing Limit	Stream Height
14-23	White	15-25 psi (1-1.8 bar)	11' (3.4 m)	20-39" (51-99 cm)
24-39	Tan			10-18" (25-46 cm)
40-50	Black	15-30 psi (1-2 bar)		29-41" (74-104 cm)

PART-CIRCLE FOR END OF SYSTEM

Gain added end of system acreage at low pressure. Complement traditional end gun packages to fill the pattern going in and out of corners.

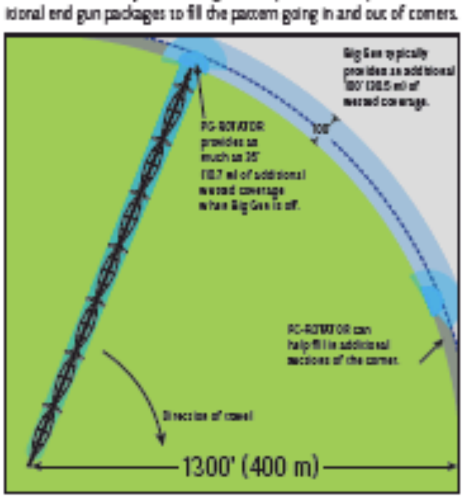

INTEGRATE THE PC-ROTATOR WITH THE PREMIERE PIVOT SPRINKLER — THE R3030 ROTATOR®.

ENGINEERED SPEED CONTROL & THE RIGHT BALANCE OF ROTATING STREAMS. Designed specifically for providing the very best water application on center pivots, the controlled rotation of engineered streams provides superior throw, superior uniformity and the best available conditions for getting the water into the ground.

GREATEST THROW ON DROPS. The Rotator® applies water further ahead of the machine than any other pivot sprinkler and wets the field with intermittent applications of larger droplets for optimal soil infiltration conditions.

YEARS OF FIELD RESULTS & SCIENTIFIC RESEARCH SHOW THE PIVOT ROTATOR GETS WATER INTO THE GROUND. The wide throw delivers the lowest Average Application Rates on drop tubes — and testing shows that the Pivot Rotator is the best in class at minimizing runoff and soil erosion.

NEW 3NV NOZZLE IN THE 3030 SERIES. This side-inlet, quick-change nozzle combines multiple functions so you can more effectively manage your system. Gain lots - give up nothing!

PART CIRCLE SPINNER

The Part Circle Spinner distributes water to one side in an approximate semicircle. It can be used to minimize application on pivot towers or other structures. The Part Circle Spinner utilizes the 3TN nozzle (PC-S3000) or 3NV Nozzle (PC-S3030). The directional control is provided by a 'stream deflector' which is inserted between the nozzle and the spinner body.

OPERATING SPECS:

- 10–20 PSI (0.7–1.4 bar)
- #14-#40 3TN or 3NV Nozzle
- Mount on a rigid drop assembly

PERFORMANCE:

- 190° Arc (varies slightly with flowrate)
- Gentle, Rain-like Droplets
- High Uniformity
- Low Instantaneous Rates

THROW RADIUS:

(At midpoint of arc, throw to the sides may be less.)

- 15 PSI (1.0 BAR)
- #36 3TN or 3NV Nozzle
- Stream Height = 20 in. (51 cm)

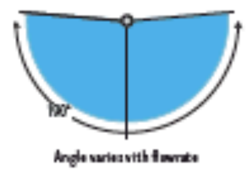

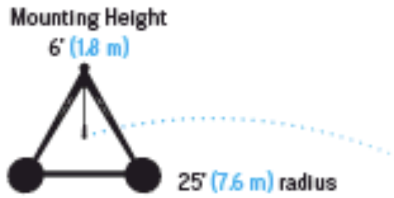

PART CIRCLE SPRAYHEAD

The Part Circle Sprayhead has a 170° arc setting to provide part-circle operation for applications at the span towers or offset drops or boombacks. The Part Circle spray plate provides stream definition similar to the spray plate geometry of the #9493 Blue spray plate. The medium grooves and concave trajectory provide wind-penetration and wide throw distance.

OPERATING SPECS:

- 6–20 PSI (0.4–1.4 bar)
- #9-#50 3TN or 3NV Nozzle
- Mount on a rigid drop assembly

PERFORMANCE:

- 170° Arc (varies slightly with flowrate)
- Low Trajectory
- Concave Medium Groove Blue Spray Plate

THROW RADIUS:

(At midpoint of arc, throw to the sides may be less.)

- 10 PSI (.7 BAR)
- #36 3TN or 3NV Nozzle
- Stream Height = 6 in. (15 cm)

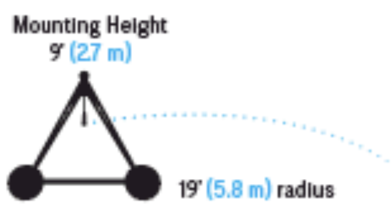

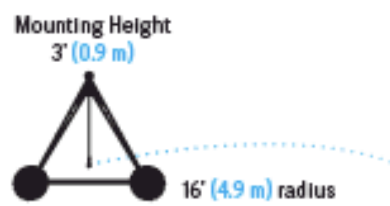

DESIGNING WITH PART CIRCLE SPRINKLERS

PART-CIRCLE SPRINKLERS CAN BE INSTALLED IN A VARIETY OF CONFIGURATIONS

BOOMBACKS
INSTALLATIONS ON BOOMBACKS MINIMIZE THE COMPROMISE IN UNIFORMITY THAT OCCURS WHEN PART-CIRCLE DEVICES ARE UTILIZED.

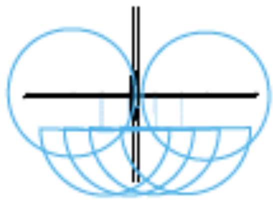

STRAIGHT DROPS
INSTALLATIONS ON STRAIGHT DROPS REQUIRE CAREFUL ADJUSTMENT OF THE ORIENTATION.

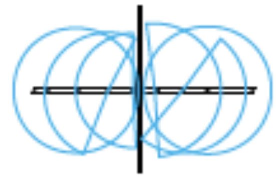

STEP 1: PLAN THE SYSTEM WITH CONVENTIONAL FULL CIRCLE SPRINKLERS.

For Linears/Laterals select sprinkler spacing and determine the nozzle size to deliver your desired application rate. For pivot systems, planning should include a Sprinkler Package Chart. Nelson part circle devices will fit best in packages with sprinkler spacing of 11 feet (3.3 m) or less. If the part circle devices are to be mounted on boombacks, maintain uniform spacing between all sprinklers. The IACO 15' Hose Boom is the only "boomback" style configuration recommended for the Part Circle Rotator. If the devices will be mounted on conventional drops, a distance of 1 to 3 feet (0.3 to 1 m) between the wheel and the closest sprinkler on each side is optimal.

STEP 2: DETERMINE WHICH OUTLETS NEED MODIFIED SPRINKLERS.

Use the preliminary design to compare the distance to the tower with the radius for each sprinkler. If you are working from a Sprinkler Package Chart, adjust the listed Tower location for the wheel offset. An offset of 2 feet (0.6 m) is common. Coverage diameter information on other Nelson Pivot Sprinklers is available at www.nelsonirrigation.com or by contacting Nelson Irrigation.

STEP 3: PLAN THE ORIENTATION ANGLES FOR THE PART CIRCLE SPRINKLERS.

The semicircular pattern of the Part Circle Sprinklers adjacent to the towers should be oriented as close to perpendicular to the main pipe as possible. On boombacks, they should face directly away from the main pipe as shown in the diagram. On straight drops, they should be adjusted so the edge of the semicircle falls immediately behind the rear tower wheel. If possible, orient adjacent part circles at opposite directions from the pipe. This reduces the application rate.

ADDITIONAL CAUTIONS:

It is important to mount Part Circle Sprinklers on rigid drops or Hose Booms. Side thrust will cause extreme movement of flexible drops. Part Circle Sprinklers cannot provide the whole solution to traction, rutting, or runoff problems. If you are trying to utilize mechanized irrigation systems on steep slopes or heavy soils you should carefully consider all aspects of system design and management that can contribute to reduced soil loading and application rate minimization. The distribution profile of the Part Circle Sprinklers provides good overlaps with conventional sprinklers in most configurations. However, it is likely that a system intended to minimize application at the tower will not achieve the high uniformity possible with a well designed conventional system. For best results keep the spacing within the limits described above. Part Circle Sprinklers can be used to minimize, but they will not totally eliminate, application on the towers or wheel tracks.

NELSON IRRIGATION CORPORATION
848 Airport Rd., Walla Walla, WA 99362 USA
Tel: 509.525.7660 Fax: 509.525.7907 info@nelsonirrigation.com

NELSON IRRIGATION CORPORATION OF AUSTRALIA PTY. LTD.
35 Sudbury Street, Darra QLD 4074 info@nelsonirrigation.com.au
Tel: +617 3715 8555 Fax: +61 7 3715 8666

NELSON 3000 & 3030 Series Pivot Products

3TN & 3NV NOZZLE CHART

14 15 16 17 18 19

The nozzle sizing system is based on 128th inch increments, e.g. 3TN/3NV Nozzle #26 has an orifice diameter of 26/128th inches while 3TN/3NV Nozzle #27 has an orifice diameter of 27/128th inches. For 3TN Nozzles, the odd-numbered nozzles have a color box around the number marking. This color box denotes the color of the next larger nozzle size. The odd-numbered 3NV Nozzles have a scalloped edge rather than secondary coloring.

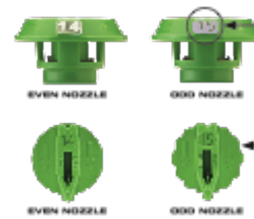

NOZZLE #		#9		#10		#11		#12		#13		#14		#15		#16		#17		#18		#19	
Color		Light Blue		Beige		Beige		Gold		Gold		Lime		Lime		Lavender		Lavender		Gray		Gray	
Stripe		Beige				Gold				Lime				Lavender				Gray				Turquoise	
PSI	BAR	GPM	LPM	GPM	LPM	GPM	LPM	GPM	LPM	GPM	LPM	GPM	LPM	GPM	LPM	GPM	LPM	GPM	LPM	GPM	LPM	GPM	LPM
6	0.4	0.34	1.28	0.42	1.59	0.50	1.89	0.61	2.30	0.71	2.68	0.82	3.10	0.95	3.59	1.08	4.08	1.22	4.61	1.36	5.14	1.53	5.79
10	0.7	0.44	1.66	0.54	2.04	0.65	2.46	0.79	2.99	0.92	3.48	1.06	4.01	1.23	4.65	1.40	5.29	1.58	5.98	1.75	6.62	1.97	7.45
15	1.0	0.53	2.00	0.66	2.50	0.79	2.99	0.96	3.63	1.13	4.27	1.29	4.88	1.51	5.71	1.71	6.47	1.93	7.30	2.14	8.09	2.41	9.12
20	1.4	0.62	2.34	0.76	2.87	0.92	3.48	1.11	4.20	1.30	4.92	1.49	5.63	1.74	6.58	1.98	7.49	2.23	8.44	2.48	9.38	2.79	10.56
25	1.7	0.69	2.61	0.85	3.22	1.02	3.86	1.24	4.69	1.46	5.52	1.67	6.32	1.95	7.38	2.21	8.36	2.50	9.46	2.77	10.48	3.12	11.81
30	2.1	0.76	2.87	0.93	3.52	1.12	4.23	1.36	5.14	1.59	6.01	1.83	6.92	2.14	8.09	2.42	9.15	2.74	10.37	3.03	11.46	3.41	12.90
40	2.8	0.87	3.29	1.07	4.05	1.29	4.88	1.57	5.94	1.84	6.96	2.11	7.98	2.47	9.34	2.80	10.59	3.16	11.96	3.50	13.24	3.94	14.91
50	3.4	0.97	3.67	1.20	4.54	1.45	5.48	1.76	6.66	2.06	7.79	2.36	8.93	2.76	10.44	3.13	11.84	3.53	13.32	3.91	14.79	4.41	16.69

NOZZLE #		#20		#21		#22		#23		#24		#25		#26		#27		#28		#29		#30	
Color		Turquoise		Turquoise		Yellow		Yellow		Red		Red		White		White		Blue		Blue		Dark Brown	
Stripe				Yellow				Red				White				Blue				Dark Brown			
PSI	BAR	GPM	LPM	GPM	LPM	GPM	LPM	GPM	LPM	GPM	LPM	GPM	LPM	GPM	LPM	GPM	LPM	GPM	LPM	GPM	LPM	GPM	LPM
6	0.4	1.70	6.43	1.84	6.96	2.04	7.72	2.22	8.40	2.44	9.23	2.64	9.99	2.87	10.86	3.07	11.61	3.35	12.68	3.58	13.55	3.83	14.49
10	0.7	2.19	8.28	2.38	9.00	2.64	9.99	2.86	10.82	3.16	11.96	3.41	12.90	3.70	14.00	3.97	15.00	4.32	16.35	4.62	17.48	4.94	18.69
15	1.0	2.69	10.18	2.91	11.01	3.23	12.22	3.50	13.24	3.86	14.61	4.17	15.78	4.53	17.14	4.86	18.39	5.29	20.02	5.66	21.42	6.06	22.93
20	1.4	3.10	11.73	3.36	12.71	3.73	14.11	4.05	15.32	4.46	16.88	4.82	18.24	5.23	19.79	5.61	21.23	6.11	23.12	6.53	24.71	6.99	26.45
25	1.7	3.47	13.13	3.76	14.23	4.17	15.78	4.52	17.10	4.99	18.88	5.38	20.36	5.85	22.14	6.27	23.73	6.83	25.85	7.30	27.63	7.82	29.59
30	2.1	3.80	14.38	4.12	15.59	4.56	17.25	4.96	18.77	5.47	20.70	5.90	22.33	6.41	24.26	6.87	26.00	7.48	28.31	8.00	30.28	8.56	32.39
40	2.8	4.39	16.61	4.76	18.01	5.27	19.94	5.72	21.65	6.31	23.88	6.81	25.77	7.40	28.00	7.94	30.65	8.64	32.70	9.24	34.97	9.89	37.43
50	3.4	4.90	18.54	5.32	20.13	5.89	22.29	6.40	24.22	7.06	26.72	7.61	28.80	8.28	31.33	8.87	33.57	9.66	36.56	10.33	39.13	11.06	41.86

NOZZLE #		#31		#32		#33		#34		#35		#36		#37		#38		#39		#40		#41	
Color		Dark Brown		Orange		Orange		Dark Green		Dark Green		Purple		Purple		Black		Black		Dark		Dk. Turquoise	
Stripe		Orange				Dark Green				Purple				Black				Dk. Turquoise		Turquoise		Mustard	
PSI	BAR	GPM	LPM	GPM	LPM	GPM	LPM	GPM	LPM	GPM	LPM	GPM	LPM	GPM	LPM	GPM	LPM	GPM	LPM	GPM	LPM	GPM	LPM
6	0.4	4.06	15.36	4.36	16.50	4.65	17.60	4.94	18.69	5.20	19.68	5.47	20.70	5.84	22.10	6.18	23.39	6.52	24.68	6.85	25.92	7.26	27.48
10	0.7	5.24	19.83	5.63	21.30	6.00	22.71	6.37	24.11	6.72	25.43	7.06	26.72	7.54	28.54	7.97	30.16	8.42	31.87	8.85	33.49	9.37	35.47
15	1.0	6.41	24.26	6.89	26.07	7.35	27.81	7.81	29.56	8.23	31.15	8.65	32.74	9.24	34.97	9.77	36.98	10.31	39.02	10.84	41.02	11.48	43.45
20	1.4	7.40	28.00	7.96	30.12	8.49	32.13	9.01	34.10	9.50	35.95	9.98	37.77	10.67	40.38	11.28	42.69	11.91	45.08	12.51	47.35	13.26	50.19
25	1.7	8.28	31.34	8.90	33.68	9.49	35.91	10.08	38.15	10.62	40.19	11.16	42.24	11.92	45.11	12.61	47.72	13.31	50.38	13.99	52.95	14.82	56.09
30	2.1	9.07	34.32	9.75	36.90	10.39	39.32	11.04	41.78	11.64	44.05	12.23	46.29	13.06	49.43	13.81	52.27	14.58	55.19	15.33	58.02	16.23	61.43
40	2.8	10.47	39.62	11.26	42.62	12.00	45.42	12.75	48.25	13.44	50.87	14.12	53.44	15.08	57.07	15.95	60.37	16.84	63.74	17.70	66.99	18.75	70.97
50	3.4	11.71	44.32	12.59	47.65	13.42	50.79	14.25	53.93	15.02	56.85	15.79	59.76	16.86	63.81	17.83	67.48	18.81	71.20	19.79	74.90	20.96	79.33

NOZZLE #		#42		#43		#44		#45		#46		#47		#48		#49		#50	
Color		Mustard		Mustard		Maroon		Maroon		Cream		Cream		Dark Blue		Dark Blue		Copper	
Stripe				Maroon				Cream				Dark Blue				Copper			
PSI	BAR	GPM	LPM	GPM	LPM	GPM	LPM	GPM	LPM	GPM	LPM	GPM	LPM	GPM	LPM	GPM	LPM	GPM	LPM
6	0.4	7.60	28.76	7.96	30.13	8.33	31.52	8.73	33.04	9.12	34.51	9.58	36.26	9.96	37.69	10.31	39.02	10.77	40.76
10	0.7	9.81	37.13	10.28	38.91	10.75	40.68	11.27	42.66	11.77	44.54	12.36	46.78	12.86	48.67	13.31	50.38	13.91	52.64
15	1.0	12.01	45.45	12.59	47.65	13.17	49.84	13.80	52.23	14.41	54.54	15.14	57.30	15.75	59.61	16.30	61.70	17.03	64.45
20	1.4	13.87	52.49	14.54	55.03	15.20	57.53	15.93	60.30	16.64	62.98	17.49	66.20	18.19	68.84	18.82	71.23	19.67	74.45
25	1.7	15.51	58.70	16.25	61.51	17.00	64.34	17.81	67.41	18.61	70.43	19.55	74.00	20.33	76.94	21.05	79.67	21.99	83.23
30	2.1	16.99	64.30	17.80	67.37	18.62	70.47	19.51	73.85	20.38	77.13	21.42	81.07	22.28	84.32	23.05	87.24	24.09	91.18
40	2.8	19.61	74.22	20.56	77.82	21.50	81.37	22.53	85.28	23.54	89.09	24.73	93.60	25.72	97.35	26.62	100.76	27.82	105.29
50	3.4	21.93	83.00	22.98	86.98	24.04	90.99	25.19	95.34	26.31	99.58	27.65	104.66	28.76	108.85	29.76	112.64	31.10	117.71

This flow data was obtained under ideal test conditions and may be adversely affected by poor hydraulic entrance conditions, turbulence or other factors. Nelson Irrigation makes no representation regarding sprinkler flow rate accuracy under various plumbing and drop pipe conditions.

Tel: +1 509.525.7660 / Fax: +1 509.525.7907 / nelsonirrigation.com / info@nelsonirrigation.com

Cut-away of Pressure Regulator

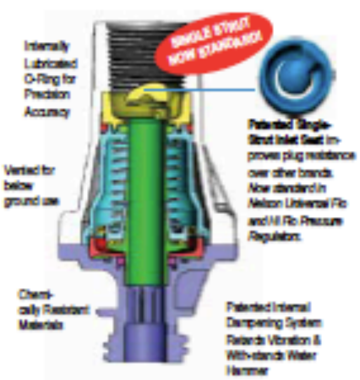

TECHNICAL TIPS FOR REGULATING SYSTEMS

IMPORTANT: Allow approximately 5 PSI (.35 BAR) extra pressure in order for the regulator to function properly. For example, the minimum design pressure for a 20 PSI (1.4 BAR) pressure regulator is 25 PSI (1.7 BAR).

IMPORTANT: If your system is designed with Nelson sprinklers, use Nelson Pressure Regulators. Individual manufacturers' pressure regulator performance varies. Interchanging could result in inaccurate nozzle selection.

NELSON

SAVE WATER, SAVE ENERGY AND DO A BETTER JOB OF IRRIGATING

NELSON'S UNIVERSAL FLO AND HI FLO REGULATORS

The function of a pressure regulator is to fix a varying inlet pressure to a set outlet pressure, regardless of changes in the system pressure due to hydraulic conditions, elevation changes, pumping scenarios, etc. The benefits include a uniform depth of water application, controlled sprinkler performance (droplet size and throw distance), and flexibility in system operation.

FEATURES & BENEFITS:

SINGLE STRUT SEAT DESIGN STANDARD WITH UNIVERSAL FLO. The new "single-strut" technology in the Universal Flo regulator minimizes "hair-pinning" of debris around the inlet seat, providing more plug resistance for systems operating in dirty water condtions.

PATENTED DAMPENING SYSTEM. The patented o-ring dampening system of all Nelson pressure regulators handles severe pressure surges to withstand water hammer.

WIDE FLOW RANGE. The Nelson Universal Pressure Regulator has a flow up to 12 GPM (2.7 M³/H) at 15 PSI (1.0 BAR) and above.

EXTENDED PERFORMANCE AND PRECISION ACCURACY. Precision components coupled with an internally lubricated o-ring minimize frictional drag and hysteresis.

PRECISION MANUFACTURED. Made of the toughest chemically resistant materials. 100% tested for accuracy.

UNIVERSAL 3000 SERIES CONNECTION OPTION. Integral adapter connects directly into all Nelson 3000 Series Pivot Sprinklers and creates an easy to assemble, economical pivot sprinkler package.

> UNIVERSAL FLO and HIGH FLO — CONNECTIONS & PERFORMANCE

PIPE THREAD CONNECTION

INLET
3/4" FNPT

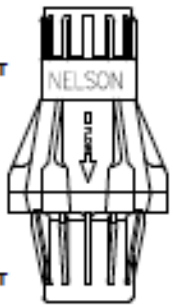

OUTLET
3/4" FNPT

3000 SERIES PIVOT CONNECTION

(Integral adapter for 3000 Series Pivot Products)

INLET
3/4" FNPT

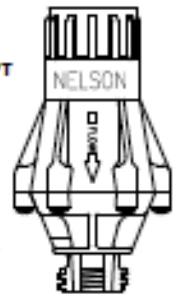

OUTLET
3000 ST

HOSE THREAD CONNECTION

(Connections for Micro/Drip)

INLET
3/4" FHT

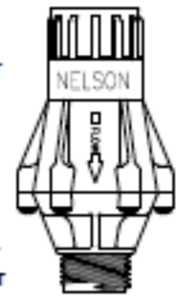

OUTLET
3/4" MHT

ORDERING SPECIFICATIONS: When ordering Nelson Pressure Regulators specify Pressure, Flow (Universal Flo or Hi Flo) & Connection (Inlet x Outlet). (Example: 10 PSI Hi Flo 3/4"FNPT x 3/4"FNPT.) **More connection options available — please contact Nelson factory for more information.**

UNIVERSAL FLO REGULATOR

PSI	BAR	GPM	M³/HR	CONNECTIONS AVAILABLE ■ 3/4" FNPT 3/4" FNPT	3/4" FNPT 3/4" ST	3/4" FHT 3/4" MHT
6	0.41	0.5-8	0.11-1.82	■	■	■
10	0.70	0.5-10	0.11-2.27	■	■	■
15	1.0	0.5-12	0.11-2.72	■	■	■
20	1.4	0.5-12	0.11-2.72	■	■	■
25	1.7	0.5-12	0.11-2.72	■	■	■
30	2.0	0.5-12	0.11-2.72	■	■	■
40	2.8	0.5-12	0.11-2.72	■	■	■
50	3.4	0.5-12	0.11-2.72	■	■	■

HI-FLO REGULATOR

PSI	BAR	GPM	M³/HR	CONNECTIONS AVAILABLE ■ 3/4" FNPT 3/4" FNPT	3/4" FNPT 3/4" ST
6	0.41	4-16	.91-3.63	■	■
10	0.70	4-16	.91-3.63	■	■
15	1.0	2-20	.45-4.54	■	■
20	1.4	2-20	.45-4.54	■	■
25	1.7	2-20	.45-4.54	■	■
30	2.0	2-20	.45-4.54	■	■
40	2.8	2-20	.45-4.54	■	■
50	3.4	2-20	.45-4.54	■	■

APPLICATION NOTES

Nelson Pressure Regulators can be used in a variety of applications (e.g. Center Pivot, Solid Set, Tree & Vine). Choose the proper pressure rating for your application.

Performance Tables. Contact the Nelson factory for detailed performance information.

Design Considerations. Maintain a 5 PSI (0.35 BAR) threshold above the nominal spring rated pressure.

CAUTION! Pressure regulators should be installed downstream from all shut-off valves.

NELSON
Nelson Irrigation Corporation
848 Airport Rd., Walla Walla, WA 99362 USA
Tel: 509.525.7660 Fax: 509.525.7907 **info@nelsonirrigation.com**
Nelson Irrigation Corporation of Australia Pty. Ltd.
35 Sudbury Street, Darra QLD 4074 **info@nelsonirrigation.com.au**
Tel: +61 7 3715 8555 Fax: +61 7 3715 8666

WWW.NELSONIRRIGATION.COM

Electricsolenoidvalves.com

The Brass - Series Semi-Direct acting, 2 Way General Purpose Solenoid Valves provide and on-off control of inherit liquids and gases. Suitable for commercial and residential applications. This valve type is gravity feed capable and is deal for low pressure fluid appliations. Available in sizes from 3/8" - 2" in both Normally Closed and Normally Open operating positions.

*These valves are not intended for use in medical life support, combustion, aviatiion, aerospace, automotive or similar applications.

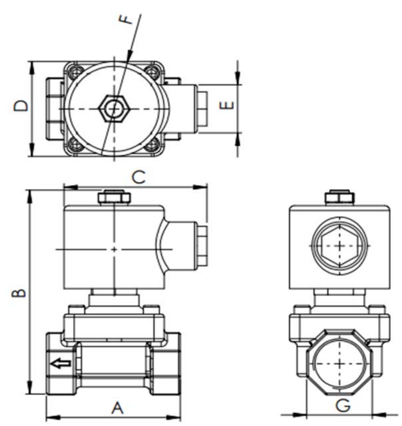

Materials	
Valve Body	Brass
Seal	FKM
Shading Ring	Copper
Hardware	S/S

Electrical				
Connection Type	N/C - 5.5" Lead		N/O - DIN	
Protection Class	NEMA 3	IP54		
Available Voltages	DC: 24V	DC: 12V	AC: 24V/60Hz	AC: 110V/60Hz
Power 3/8" - 1"	28 W	18 W	28 W	28 W
Power 1-1/4" - 2"	40 W	30 W	40 W	40 W

Brass - Series

Port Size	Thread	Orifice	Cv Value	Min PSI	Max PSI	Operating Temp Min	Operating Temp Max	Duty Cycle	Weight	Dimensions A	B	C	D	E	F	G
Normally Closed																
3/8"	NPT	5/8	4.8	0	AC145 DC115	15°F	250°F	100%	1lb 7oz	2.36"	4.00"	2.83"	2.00"	1.00"	1.96"	1.05"
1/2"	NPT	5/8	4.8	0	AC145 DC115	15°F	250°F	100%	1lb 7oz	2.36"	4.00"	2.83"	2.00"	1.00"	1.96"	1.06"
3/4"	NPT	3/4	7.6	0	AC145 DC115	15°F	250°F	100%	1lb 10oz	2.65"	4.25"	2.83"	2.00"	1.00"	1.96"	1.30"
1"	NPT	1	12	0	AC145 DC115	15°F	250°F	100%	2lb 5oz	3.25"	4.50"	2.83"	2.60"	1.00"	1.96"	1.57"
1-1/4"	NPT	1 1/4	24	0	AC145 DC90	15°F	250°F	100%	4lbs 11oz	4.00"	5.80"	3.55"	3.22"	1.00"	2.70"	1.95"
1-1/2"	NPT	1 4/7	29	0	AC145 DC90	15°F	250°F	100%	4lbs 14oz	4.33"	6.00"	3.55"	3.35"	1.00"	2.70"	2.20"
2"	NPT	1 7/8	48	0	AC145 DC90	15°F	250°F	100%	7lbs	5.30"	6.50"	3.55"	4.25"	1.00"	2.70"	2.66"
Normally Open																
1/2"	NPT	5/8	4.8	0	90	15°F	250°F	100%	1lb 9oz	2.36"	4.50"	3.50"	1.95"	.80"	1.96"	1.06"
3/4"	NPT	3/4	7.6	0	90	15°F	250°F	100%	1lb 13oz	2.65"	4.70"	3.50"	2.00"	.80"	1.96"	1.30"
1"	NPT	1	12	0	90	15°F	250°F	100%	2lb 7oz	3.20"	5.00"	3.50"	2.60"	.80"	1.96"	1.57"
1-1/2"	NPT	1 4/7	29	0	90	15°F	250°F	100%	5lb 2oz	4.33"	7.00"	4.50"	3.25"	1.15"	2.75"	2.25"
2"	NPT	1 7/8	48	0	90	15°F	250°F	100%	7lb 8oz	5.30"	7.50"	4.50"	4.25"	1.15"	2.75"	2.75"

*Consult a chemical compatibility expert for correct seal and valve body material choice.
*Weight and dimensions may vary slightly from production.

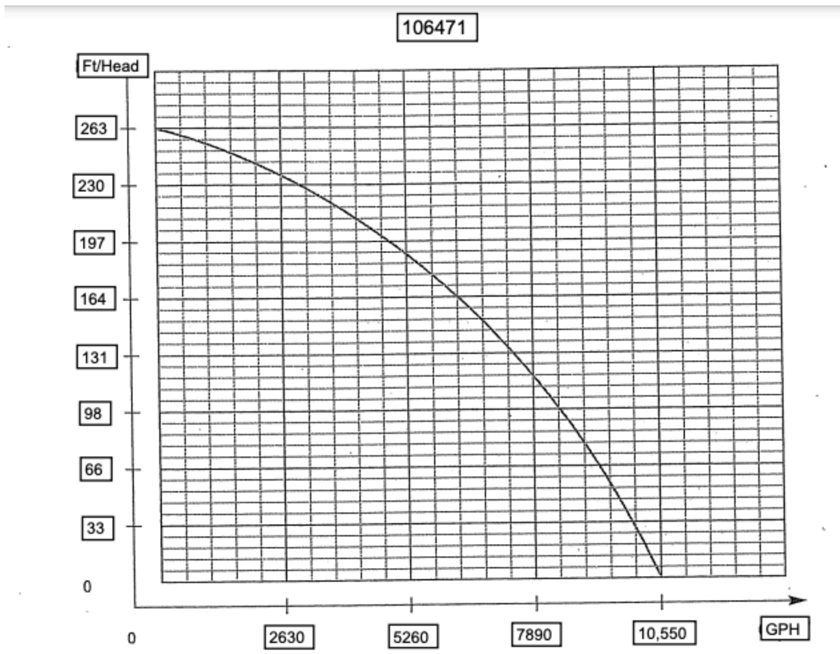

NorthStar 3 in. High Pressure Pump Curve Model No. 106471